SYNTHESIS OF DINUCLEAR COMPLEXES. FROM LIGAND DESIGN TO CATALYSIS

Oriol Martínez Ferraté

Dipòsit Legal: T.1429-2013

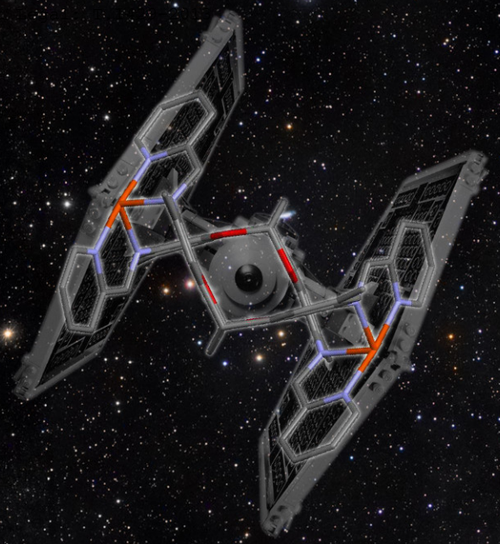

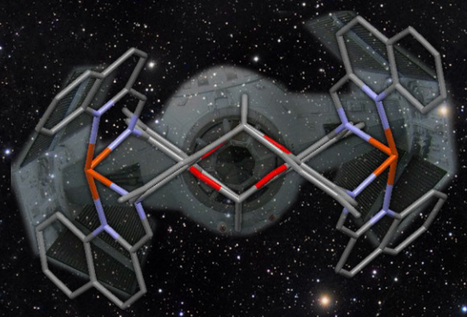

Synthesis of Dinuclear Complexes. From Ligand Design to Catalysis.
Oriol Martínez Ferraté, Doctoral Thesis, Tarragona 2013

ICIQ

SYNTHESIS OF DINUCLEAR COMPLEXES. FROM LIGAND DESIGN TO CATALYSIS.

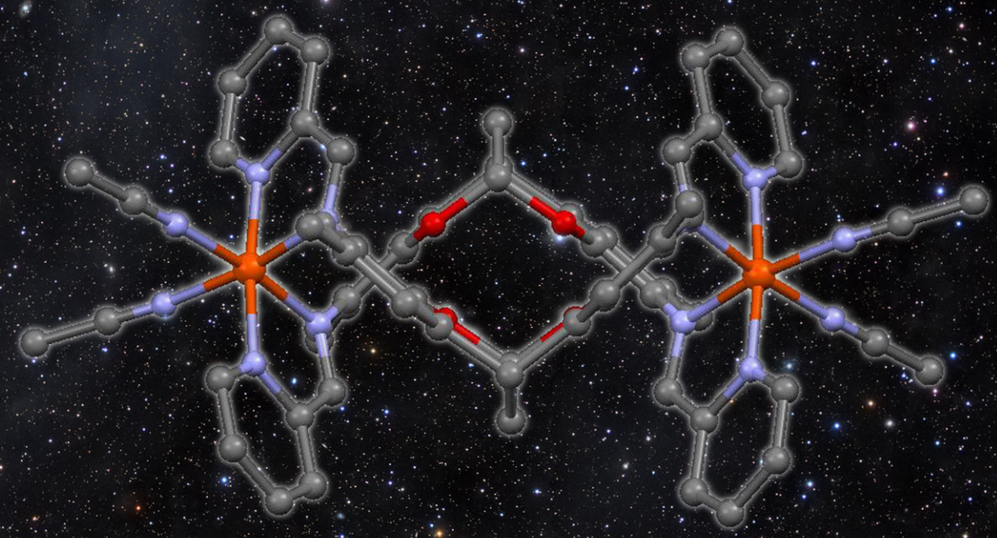

Oriol Martínez Ferraté

Doctoral Thesis

Tarragona 2013

Oriol Martínez Ferraté

"Synthesis of Dinuclear Complexes. From Ligand Design to Catalysis."

DOCTORAL THESIS

Supervised by

Prof. Dr. Carmen Claver Cabrero and Prof. Dr. Piet van Leeuwen

UNIVERSITAT ROVIRA I VIRGILI

Tarragona, 2013

UNIVERSITAT ROVIRA I VIRGILI

UNIVERSITAT ROVIRA I VIRGILI
Departament de Química Física i Inorgànica
Campus Sescelades
Carrer Marcel.lí Domingo,s/n
43007 Tarragona
Tel. 977 55 81 37

Prof. Dra. Carmen Claver Cabrero, catedràtica del Departament de Química Física i Inorgànica de la Universitat Rovira i Virgili,

FAIG CONSTAR:

Que el present treball, titulat “Synthesis of dinuclear complexes. From ligand design to catalysis”, que presenta el Sr. Oriol Martínez Ferraté per a l’obtenció del títol de Doctor en Química, ha estat realitzat sota la meva direcció i la co-direcció del Prof. Dr. Piet van Leeuwen cap de grup de l’Institut Català d’Investigació Química, al Departament de Química Física i Inorgànica i a l’ Institut Català d’Investigació Química i compleix els requisits per a optar a la Menció Europea.

Tarragona, juny 2013

Prof. Dra. Carmen Claver Cabrero

Prof. Dr. Piet van Leeuwen

UNIVERSITAT ROVIRA I VIRGILI
SYNTHESIS OF DINUCLEAR COMPLEXES. FROM LIGAND DESIGN TO CATALYSIS
Oriol Martínez Ferraté
Dipòsit Legal: T.1429-2013

El present treball ha estat desenvolupat amb una beca BDRI finançada per la Universitat Rovira i Virgili i Fundació Institut Català d'Investigació Química. El treball que descriu la següent tesi ha estat finançat pels següents projectes:

URV 2010PFR-URV-B2-01
Generalitat de Catalunya 2009 SGR 116
CONSOLIDER-Intecat CSD2006-0003
MCIN CTQ2010-14938

UNIVERSITAT ROVIRA I VIRGILI

UNIVERSITAT ROVIRA I VIRGILI
SYNTHESIS OF DINUCLEAR COMPLEXES. FROM LIGAND DESIGN TO CATALYSIS
Oriol Martínez Ferraté
Dipòsit Legal: T.1429-2013

Agraïments

Abans de començar vull comentar que hi ha molta gent que d'una manera o altra a contribuït d'una manera o altre en el desenvolupament d'aquesta tesis. Vull agrair a tothom la seva col·laboració, i espero no oblidar a cap d'ells.

En primer lloc voldria agrair a la Carmen i al Piet per donar-me l'oportunitat de realitzar aquesta tesis. Per haver tingut la suficient confiança en mi com per deixar-me "volar sol" però sabent que hi estàveu com a xarxa de seguretat i guia per si sorgia cap problema o em perdia. M'heu ensenyat moltes coses durant la tesis, i el que trobo més important, no només de química. Així que gràcies per tot.

I want also to thank George Britovsek to give me the chance to work in his laboratory for 3 months. I can assure that final results of this thesis would be really different without my time in Imperial College of London.

També m'agradaria donar les gràcies a les persones que han ajudat a que el meu treball fos més senzill, a les secretaries tant del departament de Químca Física i Química Inorgànica (Marisol Romero, Silvia Duran i Yolanda Albero)com les de Piet a l'ICIQ (Mª José Gutierrez i Marta Moya) per la seva ajuda indispensable a l'hora de preparar i presentar tràmits.

No em puc deixar d'agrair als tècnics del servei de recursos de la URV: Ramon, Rosa, Maria José, Jordi, Arantxa i Raquel; com no també als de l'ICIQ: Jordi, Marta M., Eddy, Eduardo, Marta G. Yvette, Mariona, Simona, Gabriel, Kerman, Israel, Noemi, Sofia i Vanesa.

També, agraeixo l'ajuda dels grups *leader* de la URV: Ana Mª Masdeu, Elena Fernández Sergio Castillón, Oscar Pàmies, Montse Dieguez i Aurora Ruiz.

En tot aquest temps he tingut la possibilitat de compartir laboratori amb moltíssims companys que han fet aquest camí més agradable i divertit. Ariadna, Marta, Siham, Javi M., Eva , Mercè, Marc , Sabina, Jèssica M., Amo, Xavi, Gerard, Manuel, Cris S., Henrik, Jèssica C., Isabel, Dolores, Tatiana. I

també als del màster Lourdes, Isi, Núria, Miriam, Moira, Carlo i David. Espero no oblidar-me de ningú.

Menció especial per a l'Amadeu al qual crec que puc considerar a un amic. Estic segur que s'ha espantat al no veure el seu nom en la llista jeje. No et preocupis que no m'oblido de tu.

Durant el doctorat he tingut la sort de treballar al grups dels meus dos supervisors, a tots ells també he de donar les gràcies per ajudar-me i aguantar-me pel laboratori. Primer agrair a la gent del grup de Carmen per suportar-me durant els primers 2 anys: Cyril, Aitor, Jamin, Bernabé, Nico, Doris, Carolina, Verònica, Angelica, Jessi, Eli, Jorge, Norbert, Quique, Tatiana, Dagoberto, Bianca, Mónica i Alberto. I un agraïment especial per a l'Olivier per ensenyar-me a sobreviure en el laboratori i a Alí que va haver de patir-me quan Olivier va anar a l'ICIQ.

I per acabar, al a gent del grup de Piet, pels bons moments i les discussions sobre química: Josep Mª, Marta, Nic, Hugo, David, Anzhelika, Rick, Matthieu R., Eion, Piotr, Isra, Andy, Matthieu T., Prasad, Ece, Marcos, Olivier D. i Deniz

A tots i a totes us dono les gràcies per haver compartit aquesta aventura de la tesis!!! Molta sort a tots!!!

Fora de l'àmbit del doctorat vull agrair especialment als del poble (Frías, Tajon, Tita, Migui, Nacho y Gump) perquè he tingut la sort de créixer amb vosaltres. També a l'Antonio i el Xavi, perquè sembla mentida que després de tant de temps l'amistat encara perduri i finalment als companys de la Uni: Paco, Rafa i Edu perquè vau fer l'estada a la universitat molt divertida, tant que es va allargar massa XD

A la Cristina, per tot i més. No sé com expressar com d'important ets per a mi, no tornis a marxar sense mi. Et trobo massa a faltar. ☺

I per acabar a mons pares, per haver estat sempre quan els he necessitat, per ser com són i per haver-me portat fins on sóc ara. No us ho dic gaire però us estimo molt!!!!

UNIVERSITAT ROVIRA I VIRGILI
SYNTHESIS OF DINUCLEAR COMPLEXES. FROM LIGAND DESIGN TO CATALYSIS
Oriol Martínez Ferraté
Dipòsit Legal: T.1429-2013

“Es intentando lo imposible como se realiza lo posible.”
— Henri Barbusse

CONTENTS

Abbreviations

Å	angström
^{1}H	proton
Ac	acetyl
ACN	acetonitrile
Ar	aryl group
atm	atmosphere
b	broad
BFBF	2,9-dimethyl-5a,10b-dihydrobenzofuro[2,3-b]benzofuran
BINAP	2,2'-Bis(diphenylphosphino)-1,1'-binaphthyl
Bn	benzyl
BOX	bisoxazoline
BPMEN	N^1,N^2-dimethyl-N^1,N^2-bis(pyridin-2-ylmethyl)ethane-1,2-diamine
brine	saturated NaCl-solution in water
BuLi	butyllithium
calcd	calculated
cat.	catalyst
$CDCl_3$	deuterated chloroform
conv.	conversion
COSY	correlated spectroscopy
DBDOC	2,10-dimethyl-12H-6,12-methanodibenzo[d,g][1,3]dioxocine
DCM	dichloromethane
det	detector
DFT	Density functional theory
DIBALH	Diisobutylaluminium hydride
DIOP	2,3-O-Isopropylidene-2,3-dihydroxy-1,4-bis(diphenylphosphino)butane
DIPAMP	Ethane-1,2-diylbis[(2-methoxyphenyl)phenylphosphane]
DMAP	4-dimethylaminopyridine
DME	Dimethoxyethane
DMF	*N,N*-dimethyl formamide
DMSO	dimethylsulfoxide
DPEphos	Bis[(2-diphenylphosphino)phenyl]
dppe	1,2-Bis(diphenylphosphino)ethane
dppf	1,1'- Bis(diphenylphosphino) ferrocene
dppm	1,1-Bis(diphenylphosphino)methane
dppp	1,3-Bis(diphenylphosphino)propane
Duphos	1,2-Bis(2,5-dimethylphospholano)benzene
Ea	Activation energy
EDG	Electron donating group
ee	enantiomeric excess

EI	electron ionization
eq.	equivalent
ESI	Electrospray ionization
Et	ethyl
Et_2O	diethyl ether
Et_3N	trietylamine
EtOAc	ethyl acetate
EtOH	ethanol
EWG	Electron withdrawing group
g	gram
GC	gas cromatography
GC-MS	Gas chromatography–mass spectrometry
glup	(((2R,4aR,6S,7R,8R,8aR)-6-phenoxy-2-phenylhexahydropyrano-[3,2-d][1,3]dioxine-7,8-diyl)bis(oxy))bis(diphenylphosphine)
h	hours
HPLC	high pressure liquid chromatography
Hz	hertz
inj	injector
^{i}Pr	*iso*-propyl
IPr	1,3-Bis(2,6-Diisopropylphenyl)imidazol-2-ylidene
J	coupling constant
L	ligand
L	litre
LHMDS	lithium bis(trimethylsilyl)amide
LSIMS	Liquid secondary ion mass spectrometry
M	molar
m	meta
m	multiplet
MALDI	Matrix-Assisted Laser Desorption/Ionization
MAO	Methylaluminoxane
m-CPBA	*meta*-chloroperbenzoic acid
Me	methyl
MEK	butanone
MeOH	methanol
min	minute
MMO	methane monooxygenase
Ms	methanesulfonyl
mw	microwaves
NBS	N-bromosuccinimide
NHC	N-Heterocyclic Carbene
NMR	nuclear magnetic resonance
NOESY	nuclear overhauser effect spectroscopy

o	ortho
ox	oxidant
p	para
Pa	pascal
PDP	(2S,2'S)-1,1'-bis(pyridin-2-ylmethyl)-2,2'-bipyrrolidine
PEMB	5-Ethyl-2-methylpyridine borane
PFOA	Perfluorooctanoic acid
Ph	phenyl
phen	phenanthroline
ppm	parts per million
Pr	propyl
Py	pyridine
q	quartet
Qphos	pentaphenyl(di-tert-butylphosphino)ferrocene
R	alkyl group
rt	room temperature
s	singlet
S	solvent
salen	2,2'-ethylenebis(nitrilomethylidene)diphenol
salphen	*N,N*'-bis(3,5-di-tert-butyl salicylidine-1,2-benzenediamine)
sel	selectivity
Selectfluor	N-Chloromethyl-N′-fluorotriethylenediammonium bis(tetrafluoroborate)
SIPr	1,3-Bis(2,6-di-i-propylphenyl)imidazolidin-2-ylidene
SPAN	4,4,4',4',6,6'-hexamethyl-2,2'-spirobi[chroman]
S-Phos	2-Dicyclohexylphosphino-2',6'-dimethoxybiphenyl
T	temperature
t	triplet
TACN	1,4-dimethyl-7-(pyridin-2-ylmethyl)-1,4,7-triazonane
^{t}Bu	*tert*-butyl
TEOF	triethylorthoformate
Tf	trifluoromethanesulfonyl
TFA	trifluoroacetic acid
THF	tetrahydrofuran
TLC	thin layer chromatography
TMEDA	tetramethylethylenediamine
TMS	Tetramethylsilane
TOF	turnover frequency
TON	turnover number
TPA	tris(pyridin-2-ylmethyl)amine
TPhOA	amine triphenolate
TRANSPHOS	2,11-bis((diphenylphosphino)methyl)benzo[c]phenanthrene
TRAP	2,2''-bis[1-(diphenylphosphino)ethyl]-1,1''-biferrocene

Ts	*p*-toluenesulfonyl
vs.	versus
X	halide
Xantphos	4,5-Bis(diphenylphosphino)-9,9-dimethylxanthene
δ	chemical shift in parts per million

Chapter 1
General introduction and objectives.

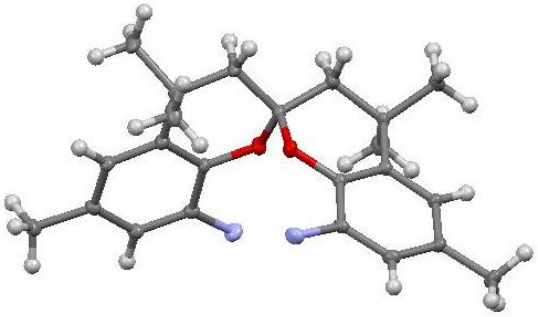

1.1. Homogeneous catalysis and industrial applications

A common definition for a catalyst is the following one: "A catalyst is a substance that increases the rate at which a chemical reaction approaches equilibrium without becoming itself permanently involved".[1] Depending on the phase of the catalyst and the substrates they can be classified as either homogeneous or heterogeneous catalysts.

A broad spectrum of substances can function as homogeneous catalysts: Brønsted and Lewis acids, bases, organic molecules such as proline and quinine, and metal complexes. Organometallic and coordination complexes play an important role in homogeneous catalysis. These substances are composed of a central metal surrounded by ligands (organic or inorganic). The reactivity of organometallic complexes relies on the metal and the type of ligands in the coordination sphere.[1] The activity and selectivity of a catalytic system can be tuned by modifying the ligands. In doing so, the number of catalysts and processes has grown enormously in the last decades and a large number of new processes using organometallic and coordination complexes has come on stream. Accelerations of many orders of magnitude have been reported — often the non-catalytic reaction does not proceed at all — and selectivities have been improved similarly.

Those high activities and selectivities are due the presence of a catalyst, for instance the activation of bromine in an electrophilic aromatic substitution reaction. Iron tribromide forms a complex with bromine increasing the electrophicility of bromine and facilitating the reaction for non-activated substrates. The catalytic process between iron and bromine has only one intermediate. Usually more than one intermediate could participate in a catalytic reaction. As a general trend, an organometallic complex in a reaction media will affect the reactivity, since the substrates will be activated through coordination to the metal center, providing an alternative mechanism which shows a different transition state with lower activation energy (Figure 1.1). Moreover, the catalyst will enable reactions, which although thermodynamically feasible, would not occur in the absence of a catalyst. This new pathway usually includes several new intermediates and steps which together present the reaction mechanism.

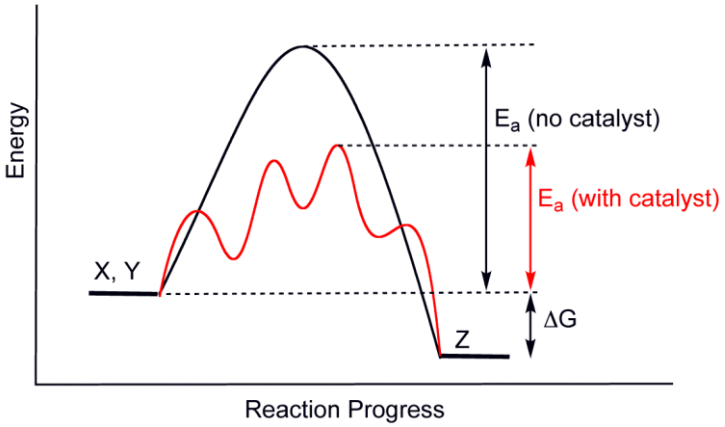

Figure 1.1 *Energy profile for a catalyzed multi-step reaction (in red) and an uncatalyzed reaction (in black).*

Activity is a key issue. In order to compare the activity of various modified catalysts, we need to quantify the catalyst activity. The activity of a catalytic system can be expressed by the turnover number (TON) and the turnover frequency (TOF). The TON is the total number of substrate molecules that a catalyst converts into product molecules. The TOF is the TON per unit of time.

Selectivity is equally important in chemical transformations. Several kinds of selectivity can be distinguished in a catalytic process, or any chemical reaction. The first kind of selectivity is named chemoselectivity by which we mean that one functional group is transformed preferentially in the presence of other functionalities. For instance, the hydrogenation of alkenes in the presence of carbonyl groups may occur with a certain chemoselectivity. The second type is regioselectivity that is defined as the selective conversion of one of the same reactive centers in a molecule, for example in electrophilic aromatic substitution or hydroformylation. When one of the stereoisomers is formed preferentially, this is named stereoselectivity. The next type is enantioselectivity defined as the conversion of an achiral substrate selectively into one of the possible enantiomers. If in a racemic mixture, only one of the enantiomers is reacting, a kinetic resolution is taking place. The maximum yield in this type of reactions is 50%. A special case, in which it is possible to achieve 100% yield is the so-called dynamic kinetic resolution. This process consists in predominant conversion of one enantiomer of the racemic mixture, while continuously

racemization maintains the equilibrium of the racemate until the end of the reaction. Examples of all these kinds of selectivity are depicted in Scheme 1.1.

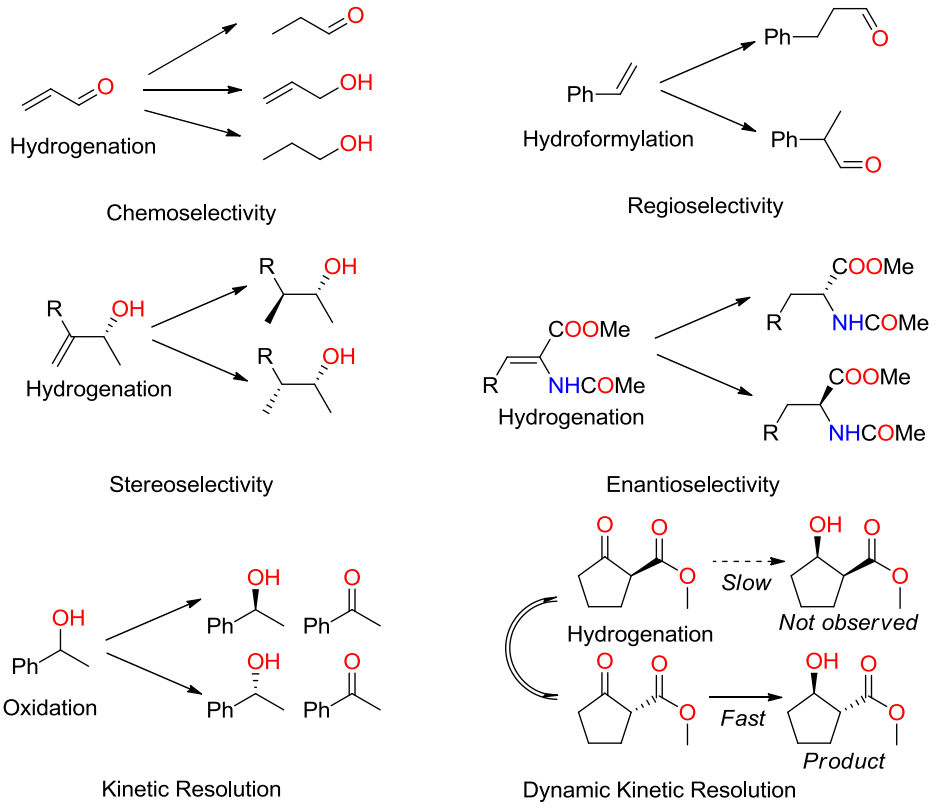

Scheme 1.1 *Selectivities of chemical conversions.*

Catalysts have a long history in chemical industry. For instance, as early as 1900 catalysts were already used in industry for making organic products, e.g. nickel on a silica support for the hydrogenation of fatty acids ("fat hardening"). Heterogeneous catalysts are more widely used in industrial processes than homogeneous catalysts. The first main advantage of heterogeneous catalysts with respect to homogeneous ones is the easier recovery of the former for reuse, since reagents and products are in a different phase. In contrast, recycling of homogeneous catalysts is more difficult. Consequently several heterogenization methods have been investigated in order to facilitate the recovery of the catalyst. Other important advantages of heterogeneous catalysts are their high thermal stability and their ease of regeneration,

especially for oxidic catalysts. However, homogeneous catalyst have several advantages such as a general tunability with small modifications in the nature of the organometallic catalyst; mechanisms are considerably easier to study, — where such powerful methods as NMR can be used to both assign structures and follow reaction kinetics —; and diffusion and dissipation of heat rarely is an issue.[2,3]

Many industrial processes are performed with the use of heterogeneous catalysts. For example in oil refining, which is an order of magnitude larger by volume than chemicals manufacturing, nearly all processes use heterogeneous catalysts. The Fischer-Tropsch process, ethylene oxide synthesis, Haber-Bosch process, Ziegler-Natta polymerization, sulphuric acid synthesis, among different reactions are industrial processes conducted with heterogeneous catalysts.[4]

Even so, a wide variety of products are synthesized using homogeneous catalysts. As is shown in Scheme 1.2, substances within the ovals are the basic building blocks obtained from coal, gas, and petroleum refining and products within the squares are manufactured from these raw materials by homogeneous catalysts. Except the fine chemicals and intermediates, the other products are manufactured on a large scale.[5]

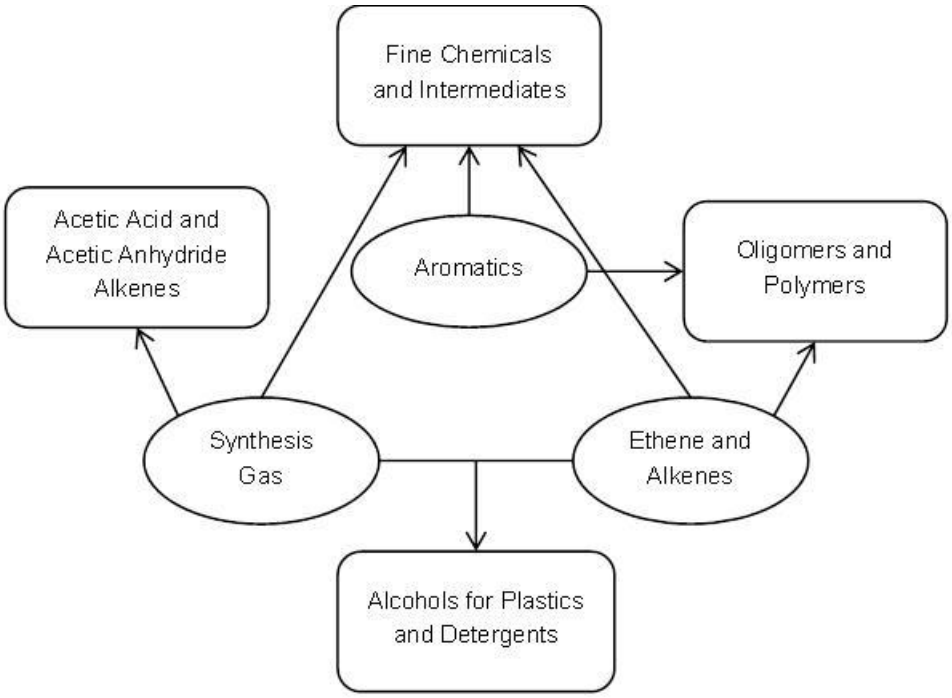

Scheme 1.2 *Chemicals and classes of chemicals that are manufactured by homogeneous catalytic processes (from reference 5).*

For instance, synthesis gas is converted into methanol by a heterogeneous catalyst and then the carbonylation of methanol is performed by a homogeneous catalyst to produce acetic acid. Acetic anhydride is obtained by carbonylation of methyl acetate; both processes are carried out on a large scale. The hydroformylation of alkenes allows the formation of aldehydes which are hydrogenated to produce alcohols, which are used for the generation of esters, solvents and detergents. More recently homogeneous catalysts are also used for processes which yield high added value products, such as fine chemicals, intermediates, agrochemicals and pharmaceutical compounds, L-Dopa being an early example.[6,7] Often these compounds are optically active, and in most of the cases only one enantiomer is of interest. For this reason, enantioselective synthetic procedures catalyzed by metal complexes can be a powerful synthetic tool in the pharmaceutical, agrochemical and flavours or fragrances companies.[6,7] There are only very few examples of enantioselective heterogeneous catalysts. Some of the most successful chiral ligands applied in homogeneous catalysis are depicted in Figure 1.2.

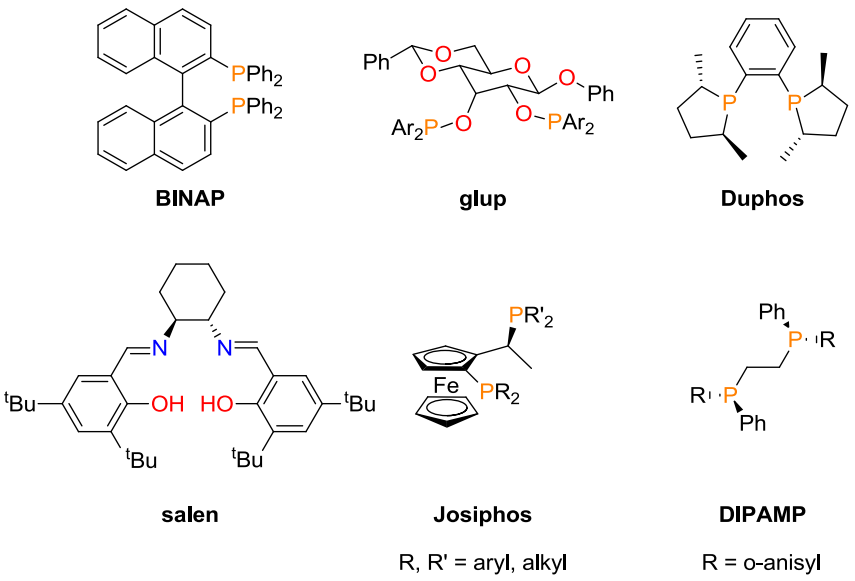

Figure 1.2 A *selection of successful chiral ligands.*

Some examples of products synthesized by homogeneous catalysts in industry are presented in Table 1.1.[5]

Table 1.1 *Products synthesized via homogeneous catalysis.*

Structure	Name	Use	Process
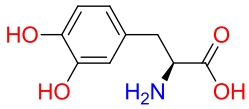	L-Dopa	Drug for Parkinson's disease	Asymmetric hydrogenation
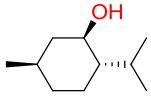	L-Menthol	Flavoring agent	Asymmetric isomerization
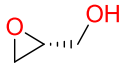	(R)-Glycidol	Component of heart drug	Asymmetric epoxidation
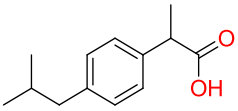	Ibuprofen	Analgesic	Carbonylation
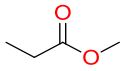	Methyl Propanoate	Synthesis of methyl methacrylate	Methoxycarbonylation

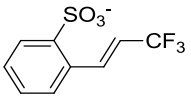	Intermediate for Prosulfuron	Herbicide	C-C coupling

1.2. Application of N-donor ligands in catalysis

Ever since the publication of the Wilkinson's catalyst for highly efficient homogeneous catalytic hydrogenation,[8] the most common ligands employed in organometallic catalysis have been phosphorus containing compounds. Prior to this report, also nitrogen compounds, such as amines and pyridines, were ubiquitous ligands both in coordination chemistry and in catalysis.[9–11] Phosphines have been studied extensively, but the use of nitrogen ligands can be interesting due to their properties which provide some advantages:

- Nitrogen ligands are more stable than phosphines and phosphites towards oxidation and hydrolysis, which enables the use of solvents without purification.[12] This stability allows easier access to recycling of the catalyst.

- Many of these precursors/ligands are available in enantiomerically pure form, either in the chiral pool as aminoacids, quinine, cinchonine, sparteine, strychnine and emetine or industrial products like 1,2-diaminocyclohexane.[13]

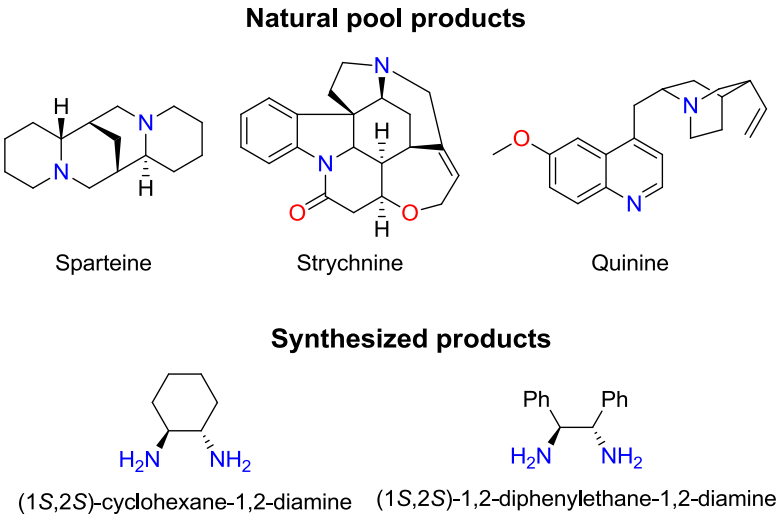

Figure 1.3 *Some examples of commercial available amines.*

- The chemistry of nitrogen is better known than that of phosphorus and it provides numerous synthetic solutions to each possible transformation of these compounds. It is easier to modify a backbone with amine groups (RNH_2),[14–16] than one with phosphine group (RPH_2).[17]

However nitrogen ligands also have several disadvantages, such as:

- Low sensibility for NMR techniques. For this reason it is difficult to determine structures of catalysts and catalytic intermediates in solution.

- Chirality on the nitrogen atom is difficult to obtain, as nitrogen atoms instantaneously epimerize at room temperature. The only possible way to have chiral nitrogen atom is in polycyclic structures. In contrast, this chirality is very common for phosphorus compounds like DIPAMP.[18]

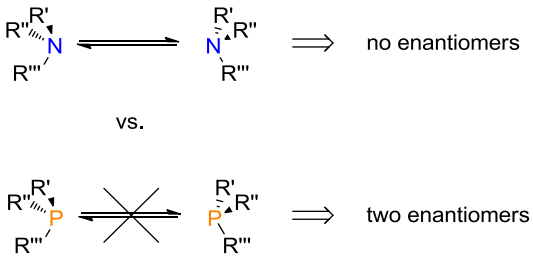

Scheme 1.3 *Representation of epimerization for nitrogen and phosphorus.*

Nitrogen and phosphorus ligands have several different properties in terms of sterics and electronics. These properties could be considered either an advantage or a drawback depending on the system and the desired reactivity.

- Steric hindrance is larger for nitrogen ligands. Substituents at nitrogen are closer to the metal as the nitrogen bonds are shorter than phosphorus bonds. Tolman's cone angle for nitrogen and phosphorus analogues are summarized in Table 1.2.[19,20]

Table 1.2 *Tolman's cone angle for P and N compounds.*

Ligand	θ_P (º)	θ_N (º)
XH_3	87	94
XMe_3	118	132
XEt_3	132	150
XPh_3	145	166
X^iPr_3	160	220

- The stabilization of metal complexes with nitrogen and phosphorus is different since they have different electronic properties. Unlike nitrogen complexes, back-donation is possible in phosphorus complexes due to the involvement of empty σ* orbitals with the appropriate energy.[21]

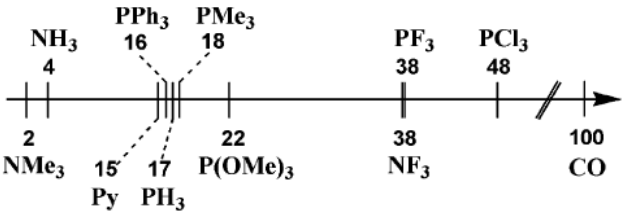

Figure 1.4 *Caculated π-acceptor index for P- and N- based ligands.*

In general the hybridization for nitrogen atoms present in the ligands is an sp^3 or sp^2 hybridization. Examples of sp^3 nitrogen compounds are amines, pyrrolidines, amides, anilines and others. These ligands are strong and hard σ-donors, moreover the absence of low-lying empty orbitals disables the back-donation which takes place in phosphorus ligand complexes. Thus nitrogen ligands stabilize metals in high valence states.[1] Nitrogen compounds that exhibit sp^2 hybridization are imine, pyridine, oxazoline, imidazoline, etc. In this case they are strong σ-donors and low to moderate π-acceptors, consequently they stabilize metals of high and intermediate valency.[21,22]

Nitrogen atoms are present in multidentate ligands in combination with other nitrogen, phosphorus, sulphur, oxygen or carbon atoms.[13,23–25] Some examples of N-X ligands are shown in Figure 1.5.

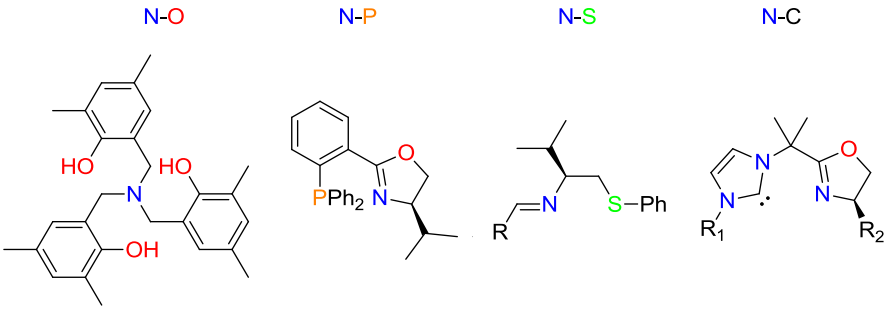

Figure 1.5 *Examples of nitrogen-heteroatom ligands.*

Nitrogen ligands are used in many metal catalyzed reactions such as epoxidation, oxidation of alcohols, oxidative coupling of phenols, hydrosilylation, hydrogen transfer, alkene polymerization, alternating CO/alkene polymerization, reduction of nitro compounds, C–H activation, etc. Some of these reactions are catalyzed by metals modified with nitrogen-heteroatom ligands.[1,13,21,26,27]

Several successful N-donor containing ligands applied in homogeneous catalysis are depicted in Figure 1.6

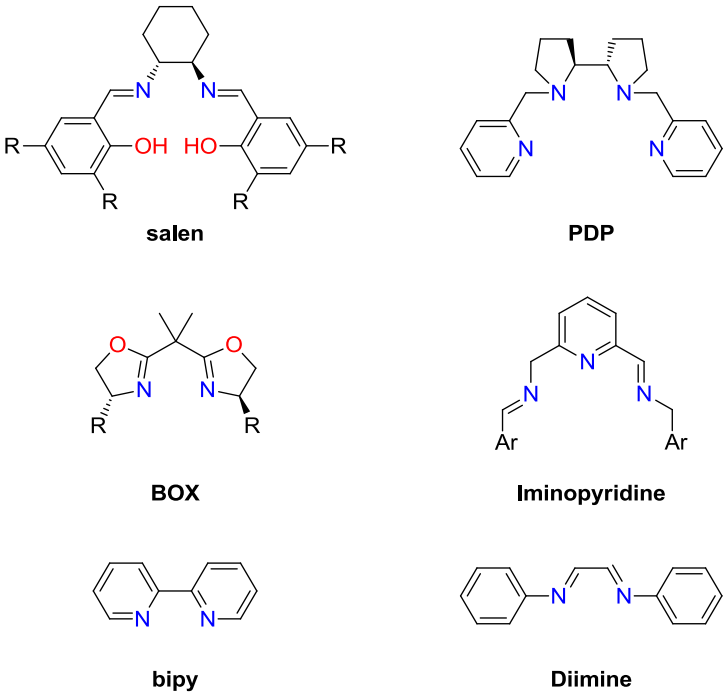

Figure 1.6 *Successful N-donors ligands in catalysis.*

Salen[i] type ligands were first reported by Pfeiffer and co-workers in 1933. [28] It is a very modular family of ligands that can coordinate with a wide range of transition metal such as: Mn, Ru, Co, V, Cr, Ti, etc.[13,27,29] Asymmetric catalytic epoxidation of alkenes with Mn complexes is an example of a successful reaction for salen ligands.[24,29] These ligands were successfully applied in metal catalyzed CO_2 activation which is an interesting and active field in current chemistry research. Several metals such as Zn, Co or Cr have been applied in the catalytic activation of CO_2 and epoxides to yield cyclic carbonates or co-polymers Scheme 1.4.[30–33] Salen complexes have also been employed in: alkene aziridinations, epoxide ring openings, hydroxylations, cyclopropanation, etc.[29]

[i] Salen refers to N,N'-ethylenebis(salicylimine). The name is often used for other diamines as well. 1,2-Diaminobenzene derived Schiff bases are referred to as Salphen.

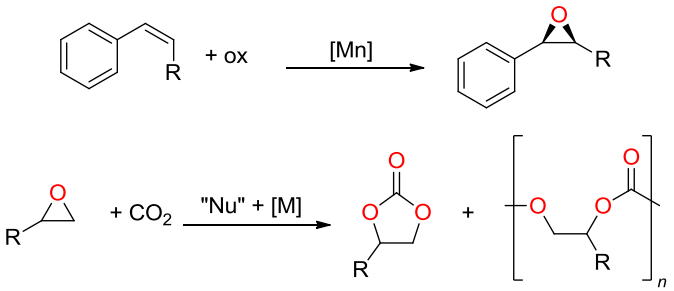

Scheme 1.4 *Examples of catalytic reactions mediated by salen complexes.*

Aminopyridine ligands as modifiers of iron catalysts were found to be active catalyst for oxidation such as epoxidation of alkenes, *cis*-hydroxylation of alkenes, and C–H activation.[34–37] Iron catalyst modified by PDP ligand (Figure 1.6) was reported by White and co-workers as a powerful catalyst in C–H oxidations. In this work hydrogen is considered as a functional group with predictable reactivity and selectivity. It allows the selective oxidation of one C–H "functional group" in a complex molecule (Scheme 1.5).[38–40]

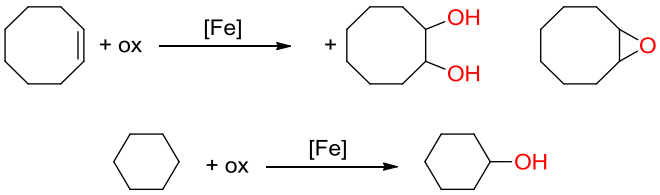

Scheme 1.5 *Oxidation reactions catalyzed by Ir aminopyridine compounds.*

Bisoxazoline ligands (BOX) constitute a popular family of nitrogen ligands in asymmetric catalysis. They present several advantageous properties, such as easy preparation of enantiopure ligands from readily available aminoalcohols, their stability towards oxygen and water, and the formation of complexes with a wide variety of metals (Cu, Pd, Fe, W, Zn, Rh, Ru, Ni). Copper (I) catalyzed asymmetric cyclopropanation of alkenes and copper (II) catalyzed enantioselective Diels-Alder reaction were the first examples of BOX as ligands. Since then, BOX ligands were applied in a wide variety of reactions such as aziridinations, desymmetrisation of *meso*-diols, kinetic resolution of racemates, aldol reaction, allylic substitutions, etc. Scheme 1.6 summarizes two examples of reactions catalyzed by BOX ligands.[13,41]

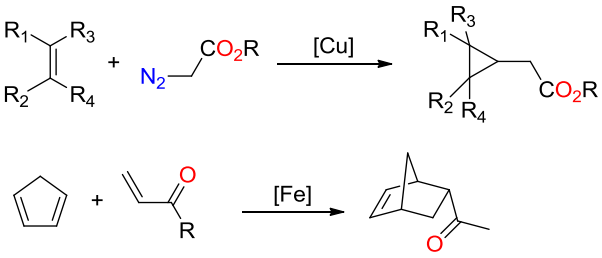

Scheme 1.6 *Copper and iron BOX ligands applications.*

Iminopyridine and bisiminopyridine are families of very modular ligands as they are prepared *via* a Schiff base condensation. These ligands form complexes with several metals such as Fe, Co, Cu, Ru, Rh, Pd, Ti, etc.[13,42,43] One remarkable catalytic application of these ligands is the Fe and Co catalyzed polymerization of ethene and 1-alkenes (Scheme 1.7). Other catalytic applications of these ligands are: benzylic oxidatons, hydrogenation of alkenes, and hydrosilylation.[44–47]

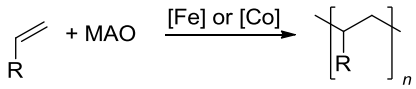

Scheme 1.7 *Iron or cobalt catalyzed polymerization of alkenes.*

Bipyridine (bipy) ligands are widely used family of ligand due to their several advantages such as their high stability against moisture and oxygen in the atmosphere and their interesting coordination chemistry. A wide scope of metals is known to form complexes with bipy, for instance Fe, Ru, Cu, Mn, Ir.[48,49] One of the most successful application of derivative of bipyridine in catalysis is related with its high stability towards oxidation. Due to that they were widely applied in water oxidation promoted by ruthenium complexes (Scheme 1.8).[50] Chiral derivatives of bipy were also applied in different reaction with good activities and selectivities, for example, alcoholysis and aminolysis of *meso*-epoxides, allylic oxidations, or cyclopronations. [48,49]

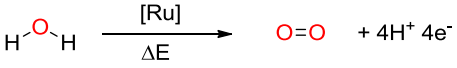

Scheme 1.8 *Example of catalytic reaction promoted by bipy complexes.*

One of the main advantages of diimines is the easy preparation. Like salen or iminopyridine ligands they are prepared by a simple Schiff base condensation which allows them to be a very modular family of ligands. Dimine Pd (II) and Ni (II) complexes are capable to promote the polymerization of ethylene and α-olefins (Scheme 1.9).[51–53] The usage of chiral amines or aldehyde lead the formation of chiral ligands which are applied in different catalytic reactions, such as, Zn-hydrosilylation, Cu-aziridination and Cu-cyclopropanation.[54–56]

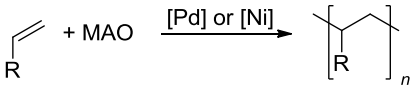

Scheme 1.9 *Palladium or nickel catalyzed polymerization of alkenes.*

1.3. Bite angle effects in catalysis and *trans*-coordinating ligands

Monodentate ligands can coordinate to transition metals to form several isomers. An example is *cis*- or *trans*-coordination in square-planar complexes. The use of bidentate ligands reduce the number of isomers formed because the backbone ensures the formation of more rigid chelates (Scheme 1.10).

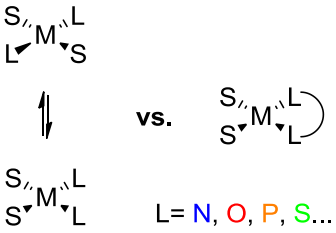

Scheme 1.10 *Square-planar rearrangements for mono- and bidentate ligands.*

The bite angle is defined as the angle between L-M-L in a coordination complex and depends on the backbone, the metal and the other molecules coordinated to the metal. The *natural* bite angle is defined as the calculated angle for coordination of a bidentate ligand to a “dummy” metal that has no geometric preferences (using Molecular Mechanics) and thus this is the preferred bite angle. The bite angle obtained from crystallographic structures can also be used as a yardstick. *Cis*-chelating ligands, with bite angles around 90º are the

most common in literature. Figure 1.7 includes some bidentate ligands with their bite angles.[1,57–61]

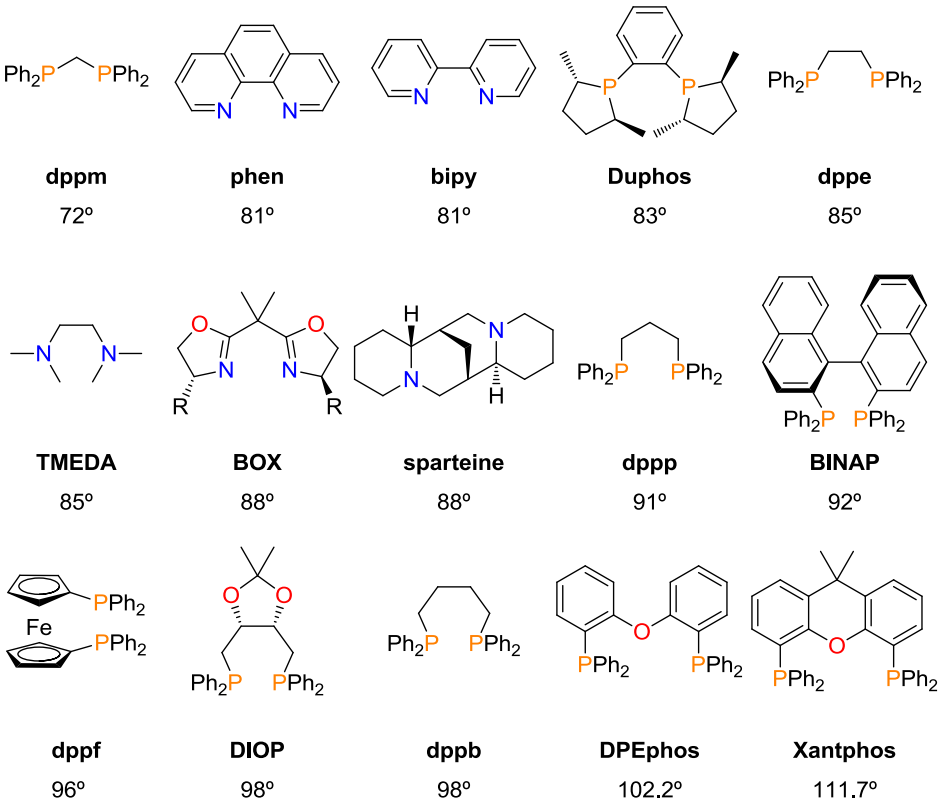

Figure 1.7 *Commercial available bidentate phosphines and their bite angles.*

It was observed that catalytic performance is related to the geometry of catalytic metallic species. The design and synthesis of new wide bite angle ligands showed a correlation between ligand bite angles, catalyst activities, and selectivity. For example, it was observed in hydroformylation and hydrocyanation reactions. These differences in catalytic reactivity can be rationalized by two different effects.[62]

The first one, the steric bite angle effect is related with the steric hindrance around the metal. It depends directly on the steric interaction between the ligand and other molecules in the metal's coordination sphere. It can alter the energies of the different species during the catalytic cycle thus changing the

catalytic activity or selectivity. An example is the use of wide bite angle ligands like Xantphos ((9,9-dimethyl-9H-xanthene-4,5-diyl)bis(diphenylphosphine)) in rhodium catalyzed hydroformylation of alkenes. The preferential coordination of the phosphines in the equatorial-equatorial position and the bulkiness of their substituents are crucial for the formation of linear aldehydes. [62–64]

The second one is the electronic bite angle effect. It consists in an orbital effect due to the modification of the metal hybridization and it can produce changes in the metal orbital energies and reactivity. For instance in the nickel catalyzed hydrocyanation, an increase of activity and stability are obtained with the use of wide bite angle ligands which destabilize square-planar geometries, and stabilize the active tetrahedral Ni(0) compounds. These facts are reflected in two cooperative effects: the formation of Ni(II) species more resistant to deactivation and an increase of the reductive elimination step.[62,65]

Both bite angle effects can never be fully separated and predictions remain uncertain, but it seems always worthwhile modifying bite angles in the search for improved chemo-, regio-, diastereo- and enantioselectivity. The Xantphos family is an example of wide bite angle ligands showing good conversion and enantiomeric excess (when a chiral derivative is used) in several reactions.[62,66]

Extending the theme, the design of proper *trans*-ligands is an interesting area. Whereas the synthesis of *cis*-ligands has shown an enormous development,[67–69] only a few examples of *trans*-ligands have been reported. The first example of *trans*-ligands was reported by Issleib and Hohlfeld in 1961, However, it was not until 1976 when Venanzi and co-workers published the first diphosphine designed to be a *trans*-ligand.[70,71] The main drawbacks in the design of *trans*-ligands are the flexibility of the designed backbones which allows other coordination modes (*cis*-monomers, dimers, oligomers or dinuclear species [72]) and *ortho*-metallation of the backbone leading to a polydentate P–X_n–P (X=C, N). In order to overcome these problems the ligands should contain relatively large and rigid backbones.[68,69,73,74] Several *trans*-coordinating diphosphines are depicted in Figure 1.8.

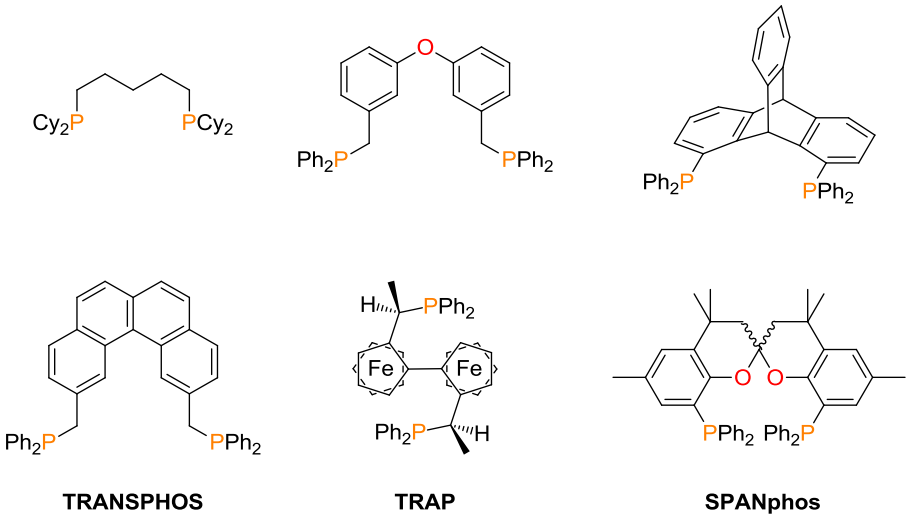

TRANSPHOS **TRAP** **SPANphos**

Figure 1.8 *Diphosphines with trans-coordination complexes known.*

As expected, *trans*-ligands can improve the performance of several catalytic processes and sometimes they even allow new transformations. For instance, TRAP ligands ((*S*,*S*)-2,2'-bis[(*R*)-1-(dialkylphosphino)ethyl]-1,1'-biferrocenes) were able to promote the ruthenium or rhodium catalytized hydrogenation of heterocyclic compounds reaching good yields and selectivities.[75–78] Likewise SPANphos (8,8'-Bis(diphen-ylphosphino)4,4,4',4',6,6'-hexamethylspiro-2,2'-bichroman) presents different behaviour to *cis*-ligands in palladium-catalyzed asymmetric fluorination of α-cyanoacetates.[79]

Despite the advantages of nitrogen ligands, few examples of *trans*-ligands were known. In 2001, Bunz and co-workers published a bipyridine derivative with *trans*-coordination mode.[80] The pyridine derivatives shown in Figure 1.9 led to the formation of various *trans*-complexes.[81,82]

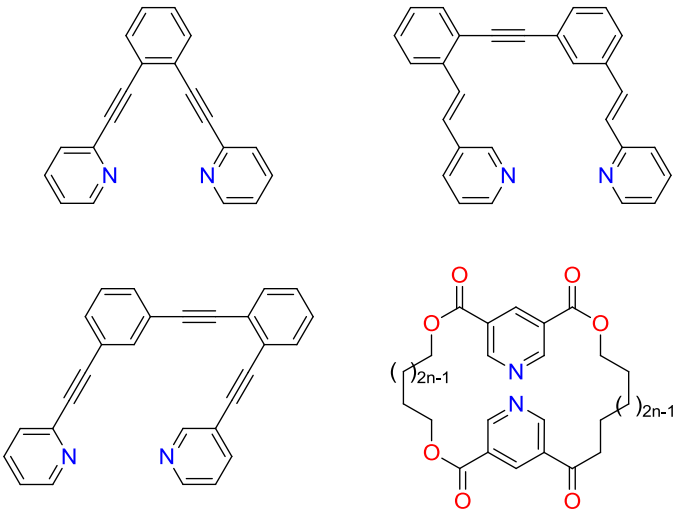

Figure 1.9 *Examples of N-donor trans-coordinating ligands.*

1.4. Dinuclear complexes in catalysis

Metalloproteins play an important role in bioorganic chemistry processes, for instance oxygen transport is carried out by haemoglobin, or redox reactions such as photosynthesis. Their active site contains various metals, usually first row transition metals. For several metalloproteins these active sites are composed of metal clusters which can contain metals such as iron, manganese, copper, etc.[83–86] These metals are stabilized by nitrogen, oxygen and sulphur containing groups in the protein. Clusters usually have as bridging groups, sulphides, carboxylic acids, hydroxygroups, etc. (Figure 1.10). The reactivity of the bimetallic metalloproteins differs from known organometallic compounds. A remarkable case is methane monoxygenase which is able to activate methane to undergo oxidation to methanol.[87]

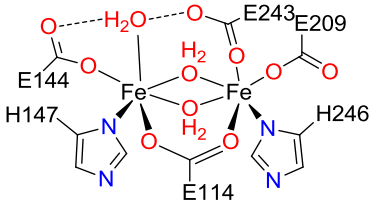

Methane monoxygensae active site

Figure 1.10 *Schematic representation of dinuclear metalloproteins cores.*

Bimetallic compounds are not only present in metalloproteins but they also exist in organometallic chemistry, for instance halide or methoxide bridged compounds are common starting materials in the synthesis of organometallic compounds.[88–91] Unfortunately, donor ligands such as phosphines, amines or pyridines may cause cleavage of the bridging species and we may lose the bimetallic nature. [89,92,93] Even double decomposition of halide bridging compounds and mononuclear complexes could formed stable bimetallic compounds (Scheme 1.11).[94]

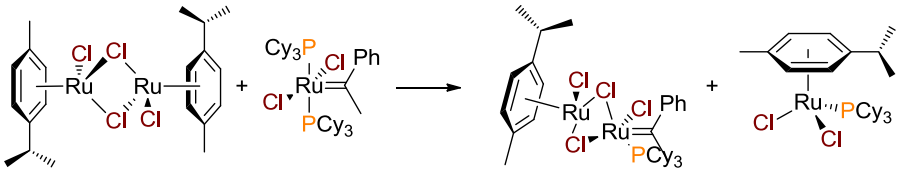

Scheme 1.11 *Synthesis of dinuclear complexes by double decomposition.*

Likewise in metalloproteins, bimetallic species often show properties different from those of homologous single metal compounds. As homogeneous catalysts, they can promote reactions that cannot be accomplished by monometallic complexes or they improve activities and selectivities. Several examples of bimetallic systems that show a different reactivity have been reported in literature, for instance catalysts for methanol carbonylation, copolymerization of epoxides and carbon dioxide, and olefin metathesis.[95–101] Thus, the different activity is attributed to a cooperative effect between the two metal centers which is possible when two metal centers are in close proximity (often less than 5 Å apart).[102–104] A few examples of bimetallic complexes which are active in catalysis are depicted in Figure 1.11.

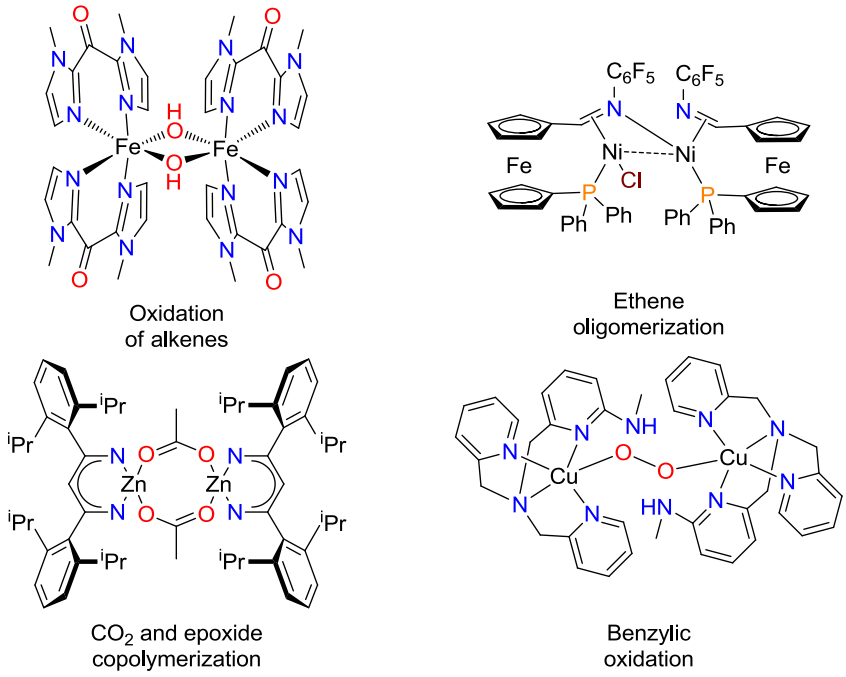

Figure 1.11 *Examples of dinuclear complexes active in catalysis.*

Several of these active species are formed *in situ* when the components are brought together in solution. In order to enforce the formation of bimetallic compounds rather than being dependent of their accidental formation, we can use ligand design to achieve this goal. This means that in the designed framework the metals should be close enough to show a cooperative effect.[99,104] Examples of designed bimetallic compounds are collected in Figure 1.12. Several strategies were used in the design of ligands which promote the formation of bimetallic compounds. The first one is the synthesis of two multidentante ligands separated by a spacer (structures **I** and **III** in Figure 1.12 or Figure 1.14). Secondly, the proximity of the metals can be further promoted if the spacer contains a donor atom in the middle capable of coordinating to both metals, such as an amido nitrogen atom, an alkoxide or sulfide (structure **I** in Figure 1.12).[105] Also the spacer can promote the formation of two differentiated catalytic centres. (structure **III** in Figure 1.12)[106] The next one is the use of pincer ligands, in which the central atom has two pairs of electrons available for coordination to two metals. (structure **II** in Figure 1.12).[107]

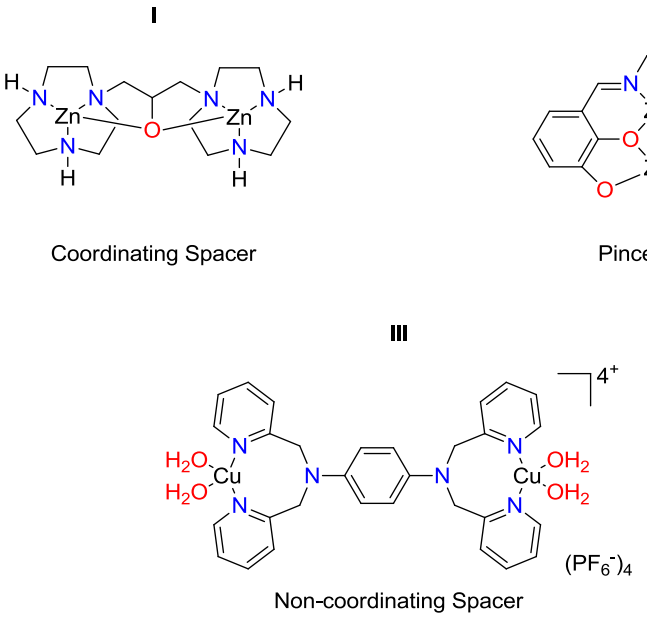

Figure 1.12 *Designed bimetallic complexes*.

The designed dinuclear complexes were applied in various homogeneous catalytic reactions in which a cooperative effect was observed.[108] For instance, several copper dinuclear systems were applied in oxidative phenol coupling or azide–alkyne cycloadditions with high activities and selectivities for both reactions.[109–111] Zinc dinuclear complexes were also applied in various reactions with excellent results, for example desymmetrization of *meso*-diols, asymmetric aldol reaction, or catalytic synthesis of cyclic carbonates. [107,112,113] Examples of two dinuclear catalysts and the catalytic reaction are shown in Scheme 1.12.

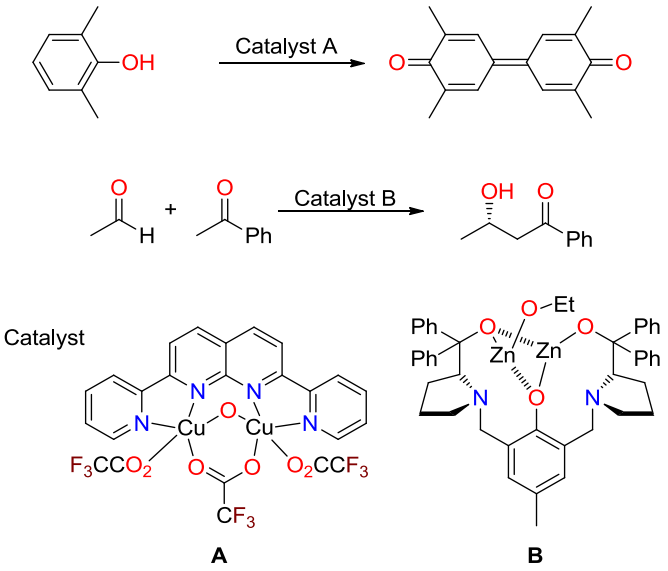

Scheme 1.12 *Dinuclear complexes and their application in catalysis.*

Our group synthesized the phosphine derivatives of 4,4,4',4',6,6'-hexamethylspiro-2,2'-bichroman (Span), 2,9-dimethyl-5a,10b-dihydrobenzofuro-[2,3-b]benzofuran (BFBF) and 2,10-dimethyl-12H-6,12-methanodibenzo[d,g]-[1,3]dioxocine which were able to form bimetallic complexes. Methanol carbonylation was carried out with these complexes and they were found to be the most active catalysts for this reaction (Scheme 1.13).[95,99]

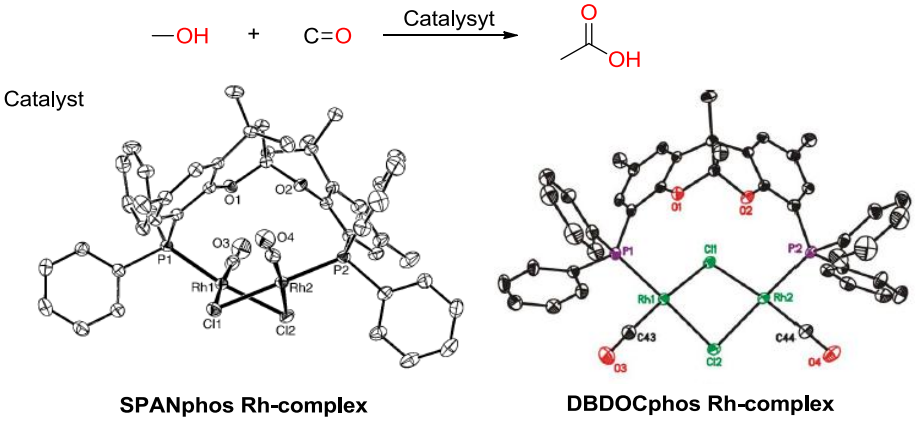

Scheme 1.13 *SPANphos and DBDOCphos dinuclear complexes applied in methanol carbonylation.*

1.5. Objectives

With these precedents in mind, this thesis focus on the development of novel N-donor ligands with non-typical coordination mode and their application in homogeneous catalysis with the usage of green metals and/or processes. The main goals of the study are:

- To improve or design new synthetic routes for the formation of the three backbones shown in Figure 1.13. These three backbones will be used to develop three closely related families of polydentate ligands.

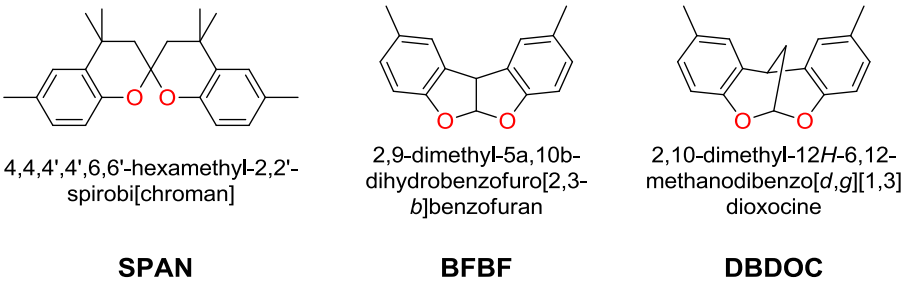

Figure 1.13 *Different backbone to be synthesized.*

- To introduce an amino group *ortho* to the oxygen atom in all backbones, to synthesize and characterize a library of ligands.

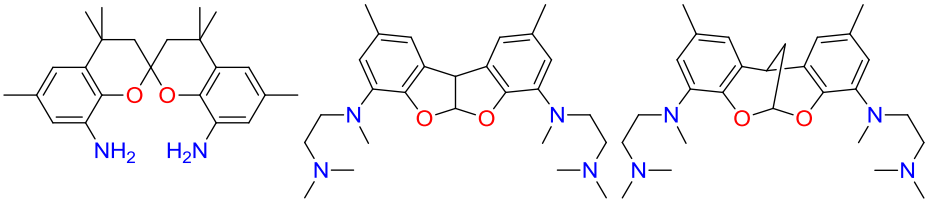

Figure 1.14 *Different ligand families to be synthesized.*

- To synthesize and characterize different metal complexes (Rh, Pd, Cu and Fe) for these three ligand types. To study the non-classical coordination behaviour for each one.

- To study the *trans* coordination of SPANamine derivatives and formation of dinuclear compounds for BFBF and DBDOC derivatives.

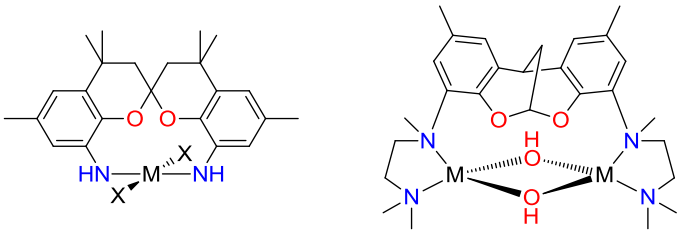

Figure 1.15 *Desired coordination modes for different families.*

- To explore and study the activity of the metal complexes synthesized in various catalytic reactions. The catalytic reactions can be classified in two main groups depending on the denticity of ligands:

    - To study bidentate ligands in:
        - Rh-catalyzed asymmetric hydrogenation of alkenes.
        - Rh-catalyzed asymmetric hydrosilylation of ketones.
        - Cu-catalyzed asymmetric oxidation of *meso*-diols.

    - To study tetradentate ligands in:
        - Zn-catalyzed cyclic carbonate formation.
        - Fe-catalyzed cyclic carbonate formation.
        - Fe-catalyzed benzylic C–H oxidation.

1.6. References

1. P. W. N. M. Leeuwen, *Homogeneous Catalysis: Understanding the Art*, Kluwer, Dordrecht, 2004.
2. L. A. Oro and E. Sola, *Fundamentos y aplicaciones de la catálisis homogénea*, Prensas Universitarias de Zaragoza, Zaragoza, 2000.
3. B. Cornils and W. A. Herrman, *Applied Homogeneous Catalysis with Organometallic Compounds*, Wiley-VCH, Wienheim, 1996.
4. R. B. King, R. H. Crabtree, C. M. Lukehart, D. A. Atwood, and R. A. Scott, Eds., *Encyclopedia of Inorganic Chemistry*, John Wiley & Sons, Ltd, Chichester, UK, 2006.
5. S. Bhaduri and D. Mukesh, *Homogeneous Catalysis: Mechanisms and Industrial Applications*, Wiley-Interscience, New York, 2000, vol. 8.
6. I. Ojima, *Catalytic Asymmetric Synthesis, 3rd Edition*, Wiley, New Jersey.
7. R. Noyori, *Asymmetric Catalysis In Organic Synthesis*, Wiley, New York, 1994.
8. J. A. Osborn, F. H. Jardine, J. F. Young, and G. Wilkinson, *J. Chem. Soc. (A)*, 1966, **0**, 1711–32.
9. G. F. Endres and A. S. Hay, *J. Org. Chem.*, 1963, **28**, 1300–5.
10. R. Gillard and G. Wilkinson, *J. Chem. Soc.Chem. Soc.*, 1963, 3594–9.
11. B. Martin and G. M. Waind, *J. Chem. Soc.*, 1966, 4284–8.
12. R. T. Halle, A. Breheret, E. Schulz, C. Pinel, and M. Lemaire, *Tetrahedron: Asymmetry*, 1997, **8**, 2101–8.
13. C. Caputo and N. D. Jones, *Dalton Trans.*, 2007, 4627–40.
14. A. I. Vogel, A. R. Tatchell, B. S. Furnis, A. J. Hannaford, and P. W. G. Smith, *Practical Organic Chemistry (5th Edition)*, Prentice Hall, London, 1996.
15. J. Royer and H. P. Husson, 2009, 425.
16. N. Ono, *The Nitro Group in Organic Synthesis*, John Wiley & Sons, 2003.
17. P. C. J. Kamer and P. W. N. M. van Leeuwen, *Phosphorus(III)Ligands in Homogeneous Catalysis: Design and Synthesis*, Wiley, 2012.
18. B. D. Vineyard, W. S. Knowles, M. J. Sabacky, G. L. Bachman, and D. J. Weinkauff, *J. Am. Chem. Soc.*, 1977, **99**, 5946–52.
19. C. A. Tolman, *Chem. Rev.*, 1977, **77**, 313–48.

20. A. L. Seligson and W. C. Trogler, *J. Am. Chem. Soc.*, 1991, **113**, 2520–7.
21. A. Togni and L. Venanzi, *Angew. Chem. Int. Ed.*, 1994, **33**, 497–526.
22. T. Leyssens, D. Peeters, A. Orpen, and J. Harvey, *Organometallics*, 2007, **26**, 2637–45.
23. H. Adams, J. C. Anderson, R. Cubbon, D. S. James, and J. P. Mathias, *J. Org. Chem.*, 1999, **64**, 8256–62.
24. E. N. Jacobsen, W. Zhang, and A. Muci, *J. Am. Chem. Soc.*, 1991, **113**, 7063–4.
25. N. Schneider, M. Kruck, S. Bellemin-Laponnaz, H. Wadepohl, and L. H. Gade, *Eur. J. Inorg. Chem.*, 2009, **2009**, 493–500.
26. E. N. Jacobsen, A. Pfaltz, and H. Yamamoto, *Comprehensive Asymmetric Catalysis*, Springer, Heidelberg, 1999.
27. F. Fache, E. Schulz, M. L. Tommasino, and M. Lemaire, *Chem. Rev.*, 2000, **100**, 2159–232.
28. P. Pfeiffer, E. Breith, E. Lübbe, and T. Tsumaki, *Liebigs Ann. Chem.*, 1933, **503**, 84–130.
29. C. Baleizão and H. Garcia, *Chem. Rev.*, 2006, **106**, 3987–4043.
30. M. North, R. Pasquale, and C. Young, *Green Chem.*, 2010, **12**, 1514–39.
31. M. Taherimehr, A. Decortes, S. M. Al-Amsyar, W. Lueangchaichaweng, C. J. Whiteoak, E. C. Escudero-Adán, A. W. Kleij, and P. P. Pescarmona, *Catal. Sci. & Tech.*, 2012, **2**, 2231–7.
32. A. Decortes and A. W. Kleij, *ChemCatChem.*, 2011, **3**, 831–4.
33. D. J. Darensbourg and S. J. Wilson, *Green Chem.*, 2012, **14**, 2665–71.
34. A. Company, L. Gómez, X. Fontrodona, X. Ribas, and M. Costas, *Chem. Eur. J.*, 2008, **14**, 5727–31.
35. K. Chen, M. Costas, J. Kim, A. K. Tipton, and L. Que, *J. Am. Chem. Soc.*, 2002, **124**, 3026–35.
36. P. D. Oldenburg, Y. Feng, I. Pryjomska-Ray, D. Ness, and L. Que, *J. Am. Chem. Soc.*, 2010, **132**, 17713–23.
37. T. Okuno, S. Ito, S. Ohba, and Y. Nishida, *Dalton Trans.*, 1997, 3547–51.
38. M. S. Chen and M. C. White, *Science*, 2007, **318**, 783–7.
39. M. S. Chen and M. C. White, *Science*, 2010, **327**, 566–71.
40. M. C. White, *Science*, 2012, **335**, 807–9.
41. G. Desimoni, G. Faita, and K. A. Jørgensen, *Chem. Rev.*, 2006, **106**, 3561–651.

42. A. Abu-Surrah and K. Lappalainen, *J. Organomet. Chem.*, 2002, **648**, 55–61.
43. S. S. Karpiniec, D. S. McGuinness, G. J. P. Britovsek, and J. Patel, *Organometallics*, 2012, **31**, 3439–42.
44. C. HILLAIRET and G. MICHAUD, *WO Patent WO/2007/122,139*, 2007.
45. A. M. Tondreau, E. Lobkovsky, and P. J. Chirik, *Org. Lett.*, 2008, **10**, 2789–92.
46. P. Shejwalkar, N. P. Rath, and E. B. Bauer, *Dalton Trans.*, 2011, **40**, 7617–31.
47. K. Junge, K. Schröder, and M. Beller, *Chem. Comm.*, 2011, **47**, 4849–59.
48. B. Plancq and T. Ollevier, *Aust. J. Chem.*, 2012, 1564–72.
49. H. Kwong, H. Yeung, C. Yeung, W. Lee, C. Lee, and W. Wong, *Coord. Chem. Rev.*, 2007, **251**, 2188–222.
50. J. K. Hurst, J. L. Cape, A. E. Clark, S. Das, and C. Qin, *Inorg. Chem.*, 2008, **47**, 1753–64.
51. S. D. Ittel, L. K. Johnson, and M. Brookhart, *Chem. Rev.*, 2000, **100**, 1169–204.
52. L. K. Johnson, C. M. Killian, M. Brookhart, C. Hill, and N. Carolina, *J. Am. Chem. Soc.*, 1995, 6414–5.
53. G. Britovsek, *Angew. Chem. Int. Ed.*, 1999, **38**, 428–47.
54. X. Wang and K. Ding, *Chem. Eur. J.*, 2006, **12**, 4568–75.
55. H. Mimoun and J. de Saint Laumer, *J. Am. Chem. Soc.*, 1999, 6158–66.
56. M. Hechavarría Fonseca, E. Eibler, M. Zabel, and B. König, *Inorg. Chim. Acta*, 2003, **352**, 136–42.
57. R. C. Boyle, J. T. Mague, and M. J. Fink, *Acta Cryst.*, 2004, **60**, m40–1.
58. K. Ha, *Acta Cryst.*, 2010, **66**, m38.
59. S. K. Mandal and M. S. Sigman, *J. Org. Chem.*, 2003, **68**, 7535–7.
60. M. Zehnder, M. Neuburger, P. von Matt, and A. Pfaltz, *Acta Cryst.*, 1995, **51**, 1109–12.
61. R. A. Adrian, S. Zhu, K. K. Klausmeyer, and J. A. Walmsley, *Inorg. Chem. Comm.*, 2007, **10**, 1527–30.
62. Z. Freixa and P. W. N. M. van Leeuwen, *Dalton Trans.*, 2003, **34**, 1890–901.
63. M. Kranenburg, Y. van der Burgt, P. C. J. Kamer, and P. W. N. M. van Leeuwen, *Organometallics*, 1995, **14**, 3081–9.
64. J. J. Carbó, F. Maseras, C. Bo, and P. W. N. M. van Leeuwen, *J. Am. Chem. Soc.*, 2001, **123**, 7630–7.

65. M. Kranenburg, P. C. J. Kamer, D. Vogt, W. Keim, and P. W. N. M. Leeuwen, *J. Chem. Soc., Chem. Comm.*, 1995, 2177–8.
66. M.-N. Birkholz, Z. Freixa, and P. W. N. M. van Leeuwen, *Chem. Soc. Rev.*, 2009, **38**, 1099–118.
67. X. Sala, E. J. García Suárez, Z. Freixa, J. Benet-Buchholz, and P. W. N. M. van Leeuwen, *Eur. J. Org. Chem.*, 2008, **2008**, 6197–205.
68. Z. Freixa and P. W. N. M. van Leeuwen, *Coord. Chem. Rev.*, 2008, **252**, 1755–86.
69. C. A. Bessel, P. Aggarwal, A. C. Marschilok, and K. J. Takeuchi, *Chem. Rev.*, 2001, **101**, 1031–66.
70. K. Issleib and G. Hohlfeld, *Z. Anorg. Allg. Chem.*, 1961, **312**, 169–79.
71. N. J. DeStefano, D. K. Johnson, R. M. Lane, and L. M. Venanzi, *Helvetica Chimica Acta*, 1976, **59**, 2674–82.
72. W. E. Hill, D. M. A. Minahan, J. G. Taylor, and C. A. McAuliffe, *J. Am. Chem. Soc.*, 1982, **104**, 6001–5.
73. C. Azerraf, O. Grossman, and D. Gelman, *J. Org. Chem.*, 2007, **692**, 761–7.
74. C. Jiménez-Rodríguez, F. X. Roca, C. Bo, J. Benet-Buchholz, E. C. Escudero-Adán, Z. Freixa, and P. W. N. M. van Leeuwen, *Dalton Trans.*, 2006, 268–78.
75. R. Kuwano, N. Kameyama, and R. Ikeda, *J. Am. Chem. Soc.*, 2011, **133**, 7312–5.
76. R. Kuwano, M. Kashiwabara, K. Sato, T. Ito, K. Kaneda, and Y. Ito, *Tetrahedron: Asymmetry*, 2006, **17**, 521–35.
77. R. Kuwano and M. Kashiwabara, *Org. Lett.*, 2006, **8**, 2653–5.
78. R. Kuwano, K. Sato, T. Kurokawa, D. Karube, and Y. Ito, *J. Am. Chem. Soc.*, 2000, **122**, 7614–5.
79. O. Jacquet, N. D. Clément, C. Blanco, M. M. Belmonte, J. Benet-Buchholz, and P. W. N. M. van Leeuwen, *Eur. J. Org. Chem.*, 2012, **2012**, 4844–52.
80. J. E. Fiscus, S. Shotwell, R. C. Layland, M. D. Smith, H.-C. Loye, U. H. F. Bunz, and H.-C. zur Loye, *Chem. Comm.*, 2001, 2674–5.
81. P. D. Zeits, G. Pietro Rachiero, F. Hampel, J. H. Reibenspies, and J. A. Gladysz, *Organometallics*, 2012, **31**, 2854–77.
82. D. C. Hamm, L. A. Braun, A. N. Burazin, A. M. Gauthier, K. O. Ness, C. E. Biebel, J. S. Sauer, R. Tanke, B. C. Noll, E. Bosch, and N. P. Bowling, *Dalton Trans.*, 2013, **42**, 948–58.
83. E. a Lewis and W. B. Tolman, *Chem. Rev.*, 2004, **104**, 1047–76.

84. D. C. Johnson, D. R. Dean, A. D. Smith, and M. K. Johnson, *Ann. Rev. Biochem.*, 2005, **74**, 247–81.
85. L. R. Scolnick, Z. F. Kanyo, R. C. Cavalli, D. E. Ash, and D. W. Christianson, *Biochem.*, 1997, **36**, 10558–65.
86. R. G. Wilkins, *Chem. Soc. Rev.*, 1992, **21**, 171–8.
87. S. Friedle, E. Reisner, and S. J. Lippard, *Chem. Soc. Rev.*, 2010, **39**, 2768–79.
88. J. A. Osborn and R. R. Schrock, *J. Am. Chem. Soc.*, 1971, **93**, 2397–407.
89. T. G. Schenck, J. M. Downes, C. R. C. Milne, P. B. Mackenzie, T. G. Boucher, J. Whelan, and B. Bosnich, *Inorg. Chem.*, 1985, **24**, 2334–7.
90. J. Chatt and L. Venanzi, *J. Chem. Soc.*, 1957, 4735–41.
91. M. Green, T. Kuc, and H. Taylor, *J. Chem. Soc.*, 1971, 2334–7.
92. L. Nindakova, N. Chipanina, M. Turchaninov, and B. Shainyan, *Russ. Chem. Bull.*, 2005, **54**, 2343–7.
93. M. S. Viciu, R. F. Germaneau, O. Navarro-Fernandez, E. D. Stevens, and S. P. Nolan, *Organometallics*, 2002, **21**, 5470–2.
94. K. Severin, *Chem. Eur. J.*, 2002, **8**, 1514–8.
95. Z. Freixa, P. C. J. Kamer, M. Lutz, A. L. Spek, P. W. N. M. van Leeuwen, and P. W. N. M. Leeuwen, *Angew. Chem. Int. Ed.*, 2005, **44**, 4385–8.
96. D. R. Moore, M. Cheng, E. B. Lobkovsky, and G. W. Coates, *J. Am. Chem. Soc.*, 2003, **125**, 11911–24.
97. E. Dias and R. Grubbs, *Organometallics*, 1998, **7333**, 2758–67.
98. I. Guzei, K. Li, G. Bikzhanova, J. Darkwa, and S. Mapolie, *Dalton Trans.*, 2003, 715–722.
99. J. M. López-Valbuena, E. C. Escudero-Adán, J. Benet-Buchholz, Z. Freixa, P. W. N. M. van Leeuwen, and P. W. N. M. Leeuwen, *Dalton Trans.*, 2010, **39**, 8560–74.
100. D. Maiti, J. S. Woertink, A. A. N. Sarjeant, E. I. Solomon, and K. D. Karlin, *Inorg. Chem.*, 2008, **47**, 3787–3800.
101. Z. Weng, S. Teo, Z. Liu, and T. S. A. Hor, *Organometallics*, 2007, **26**, 2950–2.
102. O. Iranzo, T. Elmer, J. P. Richard, and J. R. Morrow, *Inorg. Chem.*, 2003, **42**, 7737–46.
103. D. McCollum and B. Bosnich, *Inorg. Chim. Acta*, 1998, **270**, 13–9.
104. B. Bosnich, *Inorg. Chem.*, 1999, **38**, 2554–62.
105. A. L. Gavrilova and B. Bosnich, *Chem. Rev.*, 2004, **104**, 349–83.

106. S. Turba, O. Walter, S. Schindler, L. P. Nielsen, A. Hazell, C. J McKenzie, F. Lloret, J. Cano, and M. Julve, *Inorg. Chem.*, 2008, **47**, 9612–23.
107. R. M. Haak, A. Decortes, E. C. Escudero-Adán, M. Martínez Belmonte, E. Martin, J. Benet-Buchholz, and A. W. Kleij, *Inorg. Chem.*, 2011, **50**, 7934–6.
108. J. Park and S. Hong, *Chem. Soc. Rev.*, 2012, **41**, 6931–43.
109. B.-S. Liao, Y.-H. Liu, S.-M. Peng, and S.-T. Liu, *Dalton Trans.*, 2012, **41**, 1158–64.
110. J. Gao, J. H. Reibenspies, and A. E. Martell, *Angew. Chem. Int. Ed.*, 2003, **42**, 6008–12.
111. R. Berg, J. Straub, E. Schreiner, S. Mader, F. Rominger, and B. F. Straub, *Adv. Syn. & Cat.*, 2012, **354**, 3445–50.
112. B. Trost and H. Ito, *J. Am. Chem. Soc.*, 2001, **122**, 12003–4.
113. B. M. Trost and T. Mino, *J. Am. Chem. Soc.*, 2003, **125**, 2410–1.

Chapter 2
Synthesis of Novel N-Donor Ligands: Spirobichroman, Dehydrobenzofurobenzofuran and Methanodibenzodioxocine Aminoderivatives.

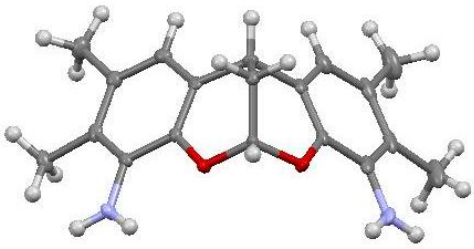

This chapter focus on the synthesis of novel N-donor ligands, describing optimized synthetic routes. The backbones can be synthesized in the follow steps. Firstly *p*-cresol is condensated with different carbonyl derivatives (Scheme 2.1). Next transformation is the halogenation of the backbones. Then primary aminoderivatives are synthesized *via* cross-coupling reaction and finally tetradentate ligands can be synthesized by Schiff condensation or reductive amination.

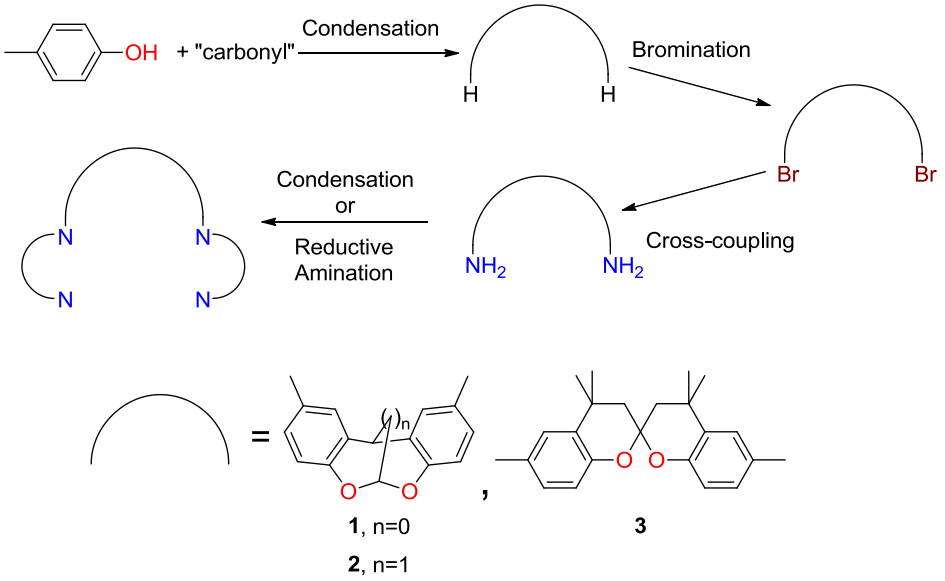

Scheme 2.1 *Designed synthetic route to the formation of novel tetradentate ligands.*

The following introduction is a short overview of the state of the art in these different transformations. The first two synthetic steps – condensation and bromination – are summarized in point 2.1. The cross-coupling reaction is described for two different metals Pd and Cu in section 2.2.1 and 2.2.2, respectively. And the final transformation is explained in point 2.3.

2.1. Electrophilic Aromatic Substitutions

Electrophilic aromatic substitution is an important synthetic transformation to functionalize aromatic compounds. These transformations are well documented in the literature and the most studied are: nitration, sulfonation, halogenation

and Friedel-Crafts alkylation and acylation.[1] In this chapter, reactions related to the synthesis of dehydrobenzofurobenzofuran and methanodibenzodioxocine backbones will be discussed.

2,9-Dimethyl-5*a*,10*b*-dihydrobenzofuro[2,3-*b*]benzofuran (BFBF) and 2,10-dimethyl-12*H*-6,12-methanodibenzo[*d*,*g*][1,3]dioxocine (DBDOC) were reported by Bhima Rao in 1966 and Rahmatpour in 1999 respectively.[2,3] The formation of BFBF and DBDOC backbones is an acid catalyzed reaction. The reaction mechanism proceeds through condensation of an aldehyde or acetal with *p*-cresol followed by intramolecular acetal formation.[3,4] The reaction mechanism for the formation of BFBF backbone is shown in Scheme 2.2.

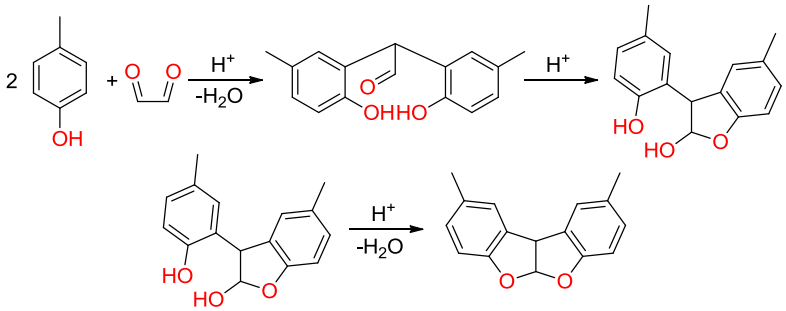

Scheme 2.2 *Reaction mechanism for the formation of BFBF.*

In the first step of the reaction, the formation of the two C–C bonds (activated phenol with an aldehyde or acetone), can be either acid or base catalyzed.[5,6] The synthesis of BFBF and DBDOC derivatives is generally carried out with the use of strong Brönsted acids such as sulphuric, methanesulfonic and trifluoroacetic acid,[2,3] although the use of Brönsted bases or Lewis acids has also been reported for the synthesis of these backbones and their analogues, e.g. xanthenes.[7–10]

Electrophilic aromatic halogenation is a common reaction involving a cationic halide X^+. The first examples of aromatic brominations were reported with molecular bromine and iron.[1] Later on, less toxic reagents and new bromine sources were introduced in the electrophilic aromatic bromination reactions. Reagents used are for instance, N-bromosuccinimide (NBS), organic tribromide or the oxidative brominations in which a bromide is converted to a bromonium ion *via* an umpolung strategy using an oxidant (Scheme 2.3).[11–15]

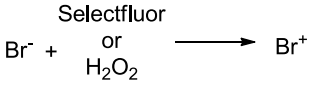

Scheme 2.3 *Examples of auxiliary reagents in oxidative brominations.*

2.2. Aromatic C–N bond Formation

The conventional strategy for the synthesis of aromatic amines involves a nitration, reduction, and alkylation sequence. However, this synthesis is not environmentally friendly and has several drawbacks such as long reaction times, use of hazardous acids and toxic reagents. Moreover the nitration can be dangerous because of possible formation of explosive products due to excess of nitration. As regards the present target molecules, the acetal backbones decompose in the nitration reaction medium or work-up medium. Thus, alternative strategies for the formation of aromatic C–N bond were developed, such as transition metal catalyzed cross-coupling reactions between aryl halides or arene sulfonates and amines (Scheme 2.4).[16] The cross-coupling reaction avoids most of the disadvantages of the traditional aromatic amine synthesis.

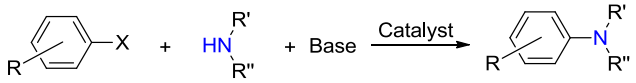

Scheme 2.4 *C–N bond formation via cross-coupling reaction.*

2.2.1. The Buchwald-Hartwig Coupling Reaction

The formation of an aromatic C–N bond catalyzed by palladium complexes is known as Buchwald-Hartwig amination.[17–20] This reaction was developed simultaneously by the Buchwald and the Hartwig group in the 90s and has been extensively studied.[17–20] Nowadays, numerous amines, having functional groups, can be prepared with high selectivities and high yields.[21] A wide range of reaction conditions were reported for this reaction (polar/nonpolar solvents, weak/strong and organic/inorganic bases, reaction temperatures), depending on the substrate properties.[22]

Aryl bromides are the most reactive substrates for this reaction followed by chloroarenes.[23] Aryl iodides are usually more reactive in other cross-coupling reactions, but they exhibit less reactivity for C–N bond formation.[19,24] Arenesulfonic esters, such as triflate or mesylate are also suitable substrates for the Buchwald-Hartwig coupling reaction (Figure 2.1).[22,25] As expected, substituents on the aromatic moiety can affect the reactivity of the halogenated arene in two different manners: Sterically and electronically. Thus, for steric reason *ortho*-substituted compounds are more challenging than *meta* and *para*-analogues and electron withdrawing groups (EWG) often give higher yields.[26]

Nowadays, a broad range of primary and secondary amines can be used as coupling partners in this cross coupling reaction. The performance of the catalytic system depends on the nature of the amine for example, to couple primary amines, hindered bisphosphine ligands are the most active and selective ligands, but for secondary amines the best catalytic systems consists of bulky monodentate ligands.[27–31] Even ammonia and ammonia surrogates or lithium amide can be coupled to aryl halides using electron-donating and sterically hindered monophosphines and bisphosphines. Benzophenone imine and lithium bis(trimethylsilyl)amide (LHMDS) are the most common ammonia substitutes (Figure 2.1).[22,25]

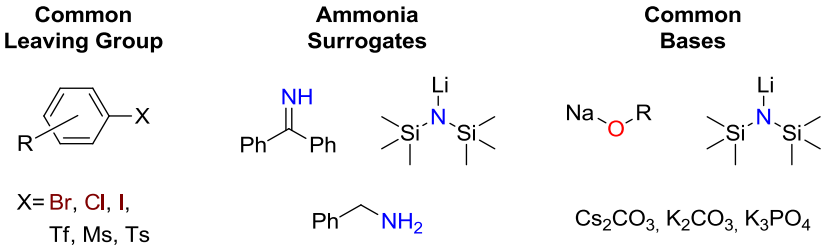

Figure 2.1 *Common reagents used in Buchwald-Hartwig amination.*

It is important to note that the base plays a critical role in the reaction. Many types of bases were applied in this reaction, from strong to weak bases which can be either organic or inorganic. Sodium and potassium alkoxides were widely used in aromatic amination; their main problem is the functional group tolerance. LMHDS is an interesting base as it is compatible with protic functional groups such as phenols. Inorganic salts such as carbonates or

phosphates show the highest tolerance toward functionalities, but the main problem of these bases is their low solubility in the reaction media.[22,24,29,30,32]

Obviously, the most important factor in catalyst performance is the ligand. Palladium modified with tri-o-tolylphosphine was the first catalyst reported that promotes the coupling reaction between aryl bromides and secondary amines.[19,20] With the usage of bidentate ligands such as BINAP, dppf and Xantphos the scope of the reaction was expanded.[33] At this stage, aryl chlorides were still a challenging substrate, but nowadays these can be activated thanks to the development of bulky strong σ-donor ligands such as N-heterocyclic carbenes or dialkylbiaryl phosphines.[29,34] Figure 2.2 depicts several ligands applied in the Buchwald-Hartwig amination.

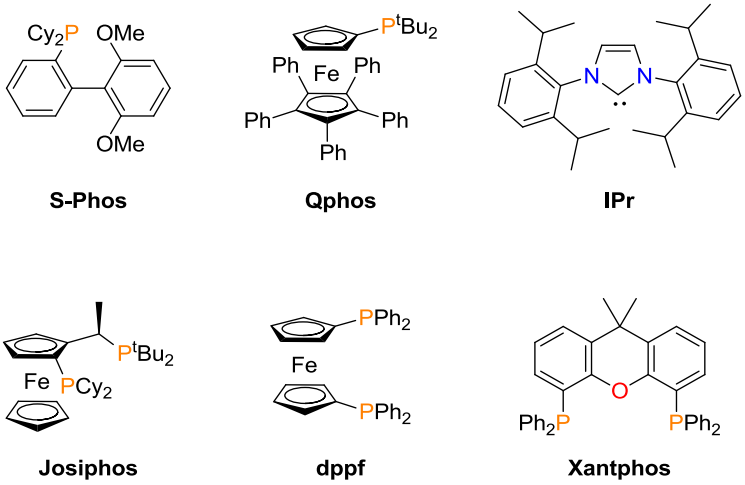

Figure 2.2 *Successful ligands applied in the Buchwald-Hartwig amination.*

The mechanism of this catalytic transformation starts with the oxidative addition of the aryl halide to a Pd(0) to form a Pd(II) species. The second step is the coordination of the amine to Pd(II) formed previously and subsequent deprotonation led to the arylpalladium-amido complex which can undergo reductive elimination to generate the desired arylamine product which is highlighted with a green frame in Scheme 2.5. As a competitive reaction β-hydrogen elimination may take place, which results in the formation of an imine and reduced aryl ring (both products are placed in a red frame in Scheme

2.5).[26,35–37] The mechanism of the Buchwald-Hartwig amination is shown in Scheme 2.5.

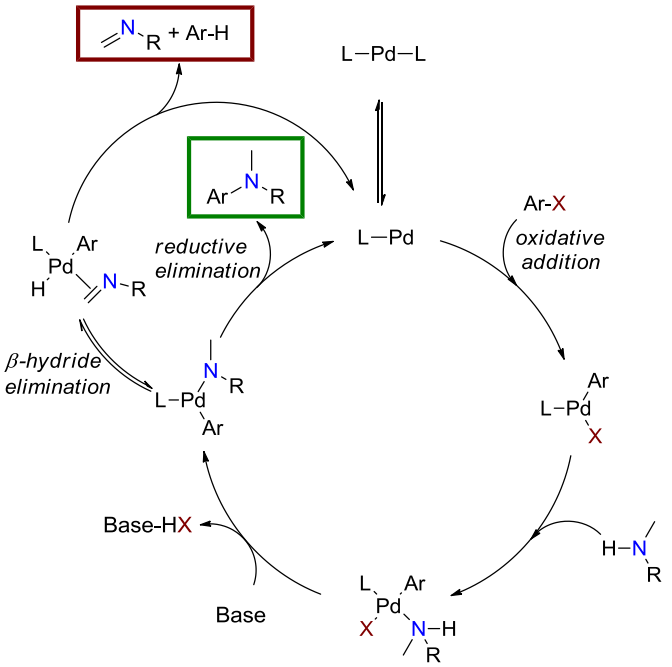

Scheme 2.5 *The mechanism of the Buchwald-Hartwig amination. The green marked compound is the target one and red product is formed by reduction of the aryl halide.*

Thus, the selectivity of the process lies in the competition between reductive elimination and β-hydrogen elimination processes. The palladium species involved are either 14 electron, three-coordinate palladium compounds, in the case of monodentate ligands or tetra-coordinated species with 16 electrons when bidentate ligands are used. [26,35,36] Several ligand properties have been varied in attempts to avoid *β*-elimination. The first one is the denticity of the ligands. The use of bidentate ligands forming tetracoordinated palladium species slows *β*-hydrogen elimination, as this reaction requires a free coordination site and thus reductive elimination is relatively favoured.[38] For bidentate ligands, the bite angle is important for the reductive elimination step, since large bite angle ligands such as Xantphos or DPEphos enhance this reaction step.[33] The second factor that decreases undesired β-hydrogen elimination is to increase the steric hindrance on Pd as this hinders the

reductive elimination. This also holds for monodentate ligands, although the mechanistic details are less clear for monodentate ligands than for bidentates.[35]

2.2.2. The Ullmann C–N Coupling Reaction

In 1901 Ullmann and Bielecki reported the coupling aryl halides with stoichiometric amounts of copper, which was later named the Ullmann reaction.[39] Coupling of nucleophiles such as amines and thiols with aryl halides was also achieved with the use of stoichiometric quantities of copper. Three years later Goldberg reported the first catalytic example of an aniline and bromobenzene with an *ortho*-carboxylic acid as directing group (Scheme 2.6).[40] Copper-assisted Ullmann coupling reactions are valuable transformations in organic synthesis. The Ullmann coupling reaction was extensively applied in the synthesis of pharmaceutical, agrochemical and polymeric compounds.[41,42]

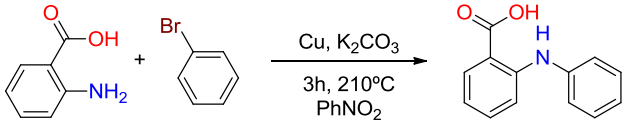

Scheme 2.6 *First example of catalytic C-N bond formation promoted by copper.*

However, this transformation has several drawbacks: copper is used in stoichiometric amounts and, substrate scope is limited, due to high temperatures required for this transformation. The solvent that can be used is restricted by the high temperature required, thus the condensation is usually conducted in high-boiling polar solvents such as N-methyl-pyrrolidone, nitrobenzene, or dimethylformamide.[43] The use of ligands for this reaction was reported for the first time in 1999 and allowed the use copper in catalytic amounts and milder reaction conditions.[44–46] As copper is a first row metal, coordination with hard donors such as oxygen or nitrogen is preferred over phosphorus containing ligands. Thus diamines, diols, diketones, aminoacid derivatives, among others are used as ligands in the Ullmann coupling (Figure 2.3).[41,42]

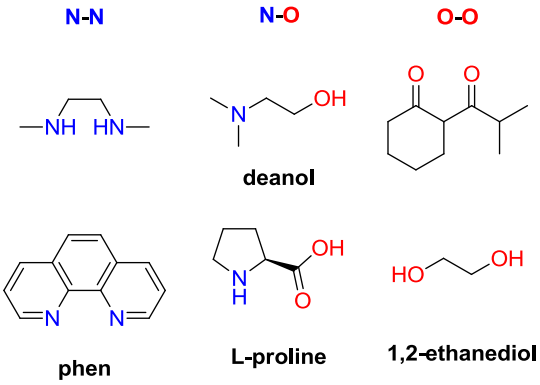

Figure 2.3 *Ligands applied in the Ullmann reaction.*

The development and application of the Ullmann coupling reaction increase the scope and limitation of the reaction. The reactivity of aryl halide is different from the Buchwald-Hartwig amination, iodides being the most active substrates, but chlorides show a low reactivity and few examples are reported.[47–52] The steric hindrance on the aryl halide plays an important role in the reactivity of the reagents. The reaction with unfunctionalized *ortho*-substituted aromatics are the most challenging substrates.[41] However, coordinating *ortho*-groups activate the substrates, even aryl chloride derivatives.[40,41]

Historically this reaction was applied in the synthesis of aryl amines, but the use of ligands in the catalytic system expanded the scope of nitrogen nucleophiles. Thus, primary and secondary aryl amines were coupled with aryl halides under mild conditions with catalytic amounts of copper salts and ligands such as phenanthroline and aminoacids.[48,53] Alkyl amines were not reactive with copper ligand-free systems. However, with ligands such as diketone or aminoacids, diols or others, the coupling of primary amines and cyclic secondary amines was described under mild conditions.[51,54,55,44] Other nitrogen-containing groups able to couple with aryl halides includes azides, ammonia, heterocyclic amines, and amides (Figure 2.4).[52,56–58]

Several copper sources were used in this reaction. Cu(I) compounds are widely used, for example copper halides, cyanide and oxides. Preformed complexes were also applied in this reaction (Figure 2.4).[41] Inorganic bases such as, phosphates, carbonates, hydroxides or alkoxydes were required to promote this reaction.

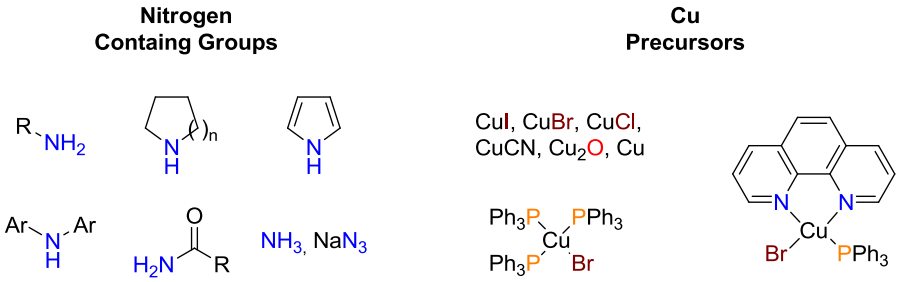

Figure 2.4 *Nitrogen starting materials and copper precursors used in the Ullmann coupling.*

Several mechanisms were proposed for the Ullmann C–N coupling reaction involving aromatic substitution from the π-complex or single-electron transfer or generation of Cu (III) intermediates by oxidative addition of the aryl halide.[59] The most widely accepted mechanism involves coordination of the ligand to the copper precursor. The first step is the coordination of the amine to the Cu(I) complex. The aryl halide then adds *via* oxidative addition to form a Cu(III) species which can undergo reductive elimination to generate the desired arylamine product which is highlighted with a green square in Scheme 2.7.[59]

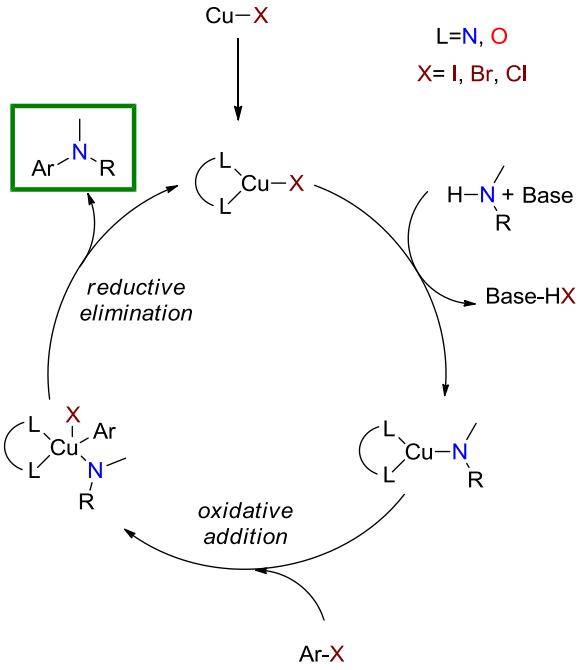

Scheme 2.7 *Catalytic cylce for Ullmann coupling.*

Several evidences are in agreement with the mechanism of Scheme 2.7. For instance, aryl iodides which are the best leaving group present faster reactions and electron-withdrawing groups on the aryl halide favoured the coupling reactions.[59] Several intermediates of the oxidative addition/reductive elimination mechanism have been isolated showing the feasibility of this mechanism (Scheme 2.8, **A** and **B**).[57,60] To eliminate the occurrence of radicals in the reaction a so-called radical clock was used in this reaction and only product was obtained (Scheme 2.8, **C**). Different reactivity bromine and chlorine compounds with similar rates of halide dissociation from the radical were consistent with catalytic cycle depicted in Scheme 2.7.[57]

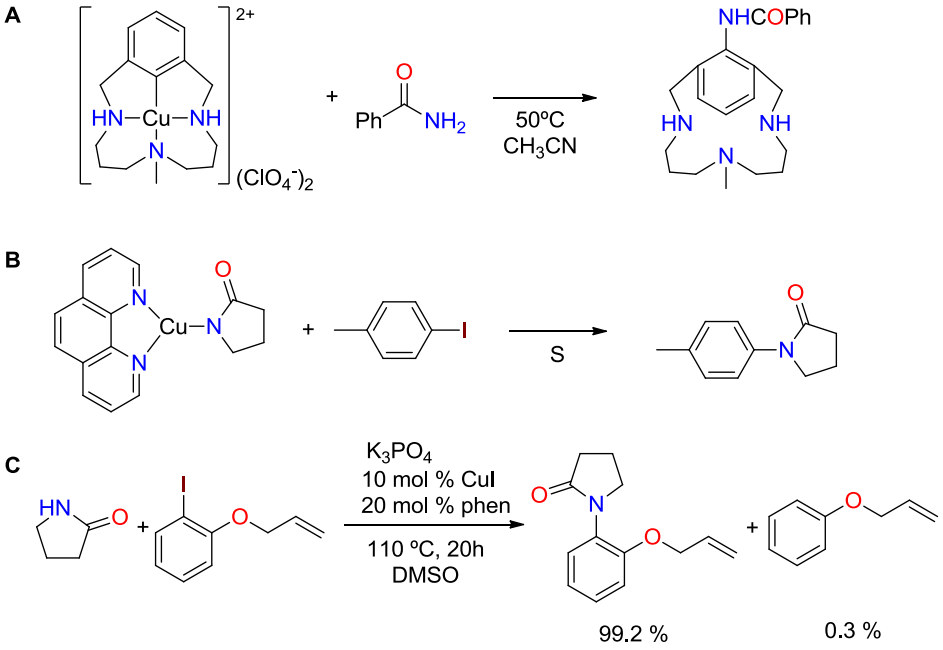

Scheme 2.8 *Reactivity of isolated intermediates of Ullmann coupling.*

2.3. Imine Formation and Reductive Amination

Generally imines are synthesized by the reaction of ammonia or primary amine with aldehydes or ketones. The mechanism of the reaction involves two different steps. First the hemiaminal intermediate is formed by nucleophilic attack of amino group to the carbonyl followed by dehydration. In solution the reaction is an equilibrium between the imine, water, and the starting reagents (the carbonyl compound and the amine).[61] Catalytic amounts of acid promote the formation of the imine. In order to increase the imine yield, the use of dehydrating agents, such as magnesium sulphate or molecular sieves or azeotropic distillation is necessary to remove the water formed. [62–64]

The reduction of imines leads to the formation of primary or secondary amines. Several reducing agents can be applied in this reduction, such as lithium aluminiumhydride derivatives, borohydride derivatives, borane derivatives, etc...[65,66] Catalytic hydrogenation of imines has been extensively investigated,

as well as the enantioselective reaction, with ruthenium, iridium or rhodium as catalyst.[67,68]

The direct formation of the amine in one-step is also possible and this reaction is known as the reductive amination reaction. In this reaction imine formation and reduction take place simultaneously. The reducing agent should be more active toward the iminium intermediates than to aldehydes such as sodium acetoxyborohydride, sodium cyanoborohydride or 5-ethyl-2-methylpyridine borane (PEMB) which are common reducing agents in this reaction.[65,66,69] General representation of the reductive amination is shown in Scheme 2.9.

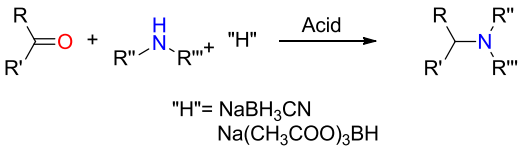

Scheme 2.9 *The reductive amination reaction.*

2.4. Results and Discussion

2.4.1. Backbone Synthesis

Several backbones were prepared using acid catalyzed condensation of *p*-cresol with different carbonyl derivatives according to literature procedures.[3,70,71] **1**, **2** and **3** were obtained in moderate yields (up to 50%, Scheme 2.10).

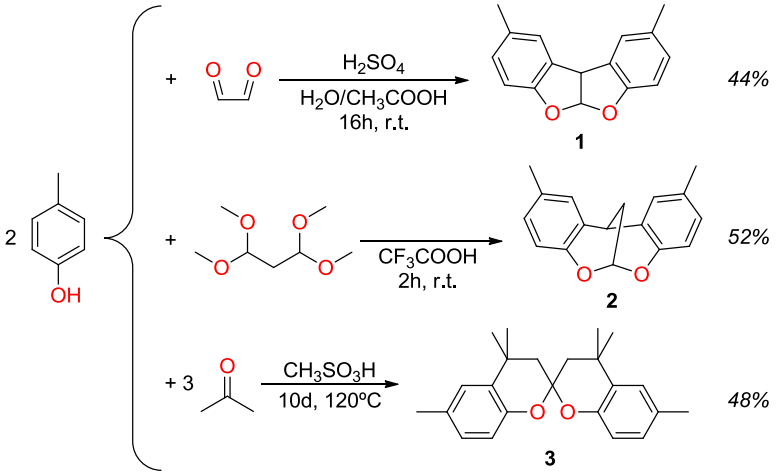

Scheme 2.10 *Results in the synthesis of BFBF, DBDOC and SPAN backbones.*

In order to synthesize new backbones with slightly different steric and electronic properties, substituted *p*-cresol derivatives or other carbonyl compounds such as 2,4-pentadione were used as substrates. The general synthetic route to amino substituted backbones involves two steps, bromination of arenes in **1**, **2**, **3**, followed by C–N bond formation *via* a cross coupling reaction. We hypothesized that the reaction between 2-bromo-4-methylphenol and the carbonyl compound could give the brominated backbones in one step, avoiding the bromination step, thus, making our synthesis faster, more economic and greener. The preliminary study was performed for synthesizing DBDOC backbone derivatives and the results are summarized in Table 2.1. Compound **2** was obtained in moderate yield (52%) by a literature procedure using trifluoroacetic acid (TFA) as catalyst.[3]

The *p*-cresol derivatives carrying electron-withdrawing groups did not yield the desired product (entries 2 to 5). This could be due to deactivation of the phenol derivatives. Increasing reaction time and temperature and using different acids had no influence on the reactivity. Even the 2-amido substituted phenol, a moderately activating group in electrophilic aromatic substitution, showed no reactivity under the same reaction conditions.

Table 2.1 *Condensations of p-cresol derivatives with different acid catalysts*

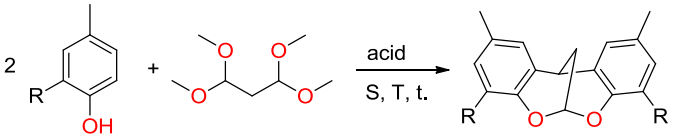

R= H, Br, NO_2, $NHCOCH_3$

Entry	R	Acid	T(ºC)	t (d)	Yield %
1	H	TFA	r.t.	1	52
2	NO_2	TFA	r.t.	3	0
3[a]	NO_2	H_2SO_4	70	3	0
4	Br	TFA	r.t.	3	1
5	Br	TFA	70	3	1
6	$NHCOCH_3$	TFA	r.t.	3	0
7[b]	$NHCOCH_3$	$ZnCl_2$	70	2	0
8[b]	$NHCOCH_3$	$AlCl_3$	70	2	0
9[c]	$NHCOCH_3$	P_2O_5	80	1	0

Reaction conditions: ratio (alcohol/acetal/acid): 1/2/7, 2 mmol of alcohol. [a] *ratio: 1/2/3, in 3 mL of acetic acid.* [b] *ratio: 1/2/3.* [c] *1/2/0.2.*

The *p*-cresol derivatives carrying electron-withdrawing groups did not yield the desired product (entries 2 to 5). This could be due to deactivation of the phenol derivatives. Increasing reaction time and temperature and using different acids had no influence on the reactivity. Even the 2-amido substituted phenol, a moderately activating group in electrophilic aromatic substitution, showed no reactivity under the same reaction conditions.

Concomitantly, the synthesis of modified DBDOC and BFBF were explored under these reaction conditions. Figure 2.5 summarizes the different phenol derivatives and dicarbonyl compounds tested in this reaction.

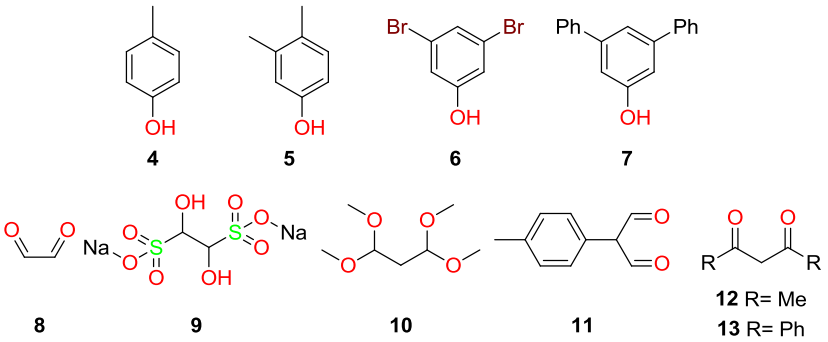

Figure 2.5 *Different starting materials used in the condensation reaction.*

The results of condensation of aldehydes with *p*-cresol derivatives are shown in Table 2.2. It was observed that sulphuric acid was a convenient catalyst and media for the synthesis BFBF (entry 1). In order to improve the yield of the product we have replaced the H_2SO_4 with a phosphorus pentoxide (entries 2-4). This Lewis acid could promote the condensation of **8** and the aromatic ring. Conversions were lower when compared to the sulphuric acid promoted reactions, although comparable conversions were achieved with longer reaction times. As phosphorus pentoxide promoted the condensation between aldehydes and *p*-cresol, same reaction conditions were used to synthesize DBDOC. Unfortunately the reaction did not proceed under similar reaction conditions (entry 5). The presence of aldehyde is required in order the condensation to proceed; this is in agreement with the lack of activity when **9** was used (entry 4). When water was added the reactions proceeded with low yields.

Table 2.2 *Condensations of phenol derivatives with different dialdehyde derivatives*

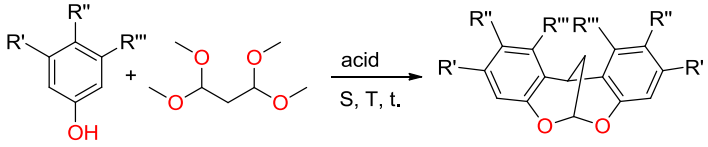

4 R'=R'''=H, R''=Me
5 R'=R''=Me, R'''=H
6 R'=R'''=Br, R''=H
7 R'=R'''=Ph, R''=H

R'=R'''=H, R''=Me
R'=R''=Me, R'''=H
R'=R'''=Br, R''=H
R'=R'''=Ph, R''=H

Entry	Phenol	Aldehyde	Acid	T(ºC)	t (h)	Yield %
1[a]	**4**	**8**	H_2SO_4	r.t.	16	44
2	**4**	**8**	P_2O_5	80	16	32
3	**4**	**8**	P_2O_5	80	40	43
4	**4**	**9**	P_2O_5	80	16	1
5	**4**	**10**	P_2O_5	80	16	0
6[b]	**4**	**10**	P_2O_5	80	16	15
7[c]	**5**	**10**	TFA	r.t.	2	37
8[c]	**6**	**10**	TFA	r.t.	16	0
9[c]	**7**	**10**	TFA	r.t.	16	0
10[c]	**4**	**11**	TFA	r.t.	16	0
11[c]	**4**	**11**	TFA	r.t.	280	20
12[c]	**4**	**11**	PFOA	120	16	0
13[a]	**4**	**11**	H_2SO_4	r.t.	16	0
14[c]	**4**	**11**	H_2SO_4	r.t.	160	0
15	**4**	**11**	P_2O_5	80	40	0

Reaction conditions: ratio (alcohol/carbonyl/acid): 1/2/0.2, 2 mmol of alcohol. [a] *ratio: 1/2/3, in 3 mL of acetic acid.* [b] *Addition of 2 eq. of water.* [c] *ratio: 1/2/7.*

The mechanism of the reaction consists in the cleavage of the acetals, in a first step, releasing the activated aldehyde followed by condensation with the aromatic ring to form the backbone. The condensation of substituted phenol was investigated. (The condensation of different bulky phenol derivatives such as **7** was unsuccessful). Compound **5** exhibited a similar reactivity as **4**. The corresponding product was isolated in moderate yields up to 37% after very fast and exothermic reaction (entry 7, Table 2.2). In contrast *meta* disubstituted phenols **6** and **7** did not react under these reaction conditions. The lack of reactivity can be attributed to the low solubility of these compounds in TFA and the steric hindrance in *meta* position to alcohol. Aldehyde **11** is not only interesting for the new steric properties; also it is remarkable that final product would have a chiral carbon atom. Having in mind the precedent aldehyde reactivity, it can be expected moderate yields in a fast reaction. In contrast long reaction time was to afford some of the product (entry 11). In order to remove the water formed during the reaction and to displace the equilibrium, the

reaction was carried out at 120ºC and perfluoroctanoic acid (PFOA) was used as a catalyst. Under these reaction conditions, **15** was not detected by ^{1}H NMR. Different catalysts such as sulphuric acid and phosphorus pentoxide were applied as acid catalyst, but no conversion was achieved even with long reaction times. The explanation of the low reactivity for **11** can be attributed to the influence of the aryl substituent that can delocalize the charge during the condensation, braking the reaction rate.

Table 2.3 *p-cresol condensations with different diketones derivatives*

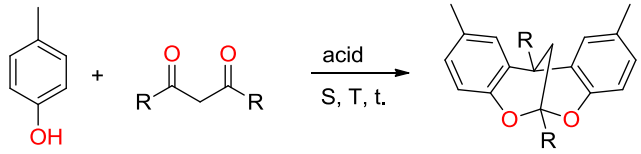

12 R= Me
13 R= Ph

R= Me
R= Ph

Entry	Ketone	Acid	T(ºC)	t (h)	Yield %
1	**12**	$ZnCl_2$	r.t.	48	0
2[a]	**12**	$ZnCl_2$	r.t.	48	0
3	**12**	$AlCl_3$	r.t	48	0
4[a]	**12**	$AlCl_3$	r.t	48	0
5[b]	**12**	TFA	r.t	16	0
6[c]	**12**	P_2O_5	80	16	0
7[d]	**12**	H_2SO_4	r.t.	7 d	6
8	**12**	H_2SO_4	100	7 d	0
9	**13**	H_2SO_4	r.t.	7 d	0

Reaction conditions: ratio (alcohol/carbonyl/acid): 1/2/3, 2 mmol of alcohol. [a] in 1 mL of THF. [b] ratio: 1/2/7. [c] ratio: 1/2/0.2 .[d] ratio:1/2/11, 20 mmol of alcohol.

The use of 1,3-diketones as carbonyl source in acid catalyzed condensation, would led to modified DBDOC backbone with higher steric hindrance at the acetal moiety. Different results for this transformation are summarized in Table

2.3. Compound **16** was previously reported by Narsinh and co-workers.[7] Unfortunately the synthesis was not reproducible under reported conditions using $ZnCl_2$ as catalyst in our hands. As the reaction is performed in solid state, the addition of THF solubilized the system, but no improvement in the activity was observed (entry 2). The same behaviour was observed using $AlCl_3$ as catalyst. TFA and P_2O_5, which previously catalyzed aldehyde condensation, were not active in the case of ketones (entry 5-6). In entry 7 sulphuric acid was used as solvent and catalyst. One of the reasons of using this acid is its hygroscopic character. Water formed during the condensation is absorbed and it could favour the formation of the desired compound. For the first time, compound **16** was isolated. In order to study the effect of temperature, the reaction was carried out at 100ºC degree but only starting materials were recovered after the work up. When **13** is used as reagent, only starting materials were recovered. It could be attributed to electron delocalization in the substrate and to high steric hindrance of the phenyl ring during the condensation step.

Synthesized ligands and their best isolated yield are summarized in Figure 2.6.

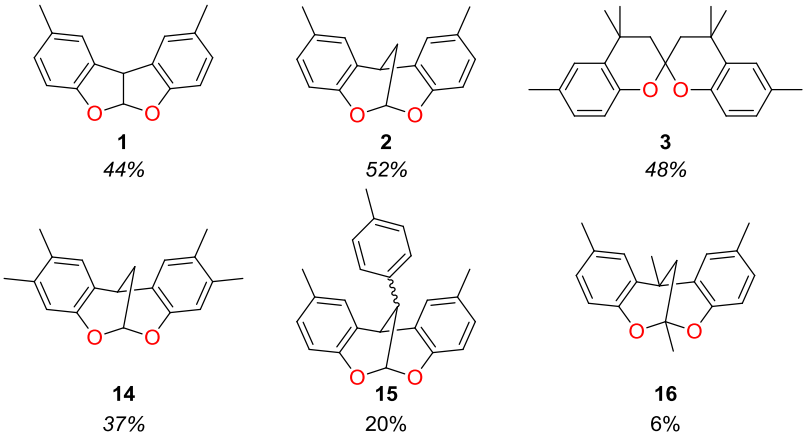

Figure 2.6 *Summary of the different synthesized backbones.*

2.4.2. Halogenation

Backbones **1**, **2** and **3** were brominated using the previously reported procedure.[71,72] Modified procedure was used for **14** and **16** (Scheme 2.11).

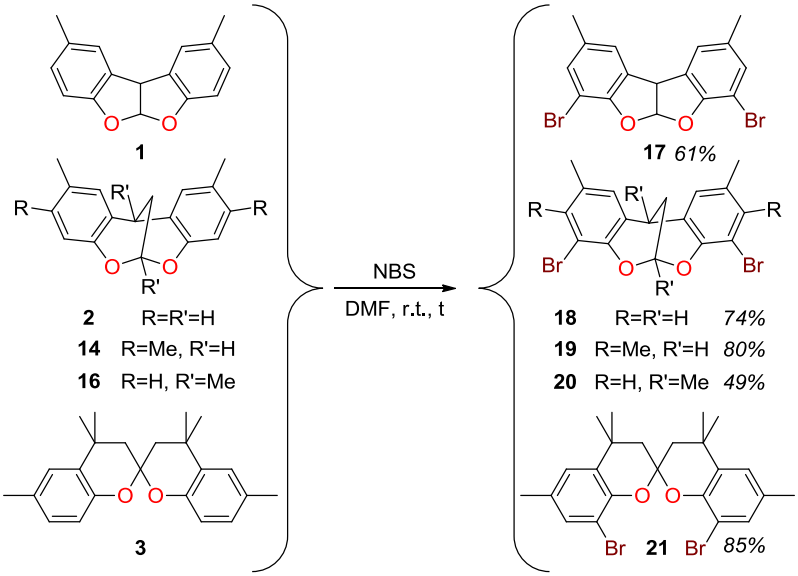

Scheme 2.11 *General synthetic conditions in bromination.*

The bromination for **1** was studied with NBS. After 16h, only starting material was observed in the presence of 3 equivalents of NBS. The system evolved after 24h with the addition of three equivalents of NBS. However the major compound was the monobrominated BFBF. This product could be interesting to prepare C_1-symmetry ligands. The desired product **17** was obtained in moderate yield (61%) after the addition of 2 extra equivalents of NBS (8 eq. in total). In Figure 2.7, the chromatogram showing the evolution of the different compound ratio with different amounts NBS is presented. Final product was recovered in two fractions; one of them presented bromine impurities that could affect reactivity in further reaction.

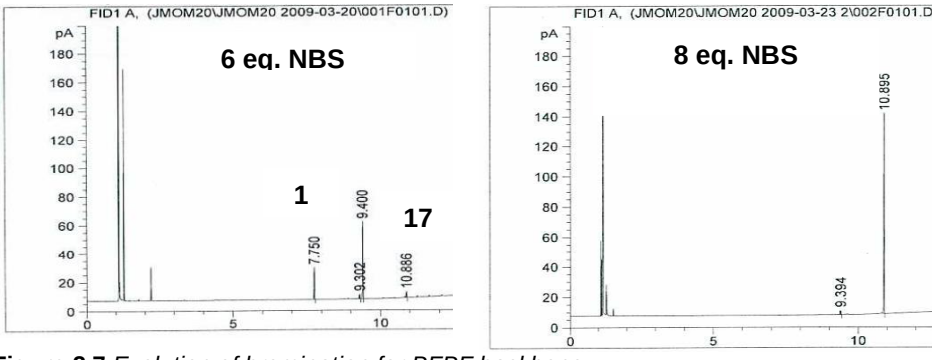

Figure 2.7 *Evolution of bromination for BFBF backbone.*

In the case of **2**, **14** and **16**, a large excess of NBS (8 eq.) was also required. Using less than 8 equivalents favour the formation of product mixture. Only backbone **3** could be brominated with a slightly excess of NBS, in return longer reaction times were necessary.

In order to improve the preparation of the brominated backbones, different bromine sources were explored in the electrophilic aromatic bromination of **2**. Bromine and Fe system was applied in this reaction (Table 2.4). In entry 1, only 50% selectivity for **18** was observed with high conversions of **2** (90%). To enhance the complete conversion to desired product an extra equivalent of bromine was added which led to over brominated backbone as the major product (entry 2). The nature of the iron source was changed in entries 3 and 4. Iron fillings proved to be more efficient towards dibromination, and desired product is form with higher selectivity compared to entry 1. The problem of overbromination was also detected with the addition of extra NBS.

Table 2.4 *Results in DBDOC bromination using Br_2.*

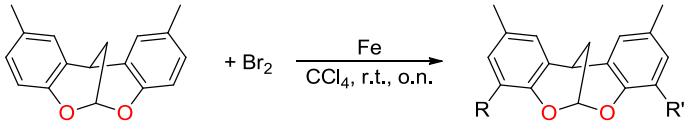

Entry	Br_2 eq.	Conv. (%)	Sel. 22 (%)	Sel. 18 (%)	Sel. overbromo (%)
1[a]	2.1	90	50	50	0
2[a]	3.1	100	0	45	55
3[b]	2.1	89	28	72	0
4[b]	2.6	100	5	80	15

*Reaction conditions: **2**/Fe (1/0.1), 1 mmol of **2**. Conversion determined by ^1H NMR. [a] Iron powder. [b] Iron fillings.*

In a different approach organic tribromide **23** was used as a bromine source in the bromination of DBDOC backbone (Scheme 2.12). Compound **2** was brominated using an established protocol.[73] With 2.2 equivalents of **23**, the reaction proceeded slowly, at room temperature. After 6 hours only 30% of

conversion to **22** was achieved and after 4 days, 72% of conversion was determined with only 11% yield toward the desired compound. To favour the bromination process, two equivalents of **23** were added which increased selectivity up to 80% but total conversion remained invariable. To afford **18** were necessary 14 equivalents of tribromide and long reaction time. In order to improve conversion and selectivity, reaction was performed at 50 ºC with 2.2 equivalents of tribromide. Under these conditions complete conversion of the starting material was observed; unfortunately the selectivity towards **22** was high, up to 85%. If 4 equivalents of brominating agent were used at 50 ºC, the selectivity to the desired product was increased but the major product was still monobrominated (55%). These results prompted us to use a large excess of **23** to afford desired dibrominated product.

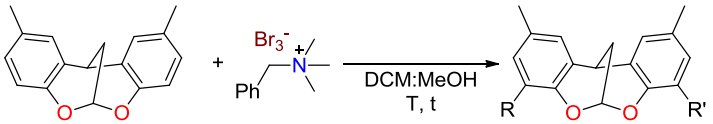

2 **23**

Scheme 2.12 *Bromination reaction with the usage of organic tribromides.*

Oxidative bromination was the last attempt to synthesize **18** (Scheme 2.13).[13] Full conversion were achieved using 2 equivalents of **24** (Selectfluor) and NaBr, but the selectivity toward **18** was only 80%. It was necessary to use 3.5 equivalents of Selectfluor to achieve full conversion. This system didn't improve the behaviour of NBS and **18** was recovered with 52% yield.

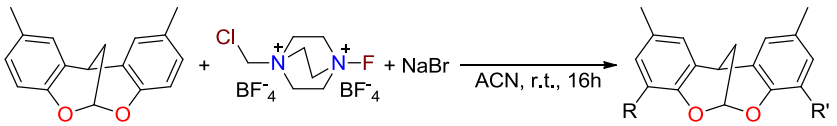

2 **24**

Scheme 2.13 *Oxidative bromination with Selectfluor and NaBr.*

We investigated different brominating agents for the bromination of **3**, and it appears that NBS was the best option in the bromination of DBDOC derivatives.

Iodine derivatives could also be interesting starting material because of the high reactivity in cross-coupling reaction. For these reason iodinated derivatives of **2**

were synthesized using iodine monochloride (Scheme 2.14). Reaction was performed in dichloromethane at room temperature yielding **25** in moderate yield, probably because of acetal cleavage which is promoted by the HCl formed during the reaction. To avoid this problem, the reaction was performed in 1,2-dichloroethane under nitrogen bubbling to remove HCl, however the final yield was lower, only 46%.

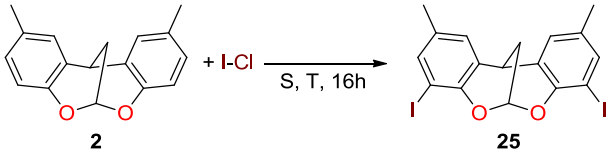

2 **25**

Scheme 2.14 *Iodination of **3** using ICl.*

2.4.3. C–N Bond Formation

The synthesis of SPANamine (4,4,4',4',6,6'-hexamethyl-2,2'-spirobi[chroman]-8,8'-diamine, compound **27**) was previously reported by our group.[62] It consisted in nitration of **3** and further reduction to yield **27** with an overall yield of 17% . The low yield is a consequence of the hard acidic conditions of both reactions that promotes the cleavage of the acetal group (Scheme 2.15). This synthetic approach was applied in our group with **1** and **2** but lot of decomposition was observed in both backbones. Thus forced us to search alternative route as cross-coupling reaction.

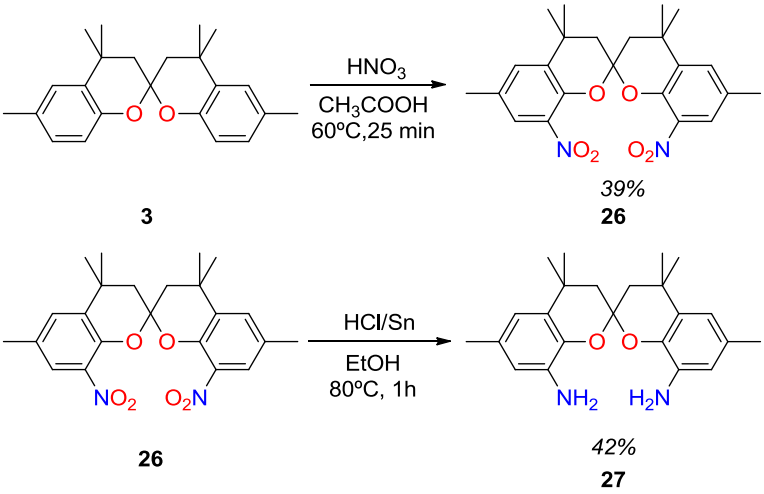

Scheme 2.15 *Nitration and reduction to led SPANamine.*

DBDOC backbone was used as substrate in Buchwald-Hartwig amination reaction. General reaction conditions and selectivity of this transformation are summarized in Scheme 2.16.

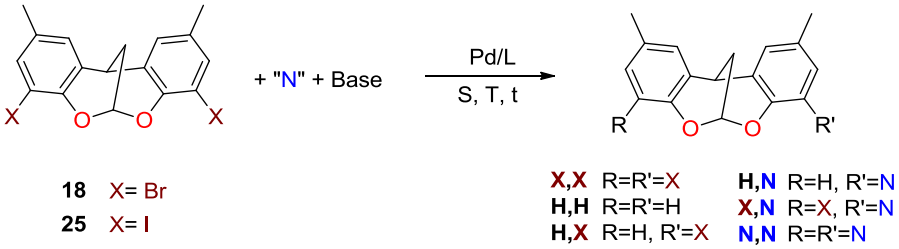

Scheme 2.16 *General selectivity for **18** and **25** in Buchwald-Hartwig amination.*

In theory, the cross-coupling with **18** and **28** leads the formation of desired compound (entry 1, Table 2.5). Unfortunately only *β*-hydride elimination was observed under this reaction condition. In order to reduce the b-H elimination and promote the reductive elimination at the palladium center during the reaction, as explained previously different ligands such as **33** and **34** were added to the catalytic system (entries 2 and 3). These two systems are more selective towards C–N bond formation, although desired compound was not detected, only starting material and reduced backbone. Monophosphine **33** was

more efficient for the reaction but long reaction time should be required for full conversion with moderate degree of bromine cleavage.

Table 2.5 *Substrate **18** in amination, with the usage of phosphines as ligands.*

"N"

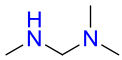

28

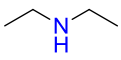

29

L

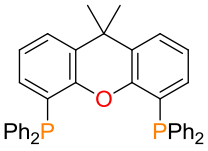

32

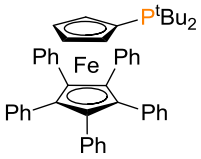

33

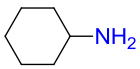

30

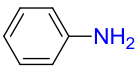

31

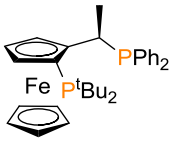

34

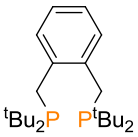

35

36

Entry	L	"N"	% Br,Br	% H,H	% H,Br	% H,N	% Br,N
1	**32**	**28**	6	89	5	0	0
2	**33**	**28**	70	2	9	3	16
3	**34**	**28**	78	2	11	2	7
4	**32**	**29**	14	16	70	0	0
5[a]	**32**	**29**	70	2	28	0	0
6	**32**	**30**	0	56	4	40	0
7	**32**	**31**	79	1	12	8	0
8	**35**	**29**	53	10	37	0	0
9	**36**	**30**	0	83	0	17	0

*T=110ºC, t=16h, N/**18**=2, S/Pd=10; KO^{t}Bu/**18**=3, L/Pd=1,1, Toluene/THF=7 conversion by GC [a] N/**18**=20.*

Amine **29** was used (entries 4 and 5) with Xantphos as a ligand to compare the bromine cleavage with **28**. Less *β*-hydride elimination was observed, but C–N formation was not detected. A lower conversion was obtained with the use of a large excess of amine, showing that saturation of the catalyst slows the oxidative addition of **18**. The use of primary amines with **32** (entries 6 and 7) led

the formation of arylamines, although *β*-hydride elimination was the major process. Bulky mono- and diphosphines were used (entries 6 and 9). However these ligands gave less active catalysts than Xantphos and *β*-hydride elimination was not suppressed. The results are summarized in Table 2.5.

Table 2.6 *Cyclic amines as substrates in the catalytic amination of **18**.*

"N"

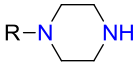

37 R=H
38 R=Me
39 R=Et
40 R=Ph

Pd/L

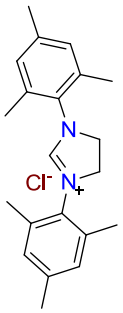

41

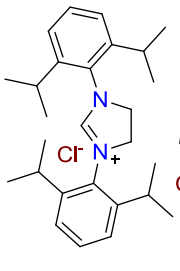

42

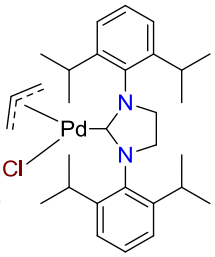

43

Entry	L	"N"	% Br,Br	% H,H	% H,Br	% H,N	% Br,N	% N,N
1	**41**	**37**	69	10	21	0	0	0
2	**41**	**38**	31	39	30	0	0	0
3	**41**	**39**	100	0	0	0	0	0
4	**41**	**40**	73	11	16	0	0	0
5	**42**	**38**	100	0	0	0	0	0
6[a]	**43**	**37**	46	8	0	0	46	0
7[a]	**43**	**38**	15	0	0	0	15	70
8[a]	**43**	**39**	30	0	0	0	18	52
9[a]	**43**	**40**	13	0	0	0	17	70

*T=70 ºC, t=16h, N/**18**=2.4, **18**/Pd=67; LHMDS/**18**=2.2, L/Pd=1.1, THF as solvent, [Pd(allyl)Cl]$_2$ as precursor, conversion by GC [a] Isolated complex, ratio **18**/Pd=33.*

The use of cyclic amines as the reagent and palladium carbene complexes as the catalyst is known to give good results in the Buchwald-Hartwig amination of bromoarenes.[27,74] This catalytic system was applied to perform the amination of compound **18**. Results of the coupling reaction are shown in Table 2.6. The difference in activity and selectivity of systems containing either NHC precursor **41** or **42** is notable in the reaction (entry 2 and 5). The ligand with less steric

hindrance was more reactive and oxidative addition of the aryl bromide did take place, but compound **18** was reduced to a large degree. On the other hand, only starting material was recovered in the catalytic system using **19,** showing that oxidative addition did not take place. When an isolated ligand-palladium complex **43** of the same ligand **42** was used as a catalyst oxidative addition did take place (entry 7), and moreover *β*-hydride elimination was completely suppressed and the product was obtained in 70% yield. The degree of conversion of the dibromides was somewhat similar for *in situ* generated catalysts and the isolated complex, although totally different selectivities were observed. This different behavior could be attributed to the fact that the isolated complex is an intermediate of the catalytic cycle, albeit that the first cycle produces an allylamine in this instance. This procedure is recommended in the literature.

Different piperazine derivatives were tested in the reaction. The best results were obtained with **38** in all cases. Moderate to high selectivity to the desired compound was observed (Table 2.6, entries 6–9) and application of different reaction conditions may lead to complete formation of the desired product. Compound **37** didn't form the doubly substituted N,N product. This could be due to lower steric hindrance of the diamine as both nitrogen atoms carry a small hydrogen substituent, which could favor the formation of chelate complexes with palladium, thus slowing the reactions.

Full conversion to the desired compound may even be feasible.

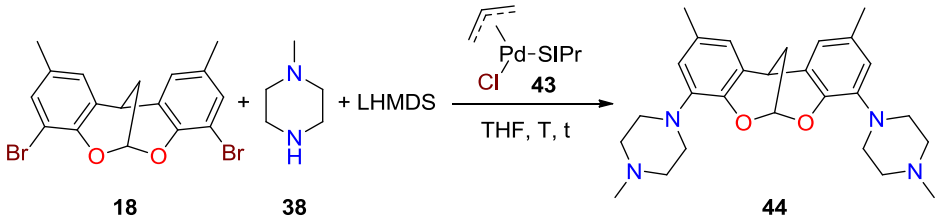

18 **38** **44**

Scheme 2.17 *Synthesis of compound **44**.*

Optimization of the reaction conditions is summarized in Scheme 2.17. An increase in catalyst loading from 1.5% to 3% led to full conversion. Compound **44** was isolated in 90% yield after 16h. Optimization studies of the reaction time demonstrated that full conversion of the dibromide was achieved after 4h but still longer reaction times were needed to improve final yield of the disubstituted

N,N compound, due to the presence Br,N compound. The best conversions and yields were obtained with 3% of catalyst loading after 6h (Graph 2.1).

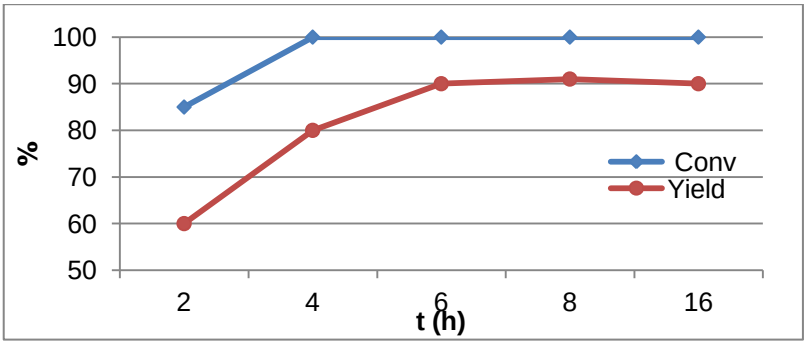

Graph 2.1 *Evolution of conversion and yield in the synthesis of **44**.*

The optimized conditions were screened with different amines depicted in Figure 2.8. Amines **28**, **45** and **46** presented similar reactivity in the reaction. They showed lower activities than **38** and large amounts of **18** were detected at the end of the reaction in all cases. This observation could be attributed to the flexibility of these amines which could coordinate as chelating ligands. More importantly, the flexibility of the chain and the increased number of *β*-hydrogens in the palladium amide intermediate facilitate *β*-hydride elimination relative to reductive elimination of the desired product. Tridentate compound **47** gives rise to a catalyst of low activity and the dibrominated DBDOC was recovered as the major product. This may be due the formation of stable Pd intermediates that do not undergo oxidative addition.

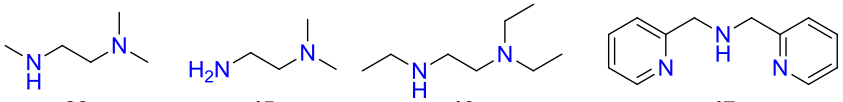

	28	**45**	**46**	**47**
% Br,Br	69	79	72	95
% H,H	4	2	5	1
% H,Br	18	19	17	4
% H,N	5	0	4	0
% Br,N	4	0	2	0
% N,N	0	0	0	0

Figure 2.8 *Different amines applied in Buchwald-Hartwig amination promoted by Pd-*

*NHC complex **43**.*

Optimized conditions were applied in the cross-coupling reaction of brominated BFBF **17**, and methylpiperazine **38**, catalyzed by Pd-NHC complexes. Unexpectedly, this reaction was not selective and gave a mixture of all possible products.

As a consequence of the poor selectivity of the dibromides with linear amines , the reactivity of iodinated DBDOC compound **25** was explored.

Table 2.7 *Amines applied in the amination of **25** catalyzed by Pd-NHC complex **43.***

"N"				Cat.
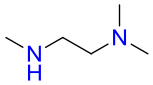	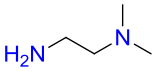	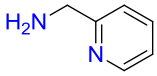	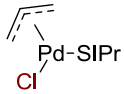	
28	**45**	**48**	**43**	

Entry	"N"	% I,I	% H,H	% H,I	% H,N	% I,N	% N,N
1	**28**	0	22	0	58	0	20
2	**45**	74	7	19	0	0	0
3	**48**	7	60	25	8	0	0

*T=70 ºC, t=16h, N/**25**=2.4, **25**/Pd=33; LHMDS/**25**=2.2, L/Pd=1.1, solvent THF, conversion by ^{1}H NMR.*

The catalytic Buchwald-Hartwig amination promoted by Pd-NHC complexes was applied with **25** and different linear amines (Table 2.7). As for the DBDOC bromoderivatives, *β*-hydride elimination was the major reaction pathway, leading to the cleavage of iodine from the DBDOC moiety. **28** was the most reactive amine in the reaction with iodinated backbone, giving full conversion of **25** and an almost statistical mixture of reduced and C–N coupled products (entry 1). Optimization of the reaction conditions could lead to major formation of H,N product which could be of great interest in order to synthesize ligands containing two different donor groups. The reaction with primary amine **45** was slow and starting material was recovered. In contrast, 2-picolylamine did react, but favored *β*-hydride elimination.

In view of the modest results obtained so far, a study of several diphosphines was performed in the coupling of diodoDBDOC (**25**) and N,N,N'-trimethyethylenediamine (**28**) with the use of palladium acetate as the precursor. The results are summarized in Table 2.8. Unlike the usual trend in C–N bond –forming reactions, in our case large bite angle ligands (entries 1 and 2) promoted the *β*-hydride elimination, and as a consequence only 10% of the H,N product was observed and none of the desired product . In the reactions with the use of phosphines having small bite angles shown in entries 3 and 4 the desired N,N compound was detected. It is thought that the bite angle effect is steric in nature, **51** causing less hindrance, rather than electronic.[33] In fact, when **51** was used as ligand similar rates for reductive amination and *β*-hydride elimination were observed. Thus, the best systems for the Buchwald-Hartwig amination of DBDOC derivatives with **28** were the Pd-NHC complex **43** and palladium acetate modified with dppe, **51**.

Table 2.8 *Amines of **25** catalyzed by Pd diphosphine complexes.*

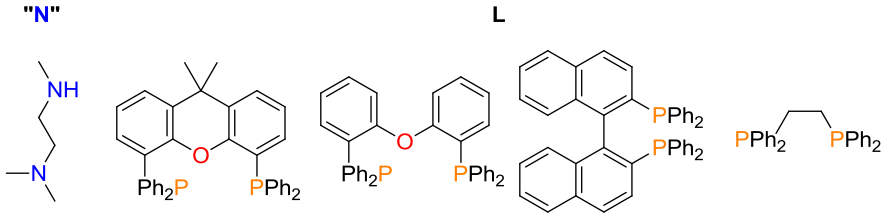

28 **32** **49** **50** **51**

Entry	L	% I,I	% H,H	% H,I	% H,N	% I,N	% N,N
1	**32**	22	28	40	10	0	0
2	**49**	26	14	54	6	0	0
3	**50**	33	13	36	9	0	9
4	**51**	0	10	24	18	28	20

*T=110ºC, t=16h, N/**25**=2.4, **25**/Pd=20; KO^{t}Bu/**25**=3, L/Pd(OAc)$_2$=1.1, solvent Toluene/THF=7, conversion by ^{1}H NMR.*

Subsequently another approach to synthesize the desired tetraamine compounds was explored, which involves the amination of the backbones with ammonia followed by introduction of a second nitrogen donor atom e.g. via a

condensation reaction with an aminoaldehyde. Efficient amination of aryl halides with ammonia is a relatively new achievement and it has been reported that it can be promoted by Pd complexes.[75,76] Bulky monodentate ligands were required for this transformation, and thus, complex **43** was used as catalyst in this reaction. The reaction is depicted in Scheme 2.18.

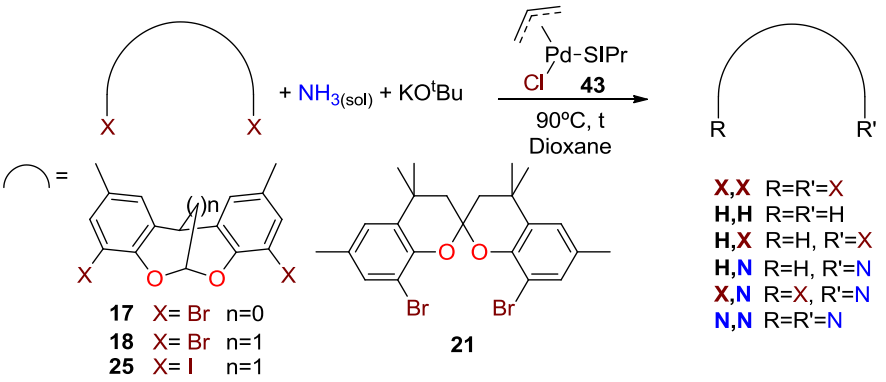

Scheme 2.18 *Buchwald-Hartwig amination with ammonia.*

The reaction conditions were optimized for dibromoSPAN **21**; The desired SPANamine was previously prepared by another route.[62] The reaction was carried out at 90 ºC in dioxane for 16 hours. The catalyst loading was 1% and 5 equivalents of ammonia were used. These reaction conditions led to 46% conversion of starting material. Higher catalyst loadings (3%) and excess of amine (10 eq.) were used and full conversion was obtained but only 36% yield was recovered. These conditions were applied to compounds **17**, **18** and **25**. **17** decomposed under these conditions and acetal cleavage was observed in the ^{1}H NMR spectra of the crude reaction mixture. All DBDOC derivatives showed similar behavior. Bromo derivative **18** reacted slightly to give 9% conversion to reduction of one bromine. The less active iodine derivative remained unaltered after 60h of reaction. The use of ammonia as nitrogen source didn't achieve the desired selectivity or activity, and thus coupling of an ammonia surrogate such as benzylamine was explored (see Scheme 2.19). Cleavage of the benzyl group is well documented.

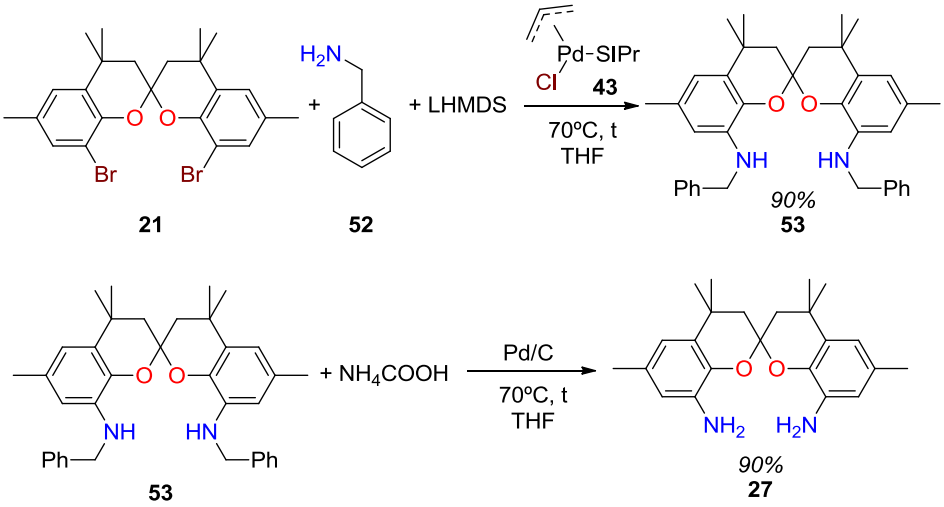

Scheme 2.19 *Alternative Spanamine synthethic route which includes a cross-coupling reaction with benzylamine followed by deprotection.*

The conditions used for the synthesis of **44** (Scheme 2.17) were applied to the synthesis of **53**. The latter was obtained in 90% yield after 16h. After optimization of the reaction a similar yield could be obtained in 4h with a catalyst loading of 1.5%. Next, cleavage of the benzyl group led to the formation of **27**, in 95% isolated yield. The monoamination of **21** was attempted unsuccessfully. The formation of first C–N bond seemed to activate the second bromine atom for substitution as only **21** and **53** were detected during the reaction. The activation of the second bromine atom might proceed by coordination of the monoamino product to the palladium center, thus enhancing the oxidative addition of second bromine-carbon function. This successful synthetic procedure of **21** was also applied to **17**, **18** and **25**, but unfortunately the selectivity was low and mixtures of all possible products were detected. The generally low selectivity in Pd cross-coupling amination for DBDOC and BFBF forced us to search for alternative synthetic routes.

In this context, the Ullmann coupling was a promising alternative to explore the formation of C–N bonds. To study the activity and selectivity of this reaction DBDOC halogenated derivatives were chosen as starting materials. The reaction is depicted in Scheme 2.20.

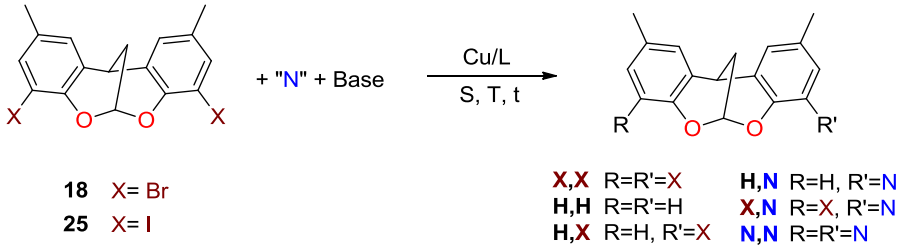

Scheme 2.20 *Possible products for **18** and **25** in Ullmann coupling.*

First, the reaction was studied with DBDOC bromine derivative **18**, under the reported conditions.[77] The results are summarized in Table 2.9. The reaction favoured the formation of C–N bonds over the β-hydride elimination (entry 1), but the activity was low and only 28% conversion was obtained. Longer reaction times, entry 2, increased the conversion, but the selectivity decreased. This might be due to the evaporation of amine. Thus, an excess of amine was added and the final conversion reached was 78%. Unfortunately, the selectivity decreased, yielding a mixture of products with a high degree of reduction, entry 3.

A solvent screening (entries 4–9, Table 2.9) was performed but all showed similar results in selectivity and conversion. The reaction done in 1,4-dioxane was the most promising in terms of conversion and selectivity, probably the coordination of the solvent to the copper metal centre has a favourable effect. The reaction in the neat amine should be faster as the starting amine probably could act as a ligand. As expected, indeed the reaction in neat N,N,N'-trimethylethyleneamine (**28**) was faster and full conversion was obtained after 16h (entry 10). As still 20% of the Br,N compound was observed, the reaction was kept at 150 ºC for an extra 24h (entry 11). The reaction continued and the desired compound was synthesized with 44% selectivity together with products related with replacement of bromine by hydrogen. Amine **38** which underwent coupling with **18** in the Pd-catalyzed Buchwald-Hartwig amination, gave a low reactivity and selectivity (entries 12 and 13) in the neat amine, similar to those found in dioxane, **57**. Since formation of C–N coupled products was neither complete nor selective, diiodide **25** was screened in this reaction, as it is known in the literature that aryl iodides usually are better substrates than bromides.[48–50]

Table 2.9 *Product distribution for **18** in ligand-free Ullmann coupling aminations.*

"N" S

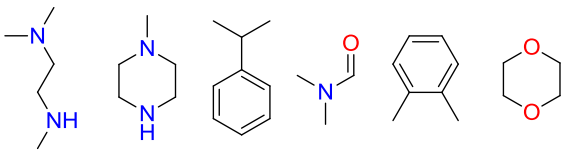

28 **38** **54** **55** **56** **57**

Entry	S	T (h)	"N"	% Br,Br	% H,H	% H,Br	% H,N	% Br,N	% N,N
1	**54**	16	**28**	72	0	4	0	24	0
2	**54**	40	**28**	60	0	10	0	30	0
3[a]	**54**	60	**28**	22	5	22	14	31	6
4	**55**	16	**28**	83	0	3	0	14	0
5	**55**	40	**28**	64	0	11	0	22	3
6	**56**	16	**28**	65	0	3	0	30	2
7	**56**	40	**28**	30	0	12	0	54	4
8	**57**	16	**28**	49	0	5	0	44	2
9	**57**	40	**28**	33	1	7	4	46	10
10[b]	-	16	**28**	0	6	7	30	19	38
11[b]	-	40	**28**	0	9	3	40	4	44
12[b]	-	16	**38**	60	12	16	7	5	0
13[b]	-	40	**38**	34	11	39	4	6	6

*T=150 ºC, N/**18**=2.4, **18**/CuI=10; K_2CO_3/**18**=5, conversion by GC.* [a] *Addition of 2,4 eq of N.* [b] *reaction in neat N, 10 eq.*

The same catalytic system was applied in the Ullmann coupling reaction of **25**. An unexpected lack of reactivity was observed and less than 10% of monoreduction of iodine was formed with the use of several solvents such as, cumene (**54**), dimethylformamide (DMF, **55**), *o*-xylene (**56**) or 1,4-dioxane (**57**). In order to improve the catalytic performance of the amination reaction, ligands such as 1,2-ethanediol or N,N'-dimethylethylenediamine were used in order to promote the copper catalyzed reaction.[78,44]

The reaction was tested with different diols and N,N,N',N'-tetramethylethylenediamine (TMEDA) as ligands.. Results are summarized in Table 2.10.

Table 2.10 *Product distribution for **18** in Ullmann coupling amination.*

"N"	L	
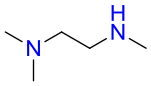	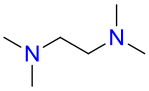	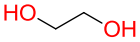
28	**58**	**59**

Entry	L	T (h)	% Br,Br	% H,H	% H,Br	% H,N	% Br,N	% N,N
1	**58**	16	71	0	8	0	11	10
2	**58**	40	60	0	10	0	13	17
3	**59**	16	74	1	2	5	3	15
4	**59**	40	60	1	1	6	4	28
5[a]	**59**	16	29	0	7	11	8	45
6[a]	**59**	40	17	0	5	8	10	60

*T=150 ºC, N/**18**=2.4, **18**/CuI=10; K_2CO_3/**18**=5,conversion by GC.* [a] *K_3PO_4 used as base.*

Similar reactivities were observed for diamines and diols when used as the solvent (entries 1–4). C–N bond formation was favored with **58**, although only 40% of conversion was achieved after 40 hours of reaction. The selectivity was higher when alcohols were used; this could be related to less steric hindrance around the copper center in their alcohol complexes – as OH groups is less sterically demanding than NMe_2 group – which could facilitate the coordination of the substrate amine and the oxidative addition of our bulky aryl bromide substrate. The base plays an important role in determining the selectivity and rate. The use of potassium phosphate enhanced the reaction rate, which provided 83% conversion and high selectivity (72%) toward diamination. As previously in similar reaction, diiodide **25** remained unreacted. Several ligands/solvents were screened, such as **59**, TMEDA, 1,2-propanediol, 1,3-propanediol and 2,4-pentanediol, yielding as major component starting material **25**. Small amounts of iodine reduction were also detected (<10%). Thus, we are still in need for a system that can activate diiodoDBDOC.

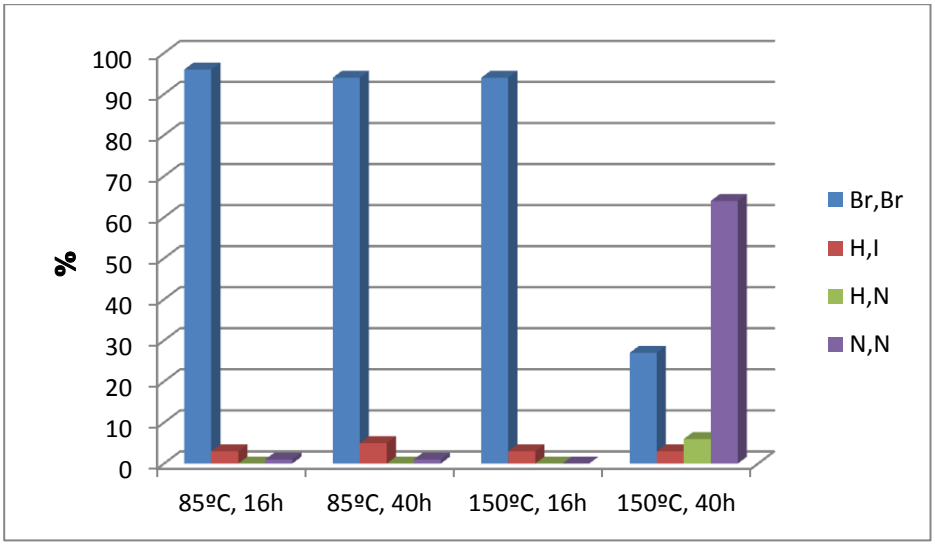

Graph 2.2 *Reactivity of copper-**59** system in Ullmann amination of **25**. Solvent isopropanol, base K_3PO_4.*

The reaction was performed at 85 ºC, but oxidative addition did not occur and starting material was recovered. Higher temperatures are needed to make the reaction proceed with good selectivity toward the desired product. Long activation times are necessary as no conversion was detected in the first 16h.

The synthesis of primary amine derivatives of BFBF and DBDOC was still unresolved. The application of Ullmann coupling with ammonia surrogates is a useful tool in the amination chemistry for instance azides.[56] The reaction is shown in Scheme 2.21. The reduction of the azide to the aniline does not require a separate step, as is usually the case, but here occurs in situ via a reaction with un unknown stoichiometry.[56] In view of the potential danger of the azide the reactions were carried on a small scale (below 150 mg).

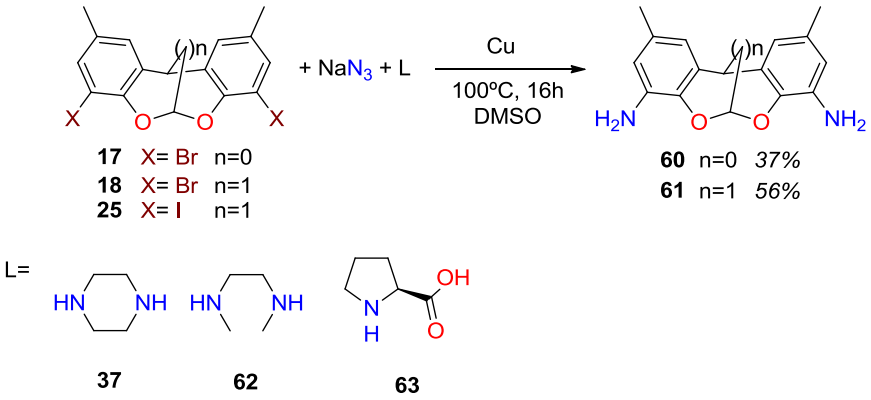

Scheme 2.21 *Primary amines synthesized via coupling with sodium azide. Reaction conditions: X= 0.5 mmol, Cu=1 mmol, L=1,3 NaN_3=3, DMSO 2mL.*

The reactions were accomplished with stoichiometric amounts of the copper precursor and an excess of ligand. The desired products were isolated in moderate yields and reduction products were also isolated for all starting materials. 42% and 44% were isolated for **18** and **25** respectively in reaction mediated by CuI and **37**; although longer reaction times were required for bromoderivatives. This is in agreement with a mechanism in which the oxidative addition step of aryl halide to copper is rate determining. Ligands **62** and **63** resulted to form most active catalyst and above 55% yields were obtained in both cases. Also the nature of the copper source was investigated, but it seems to have no influence, neither on the rate and conversion nor on the selectivity. Under optimized conditions, i.e. **61** and CuI, the amination of **17** yielded only 37% yield of the desired product. In a similar reaction with **27** the major process was dehalogenation. The monoamination of **25** was attempted but the process was not selective.

In order to improve the formation of amine derivatives with the direct coupling with ammonia was performed, previous attempts with Pd-NHC gave low yields.[79] General reaction conditions are depicted in Scheme 2.22.

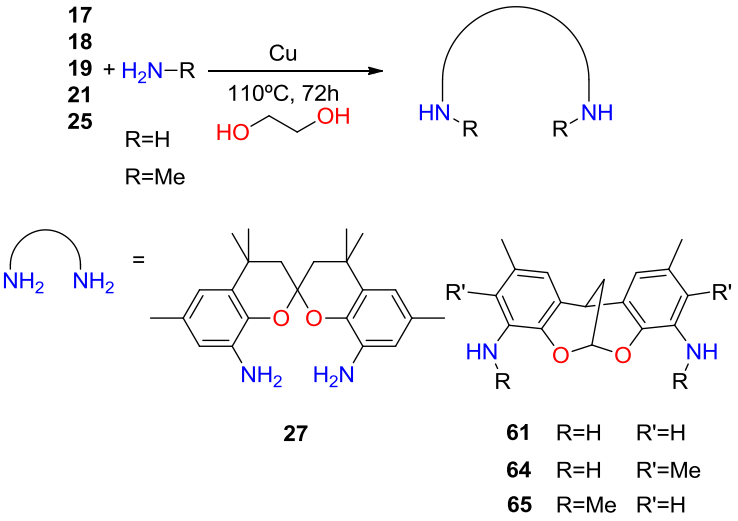

Scheme 2.22 *Ullmann copper amination for different synthesized backbones.*

The reaction was firstly performed for **18** at 110 ºC, 0,3 eq. of Cu and 50% volume 1,2-ethanediol and liquid ammonia in a reactor vessel. An important role of the experimental procedure and pressure was observed. A reaction carried out in a reactor which was nearly completely filled with liquid yielded 90% of the desired product at a gram scale. When the reactor was filled for only 2/3 with liquid the conversion and selectivity were lower and only 62% yield was obtained after 3 days. In addition an important amount of monoamination-monoreduction compound was produced. Halide effects were explored, and iodide derivatives were shown to be more active and the reaction was complete in 16 hours, but only 31% of **61** was formed due to the high degree of iodide reduction. Steric effects in the backbone turned out to be important, as could be observed in **19**, which yielded only 37% of **64**. Other effects were important as well, e.g. when methylamine was used as the source of the nitrogen nucleophile, the percentage of bromide reduction increased, as a consequence of the hydrogen atoms in the *β*-position.

Amination of SPAN and BFBF backbones was studied by Ullmann coupling but results were disappointing in most cases. SPANamine needed stoichiometric copper oxide to achieve complete conversion (otherwise up to 75% of **27** was isolated) while for BFBF only traces of the desired product were detected.

In conclusion, it appears that each backbone requires its own specific conditions and catalyst system for the amination reaction, and thus very subtle changes in the backbone (electronic, steric), can change the results of the reaction completely. SPANamine derivatives can be synthesized in two steps by a Buchwald-Hartwig amination with benzylamine and DBDOC moieties can be aminated in good yields with a direct coupling of ammonia and aromatic halides, promoted by copper catalysts. Finally, for BFBF compounds the best synthetic method is the copper mediated coupling with sodium azides.

2.4.4. Imine Formation and Reductive Amination

The Schiff base condensation of the backbones with several pyridine aldehyde derivatives and quinoline aldehydes leads the formation of tetradentate nitrogen ligands. The reaction is presented in Scheme 2.23.

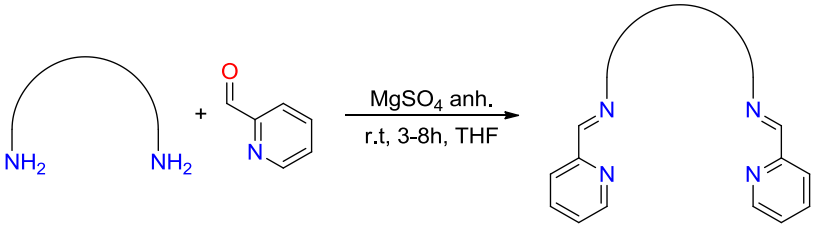

Scheme 2.23 *Schiff base condensation reaction.*

Several conditions were explored for the condensation reaction: different solvents (methanol, tetrahydrofuran, toluene or dichloromethane), temperature (from room temperature to 110 ºC) and dehydrating systems such as molecular sieves, water evaporation, and anhydrous sulfates.[62,63,80] The best yields were obtained when the reaction was carried out in tetrahydrofuran at room temperature with $MgSO_4$. The results of the condensation reactions are summarized in Figure 2.9

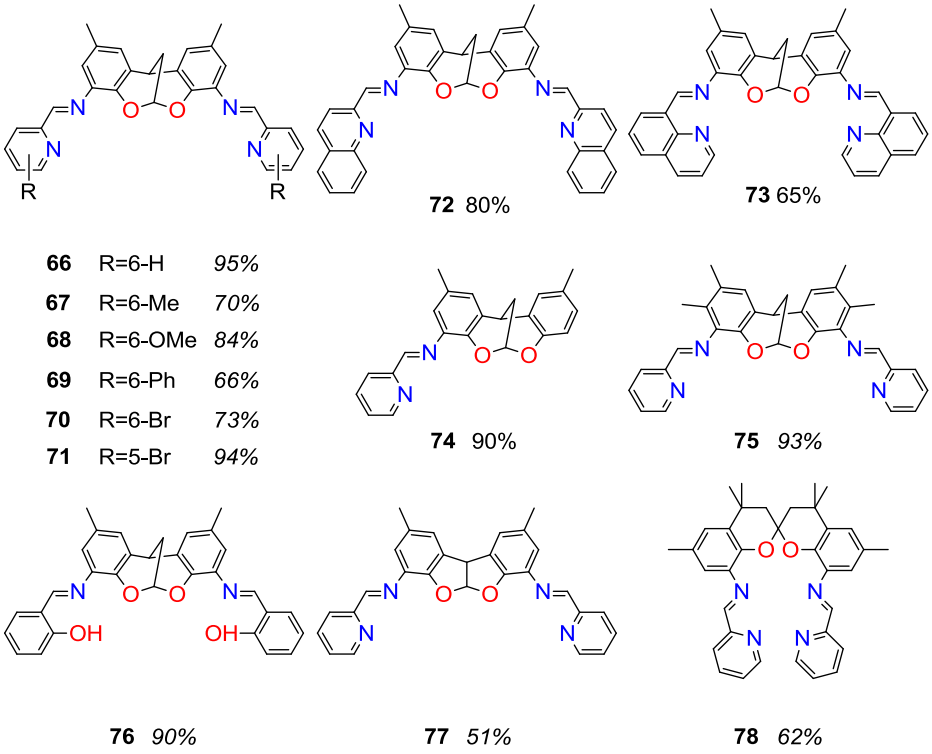

Figure 2.9 *Tetradentate ligand synthesized by condensation of amine and aldehyde.*

A wide variety of aldehydes were condensed with the backbones to give the corresponding diimine ligand. A steric influence could be observed, as for example bulky *ortho*-substituents decrease product yields significantly. For instance, isomers **70** and **71** were isolated in different yields. The synthesized compounds are very sensitive to water in solution.

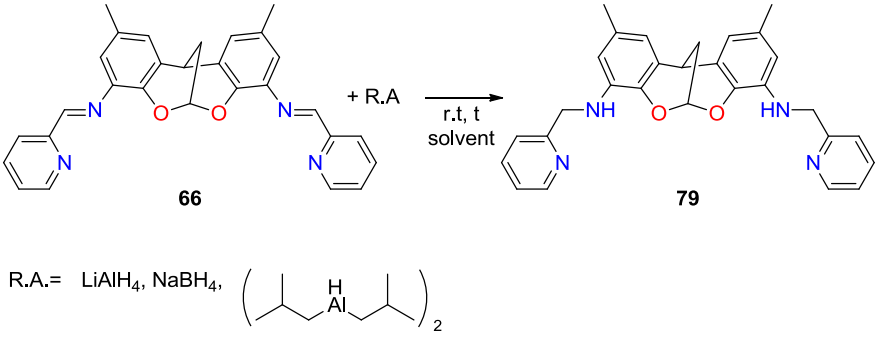

Scheme 2.24 *Imine reduction general representation.*

The final modification of the ligands involves reduction of the imine function to yield the more stable aminopyridine derivatives. The first attempt for the reduction of imine function implied a toluene-sodium borohydride system, which was used previously in the reduction of SPANimine derivatives.[62] Imine hydrolysis was observed, due to traces of water in the dry solvent. Therefore other systems were explored, for example THF-lithium aluminium hydride. This system was able to perform the reduction of the imine in good yield up to 90%, although it was important to dry the solvent beforehand with an excess of $LiAlH_4$ to avoid imine hydrolysis. Similar reactivity and selectivity was observed with the use of disiobutylaluminium hydride as reducing agent.

The amine can also be obtained in high yield in one step by reductive amination of an amine and an aldehyde, saving one synthetic step.[65,66,69] The reaction was explored and optimized for compound **66**. Several reducing agents were explored, such as PEMB **81**, sodium triacetoxyborohydride **82**, disiobutylaluminium hydride, or lithium aluminium hydride. The results are presented in Table 2.11.

Table 2.11 *Optimization of a reductive amination.*

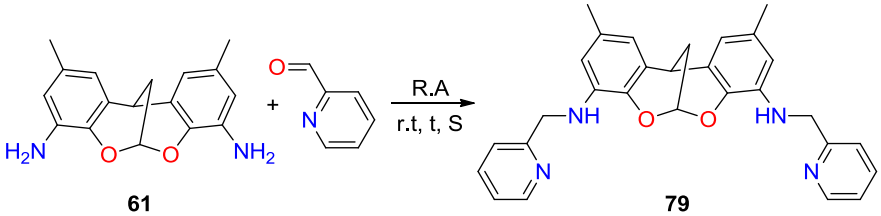

61 **79**

R.A.= $LiAlH_4$, , , $NaBH(AcO)_3$

81 **82**

Entry	R.A	Solvent	Additive	T (h)	% Conv.	% Sel.
1	**81**	MeOH	AcOH	1,5	71	73
2	**81**	MeOH	AcOH	3	73	100
3[a]	**81**	MeOH	AcOH	3	72	100
4	**81**	MeOH	-	3	59	100
5[b]	**81**	MeOH	AcOH/TEOF	3	71	100
6	**81**	THF	AcOH	3	70	46
7[c]	**82**	DCM	AcOH	3	61	100

*Aldehyde/**61**=2, **81**/**61**=1; acid/**61**=4,6, 2 mL of MeOH, 0.4 mmol **61** selectivity and conversion were determined by ^1H NMR. [a] Aldehyde/**61**=2,2. [b] TEOF/**61**=6. [c] Aldehyde/**61**=2, **82**/**61**=2,8; acid/**61**=2, 0,6 mL DCM, 0,2 mmol **61***

A known procedure was applied in the reductive amination of **61** with PEMB.[66] Promising results in terms of conversion and selectivity were observed (entry 1). Complete conversion is not observed as the starting aldehyde was reduced concomitantly during the reaction. Longer reaction times are needed to complete the formation to the disubstituted product (entries 1 and 2). The reaction was performed with an excess of aldehyde (entry 3) to increase the conversion to the desired product but the same results were obtained. The role of several additives was explored, but no improvement was observed with the addition of a desiccant such as triethyl orthoformate (TEOF) which should diminish imine hydrolysis (entry 5). Absence of acetic acid slowed the reaction, as acetic acid catalyses the reaction by activating the aldehyde reagent (entry 4). Moreover, the presence of acid enhanced the formation of an iminium ion,

which was reduced preferentially to the aldehyde. The effect of the solvent was also studied as polar solvents may favour the reaction by solubilizing the iminium intermediate (entries 2 and 6). Changing the reductant implied that the reaction conditions had to be changed completely and yet the conversion was still only 61% albeit with a high selectivity (entry 7).[69] For both procedures the product was isolated; reductive amination promoted by PEMB yielded 67% while the sodium triacetoxyborohydride system gave only 36%.

The reductive amination of **65** did not proceed for any of the reducing agents ($NaHB(CN)_3$, $NaHB(OAc)_3$ or PEMB), not even with additives, such as thionyl chloride or acetic acid.[65,66,69,81] The additives catalyze the formation of the iminium intermediate, but it seems that the reducing agent used was not able to reduce it to the corresponding amine: As a consequence of the work-up, the iminium intermediate hydrolyzed into the starting materials.

2.4.5. Other transformations

Since one of the applications of the tetraamines was their use as ligands in oxidation reactions, the synthesis of tertiary amine derivatives of DBDOC needed to be explored, because secondary amines may decompose under oxidative conditions. Methylation of secondary amine **79** would lead to compound **80** (Scheme 2.25).[62,82–84]

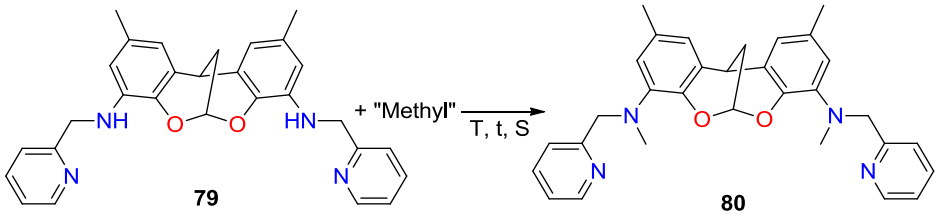

Scheme 2.25 *General methylation reaction.*

Initially methyl iodide was explored as the methylating agent. Several reaction conditions, bases, and solvents were screened such as DMF/NaH, THF/BuLi or THF/LHMDS. But unfortunately cleavage of the picolyl moiety was observed. The usage of the system dimethyl sulphate, LiHMDS and THF favoured the formation of compound **80** in high selectivities, which after purification product was isolated with 49% yield.

Similarly, nucleophilic substitution should enable the synthesis of hexadentate ligands by the double attack of each amine group of **61** to 2-(chloromethyl)pyridine hydrochloride (**83**) in basic media (Scheme 2.26).[85,86]

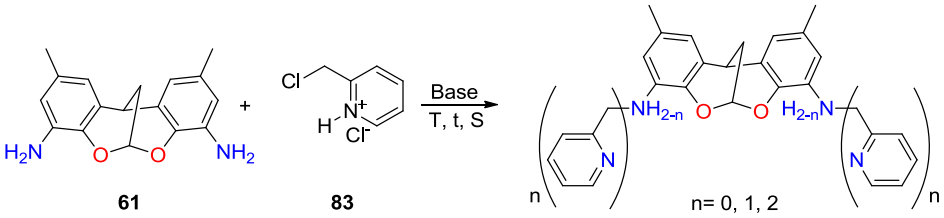

61 **83**

Scheme 2.26 *Hexadentate ligand synthesis*

The results of this reaction are summarized in Graph 2.3. The reaction was first performed in MeOH at 65 ºC and triethylamine as base. This reaction condition led to moderate conversions and the desired product was not observed, only mono and disubstituted products were formed. In order to improve the conversions and selectivities, higher temperatures and microwave irradiation were tested. Conversions improved but double alkylation on one of the nitrogen atoms was not observed, perhaps for steric reasons in combination with the low nucleophilicity of the aniline nitrogen atom. Other solvents and bases were used with the aim to increase the conversions and selectivity but no improvement could be achieved.

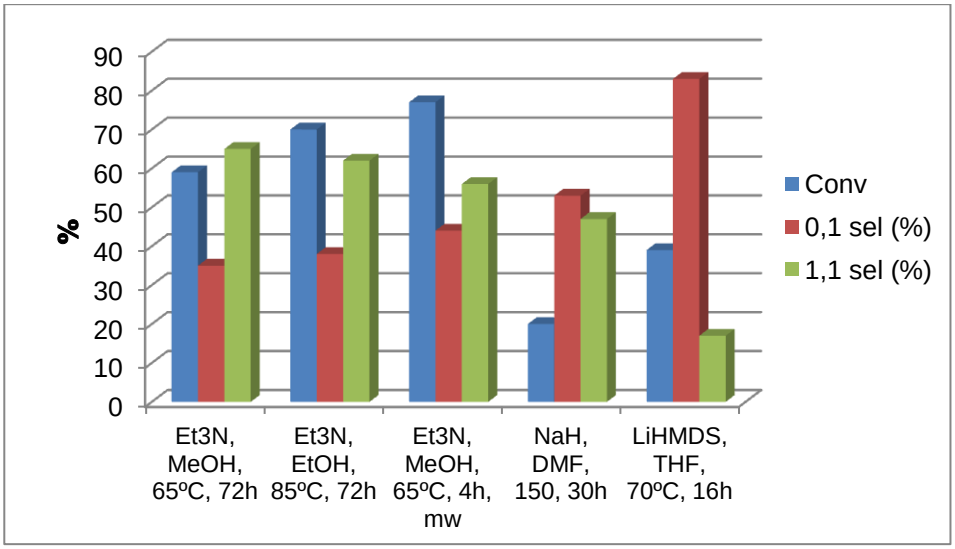

Graph 2.3 *Results for attempts in the formation of hexanuclear ligands.*

Finally, the last attempted modification of the bidentate ligand involved the formation of 2-picolyl amides. As the previous one, the reaction was performed by the nucleophilic attack of **61** to 2-picolinic acid derivatives.[87–91] The general representation of the reaction is depicted in Scheme 2.27.

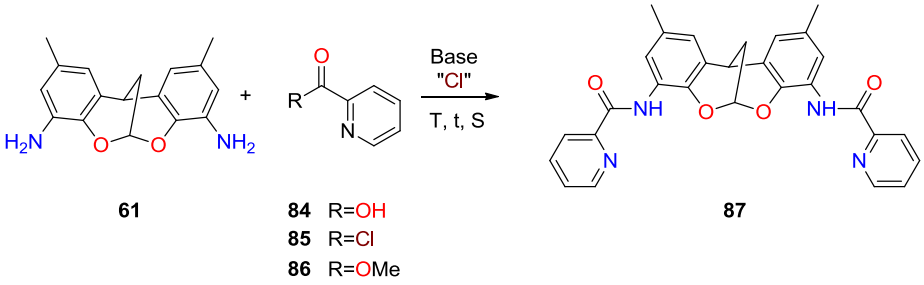

Scheme 2.27 *DBDOC amide synthesis from **61** and picolilacid derivatives.*

The reactions were performed with the use of a wide variety of reported synthesis of amides with picolinic acid derivatives.[87–91] Solvents such as DCM, THF, Toluene or EtOAc/EtOH/H_2O and bases like triethylamine or sodium hydride were screened. Also, substrate **84** was reacted first with thionyl chloride or oxalyl chloride to form **85** *in situ* or it was isolated, but in all the cases **61** was recovered. The lack of activity was attributed to the low nucleophilicity of amino

group. Finally, harsher conditions were used such as those of the Bodroux reaction, normally used for poorly nucleophilic amines.[92] Grignard reagents were used to deprotonate the amine giving the amido anion NH^- which can attack **86** and form **87**. The reported condition led to only 68% conversion and low selectivity. An increase of temperature (r.t → 65 ºC), time (4h → 16h) and another solvent, THF instead of diethyl ether; increased the conversion up to 100% and the selectivity to 90%. The product was isolated in 45% yield.

2.5. Conclusions

- The condensation reaction to of DBDOC and BFBF was performed under Lewis or Brönsted acid catalysis. The backbones were isolated with moderate yields in both cases.

- The position of the substituent in the cresol derivatives had an influence in the reaction behaviour. *Ortho* substituents to the phenol group inhibited the condensation reaction and only starting materials were recovered, in contrast *para* substituents did not affect the conversion.

- The best brominating agent is still NBS, although good yields and selectivities were obtained with the Selectfluor and sodium bromide system. The benzyl tribromide presented promising results in the formation of the monobrominated backbone.

- A new synthetic route was developed for the preparation of SPANamine. This formation of SPANbenzylamine *via* Buchwald–Hartwig coupling and further cleavage of benzyl to form SPANamine in high yield and selectivity.

- BFBF and DBDOC amino derivatives were synthesized *via* Ullmann coupling. Moderate to high yields were obtained in the coupling of $BFBFBr_2$ **17** and $DBDOCBr_2$ **18** with sodium azide and ammonia respectively.

- Different tetradentate iminopyridine ligands were synthesized for DBDOC, BFBF and SPAN backbones. These ligands were obtained in moderate to high yield and they present high water sensitivity in solution.

- Aminopiridine derivative of DBDOC **79** was prepared with high yield *via* hydrogenation of the iminopyridine with DIBALH or *via* reductive amination with PEMB as reducing agent.

- The low nucleophilicity of the compound **61** required the use of a strong base to form the amide compound which was nucleophile enough to undergo the transformation to for compound **80** and **87.**

2.6. Experimental Part

Unless otherwise stated, all reactions were performed using standard vacuum-line and Schlenk techniques under nitrogen atmosphere. Solvents were purchased from Sigma-Aldrich as HPLC grade and dried with an SPS system of ITC-inc. Reagents were used as commercially available. NMR spectra unless otherwise stated were recorded at the following frequencies: 400.13 MHz (^{1}H) and 100.63 MHz (^{13}C) NMR spectra were recorded using broad band decoupling. Chemical shifts of ^{1}H and ^{13}C NMR spectra are reported in ppm downfield from TMS, used as internal standard. Signals are quoted as s (singlet), d (doublet), t (triplet), m (multiplet), b (broad)). Gas chromatoGraph analyses were run on a Hewlett-Packard HP 5890A instrument (split/splitless injector, J&W Scientific, HP-5, 25 m column, internal diameter 0.25 mm, film thickness 0.33 mm, carrier gas: He, F.I.D. detector) equipped with a Hewlett-Packard HP3396 series II integrator. Enantiomeric resolutions were performed on. GC-MS experiments are carried with a HPLC semipreparative Waters 600 equipped with Chiralpak IC 5 µm particle size, internal diameter 10 mm and 25 cm of length. The CG-MS are done in HP 6890 Series GC System coupled to HP 5973 Mass Selective Detector, with automatic injector HP 7683 Series Injector. The column is HP 5MS (30 m x 0.25 mm, and 0.25 film thickness µm). High pressure experiments were performed in Berghof Stainless Steel SS316 reactors (25 and 40 ml) equipped with a PTFE liner, magnetic stirring and heating jacket or in a Baskerville and Lindslay LTD. 6821 (20 ml) equipped with magnetic stirring.

Synthesis of 2,9-dimethyl[5a,10b]dihydrobenzofuro[2,3-b]benzofuran, 1.[4]

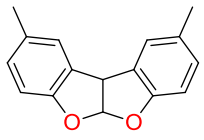

1

A round-bottomed flask (1.0 l) in a hot water bath was charged H_2O (300 mL), acetic acid (150 mL), glyoxal (12.5 mL, 110 mmol) and *p*-methylphenol (21mL, 200 mmol). A reflux condenser was fitted on the flask. After the temperature reached to 80 ºC, a dropping funnel was connected on top of the condenser and 98% H_2SO_4 was added with a rate of one drop per second, and bath temperature was kept between 80–90 C. After addition about 40 mL H_2SO_4 reaction mixture became turbid. The addition of H_2SO_4 was continued until soft green precipitates appeared in the flask. H_2SO_4 (100 mL) was consumed and the overall reaction time was about 2 h. The

cooled reaction mixture was filtered and washed with water until neutral and then with EtOH 95% until the solid turned to brilliant white. The solids were dried in air or under vacuum. 10,41 g of product are recovered (43,7%). ^{1}H NMR (400 MHz, Chloroform-d) δ= 7.17 (s, 2H, Ar–H), 6.95 (d, J = 8.8 Hz, 2H, Ar–H), 6.86 (d, J = 6.7 Hz, 2H), 6.77 (d, J = 8.1 Hz, 1H, C–H), 4.93 (d, J = 6.7 Hz, 1H, C–H), 2.30 (s, 6H, C–H_3).

Synthesis of 2,10-Dimethyl-6,12-methano-12H-dibenzo[2,1-d: 1',2'-g] [1,3]dioxocine, 2.[3]

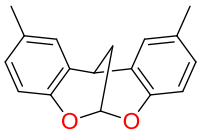
2

A 500 mL round-bottomed flask was charged p-cresol (31.3 mL, 296 mmol) in 2,2,2-trifluoroacetic acid (79 mL, 1021 mmol) to give a yellow solution. 1,1,3,3-tetramethoxypropane (25,00 mL, 148 mmol) was added. The reaction became red and a precipitate was formed. After 2 hours, 100 mL of acetic acid were added and it was filtered, washed with methanol and finally boiled with water to afford after filtration compound **2** (19.41 g, 77 mmol, 52,0 % yield) as a white-pink solid. ^{1}H NMR (400 MHz, Chloroform-d) δ= 7.00 (d, J = 2.2 Hz, 2H, Ar–H), 6.89 (ddd, J = 8.4, 2.1, 0.8 Hz, 2H, Ar–H), 6.79 (d, J = 8.2 Hz, 2H, Ar–H), 6.11 (q, J = 2.1 Hz, 1H, C–H), 3.87 (q, J = 2.6 Hz, 1H, C–H), 2.26 (s, 6H, C–H_3), 2.22 (dd, J = 3.0, 2.2 Hz, 2H, C–H_2).

Synthesis of 4,4,4',4',6,6'-hexamethyl-2,2'-spirobi[chroman], 3.[71]

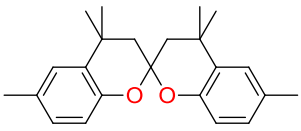
3

A two necked round bottom flask equipped with a reflux condenser was charged with 500 mL of p-cresol (4.8 mol). Methanesulfonic acid (6.3 mL, 97 mmol) was added and the temperature slowly increased to 120 ºC. At this temperature 45 mL of acetone (605 mmol) were added. The solution changed from yellow to intense orange and then to dark red. The reaction mixture was kept under reflux for several days, keeping after the second day an addition of acetone of 50 mL/day at 0.5 mL /min.The evolution of the reaction was controled by regular sampling: an aliquot is quenched with NaOH (0.1M), extracted with ether, dried over $MgSO_4$, diluted with ether, and analyzed by GCMS. After several days (5–10) the reaction mixture is cooled to room temperature (total acetone after 10 days 545 mL, 7.4 mol). The remaining p-cresol is distilled off under reduced pressure

(85–90 ºC). The black residue is dissolved in dichloromethane and quenched with NaOH 0.1 M. The aquous phase is extracted four times with dichloromethane, and the solvent evaporated. The solid obtained (a mixture of spirobischroman and tetramethylxantene) is recrystallized from MeOH to render pure spirobischroman. The average yield over several attempts is 20% calculated for p-cresol (136 g). From the remaining liquid also tetramethylxanthene can be recovered.[1]H NMR δ=7.11 (d, J = 2.6 Hz, 2H, Ar–H), 6.83 (dd, J = 8.1, 2.1 Hz, 2H, Ar–H), 6.57 (d, J = 8.2 Hz, 2H, Ar–H), 2.29 (s, 6H, C–H_3), 2.19 – 1.81 (m, 4H, C–H_2), 1.61 (s, 6H, C–H_3), 1.36 (s, 6H, C–H_3).

Synthesis of 2,3,9,10-tetramethyl-12H-6,12-methanodibenzo[d,g][1,3]dioxocine, 14.[3]

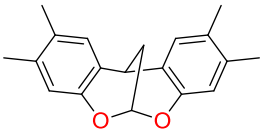
14

Compound **14** was prepared using the same procedure described above for compound **2**, but using compound 3,4.dimethylphenol as substrate. Yield: 37%. [1]H NMR (300 MHz, Chloroform-*d*) δ= 6.93 (s, 2H, Ar–H), 6.68 (s, 2H, Ar–H), 6.08 (d, *J* = 2.0 Hz, 1H, C–H), 3.82 (d, *J* = 2.5 Hz, 1H, C–H), 2.23 – 2.17 (m, 2H, C–H_2), 2.14 (d, *J* = 5.5 Hz, 12H, C–H_3).

Synthesis of 2,10-dimethyl-13-(p-tolyl)-12H-6,12-methanodibenzo[d,g][1,3]-dioxocine.

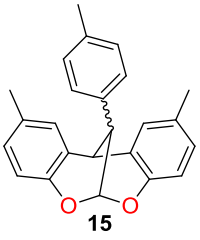
15

Compound **15** was prepared using the same procedure described above for compound **2**, but using compound 2-(p-tolyl)malonaldehyde as substrate, longer reaction time, 12 days are required. Yield: 20%. [1]H NMR (400 MHz, Chloroform-d) δ=7.16 (d, J = 8.1 Hz, 2H, Ar–H), 7.11 – 7.02 (m, 3H, Ar–H), 6.94 (ddd, J = 6.9, 2.1, 1.0 Hz, 2H, Ar–H), 6.89 – 6.84 (m, 2H, Ar–H), 6.78 (d, J = 8.2 Hz, 1H, Ar–H), 6.23 (t, J = 1.9 Hz, 1H, C–H), 4.07 (t, J = 2.2 Hz, 1H, C–H), 3.56 (t, J = 2.2 Hz, 1H, C–H), 2.30 (d, J = 4.9 Hz, 6H, C–H_3), 2.23 (s, 3H, C–H_3). [13]C NMR (101 MHz, Chloroform-*d*) δ=148.69, 148.60, 136.75, 134.10, 131.03, 130.66, 129.31, 128.66, 128.64, 128.37, 127.82, 127.47, 127.39, 123.97, 116.25, 115.97, 94.86, 39.12, 38.44, 20.99, 20.61, 20.56. ESI^+: calcd. for $C_{24}H_{22}NaO_2$ [M+] 365,15; found 365.1.

Synthesis of 6r,12r)-2,6,10,12-tetramethyl-12H-6,12-methanodibenzo[d,g]-[1,3]dioxocine.

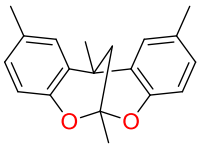

16

A 25 mL round-bottomed flask was charged p-cresol (3.87 mL, 36.6 mmol) and 2,4-pentadione (1.9 mL, 18.3 mmol) to give a yellow solution. Sulphuric acid was added dropwise (2 mL, 36.6 mmol) was added. The reaction became brown. After 7 days a precipitate was formed. The reaction was neutralized with aquous NaOH and extracted with EtOAc (10mLx3). The organic phase was evaporated and brown oil was recovered. Compound **16** was precipitated and cleaned with MeOH. Yield: 6%.^{1}H NMR (400 MHz, Chloroform-d) δ 7.11 (dd, J = 2.2, 0.9 Hz, 2H, Ar–H), 6.84 (ddd, J = 8.2, 2.1, 0.8 Hz, 2H, Ar–H), 6.73 (d, J = 8.2 Hz, 2H, Ar–H), 2.25 (t, J = 0.7 Hz, 6H, C–H_3), 2.11 (s, 2H, C–H_2), 1.82 (d, J = 3.1 Hz, 6H, C–H_3).[7]

Synthesis of 4,7-dibromo-2,9-dimethyl-5a,10b-dihydrobenzofuro[2,3-b]benzofuran, 17.[72]

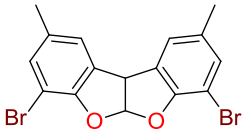

17

10.41 g of 2.9-dimethyl[5a,10b]dihydrobenzofuro[2,3-b]benzofuran (43,7 mmol) were charged in to a round bottomed flask. 500 mL of dimetylformaamide and 62.88 g of N-bromosuccinimide (349.6 mmol) are added. The reaction is stirring overnight in light absence. The solution was filtered and washed with 100 mL of DMF and with cold methanol. The product is recovered as white solid (5.02 g). The solution was removed. The solid is solved with ethanol. The NBS was extracted with a saturated solution of $Na_2S_2O_3$ (3x200mL). The organic phase was removed in vacuo. The product was isolated as a white solid (5.47 g). Total weight is 9.49 g (60,6%).^{1}H NMR (400 MHz, Chloroform-d) δ 7.14 (s, 2H, Ar–H), 7.07 (s, 2H, Ar–H), 6.94 (d, J = 6.7 Hz, 1H,C–H), 5.09 (d, J = 6.7 Hz, 1H, C–H), 2.29 (s, 6H, C–H_3).

Synthesis of 4,8-dibromo-2,10-dimethyl-12H-6,12-methanodibenzo[d,g]-[1,3]dioxocine, 18. [72]

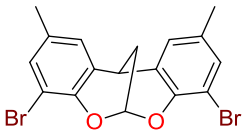

18

Compound **18** was prepared using the same procedure described above for compound **17**, but using 2,10-dimethyl-12H-6,12-methanodibenzo[d,g][1,3]-dioxocine

as substrate to brominate. Yield: 74%. ^{1}H NMR (400 MHz, Chloroform-d) δ=7.19 (dd, J = 1.9, 1.0 Hz, 2H Ar–H), 6.95 (d, J = 2.0 Hz, 2H Ar–H), 6.36 (q, J = 2.0 Hz, 1H, C–H), 3.91 (q, J = 2.7 Hz, 1H, C–H), 2.25 (d, J = 6.9 Hz, 8H, C–H_3 and C-H_2).

Synthesis of 4,8-dibromo-2,3,9,10-tetramethyl-12H-6,12-methanodibenzo-[d,g][1,3]dioxocine, 19.

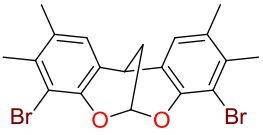

19

Compound **19** was prepared using the same procedure described above for compound **17**, but using 2,3,9,10-tetramethyl-12H-6,12-methanodibenzo-[d,g][1,3]dioxocine. ^{1}H NMR (300 MHz, Chloroform-d) δ 6.93 (s, 2H Ar–H), 6.41 – 6.35 (m, 1H C–H), 3.88 (q, J = 2.6 Hz, 1H C–H), 2.30 (s, 6H, C–H_3), 2.25 (s, 6H, C–H_3), 2.22 (t, J = 2.7 Hz, 2H, C–H_2). ^{13}C NMR (101 MHz, Chloroform-d) δ=145.91, 136.32, 130.30, 126.88, 124.41, 113.71, 92.85, 31.54, 25.49, 20.51, 19.49. ESI^{+}: calcd. for $C_{19}H_{18}Br_2NaO_2$ [M+] 460.96; found 460.9.

Synthesis of (6r,12r)-4,8-dibromo-2,6,10,12-tetramethyl-12H-6,12-methano-dibenzo[d,g][1,3]dioxocine, 20.

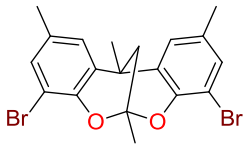

20

Compound **20** was prepared using the same procedure described above for compound **17**, but using (6r,12r)-2,6,10,12-tetramethyl-12H-6,12-methanodibenzo[d,g]-[1,3]dioxocine. ^{1}H NMR (400 MHz, Chloroform-d) δ=7.17 – 7.15 (m, 2H, Ar–H), 7.06 (dd, J = 2.1, 0.8 Hz, 2H, Ar–H), 2.26 (d, J = 0.7 Hz, 6H, C–H_3), 2.13 (s, 2H, C–H_2), 1.96 (s, 3H, C–H_3), 1.82 (s, 3H, C–H_3). ESI^{+}: calcd. for $C_{19}H_{18}Br_2NaO_2$ [M+] 460.96; found 460.9.

Synthesis of 8,8'-dibromo-4,4,4',4',6,6'-hexamethyl-2,2'-spirobi[chroman], 21.[71]

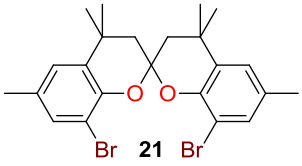

21

4,4,4',4',6,6'-hexamethyl-2,2'-spirobi[chroman] (2,5 g, 7,43 mmol), NBS (3.31 g, 18.5 mmol) and 35 mL of DMF. The resulting light oranged colured solution

was stirred at room temperature under dark for 3 days. The precipitate formed in the reaction was filtered off and the solid was washed with methanol (20 mL). The white solid was dried under vaccum. Yield: 3.05 g, 83%. ^{1}H NMR (300 MHz, Chloroform-d) δ= 7.13 – 7.02 (m, 4H, Ar–H), 2.26 (s, 6H, C–H_3), 2.25 – 2.02 (m, 4H, C–H_2), 1.75 (s, 6H, C–H_3), 1.36 (s, 6H, C–H_3).

Synthesis of 4,8-diiodo-2,10-dimethyl-12H-6,12-methanodibenzo[d,g]-[1,3]dioxocine, 25.

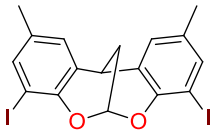

25

In a 250 mL round-bottomed flask was added 2,10-dimethyl-12H-6,12-methanodibenzo[d,g][1,3]-dioxocine (2.52 g, 10mmol) and 60 mL of DCM. Reaction was cooled to 0ºC and the iodine monochloride was added (3,73 g, 23 mmol). The reaction is stirring overnight in light absence. The purple suspension was filtered and washed with methanol. The solid was solubilized in EtOAc and extracted with saturated solution of $N_2S_2O_3$ (3x 20 mL) and water (20 mL). Organinc phase was dried over $MgSO_4$ and evapored. Yield: 3.02 g, 60%. ^{1}H NMR (400 MHz, Chloroform-d) δ=7.41 (d, J = 2.2 Hz, 2H, Ar–H), 6.97 (d, J = 2.4 Hz, 2H, Ar–H), 6.31 (q, J = 2.1 Hz, 1H, C–H), 3.84 (td, J = 2.9, 1.5 Hz, 1H, C–H), 2.24 – 2.23 (m, 6H, C–H_3), 2.21 (dd, J = 3.0, 2.2 Hz, 2H, C–H_2). ^{13}C NMR (75 MHz, Chloroform-*d*) δ=158.12, 138.43, 132.64, 128.15, 126.26, 93.30, 52.67, 32.40, 20.00, 4.24. ESI^{+}: calcd. for $C_{17}H_{14}I_2NaO_2$ [M+] 526.90; found 526.8.

Synthesis of spannitro (4,4,4',4',6,6'-hexamethyl-8,8'-dinitro-2,2'-spirobi [chroman]), 26.[62]

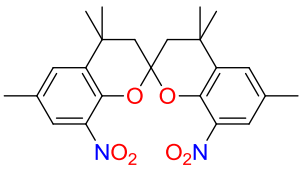

26

To SPANbackbone (10 g, 29.7 mmol) was added glacial acetic (650 mL). To the solution was then slowly added nitric acid (113 mL) at room temperature. The reaction mixture was then heated to 60°C for 25 min. Once at 55°C the mixture became clear dark orange with release of HNO_3 gas. Then ice and water was added that caused an important precipitate to come out. The precipitate was filtered and washed with important amount of water (until not acidic). Dichloromethane was then added to dissolve the solid in the filter and the organic phase separated and dried with $MgSO_4$. The dichloromethane solvent was finally removed in vacuo and the solid dried in

vacuo overnight to give pure compound **26**. Yield: 4.05 g, 33%. ^{1}H NMR (400 MHz, Chloroform-d): δ= 7.29 (s, 2 H, Ar–H), 7.25 (s, 2 H, Ar–H), 2.31 (s, 6 H, C–H_3), 2.22 (d, J = 14.3 Hz, 2 H, C–H_2), 2.12 (d, J = 14.3 Hz, 2 H, C–H_2), 1.55 (s, 6 H, C–H_3), 1.34 (s, 6 H, C–H_3).

Synthesis of spanamine ((4,4,4',4',6,6'-hexamethyl-2,2'-spirobi[chroman]-8,8'-diamine), 27. From 26 reduction. [62]

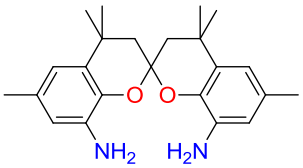

27

SPANnitro (3.78 g, 8.85 mmol) was mixed with concentrated HCl (35 mL) and ethanol (40 mL) under nitrogen. Tin powder (8.60 g, 72.5 mmol) was added portionwise and the mixture heated to reflux for 1h under nitrogen. During that time the heterogeneous solution became a yellow homogeneous solution. Ice was added to the solution that caused a precipitate to come out followed by addition of solid $NaHCO_3$ until neutralization of the mixture (pH=8). Water was also added to help neutralization. An important precipitate came out after neutralization. The mixture was then extracted with ethyl acetate (3x300mL). The combined organic layers were dried over $MgSO_4$ and then filtered over a pad of celite to remove small particles. The solvent was evaporated in vacuum to leave a brownish powder. The solid was washed with MeOH to leave an off-white powder. ^{1}H NMR (400 MHz, Chloroform-d): ^{1}H NMR (399 MHz, Chloroform-*d*) δ= 6.52 (d, *J* = 2.0 Hz, 2H, Ar–H), 6.32 (d, *J* = 0.9 Hz, 2H, Ar–H), 3.30 (b, 4H, N–H_2), 2.20 (t, *J* = 0.7 Hz, 6H, C–H_3), 2.17 (d, *J* = 14.2 Hz, 2H, C–H_2), 2.06 (d, *J* = 14.1 Hz, 2H, C–H_2), 1.55 (s, 6H, C–H_3), 1.33 (s, 6H, C–H_3).

SPANamine enantiomeric resolution

The composition for mobile phase was, 66% $CHCl_3$, 33% hexane, 0.9% isopropanol, 0.1% diethylamine. The SPANamine was solved in the mobile phase, filtered and injected in the column. The flux was 4.7 mL/min. The first enantiomer was the (+) spanamine at 4.0 minutes and the second the (-) Spanamine at 5.2 minutes.

General procedure for Buchwald-Hartwig amination reaction catalized by phosphine-palladium system.

A Schlenk was charged wiht Pd precursor and the ligand. Solvent was added and the solution was stirred for 30 minuts. Then halogenated compound, base, and amine were added. Reaction was heated (if it was necessary) and reaction stirred for different time. After that 0.25mL of the crude of reaction was filtered through cotton, silice and celite, 0.75 mL of DCM was added and GC analysis were performed.

General procedure for Buchwald-Hartwig amination reaction catalized by palladium-carbene complex.

A Schlenk tube was charged with halogenated compound (0.5 mmol), amine (1.2 mmol.), (SIPr)Pd(methallyl)Cl (0.03 mmol). The system was sealed with a septum. The flask was evacuated and backfilled with inert gas three times, after which lithium bis(trimethylsilyl)amide (1.1 mmol.) was added. Reaction was heated up to 70 ºC and reaction stirred for different time. After that 0.25mL of the crude of reaction was filtered through cotton, silice and celite, 0.75 mL of DCM was added and GC analysis were performed.

Synthesis of 4,4'-(2,10-dimethyl-12H-6,12-methanodibenzo[d,g][1,3]dioxocine-4,8-diyl)bis(1-methylpiperazine), 44

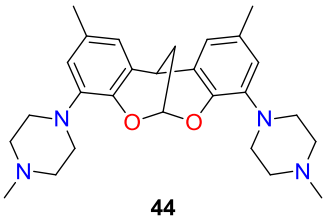

44

Compound **44** was prepared using the procedure described above for Buchwald-Hartwig amination reaction catalized by palladium-carbene complex. Reaction temperature: 70 ºC, time: 6 hours. Work up: Addition of 20 mL of EtOAc and and filtration over a pad of celite. The solution was extracted with water (3x20mL). The combined organic layer was dried over $MgSO_4$ and filtered. The solvent was evaporated in vacuum to leave a white powder. Yield: 90%. ^{1}H NMR (400 MHz, Chloroform-d) δ=6.67 (d, J = 1.6 Hz, 2H, Ar–H), 6.56 (d, J = 1.8 Hz, 2H, Ar–H), 6.31 (d, J = 1.8 Hz, 1H, C–H), 3.83 – 3.78 (m, 1H, C–H), 3.24 (b, 4H, C–H_2), 2.86 (b, 4H, C–H_2), 2.62 (b, 8H, C–H_2), 2.35 (s, 6H, C–H_3), 2.22 (s, 6H, C–H_3), 2.22 – 2.20 (m, 2H, C–H_2). ^{13}C NMR (100 MHz, Chloroform-d) δ 141.36, 140.21, 130.73, 127.29,

121.98, 117.96, 92.19, 55.48, 50.76, 46.28, 32.38, 25.17, 21.03. ESI$^+$ $C_{27}H_{36}N_4O_2$ (448,60): calcd. C, 72.29; H, 8.09; found C, 72.09; H, 8.15.

Synthesis of N^8,$N^{8'}$-dibenzyl-4,4,4',4',6,6'-hexamethyl-2,2'-spirobi-[chroman]-8,8'-diamine, 53.

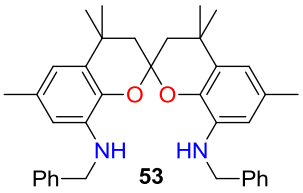

53

Compound **55** was prepared using the procedure described above for Buchwald-Hartwig amination reaction catalized by palladium-carbene complex. Reaction temperature: 70 ºC, time: 16 hours. Work up. The product was precipitated with methanol and filtered. Yield 90%. ^{1}H NMR (399 MHz, Chloroform-d) δ 7.20 – 7.10 (m, 6H, Ar–H), 6.96 – 6.90 (m, 4H, Ar–H), 6.35 (d, J = 1.8 Hz, 2H, Ar–H), 6.16 – 6.10 (m, 2H, Ar–H), 4.05 (dd, J = 13.5, 4.9 Hz, 2H, C–H_2), 3.93 – 3.82 (m, 4H, C-H_2 and N–H), 2.13 (s, 6H, C–H_3), 2.10 – 1.98 (m, 4H, C–H_2), 1.35 (s, 6H, C-H_3), 1.24 (s, 6H, C-H_3).[93]

Synthesis of Spanamine ((4,4,4',4',6,6'-hexamethyl-2,2'-spirobi[chroman]-8,8'-diamine), 27. From 53 cleavage.

A Schlenk tube was charged with SPANbnamine (2.3319 g, 4.5 mmol) and Pd/C 10% (2.3 g) and a magnetic stirrer bar. The system is sealed with a septum. The flask was evacuated and backfilled with inert gas three times. Then anhydrous methanol was added (50 mL) and the system was heated to 65ºC. At this temperature ammonium formate (22.5 mmol) was added. After two hours the solution was cooled and EtOAc was added. The solution was filtered through celite and the solution was evaporated. Yield 95%.

General procedure for Ullmann coupling reaction catalized by copper.

A Schlenk tube was charged with mixture of aryl halide (1 mmol), amine (2.4 mmol), base (10 mmol), Cu (0.1mmol) and ligand (if it was required) (0.2 mmol) in 1 mL of solvent. Reaction was heated (if it was necessary) and reaction stirred for different time. 0.25 mL of the crude of reaction was filtered through cotton, silice and celite, 0.75 mL of DCM was added and GC analysis were performed. The cooled mixture was partitioned between water and ethylacetate. The organic layer was separated, and the aqueous layer was extracted with

ethyl acetate. The combined organic layers were washed with brine, dried over Na_2SO_4, and concentrated in vacuo.

General procedure for Ullmann-amination with sodium azide

A Schlenk tube was charge with ligand (1.30 mmol), NaN_3 (130 mg, 2.00 mmol), CuI (190 mg, 1.0 mmol), and halogenated backbone (228 mg, 1.0 mmol). Degassed DMSO (2.0 mL) was added while flushing with argon. The flask was then placed in an oil bath maintained at 100 ºC. The solution turned from dark red to dark brown over the course of the reaction. After completion of the reaction as judged by TLC, the dark solution was cooled and quenched by the addition of saturated aquous NH_4Cl (3 mL) and EtOAc (2 mL). This biphasic mixture was stirred at 22 ºC for 1 h. The resulting dark green solution was filtered through a pad of Celite, which was subsequently washed with EtOAc and water. The filtrate was extracted with EtOAc and washed with brine. Finally the organic phases were combined, dried with $MgSO_4$, filtered, and concentrated.

Synthesis of 2,9-dimethyl-5a,10b-dihydrobenzofuro[2,3-b]benzofuran-4,7-diamine, 60.

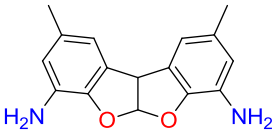

60

Compound **60** was prepared using the procedure described above for copper amination with sodium azide. Reaction time: 16 hours. The solid was loaded on a neutralized silica gel column and eluted with DCM to afford pure compound **60**. Yield: 37%. ^{1}H NMR (500 MHz, DMSO-d_6) δ = 6.88 (d, *J* = 6.7 Hz, 1H, C–H), 6.48 (d, J = 1.6 Hz, 2H, Ar–H), 6.30 (d, J = 1.5 Hz, 2H, Ar–H), 4.91 (d, *J* = 6.7 Hz, 1H, C–H), 4.70 (b, 4H, N–H_2), 2.13 (s, 6H, C–H_3). ^{13}C NMR (126 MHz, DMSO-d_6) δ = 142.41, 132.26, 131.36, 127.58, 115.11, 112.43, 51.47. ESI$^+$: calcd. for $C_{16}H_{16}N_2NaO_2$ [M+] 291.11; found 291.1

General procedure for Ullmann-amination with liquid ammonia.

A 40 mL reactor was charged with halogenated compound (6 mmol), copper oxide (I) (2 mmol), and 12 mL of 1,2-ethanediol. The mixture was cooled in an acetone/CO_2 bath, while 12 mL of ammonia were condensed with an acetone/CO_2 bath. The liquid ammonia was added to the solid solution of 1,2-

ethanediol. The reactor was closed and temperature was increased to 110ºC. Reaction was stopped after 3 days. Water (200 mL) and DCM (200 mL) were added to the dark blue solution. The aqueous phase is extracted with DCM (3x200 mL). The organic phases were combined and cleaned with 100 mL of brine. Finally the organic phase was dried with $MgSO_4$, filtered, and dried. The yellowish solid was loaded on a silica gel column and eluted with DCM to afford pure compound.

Synthesis of 2,10-dimethyl-12H-6,12-methanodibenzo[d,g][1,3]dioxocine-4,8-diamine, 61.

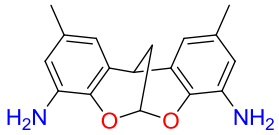

61

Compound **61** was prepared using the procedure described above for Ullmann-amination with liquid ammonia using 4,8-dibromo-2,10-dimethyl-12H-6,12-methanodibenzo[d,g]-[1,3]dioxocine as substrate. Yield: 90% ^{1}H NMR (400 MHz, Chloroform-*d*) δ= 6.45 (s, 2H, Ar–H), 6.41 – 6.34 (m, 2H, Ar–H), 6.25 (q, *J* = 2.0 Hz, 1H, C–H), 3.79 (td, *J* = 3.0, 1.4 Hz, 1H, C–H), 2.23 (dd, *J* = 3.1, 2.1 Hz, 2H, C–H_2), 2.21 (s, 6H, C–H_3). ^{13}C NMR (101 MHz, Chloroform-*d*) δ= 136.58, 134.46, 130.75, 126.44, 117.40, 114.88, 91.97, 31.32, 25.98, 20.78. ESI$^+$: calcd. for $C_{17}H_{18}N_2NaO_2$ [M+] 315.13; found 305.1.

As by-product was recovered and characterized, 2,10-dimethyl-12H-6,12-methanodibenzo[d,g][1,3]dioxocin-4-amine.

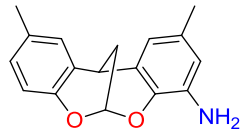

^{1}H NMR (300 MHz, Chloroform-*d*) δ = 7.03 – 6.98 (m, 1H, Ar–H), 6.90 (ddd, *J* = 8.3, 2.1, 0.8 Hz, 1H, Ar–H), 6.79 (d, *J* = 8.3 Hz, 1H, Ar–H), 6.45 (dt, *J* = 2.0, 0.7 Hz, 1H, Ar–H), 6.38 (dd, *J* = 2.0, 0.7 Hz, 1H, Ar–H), 6.18 (td, *J* = 2.2, 1.6 Hz, 1H, C–H), 3.83 (q, *J* = 2.2, 1.5 Hz, 1H, C–H), 3.73 (b, 2H, N–H_2), 2.27 (s, 3H, C–H_3), 2.23 (dd, *J* = 3.0, 2.2 Hz, 2H, C–H_2), 2.20 (s, 3H, C–H_3). ^{13}C NMR (126 MHz, Chloroform-d) δ = 148.72, 136.46, 134.69, 130.85, 130.53, 128.48, 127.96, 126.46, 117.09, 116.10, 114.84, 92.09, 31.54, 25.85, 20.77, 20.54. ESI$^+$: calcd. for $C_{17}H_{17}NNaO_2$ [M+] 290.12; found 290.1

Synthesis of 2,3,9,10-tetramethyl-12H-6,12-methanodibenzo[d,g][1,3]dioxocine-4,8-diamine, 64.

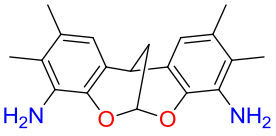

64

Compound **64** was prepared using the procedure described above for Ullmann-amination with liquid ammonia using 4,8-dibromo-2,3,9,10-tetramethyl-12H-6,12-methanodibenzo-[d,g][1,3]dioxocine as substrate. Yield: 90%. ^{1}H NMR (300 MHz, Chloroform-*d*) δ = 6.49 (s, 2H, Ar–H), 6.27 (q, *J* = 2.1 Hz, 1H, C–H), 3.77 (td, *J* = 3.1, 1.5 Hz, 1H, C–H), 3.51 (b, 4H, N–H_2), 2.23 (dd, *J* = 3.1, 2.2 Hz, 2H, C–H_2), 2.19 (s, 6H, C–H_3), 2.01 (s, 6H, C–H_3). ^{13}C NMR (75 MHz, Chloroform-*d*) δ 136.59, 132.80, 129.07, 123.75, 119.84, 117.41, 92.01, 30.93, 26.25, 19.94, 12.84. ESI^{+}: calcd. for $C_{19}H_{22}N_2NaO_2$ [M+] 333.16; found 333.1

Synthesis of N^4,N^8,2,10-tetramethyl-12H-6,12-methanodibenzo[d,g][1,3]dioxocine-4,8-diamine, 65

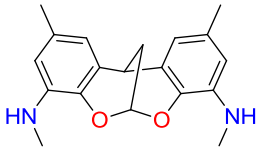

65

The reactor was charged with halogenated compound (6 mmol), copper oxide (I) (2 mmol), 12 mL of methylamine 33% in ethanol, and 12 mL of 1,2-ethanediol. The reactor was closed and temperature was increased to 110ºC. Reaction was stopped after 3 days. Water (200 mL) and DCM (200 mL) were added to the dark blue solution. The aqueous phase was extracted with DCM (3x200 mL). The organic phases were combined and cleaned with 100 mL of brine. Finally the organic phase was dried with $MgSO_4$, filtered, and evaporated. The yellowish solid was loaded on a silica gel column and eluted with DCM to afford pure compound. ^{1}H NMR (400 MHz, Chloroform-*d*) δ = 6.41 (d, *J* = 2.3 Hz, 2H, Ar–H), 6.27 (d, *J* = 1.9 Hz, 2H, Ar–H), 6.22 (q, *J* = 2.0 Hz, 1H, C–H), 3.78 (td, *J* = 3.1, 1.5 Hz, 1H, C–H), 2.82 (s, 6H, C–H_3), 2.26 (s, 6H, C–H_3), 2.22 (dd, *J* = 3.1, 2.2 Hz, 2H, C–H_2).). ^{13}C NMR (75 MHz, Chloroform-*d*) δ = 137.98, 136.16, 131.20, 125.68, 115.69, 109.64, 92.17, 31.40, 30.64, 26.21, 21.4. $C_{19}H_{22}N_2O_2$ (310,39): calcd. C, 73.52; H, 7.14; found C, 73.39; H, 7.25. ESI^{+}: calcd. for $C_{19}H_{22}N_2O_2$ [M+] 311.17; found 311.

Synthesis of (N^{4}E,N^{8}E)-2,10-dimethyl-N4,N8-bis(pyridin-2-ylmethylene)-12H-6,12-methanodibenzo[d,g][1,3]dioxocine-4,8-diamine, 66.

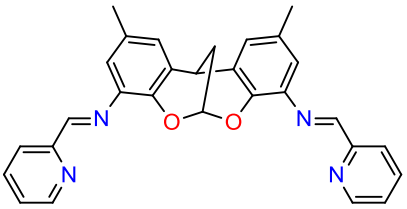

66

In a Schlenk tube was charged with 2,10-dimethyl-12H-6,12-methanodibenzo[d,g]-[1,3]dioxocine-4,8-diamine, (0.5 mmol), picolialdehyde (1 mmol) and 9 mL of THF. Then $MgSO_4$ was added. The reaction was stirred for 16 hours. Filtration was done and the solution evaporate yielding a yellow solid. Yield: 95%. ^{1}H NMR (400 MHz, Chloroform-*d*) δ = 8.72-69 (m, 2H, Ar–H), 8.60 (s, 2H, N=C–H), 8.25 (d, J = 7.9 Hz, 2H, Ar–H), 7.85 (td, J = 7.6, 1.3 Hz, 2H, Ar–H) 7.40 (ddd, J = 7.4, 4.8, 1.2 Hz, 2H, Ar–H), 7.01 (d, J= 1.7 Hz, 2H, Ar–H), 6.80 (d, J = 1.5 Hz, 2H, Ar–H), 6.30 (d, J = 1.7 Hz, 1H, C–H), 4.05 (d, J = 1.5 Hz, 1H, C–H), 2.38-35 (m, 2H, C–H_2), 2.34 (s, 6H, C–H_3). ^{13}C NMR (75 MHz, Chloroform-*d*) δ = 161.87, 154.8, 149.59, 141.67, 139.38, 136.51, 131.08, 127.48, 125.88, 125.08, 121.36, 119.36, 92.31, 31.77, 25.20, 20.27. $C_{29}H_{24}N_4O_2$ (460.19): calcd. C, 75.63; H, 5.25; found C, 75.39; H, 5.30. EI$^+$: calcd. for $C_{29}H_{24}N_4O_2$ [M+] 460; found 460.

Synthesis of (N^{4}E,N^{8}E)-2,10-dimethyl-N^4,N^8-bis(pyridin-2-ylmethylene)-12H-6,12-methanodibenzo[d,g][1,3]dioxocine-4,8-diamine, 67.

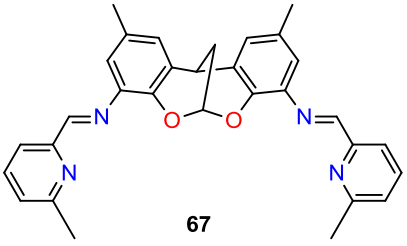

67

Compound **67** was prepared using the same procedure described above for compound **66**, but using 6-methylpicolinaldehyde. Yield: 70% ^{1}H NMR (500 MHz, Chloroform-*d*) δ = 8.58 (d, *J* = 0.6 Hz, 2H, N=C–H), 8.10 (d, *J* = 7.6 Hz, 2H, Ar–H), 7.69 (t, *J* = 7.8 Hz, 2H, Ar–H), 7.24 – 7.20 (m, 2H, Ar–H), 6.99 – 6.95 (m, 2H, Ar–H), 6.79 (dd, *J* = 2.2, 0.9 Hz, 2H, Ar–H), 6.38 (q, *J* = 2.0 Hz, 1H, C–H), 3.99 (q, *J* = 2.7 Hz, 1H, C–H), 2.63 (s, 6H, C–H_3), 2.33 – 2.30 (m, 8H, C–H_2 and C–H_3). ^{13}C NMR (126 MHz, Chloroform-d) δ = 162.07,154.21, 141.75, 137.13, 136.70, 130.77, 125.86, 124.68, 119.99, 119.09, 119.05, 117.04, 92.10, 24.34, 20.56, 1.02. $C_{31}H_{28}N_4O_2$ (488,58): calcd. C, 76.21; H, 5.78; found C, 76.02; H, 5.91 . ESI$^+$: calcd. for $C_{31}H_{28}N_4O_2Na^+$ [M+] 511.21; found 511.1.

Synthesis of (N^4E,N^8E)-2,10-dimethyl-N^4,N^8-bis((6-methoxypyridin-2-yl)methylene)-2,10-dimethyl-12H-6,12-methanodibenzo[d,g][1,3]dioxocine-4,8-diamine, 68.

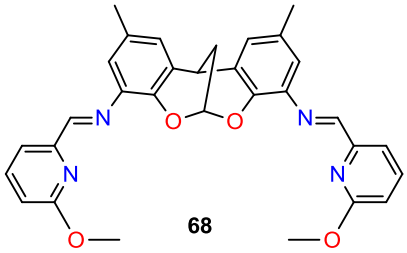

68

Compound **68** was prepared using the same procedure described above for compound **66**, but using 6-methoxypicolinaldehyde. Yield: 85%. . Yield: 70%. ^{1}H NMR (500 MHz, Chloroform-*d*) δ = 8.46 (d, *J* = 2.1 Hz, 2H, N=C–H), 7.85 (dd, *J* = 7.3, 0.9 Hz, 2H, Ar–H), 7.67 (ddd, *J* = 8.0, 7.4, 0.7 Hz, 2H, Ar–H), 6.96 (d, *J* = 2.1 Hz, 2H, Ar–H), 6.81 (dd, *J* = 8.2, 0.8 Hz, 2H, Ar–H), 6.76 (dd, *J* = 2.1, 0.8 Hz, 2H, Ar–H), 6.39 – 6.37 (m, 1H,C–H), 3.99 (s, 7H, C–H and C–H_3), 2.32 (s, 8H, C–H_2 and C–H_3). ^{13}C NMR (126 MHz, Chloroform-*d*) δ = 163.88, 161.88, 152.26, 141.76, 139.61, 138.83, 130.73, 127.25, 125.77, 119.77, 115.00, 112.56, 92.27, 53.43, 31.91, 25.24, 20.59. $C_{31}H_{28}N_4O_4$ (488,58): calcd. C, 71.52; H, 5.42; found C, 70.64; H, 5.63 . ESI$^+$: calcd. for $C_{31}H_{28}N_4O_4Na^+$ [M+] 543.20; found 543.1.

Synthesis of (N^4E,N^8E)-2,10-dimethyl-N^4,N^8-bis((6-phenylpyridin-2-yl)methylene)-12H-6,12-methanodibenzo[d,g][1,3]dioxocine-4,8-diamine, 69.

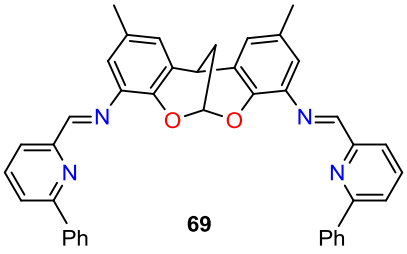

69

Compound **69** was prepared using the same procedure described above for compound **66**, but using 6-phenylpicolinaldehyde. Yield: 66% ^{1}H NMR (500 MHz, Chloroform-*d*) δ = 8.71 (s, 2H, N=C–H), 8.27 (ddd, *J* = 9.0, 7.7, 1.1 Hz, 2H, Ar–H), 8.07 (ddd, *J* = 11.0, 8.4, 1.4 Hz, 4H), 7.92 – 7.77 (m, 4H, Ar–H), 7.55 – 7.44 (m, 4H, 2H, Ar–H), 6.98 (d, *J* = 2.1 Hz, 2H, Ar–H), 6.81 (d, *J* = 2.1Hz, 2H, Ar–H), 6.33 (d, *J* = 1.9 Hz, 1H, C–H), 3.91 (d, *J* = 2.0 Hz, 1H, C–H), 2.41 – 2.25 (m, 8H, C–H_2 and C–H_3). $C_{41}H_{32}N_4O_2$ (612,25): calcd. C, 80.37; H, 5.26; found C, 80.02; H, 5.82 . EI$^+$: calcd. for $C_{41}H_{32}N_4O_2Na^+$ [M+] 635.24; found 635.1.

Synthesis of (N^4E,N^8E)-2,10-dimethyl-N^4,N^8-bis((6-bromopyridin-2-yl)methylene)-2,10-dimethyl-12H-6,12-methanodibenzo[d,g][1,3]dioxocine-4,8-diamine, 70

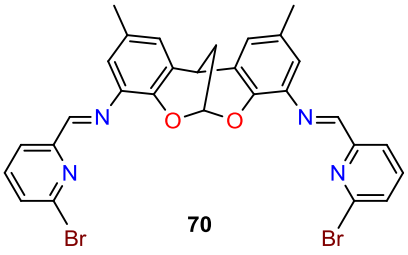

70

Compound **70** was prepared using the same procedure described above for compound **66**, but using 6-bromopicolinaldehyde. Yield: 73%. ^{1}H NMR (500 MHz, Chloroform-d) δ = 8.60 (d, J = 0.7 Hz, 2H, N=C–H), 8.27 (dd, J = 7.7, 1.0 Hz, 2H, Ar–H), 7.67 (td, J = 7.7, 0.7 Hz, 2H, Ar–H), 7.55 (dd, J = 7.8, 0.9 Hz, 2H, Ar–H), 6.98 (dt, J = 2.1, 0.7 Hz, 2H, Ar–H), 6.80 (dd, J = 2.2, 0.8 Hz, 2H, Ar–H), 6.36 (d, J = 1.9 Hz, 1H, C–H), 4.01 (q, J = 2.6 Hz, 1H, C–H), 2.36 – 2.26 (m, 8H, C–H_2 and C–H_3). ^{13}C NMR (126 MHz, Chloroform-d) δ 160.19, 156.00, 141.76, 141.55, 138.82, 138.52, 130.99, 129.39, 127.34, 126.45, 120.44, 92.26, 31.83, 25.16, 20.56, 1.03. $C_{29}H_{22}Br_2N_4O_2$ (618.32): calcd. C, 56.33; H, 3.59; found C, 55.12; H, 3.76. ESI$^+$: calcd. for $C_{29}H_{22}Br_2N_4O_2Na^+$ [M+] 641.0; found 640.9

Synthesis of (N^4E,N^8E)-2,10-dimethyl-N^4,N^8-bis((5-bromopyridin-2-yl)methylene)-2,10-dimethyl-12H-6,12-methanodibenzo[d,g][1,3]dioxocine-4,8-diamine, 71

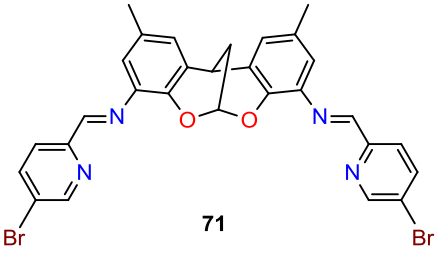

71

Compound **71** was prepared using the same procedure described above for compound **66**, but using 5-bromopicolinaldehyde. Yield: 94%. ^{1}H NMR (500 MHz, Chloroform-d) δ = 8.75 (dd, J = 2.4, 0.8 Hz, 2H, Ar–H), 8.57 (d, J = 0.7 Hz, 2H, N=C–H), 8.17 (dd, J = 8.4, 0.8 Hz, 2H, Ar–H), 7.93 (ddd, J = 8.5, 2.4, 0.7 Hz, 2H, Ar–H), 6.98 (d, J = 2.1 Hz, 2H, Ar–H), 6.78 (dd, J = 2.1, 0.9 Hz, 2H, Ar–H), 6.36 (d, J = 1.8 Hz, 1H, C–H), 4.01 (d, J = 2.2 Hz, 1H, C–H), 2.32 (s, 8H, C–H_2 and C–H_3). ^{13}C NMR (126 MHz, Chloroform-d) δ = 160.62, 153.25, 150.62, 141.71, 139.23, 138.90, 130.97, 127.33, 126.27, 122.94, 122.59, 120.16, 92.29, 31.83, 25.19, 20.57. $C_{29}H_{22}Br_2N_4O_2$ (618.32): calcd. C, 56.33; H, 3.59; found C, 56.27; H, 4.01. ESI$^+$: calcd. for $C_{29}H_{22}Br_2N_4O_2Na^+$ [M+] 641.0; found 640.9

Synthesis of (N^{4}E,N^{8}E)-2,10-dimethyl-N^4,N^8-bis(quinolin-2-ylmethylene)-12H-6,12-methanodibenzo[d,g][1,3]dioxocine-4,8-diamine, 72.

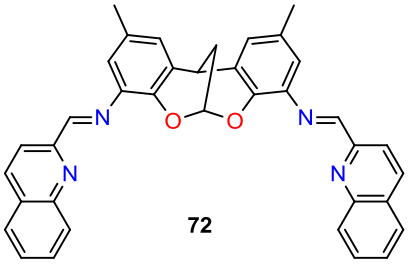

72

Compound **72** was prepared using the same procedure described above for compound **66**, but using quinoline-2-carbaldehyde. Yield: 80 %. ^{1}H NMR (400 MHz, Chloroform-*d*) δ = 8.72 (s, 2H, N=C–H), 8.34 (d, J = 8.5 Hz, 2H, Ar–H), 8.25 (d, J = 8.6 Hz, 2H, Ar–H), 8.10 (t, J = 8.7 Hz, 2H, Ar–H), 7.88 (d, J = 7.5 Hz, 2H, Ar–H), 7.74 (ddd, J = 8.4, 6.9 1.4 Hz, 2H, Ar–H), 7.59 (ddd, J = 8.0, 6.9 1.0 Hz, 2H, Ar–H), 7.01 (d, J= 1.7 Hz, 2H, Ar–H), 6.84 (d, J= 1.7 Hz, 2H, Ar–H), 6.32 (d, J = 1.7 Hz, 1H, C–H), 4.04 (d, J = 1.5 Hz, 1H, C–H), 2.36-33 (m, 2H, C–H_2), 2.31 (s, 6H, C–H_3). ^{13}C NMR (75 MHz, Chloroform-*d*) δ = 162.58, 155.59, 148.59, 142.39, 139.76, 137.07, 131.72, 130.29, 129.70, 126.46, 128.32, 128.17, 128.13, 126.77, 120.10, 119.05, 92.97, 32,35, 26.13, 20.85. $C_{37}H_{28}N_4O_2$ (560.22): calcd. C, 79.27; H, 5.03; found C, 78.39; H, 5.29. EI$^+$: calcd. for $C_{37}H_{28}N_4O_2$ [M+] 560; found 560.

Synthesis of (N^{4}E,N^{8}E)-2,10-dimethyl-N^4,N^8 -bis(quinolin-8-ylmethylene)-12H-6,12-methanodibenzo[d,g][1,3]dioxocine-4,8-diamine, 73.

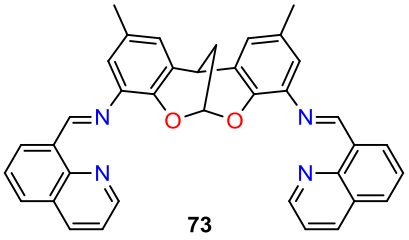

73

Compound **73** was prepared using the same procedure described above for compound **66**, but using quinoline-8-carbaldehyde. Yield: 65%. ^{1}H NMR (400 MHz, Chloroform-*d*) δ = 9.87 (s, 2H, N=C–H), 8.98 (dd, J = 4.0, 1.7 Hz, 2H, Ar–H), 8.69-66 (m, 2H, Ar–H), 8.26 (dd, J = 8.3, 1.5 Hz, 2H, Ar–H), 8.04-7.99 (m, 2H, Ar–H), 7.71 (t, J = 7.7 Hz, 2H, Ar–H), 7.49 (dd, J = 8.3, 4.1, 2H, Ar–H), 7.03 (s, 2H, Ar–H), 6.87 (s, 2H, Ar–H), 6.36 (d, J = 8.5, 1H, C–H), 4.08 (s, 1H, C–H), 2.40-39 (m, 2H, C–H_2), 2.37 (s, 6H, C–H_2). ^{13}C NMR (75 MHz, Chloroform-*d*) δ = 158.39, 150.28, 146.93, 141.99, 140.96, 136.24, 133.11, 131.11, 130.95, 128.27, 127.79, 127.41, 126.45, 125.32, 121.39, 119.19, 92.35, 31.89, 25.35, 20.35. $C_{37}H_{28}N_4O_2$ (560.22): calcd. C, 79.27; H, 5.03; found C, 78.39; H, 5.29. EI$^+$: calcd. for $C_{37}H_{28}N_4O_2$ [M+] 560; found 560.

Synthesis of (E)-2,10-dimethyl-N-(pyridin-2-ylmethylene)-12H-6,12-methanodibenzo[d,g][1,3]dioxocin-4-amine, 74.

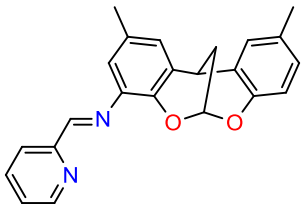

74

Compound **74** was prepared using the same procedure described above for compound **66**, but using 2,10-dimethyl-12H-6,12-methanodibenzo[d,g][1,3]dioxocin-4-amine. Yield: 90%. ^{1}H NMR (500 MHz, Chloroform-d) δ = 8.71 (ddd, J = 4.8, 1.7, 0.9 Hz, 1H, Ar–H), 8.61 (d, J = 0.7 Hz, 1H), 8.30 (dt, J = 7.9, 1.1 Hz, 1H, N=C–H), 7.85 – 7.78 (m, 1H, Ar–H), 7.37 (ddd, J = 7.5, 4.8, 1.2 Hz, 1H, Ar–H), 7.05 (dd, J = 2.2, 0.8 Hz, 1H, Ar–H), 6.96 – 6.90 (m, 2H, Ar–H), 6.82 (d, J = 8.1 Hz, 1H, Ar–H), 6.77 (dd, J = 2.1, 0.9 Hz, 1H, Ar–H), 6.26 (q, J = 2.1 Hz, 1H, C–H), 3.95 (q, J = 2.6 Hz, 1H, C–H), 2.32 – 2.29 (m, 6H, C–H_3), 2.29 – 2.25 (m, 2H, C–H_2). ^{13}C NMR (126 MHz, Chloroform-d) δ = 161.91, 154.75, 149.52, 141.73, 139.31, 136.51, 130.82, 130.59, 128.66, 127.77, 127.55, 126.15, 125.95, 125.04, 121.93, 119.88, 116.39, 92.22, 31.84, 25.46, 20.57, 20.55. $C_{23}H_{20}N_2O_2$ (356,42): calcd. C, 77.51; H, 5.66; found C, 77.24; H, 5.85. ESI$^+$: calcd. for $C_{23}H_{20}N_2O_2Na^+$ [M+] 379.14; found 379.1.

Synthesis of (N^4E,N^8E)-2,3,9,10-tetramethyl-N^4,N^8-bis(pyridin-2-ylmethylene)-12H-6,12-methanodibenzo[d,g][1,3]dioxocine-4,8-diamine, 75.

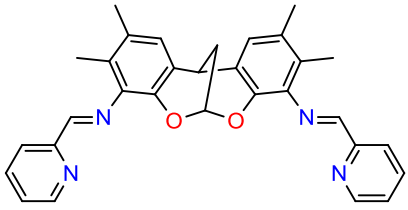

75

Compound **75** was prepared using the same procedure described above for compound **66**, but using 2,3,9,10-tetramethyl-12H-6,12-methanodibenzo-[d,g][1,3]dioxocine-4,8-diamine. Yield: 93% ^{1}H NMR (500 MHz, Chloroform-*d*) δ = 8.70 (ddd, *J* = 4.9, 1.7, 0.9 Hz, 2H, Ar–H), 8.57 (s, 2H), 8.32 (dt, *J* = 7.9, 1.1 Hz, 2H, N=C–H), 7.84 – 7.78 (m, 2H, Ar–H), 7.36 (ddd, *J* = 7.5, 4.9, 1.3 Hz, 2H, Ar–H), 6.10 (q, *J* = 2.0 Hz, 1H, C–H), 3.94 (q, *J* = 2.6 Hz, 1H, C–H), 2.26 (s, 6H, C–H_3), 2.21 (s, 2H, C–H_2), 2.13 (s, 6H, C–H_3). ^{13}C NMR (126 MHz, Chloroform-*d*) δ 164.62, 155.03, 149.35, 138.10, 137.96, 136.46, 132.97, 124.94, 124.66, 124.43, 121.43, 91.93, 31.65, 25.90, 19.62, 14.31.ESI$^+$: calcd. for $C_{31}H_{28}N_4O_2Na^+$ [M+] 511.21; found 511.1.

Synthesis of 2,2'-((1E,1'E)-((2,10-dimethyl-12H-6,12-methanodibenzo-[d,g][1,3]dioxocine-4,8-diyl)bis(azanylylidene))bis(methanylylidene))-diphenol, 76.

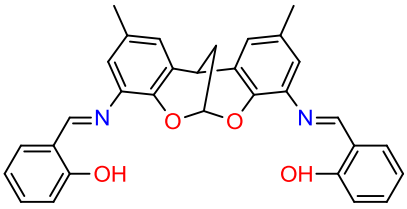

76

Compound **76** was prepared using the same procedure described above for compound **66**, but using 2-hydroxybenzaldehyde. Yield: 90% 1H NMR (500 MHz, Chloroform-d) δ = 8.68 (s, 2H, N=C–H), 7.41 – 7.34 (m, 4H, Ar–H), 7.06 – 7.02 (m, 2H, Ar–H), 6.98 (d, J = 2.0 Hz, 2H, Ar–H), 6.92 (td, J = 7.5, 1.1 Hz, 2H, Ar–H), 6.87 (dd, J = 2.1, 0.8 Hz, 2H, Ar–H), 6.34 (q, J = 2.0 Hz, 1H, C–H), 4.00 (q, J = 2.6 Hz, 1H, C–H), 2.34 (t, J = 0.7 Hz, 6H, C–H_3), 2.31 (t, J = 2.6 Hz, 2H, C–H_2). ^{13}C NMR (126 MHz, Chloroform-d) δ = 162.85, 161.51, 142.09, 135.96, 132.91, 132.09, 130.89, 127.49, 126.17, 119.63, 119.46, 118.71, 117.35, 92.17, 31.79, 25.28, 20.62.. $C_{31}H_{26}N_2O_4$ (356,42): calcd. C, 75.90; H, 5.34; found C, 74.77; H, 5.26. ESI$^+$: calcd. for $C_{31}H_{26}N_2O_4Na^+$ [M+] 513.18; found 513.1.

Synthesis of (N^4E,N^7E)-2,9-dimethyl-N^4,N^7-bis(pyridin-2-ylmethylene)-5a,10b-dihydrobenzofuro[2,3-b]benzofuran-4,7-diamine, 77.

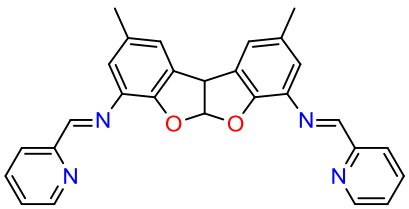

77

Compound **77** was prepared using the same procedure described above for compound **66**, but using 2 2,9-dimethyl-5a,10b-dihydrobenzofuro[2,3-b]benzo-furan-4,7-diamine. Yield: 55% ^{1}H NMR (500 MHz, Chloroform-d) δ = 8.90 (s, 2H, N=C–H), 8.75 – 8.69 (m, 2H, Ar–H), 8.30 – 8.24 (m, 2H, Ar–H), 7.84 – 7.77 (m, 2H, Ar–H), 7.36 (ddd, J = 7.4, 4.9, 1.3 Hz, 2H, Ar–H), 7.15 – 7.13 (m, 2H, Ar–H), 7.06 (d, J = 6.8 Hz, 1H, C–H), 7.01 (d, J = 1.9 Hz, 2H, Ar–H), 5.06 (d, J = 6.8 Hz, 1H, C–H), 2.37 (s, 6H, C–H_3). ^{13}C NMR (126 MHz, Chloroform-d) δ = 162.38, 149.55, 148.56, 136.52, 132.40, 128.57, 125.03, 123.10, 122.71, 121.88, 113.55, 50.26, 20.87, 1.02. ESI$^+$: calcd. for $C_{28}H_{22}N_4O_4Na^+$ [M+] 469.16; found 469.1.

Synthesis of (N^{8}E,N$^{8'}$E)-4,4,4',4',6,6'-hexamethyl-N^8,N$^{8'}$-bis(pyridin-2-ylmethylene)-2,2'-spirobi[chroman]-8,8'-diamine, 78.[94]

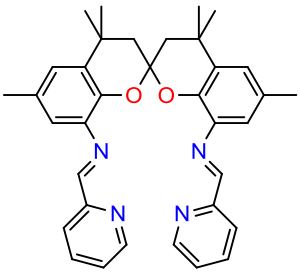

78

Compound **78** was prepared using the same procedure described above for compound **66**, but using Spanamine. Yield: 62%. ^{1}H NMR (400 MHz, , Chloroform-d) δ = 8.62 (d, 2 H, Ar–H), 8.02 (s, 2 H, Ar–H), 7.89 (d, 2H, Ar–H), 7.69 (t, 2 H, Ar–H), 7.29 (dd, 2 H, Ar–H), 6.76 (s, 2 H, Ar–H), 6.53 (s, 2 H, Ar–H), 2.19 (d, 2 H, C–H$_2$), 2.13 (s, 6 H, C–H$_3$), 2.05 (d, 2 H, C–H$_2$), 1.55 (s, 6 H, C–H$_3$), 1.31 (s, 6 H, C–H$_3$),

Synthesis of 2,10-dimethyl-N^4,N^8-bis(pyridin-2-ylmethyl)-12H-6,12-methanodibenzo[d,g][1,3]dioxocine-4,8-diamine, 79.

Procedure A, imine reduction:

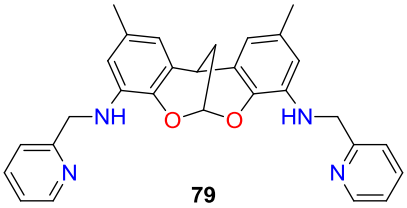

79

Under inert conditons, a Schlenk tube was charged with 2 mL of diisobutylaluminum hydride (1M) and 7 mL of diethylether. Then **66** was added (116 mg, 0.25 mmol). The reaction was stirred for 4 hours. Then 5 mL of water was added and the solution extracted with DCM (3x10 mL). The organic phase was dried over $MgSO_4$ anhydrous and evaporated yielding a yellow solid. Yield: 90%.

Procedure B, reductive amination:[66]

A Schlenk tube was charged with **61** (184 mg, 0.4 mmol) and picolylaldehyde (0.77 mL, 0.8 mmol) were added to 2 mL methanol followed by 0.1 mL of glacial acetic acid. PEMB (0.62 mL, 0.416 mmol) was added. The reaction was stirred for 4 hours. Then 1 mL of 1M HCl was added to quench the excess borane and the solution extracted with DCM (3x10 mL). Organic phases were combined and extracted with 5 mL of saturated NaOH solution. To recover desired product with 67% yield. ^{1}H NMR (500 MHz, Chloroform-d) δ = 8.61 (ddd, J = 4.9, 1.8, 0.9 Hz, 2H, Ar–H), 7.65 (td, J = 7.7, 1.8 Hz, 2H, Ar–H), 7.38 (dt, J = 8.0, 1.0 Hz, 2H, Ar–H), 7.19 (ddd, J = 7.5, 4.9, 1.2 Hz, 2H, Ar–H), 6.43 (d, J =

1.9 Hz, 2H, Ar–H), 6.33 (q, J = 2.0 Hz, 1H, C–H), 6.21 (d, J = 1.9 Hz, 2H, Ar–H), 5.08 (s, 2H, N–H), 4.47 (s, 4H, C–H_2), 3.81 (q, J = 1.5 Hz, 1H, C–H), 2.26 (dd, J = 3.0, 2.1 Hz, 2H, C–H_2), 2.19 (s, 6H, C–H_3). ^{13}C NMR (126 MHz, Chloroform-d) δ = 159.22, 149.36, 136.78, 136.57, 131.05, 125.80, 122.09, 121.57, 116.00, 110.23, 100.13, 92.16, 49.54, 31.45, 26.14, 21.29. $C_{29}H_{28}N_4O_2$ (464.56): calcd. C, 74.98; H, 6.08; found C, 73.97; H, 5.72. ESI$^+$: calcd. for $C_{29}H_{28}N_4O_2Na^+$ [M+] 487.21; found 487.1.

Synthesis of N^4,N^8,2,10-tetramethyl-N^4,N^8-bis(pyridin-2-ylmethyl)-12H-6,12-methanodibenzo[d,g][1,3]dioxocine-4,8-diamine, 80.

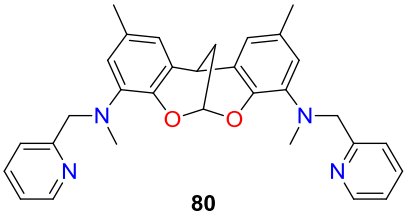

80

A Schlenk tube was charged with **79** (185 mg, 0.4 mmol) and 10 mL of THF and it was cooled to -20ºC. To the solution 1.6 mL of LHMDS 1M was added and the solution turned dark red. After 30 min the solutions was warmed up to r.t. and dimethylsulphate was added (0.153 mL, 1.6 mmol). The solution was kept under stirring for 1.5 hours. Then 10 mL of saturated ammonium chloride was added and the solution extracted with DCM (3x10 mL). The organic phase was dried over MgSO4 anhidrous and evaporated. The pure product was obtained by flash chromatography (EtOAc, to EtOAc:MeOH 10:1). To recover desired product with 49% yield. ^{1}H NMR (500 MHz, Chloroform-d) δ 8.52 (dt, J = 4.9, 1.4 Hz, 2H, Ar–H), 7.53 – 7.49 (m, 4H, Ar–H), 7.15 – 7.09 (m, 2H, Ar–H), 6.69 (d, J = 2.0 Hz, 2H, Ar–H), 6.61 (d, J = 2.0 Hz, 2H, Ar–H), 6.23 (d, J = 1.9 Hz, 1H, C–H), 4.42 – 4.26 (m, 4H, C–H_2), 3.87 (d, J = 2.1 Hz, 1H, C–H_2), 2.75 (s, 6H, C–H_3), 2.25 (s, 8H, C–H_2 and C–H_3). ^{13}C NMR (126 MHz, Chloroform-d) δ = 159.82, 148.47, 141.06, 140.27, 136.50, 130.47, 127.19, 122.68, 121.81, 120.97, 118.15, 91.77, 61.28, 39.84, 32.23, 25.45, 20.91. ESI$^+$: calcd. for $C_{31}H_{32}N_4O_2Na^+$ [M+] 515.24; found 515.1.

2.7. References

1. F. A. Carey and R. J. Sundberg, *Advanced Organic Chemistry Part B: Reactions and Synthesis*, Springer, New York, 2007.
2. K. K. Balasubramanian, B. S. Thyagarajan, and R. Bhima Rao, *Can. J. Chem*, 1966, **11**, 3–4.
3. A. Banihashemi and A. Rahmatpour, *Tetrahedron*, 1999, **55**, 7271–8.
4. A. Rahmatpour, *J. Heterocyclic Chem.*, 2010, **47**, 1011–6.
5. M. Guiso, A. Betrow, and C. Marra, *Eur. J. Org. Chem.*, 2008, **2008**, 6215–7.
6. M. Makha and C. L. Raston, *Tetrahedron Lett.*, 2001, **42**, 6215–7.
7. S. Anamik and D. Narsinh, 2002, 2002, 13.
8. T. Kito, K. Yoshinaga, M. Yamaye, and H. Mizobe, *J. Org. Chem.*, 1991, 3336–9.
9. G. C. Nandi, S. Samai, R. Kumar, and M. S. Singh, *Tetrahedron*, 2009, **65**, 7129–34.
10. G. C. Nandi, S. Samai, R. Kumar, and M. S. Singh, *Tetrahedron Lett.*, 2009, **50**, 7220–2.
11. R. Mitchell, Y. Lai, and R. Williams, *J. Org. Chem.*, 1979, **44**, 4733–5.
12. V. Kandepi and N. Narender, *Synthesis*, 2011, **44**, 15–26.
13. R. G. Syvret, K. M. Butt, T. P. Nguyen, V. L. Bulleck, and R. D. Rieth, *J. Org. Chem.*, 2002, **67**, 4487–93.
14. S. Borikar, T. Daniel, and V. Paul, *Tetrahedron Lett.*, 2009, **50**, 1007–9.
15. A. Kumar, A. Jamir, L. Jamir, D. Sinha, and U. B. Sinha, *Org. Comm.*, 2011, **4**, 1–8.
16. J. D. Senra, L. C.S. Aguiar, and A. B.C. Simas, *Curr. Org. Synt.*, 2011, **8**, 53–78.
17. A. Guram and S. Buchwald, *J. Am. Chem. Soc.*, 1994, **37**, 7901–2.
18. F. Paul, J. Patt, and J. F. Hartwig, *J. Am. Chem. Soc.*, 1994, 5969–70.
19. A. S. Guram, R. a. Rennels, and S. L. Buchwald, *Angew. Chem. Int. Ed.*, 1995, **34**, 1348–50.
20. J. Louie and J. Hartwig, *Tetrahedron Lett.*, 1995, **36**, 3609–12.
21. J. F. Hartwig, *Acc. Chem. Res.*, 2008, **41**, 1534–44.
22. D. Surry and S. Buchwald, *Chem. Sci.*, 2011, 27–50.
23. N. Marion, O. Navarro, J. Mei, E. D. Stevens, N. M. Scott, and S. P. Nolan, *J. Am. Chem. Soc.*, 2006, **128**, 4101–11.
24. M. H. Ali and S. L. Buchwald, *J. Org. Chem.*, 2001, **66**, 2560–5.

25. B. Schlummer and U. Scholz, *Adv. Syn. & Cat.*, 2004, **346**, 1599–1626.
26. M. Driver and J. Hartwig, *J. Am. Chem. Soc.*, 1997, **119**, 8232–45.
27. M. S. Viciu, O. Navarro, R. F. Germaneau, R. a. Kelly, W. Sommer, N. Marion, E. D. Stevens, L. Cavallo, and S. P. Nolan, *Organometallics*, 2004, **23**, 1629–35.
28. J. F. Hartwig, M. Kawatsura, S. I. Hauck, K. H. Shaughnessy, and L. M. Alcazar-Roman, *J. Org. Chem.*, 1999, **64**, 5575–80.
29. J. P. Wolfe, H. Tomori, J. P. Sadighi, J. Yin, and S. L. Buchwald, *J. Org. Chem.*, 2000, **65**, 1158–74.
30. X. Huang, K. W. Anderson, D. Zim, L. Jiang, A. Klapars, and S. L. Buchwald, *J. Am. Chem. Soc.*, 2003, **125**, 6653–5.
31. J. P. Stambuli, R. Kuwano, and J. F. Hartwig, *Angew. Chem. Int. Ed.*, 2002, **41**, 4746–8.
32. M. J. Cawley, F. G. N. Cloke, R. J. Fitzmaurice, S. E. Pearson, J. S. Scott, and S. Caddick, *Org. & biomol. chem.*, 2008, **6**, 2820–5.
33. M.-N. Birkholz, Z. Freixa, and P. W. N. M. van Leeuwen, *Chem. Soc. Rev.*, 2009, **38**, 1099–118.
34. J. Huang, G. Grasa, and S. P. Nolan, *Org. Lett.*, 1999, **1**, 1307–1309.
35. J. F. Hartwig, S. Richards, and D. Baran, *J. Am. Chem. Soc.*, 1996, **118**, 3626–33.
36. M. Driver and J. Hartwig, *J. Am. Chem. Soc.*, 1995, **117**, 4708–9.
37. R. Widenhoefer and S. Buchwald, *Organometallics*, 1996, **7333**, 2755–63.
38. J. F. Hartwig and N. Haven, *Organometallics*, 1996, **7863**, 7010–1.
39. F. Ullmann, *Ber. Dtsch. Chem. Ges.*, 1903, **36**, 2382–4.
40. I. Goldberg, *Ber. Dtsch. Chem. Ges.*, 1906, **36**, 1691–2.
41. G. Evano, N. Blanchard, and M. Toumi, *Chem. Rev.*, 2008, **108**, 3054–131.
42. J.-P. Corbet and G. Mignani, *Chem. Rev.*, 2006, **106**, 2651–710.
43. F. Monnier and M. Taillefer, *Angew. Chem. Int. Ed.*, 2009, **48**, 6954–71.
44. F. Y. Kwong, A. Klapars, and S. L. Buchwald, *Org. Lett.*, 2002, **4**, 581–4.
45. A. Klapars, J. Antilla, X. Huang, and S. Buchwald, *J. Am. Chem. Soc.*, 2001, **123**, 7727–9.
46. H. Goodbrand and N. Hu, *J. Org. Chem.*, 1999, **64**, 670–4.
47. H. Rao, H. Fu, Y. Jiang, and Y. Zhao, *J. Org. Chem.*, 2005, **70**, 8107–9.
48. D. Ma, Q. Cai, and H. Zhang, *Org. Lett.*, 2003, **5**, 2453–5.
49. R. K. Gujadhur, C. G. Bates, and D. Venkataraman, *Org. Lett.*, 2001, **3**, 4315–7.

50. D. Zhu, R. Wang, J. Mao, L. Xu, F. Wu, and B. Wan, *J. Mol. Cat. A, Chem.*, 2006, **256**, 256–60.
51. Z. Lu and R. J. Twieg, *Tetrahedron Lett.*, 2005, **46**, 2997–3001.
52. D. Chen, K. Yang, H. Xiang, and S. Jiang, *Tetrahedron Lett.*, 2012, **53**, 7121–4.
53. K. Moriwaki, K. Satoh, M. Takada, Y. Ishino, and T. Ohno, *Tetrahedron Lett.*, 2005, **46**, 7559–62.
54. A. Shafir and S. L. Buchwald, *J. Am. Chem. Soc.*, 2006, **128**, 8742–3.
55. H. Zhang, Q. Cai, and D. Ma, *J. Org. Chem.*, 2005, **70**, 5164–73.
56. J. T. Markiewicz, O. Wiest, and P. Helquist, *J. Org. Chem.*, 2010, **75**, 4887–90.
57. J. W. Tye, Z. Weng, A. M. Johns, C. D. Incarvito, and J. F. Hartwig, *J. Am. Chem. Soc.*, 2008, **130**, 9971–83.
58. Y. Aubin, C. Fischmeister, C. M. Thomas, and J.-L. Renaud, *Chem. Soc. Rev.*, 2010, **39**, 4130–45.
59. E. Sperotto, G. G. P. M. van Klink, G. van Koten, and J. G. de Vries, *Dalton Trans.*, 2010, **39**, 10338–51.
60. L. M. Huffman and S. S. Stahl, *J. Am. Chem. Soc.*, 2008, **130**, 9196–7.
61. A. I. Vogel, A. R. Tatchell, B. S. Furnis, A. J. Hannaford, and P. W. G. Smith, *Practical Organic Chemistry (5th Edition)*, Prentice Hall, London, 1996.
62. X. Sala, E. J. García Suárez, Z. Freixa, J. Benet-Buchholz, and P. W. N. M. van Leeuwen, *Eur. J. Org. Chem.*, 2008, **2008**, 6197–205.
63. P. Shejwalkar, N. P. Rath, and E. B. Bauer, *Dalton Trans.*, 2011, **40**, 7617–31.
64. A. Abu-Surrah and K. Lappalainen, *J. Organomet. Chem.*, 2002, **648**, 55–61.
65. R. F. Borch, M. D. Bernstein, and D. Durst, *J. Am. Chem. Soc.*, 1970, **93**, 2897–904.
66. E. R. Burkhardt and B. M. Coleridge, *Tetrahedron Lett.*, 2008, **49**, 5152–5.
67. C. Moessner and C. Bolm, *Angew. Chem. Int. Ed.*, 2005, **44**, 7564–7.
68. A. G. Becalski, W. R. Cullen, M. D. Fryzuk, B. R. James, G. J. Kang, and S. J. Rettig, *Inorg. Chem.*, 1991, **30**, 5002–8.
69. A. F. Abdel-Magid, K. G. Carson, B. D. Harris, C. a. Maryanoff, and R. D. Shah, *J. Org. Chem.*, 1996, **61**, 3849–62.
70. A. Banihashemi and A. Abdolmaleki, *Eur. Pol. J.*, 2004, **40**, 1629–35.

71. Z. Freixa, M. S. Beentjes, G. D. Batema, C. B. Dieleman, G. P. F. van Strijdonck, J. N. H. Reek, P. C. J. Kamer, J. Fraanje, K. Goubitz, and P. W. N. M. van Leeuwen, *Angew. Chem. Int. Ed.*, 2003, **42**, 1284–7.
72. J. M. López-Valbuena, E. C. Escudero-Adán, J. Benet-Buchholz, Z. Freixa, P. W. N. M. van Leeuwen, and P. W. N. M. Leeuwen, *Dalton Trans.*, 2010, **39**, 8560–74.
73. S. Kajigaeshi, M. Moriwaki, T. Tanaka, S. Fujisaki, T. Kakinami, and T. Okamoto, *J. Chem. Soc., Perkin Trans.*, 1990, 897–9.
74. M. S. Viciu, R. F. Germaneau, O. Navarro-Fernandez, E. D. Stevens, and S. P. Nolan, *Organometallics*, 2002, **21**, 5470–2.
75. G. D. Vo and J. F. Hartwig, *J. Am. Chem. Soc.*, 2009, **131**, 11049–61.
76. D. S. Surry and S. L. Buchwald, *J. Am. Chem. Soc.*, 2007, **129**, 10354–5.
77. Y. Unger, D. Meyer, O. Molt, C. Schildknecht, I. Münster, G. Wagenblast, and T. Strassner, *Angew. Chem. Int. Ed.*, 2010, **49**, 10214–6.
78. S. L. Buchwald, A. Klapars, J. C. Antilla, G. E. Job, M. Wolter, F. Kwong, G. Nordmann, and E. J. Hennessy, 2002, 306.
79. F. Lang, D. Zewge, I. N. Houpis, and R. . Volante, *Tetrahedron Lett.*, 2001, **42**, 3251–4.
80. J. Cloete and S. F. Mapolie, *J. Mol. Cat. A, Chem.*, 2006, **243**, 221–5.
81. M. P. Jensen, S. J. Lange, M. P. Mehn, E. L. Que, and L. Que, *J. Am. Chem. Soc.*, 2003, **125**, 2113–28.
82. W. A. Kinney, N. E. Lee, R. M. Blank, C. A. Demerson, C. S. Sarnella, N. T. Scherer, G. N. Mir, L. E. Borella, J. F. Dijoseph, and C. Wells, *J. Med. Chem.*, 1990, **29**, 327–336.
83. A. Arnáiz, J. V. Cuevas, G. García-Herbosa, A. Carbayo, J. a. Casares, and E. Gutierrez-Puebla, *Dalton Trans.*, 2002, **2**, 2581–6.
84. K. H. Chung, C. M. So, S. M. Wong, C. H. Luk, Z. Zhou, C. P. Lau, and F. Y. Kwong, *Chem. Comm.*, 2012, **48**, 1967–9.
85. Y. Lee, D.-H. Lee, G. Y. Park, H. R. Lucas, A. a Narducci Sarjeant, M. T. Kieber-Emmons, M. a Vance, A. E. Milligan, E. I. Solomon, and K. D. Karlin, *Inorg. Chem.*, 2010, **49**, 8873–85.
86. L. Li, N. N. Murthy, J. Telser, L. N. Zakharov, G. P. a Yap, A. L. Rheingold, K. D. Karlin, and S. E. Rokita, *Inorg. Chem.*, 2006, **45**, 7144–59.
87. S. Bagal, K. Gibson, M. Kemp, C. Poinsard, B. Stammen, S. Denton, and M. Glossop, 2008, 212.

88. K. B. Gudasi, R. S. Vadavi, R. V. Shenoy, M. S. Patil, and S. a. Patil, *Trans. Metal Chem.*, 2005, **30**, 569–74.
89. J. A. McCauley, J. W. Butcher, J. W. Hess, N. J. Liverton, and J. J. Romano, *patentscope.wipo.int*, 2010, 64.
90. M. D. Markey, Y. Fu, T. R. Kelly, B. College, and C. Hill, *Org. Lett.*, 2007, **9**, 8–10.
91. D. Marlin, *Eur. J. Inorg. Chem.*, 2002, **2002**, 859–65.
92. H. L. Bassett and C. R. Thomas, *J. Chem. Soc.*, 1954, 1188–90.
93. O. Jacquet, N. D. Clément, Z. Freixa, A. Ruiz, C. Claver, and P. W. N. M. van Leeuwen, *Tetrahedron: Asymmetry*, 2011, **22**, 1490–8.
94. J. Rich, M. Rodríguez, I. Romero, X. Fontrodona, P. W. N. M. van Leeuwen, Z. Freixa, X. Sala, A. Poater, and M. Solà, *Eur. J. Inorg. Chem.*, 2013, **2013**, 1213–24.

Chapter 3
Application of Spirobichroman bidentate amine ligands in metal catalyzed reactions.

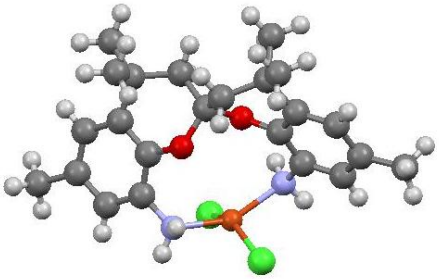

3.1. Catalysis introduction

3.1.1. Rhodium catalyzed hydrogenation of C=C bonds

Asymmetric hydrogenation of prochiral substrates catalyzed by organometallic compounds using molecular hydrogen is an efficient method for synthesizing chiral compounds (Scheme 3.1). This process has widely been used in stereoselective organic synthesis and in some cases it has been found industrial application[1–3].

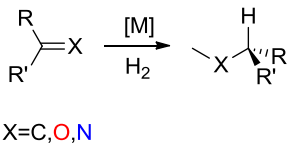

Scheme 3.1 *Asymmetric hydrogenation reaction*

The mechanism for the rhodium-catalysed hydrogenation of methyl-α-acetamidocinnamate proposed by Landis and Halpern is shown in Scheme 3.2.

Two different cycles are possible depending on the coordination face of the prochiral C=C bond.[4] The starting species of the catalytic cycle is the Rh(I) complex **1** containing one diphosphine ligand and two molecules of solvent in a square planar manner. In the first step, the substrate coordinates to complex **1** as a bidentate ligand to form the two diastereoisomeric species $\mathbf{2}^{maj}$ and $\mathbf{2}^{min}$ *via* substitution of the two molecules of solvent. The next step in the catalytic cycle is the oxidative addition of hydrogen, to form the octahedral complex **3** in which the rhodium centre is oxidized to Rh(III). Then the alkyl complex **4** is generated by migratory insertion of the olefin into one of the rhodium-hydride bonds and coordination of one solvent molecule to the vacant site. Finally, the last step is the reductive elimination in which both enantiomers are produced and the active species is regenerated. The rate and enantioselectivity determining step is the oxidative addition of hydrogen. The dominant product is the one which is formed via the minor manifold since the reactivity of the minor intermediate is higher (the reaction barrier is overall lower in energy than the barrier of the major intermediate (for the ligands studied by Halpern and Landis)).

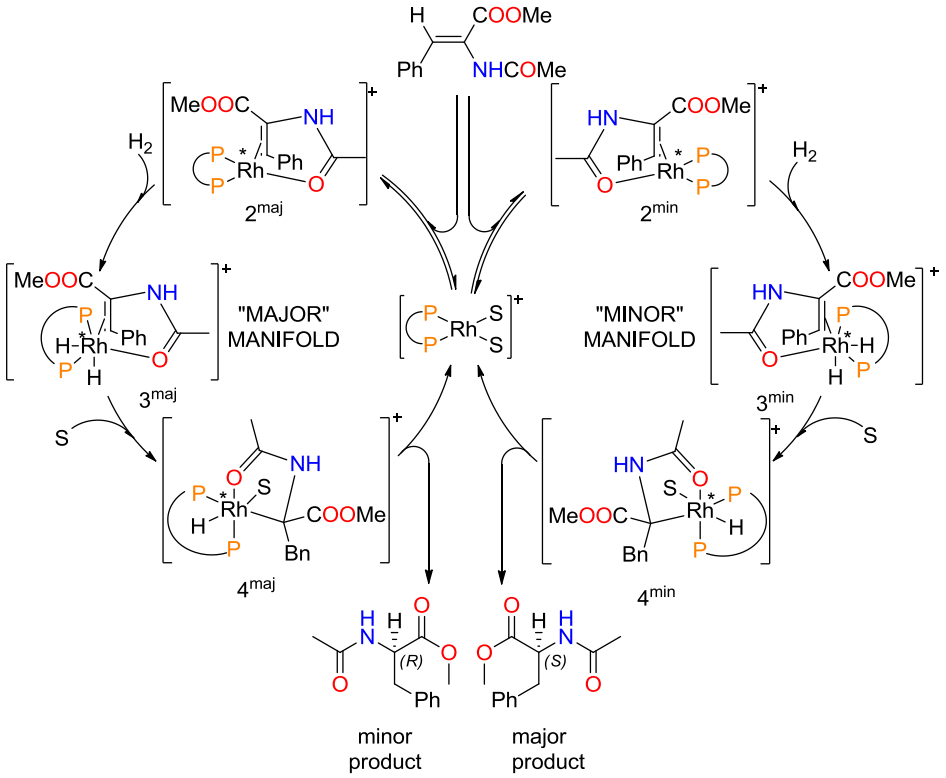

Scheme 3.2 *Catalytic cycle for asymmetric hydrogenation.*

Phosphines have been widely applied as ligands in this asymmetric hydrogenation reaction and ligands with different structural characteristics were tested in order to improve the enantioselectivity of the reaction:[2]

- Ligands containing a chiral phosphorus atom.
- Ligands having a chiral backbone.
- Ligands carrying chiral substituents on phosphorus.
- Ligands having axial chirality.
- Ligands having a planar asymmetry.

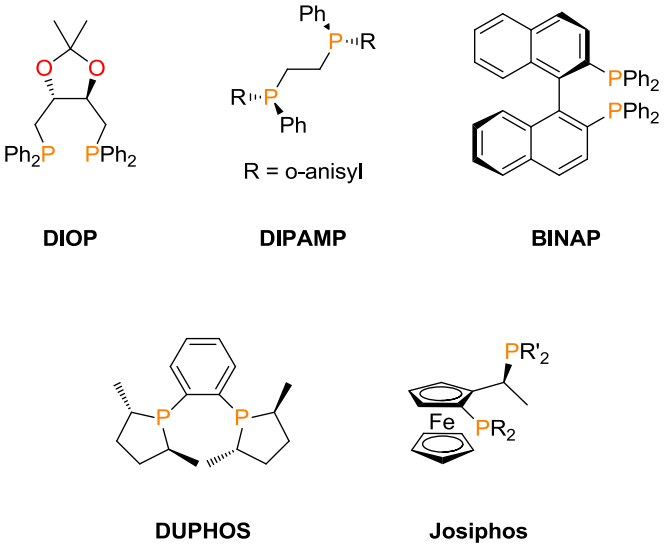

Figure 3.1 *Selection of chiral ligands that were successfully applied in Rh-catalysed asymmetric hydrogenation reactions.*

The most important examples of diphosphines with different structural characteristics are the following (Figure 3.1). DIOP ((+)-2,3-*O*-Isopropylidene-2,3-dihydroxy-1,4-bis(diphenylphosphino)butane) was reported by Kagan and coworkers[5] and represents one of the first examples of a diphosphine successfully applied in asymmetric hydrogenation. Knowles used the diphosphine ligand DIPAMP ((1R,2R)-(-)-Bis[(2-methoxyphenyl)-phenylphosphino]ethane) in this reaction.[6] This system was successfully employed in the industrial production of L-Dopa.[1] In the 1980s, Noyori and coworkers reported the use of the BINAP ((1,1'-Binaphthalene-2,2'-diyl)bis(diphenylphosphine)) ligand, which is an efficient catalyst for the hydrogenation of various substrates.[7] Burk and coworkers developed the DUPHOS ligand (1,2-bis((2S,5S)-2,5-dimethylphospholan-1-yl)benzene) with which they obtained good results in asymmetric hydrogenation of several substrates.[8] Togni and coworkers reported the synthesis and applications in different catalytic reactions of Josiphos, a diphosphine with planar asymmetry.[9] Furthermore, other ligands have been used in metal catalyzed asymmetric hydrogenation such P,N ligands, phosphites, phosphinites, and bulky monopdentate ligands, especially phosphoramidites.[2]

TRAP (Chapter 1, Figure 1.8) is a diphosphine ligand with a bis-ferrocenyl backbone which easily coordinates to metal centres in a trans geometry, and it provided interesting results in the Rh-catalysed hydrogenation of dimethyl itaconate and α-(acetoamido)acrylates. It is noteworthy that the unique application in hydrogenation of indoles was reported for TRAP complexes.[10–13]

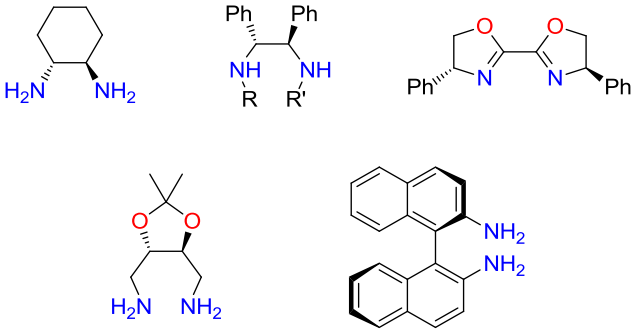

Figure 3.2 *N-ligands applied in asymmetric hydrogenation of C=C bonds.*

The use of N-donor ligands in the hydrogenation of acrylic derivatives is less common. The most representative examples gave moderate to full conversions with low enantiomeric excess.[14–19] In Figure 3.2 nitrogen ligands used in asymmetric hydrogenation of acrylic derivatives are presented.

3.1.2. Rhodium catalyzed hydrosilylation of C=O bonds

There are several ways to form organosilicon compounds. For instance, their synthesis can be performed *via* metathesis of silicon halides with organometallics, silylation of organic halides, hydrosilylation, etc... Hydrosilylation is the addition of Si-H to unsaturated compounds such as alkenes, ketones or imines (Scheme 3.3). The asymmetric version of hydrosilylation of double bonds is an interesting approach to prepare enantiopure compounds. For instance, imines and ketones can be hydrosilylated to the corresponding enantiopure amines and alcohols respectively. The alkylsilanes ($RR'HC–SiR''_3$) can be transformed into the corresponding alcohol with retention of chirality.[2,3]

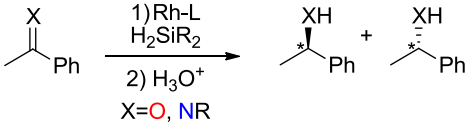

Scheme 3.3 *Asymmetric hydrosilylation reaction.*

Much work on hydrosilylation has been carried out using metal catalysts of Pd, Pt and Rh.[2,3,20] In late the 1950´s Speier used H_2PtCl_6 as hydrosilylation catalyst. This catalyst is highly active even at low catalyst loading.

A catalytic cycle for rhodium catalysed hydrosilylation was proposed by Kagan using DIOP as a ligand.[5] This mechanism includes several steps (Scheme 3.4).

1. Silane oxidative addition to the rhodium complex.
2. Coordination of ketone to the metal displacing one solvent molecule.
3. Migratory insertion of ketone into the rhodium-silicon bond.
4. Reductive elimination of alkoxysilane and regeneration of the active species.

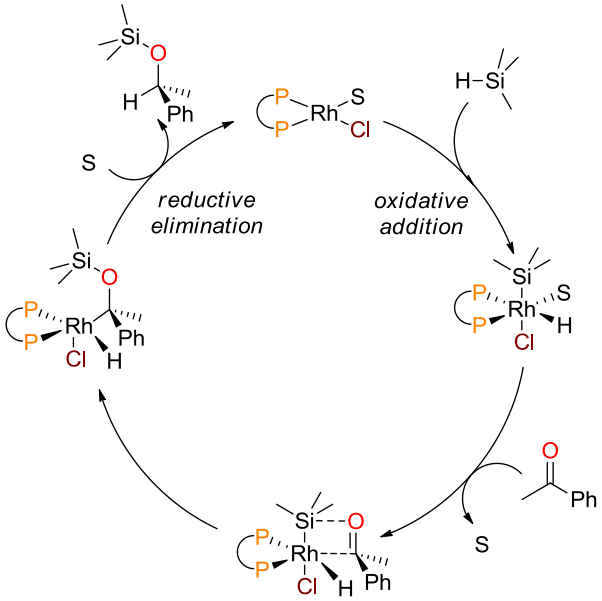

Scheme 3.4 *Proposed catalytic cycle for hydrosilylation.*

Several rhodium compounds such as $RhCl_3$, $[RhCl(COD)]_2$ or $[Rh(COD)_2]BF_4$ have been used as catalyst precursors in the hydrosilylation of ketones. The most common silanes used in this reaction are Ph_2SiH_2 and 1-NpPhSiH$_2$ and the benchmark substrate is acetophenone. A wide variety of ligands such as diphosphines, diphosphites, P-N ligands and iminopyridine have been used in asymmetric hydrosilylations. The best results have been obtained with oxazolines.[2,3,21] Some of the ligands applied are depicted in Figure 3.3.

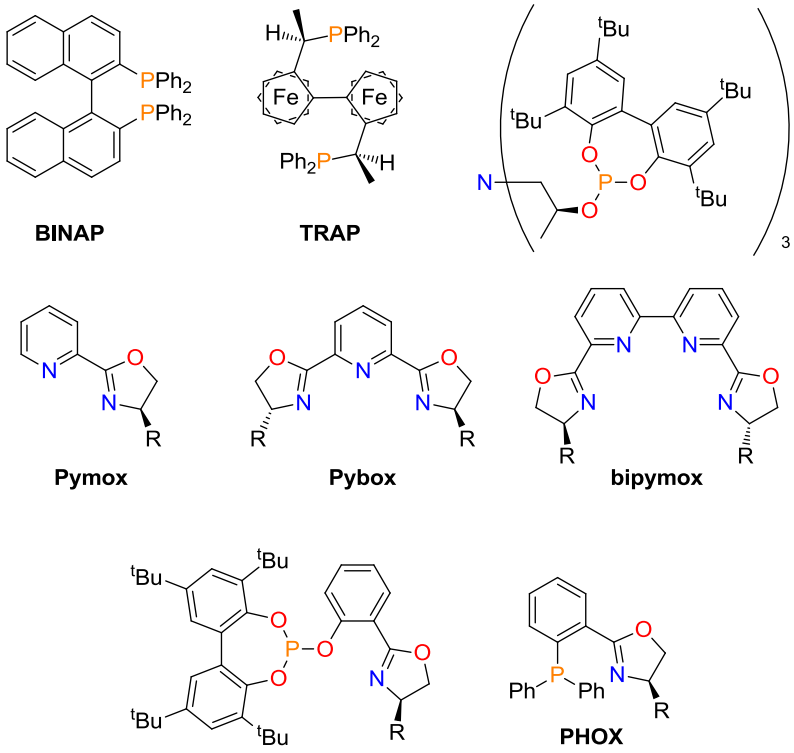

Figure 3.3 *Some ligands used in asymmetric hydrosilylation of acetophenone*

Pybox was reported in the late 80s as the ligand of choice in the hydrosilylation of ketones such as acetophenone. The Pybox ligands substituted in the oxazoline moiety have shown to give efficient catalysts.[22,23] Bipymox provided conversions up to 98% and ee up to 90% in the hydrosilylation of acetophenone using an excess of bipymox and $AgBF_4$ as additive .[24] The PHOX ligand was developed by Pfaltz and coworkers in 1993 and it was successfully used in palladium catalyzed asymmetric allylic substitution

reactions.[25] Later, this ligand was used in the rhodium-catalysed hydrosilylation of acetophenone with high enantiomeric excess.[26] Pàmies and coworkers have also used phosphite-oxazoline ligands in the rhodium-catalyzed hydrosilylation of acetophenone with moderate conversions and enantiomeric excess.[27] Various oxazoline derivatives has been used in hydrosilylation of C=O, for instance, carbene-oxazoline or bisoxazoline promoted high yields and enantioselectivities in the hydrosilylation of acetophenone.[20,28,29]

TRAP, a *trans*-coordinating diphosphine ligand, was also applied in the hydrosilylation reaction, providing high conversions and high enantionselectivities.[30,31]

Several chiral ligand containing amino group were used in the hydrosylilation of ketones with various metals such as iron, zinc, iridium, nickel, rhenium, …[32–38] For instance, zinc ($Zn(Et)_2$ as metal precursor) modified with chiral diamine ligands catalyzed hydrosilylation and provided high conversion and moderate enantioselectivities for acetophenone. Nickel-catalyzed hydrosilylation using amino-phosphine ligands provided high conversions up to 99%. Using an iron ($Fe(OAc)_2$ as metal source) system, the ketones were converted in high yields and but with moderate enantioselectivity. Some of the catalytic systems bearing amino ligands which were applied in hydrosilylation of ketones are depicted in Scheme 3.4.

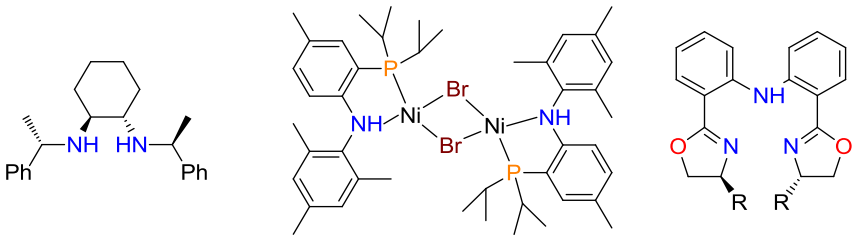

Figure 3.4 *Catalytic systems applied in hydrosilylation of ketones.*

3.1.3. Catalytic asymmetric oxidation of *meso*-diols

A wide variety of synthetic tools were applied in the oxidation of secondary alcohols to ketones[39] such as dichromate or permanganate species, aluminium alkoxide and ketone, hypervalent iodine compounds, bromine or iodide

systems, …[40–44] One interesting synthetic tool in oxidation of alcohol is the metal catalyzed oxidative kinetic resolution of alcohols in which a chiral catalyst reacts preferentially with one enantiomer. The reaction was promoted by several metals such as Ir, Rh, Ru or Pd. This reaction is represented in Scheme 3.5.[45–48]

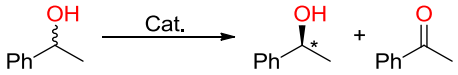

Scheme 3.5 *Oxidative kinetic resolution of secondary alcohols.*

The application of this oxidation approach to *meso*-diols is also of interest. The first example of selective monooxidation of 1,2-*meso*-diols was reported by David and coworkers in 1974.[43] They described the formation of α-hydroxy-ketones from sugars using bromine and organotin compounds as reagents. This procedure was applied in the synthesis of (+)-Spectinomycin.[49] First examples of enantioselective oxidations were reported using chiral dioxiranes or chiral hypervalent iodine compounds.[50–52] Some examples of catalytic oxidation of vicinal diols were reported. The use of various metals (Sb, Sn, Cu, Ni or Zn) and oxidizing agents such as bromine, N-bromosuccinimide (NBS) or phenyltrimethylammonium tribromide (PTAB) was successful for the formation of several α-hydroxy-ketones.[53,54]

The first catalytic asymmetric oxidation of meso-diols was reported by Onomura and coworkers in 2007.[55] $Cu(OTf)_2$ modified with the BOX ligand promoted the selective oxidation of these substrates into α-hydroxy-ketone, with high yields but moderate enantiomeric excess.[55,56] This catalytic system was also able to promote the oxidation of 1,2-hydroxyamines.[56] The asymmetric oxidation of *meso*-hydrobenzoin is depicted in Scheme 3.6.

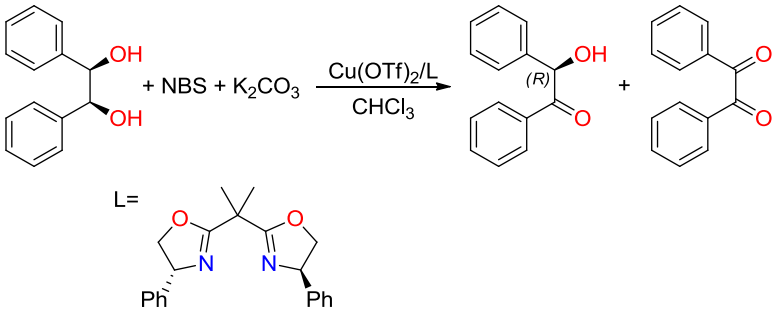

Scheme 3.6 *Catalytic oxidation of meso-hydrobenzoin by copper catalyst.*

The proposed mechanistic cycle for copper promoted oxidations of *meso*-hydrobenzoin is shown in Scheme 3.7.[56] The mechanism consists of several steps: a) coordination of the substrate to the copper complex, b) deprotonation of the coordinated *meso*-hydrobenzoin by the base present in the media, c) reaction of the alkoxide with the cationic bromide to form a copper hypobromocomplex, d) abstraction of the proton attached to the α-carbon by the base leads to the formation of the benzoin copper complex and e) the active species is regenerated by substitution of the product by a new substrate molecule.

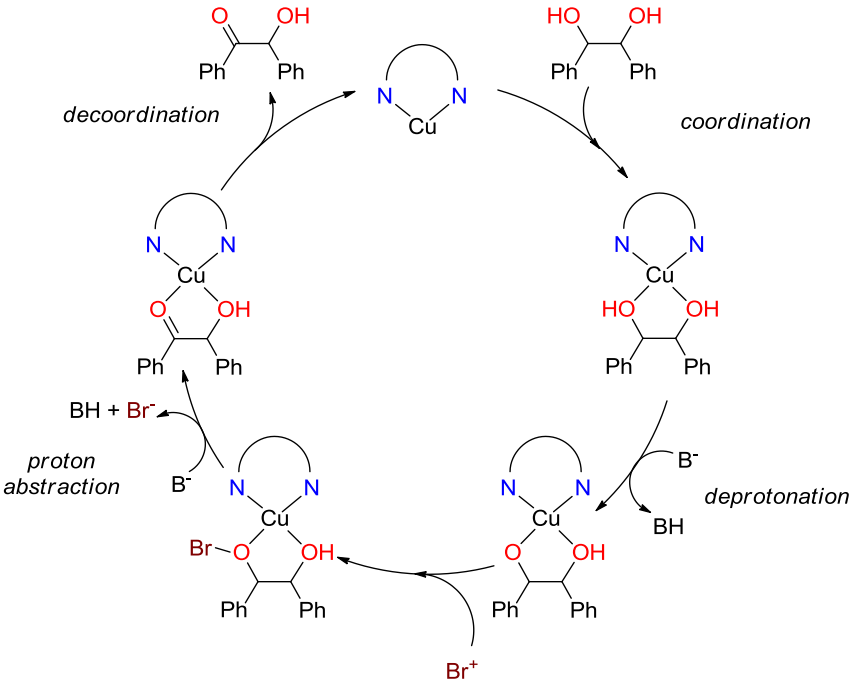

Scheme 3.7 *Proposed catalytic cycle for meso-diols oxidation.*

A proposed intermediate responsible for the enantiodiscrimination using a bisoxazoline ligand is represented in Scheme 3.8.[55] The phenyl groups of the bisoxazoline moiety decrease the accessibility towards one of the oxygen atoms, thus directing the oxidation process towards the other oxygen and the formation of diketones is avoided..

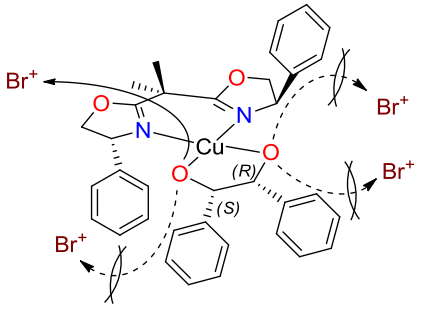

Scheme 3.8 *Proposed intermediate in the desymmetrization of meso-hydrobenzoin.*

The catalytic oxidation of *meso*-diols was performed with metals, such as iridium and ruthenium.[46,57,58] Ruthenium catalytic systems provided moderate to high conversions and enantioselectivities in the oxidation of 1,3 and 1,4 diols.[46,57] Likewise, iridium catalyst gave high conversions and selectivities for 1,3 and 1,4 diols, but the selectivity was lower in the oxidation of 1,2-*meso*-diols.[58] Examples of catalytic systems applied in the oxidation of *meso*-diols are shown in Figure 3.5.

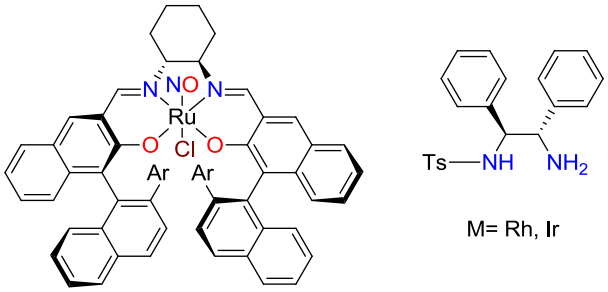

Figure 3.5 *Catalytic systems applied in oxidation of 1,3 and 1,4 meso-diols.*

With all these precedents in mind, we consider to study in this chapter the synthesis and characterization of different complexes containing *trans* coordinating ligands. These ligands and complexes were subsequently applied in the rhodium hydrogenation of C=C double bonds, the rhodium hydrosilylation of C=O double bonds, and the copper and iron catalyzed oxidation of *meso*-diols.

3.2. Results and discussion

3.2.1. Synthesis and characterization of the metal complexes

The aim of the synthesis of metal derivative complexes containing SPANamine lingad is to form *trans*-coordination complexes. The SPANamine was used as ligand in the synthesis of several complexes of rhodium, palladium, and copper (Scheme 3.9). These complexes were fully characterized.

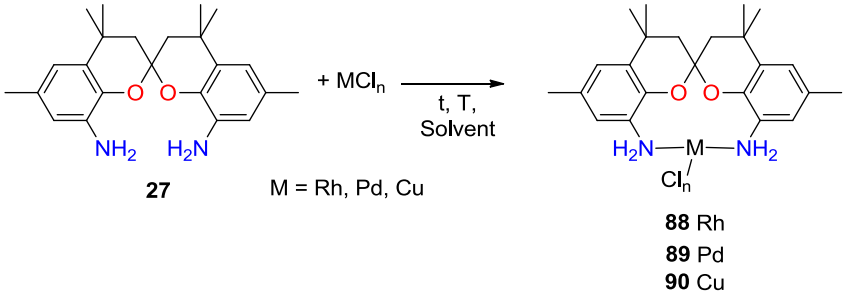

27 M = Rh, Pd, Cu

88 Rh
89 Pd
90 Cu

Scheme 3.9 *Synthesis of metal complexes with **27**.*

The resulting compounds **88**, **89**, and **90** were characterized by ^{1}H NMR, ESI mass, and X-ray diffraction. Mass analysis demonstrated that compound **88** is a dimeric species, probably with bridging chlorides, while SPANamine forms monomeric species with palladium and copper chloride precursors.

Suitable crystals of the ligands SPANamine **27** and SPANbenzylamine **53** were obtained by slow evaporation of a dichloromethane solution of these compounds, as described in Chapter 2, and both compounds were characterised by x-ray diffraction. Their molecular structures are depicted in Figure 3.6.

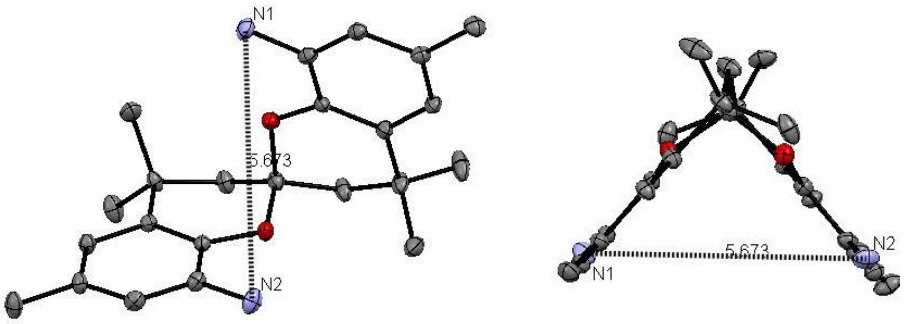

SPANamine 27

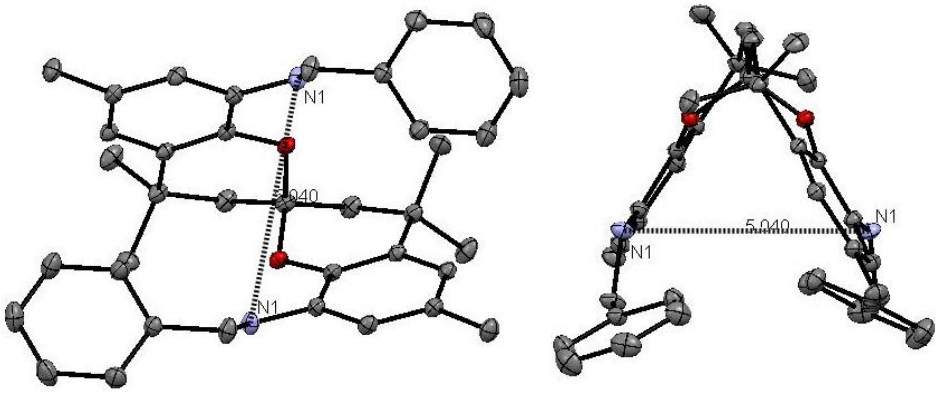

SPANbenzylamine 53

Figure 3.6 *ORTEP-plots (thermal ellipsoids shown at 50% probability levels) of complexes **27** and **53**. Non-relevant hydrogen atoms have been omitted for the sake of clarity. Nitrogen-Nitrogen distance in amstrong is shown.*

The distance between the nitrogen atoms in both compounds was large enough to allow *trans*-coordination with metals, although the only published example of Pd-complex with SPANamine had a *cis*-geometry.[59] The difference in nitrogen distance between **27** and **53** is quite remarkable. It is attributed to the packing in the solid state; the conformation of **53** allowed the formation of π-stacking interactions between benzylic rings of different molecules.

For comparison, the X-ray structures of the complexes **88** and **90** are shown in Figure 3.7.

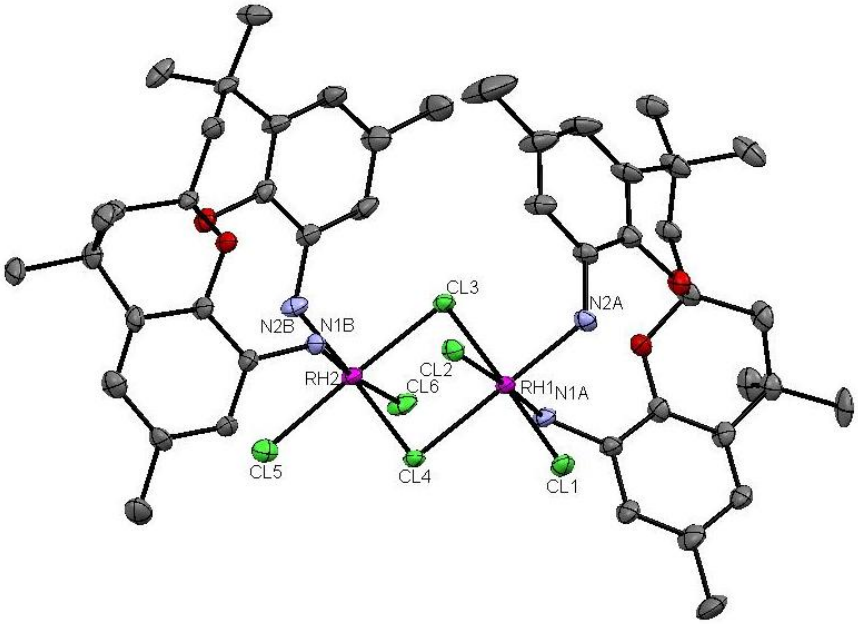

$[Rh_2Cl_4(27)_2(\mu\text{-}Cl)_2]$ 88

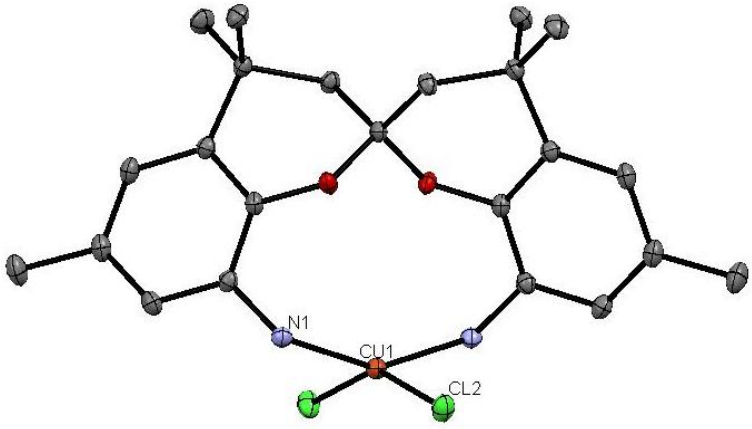

$[CuCl_2(27)]$ 90

Figure 3.7 *ORTEP-plots (thermal ellipsoids shown at 50% probability levels) of complexes **88** and **90**. Non-relevant hydrogen atoms have been omitted for the sake of clarity.*

Different coordination modes of ligand **27** were observed in **88** and **90**. The rhodium complex **88** shows an octahedral geometry with all the angles close to 90º and *cis*-coordination for SPANamine (Table 3.1). This coordination mode was previously observed for SPAN derivatives when *cis*-chelating ligands were present in the complex.[60] In this case, no *cis*-chelating ligands were present, but it can be expected that the two bridging chloride ions probably played this role, and that as a consequence, the SPANamine ligand resulted in a *cis*-coordination mode.

In contrast, the monomeric copper complex **90** presented a bite angle for SPANamine of 150º. The complex presented a distorted square-planar geometry. The distortion was attributed to the electronic repulsion between the chloride coordinated to the metal centre and the oxygen atoms of the SPAN moiety.

Finally palladium SPANamine complex **89** is a monomeric species according to the mass analysis. A *trans*-coordination is expected, as found for the analogous Pd-SPANphos complex.[61]

Table 3.1 *Selected bond distances (Å) and angles (º) for complexes **88** and **90**.*

	Distances (Å)			
88	**N_{1A}–Rh_1**	**N_{1B}–Rh_2**	**N_{2A}–Rh_1**	**N_{2B}–Rh_2**
	2.1087	2.1110	2.0936	2.0793
	Cl_1–Rh_1	**Cl_5–Rh_2**	**Cl_4–Rh_1**	**Cl_4–Rh_2**
	2.3048	2.3128	2.3746	2.3823
90	**Cu–N**	**Cu–Cl**		
	2.0215	2.2243		
	Angles (º)			
88	**N_{2B}–Rh_2–N_{1B}**	**N_{2A}–Rh_1–N_{1A}**	**N_{2A}–Rh_1–Cl_3**	**N_{2B}–Rh_2–Cl_5**
	93.99	97.36	95.76	85.07
90	**N–Cu–N**	**N–Cu–Cl**	**Cl–Cu–N**	**Cl–Cu–Cl**
	150.21	97.18	91.24	146.84

Several angles and distances for compounds **88** and **90** are summarized in Table 3.1. M–N bonds are shorter than M–Cl distances. If we compare metal distances, Cu–N or Cu–Cl distances were shorter than those of rhodium since the copper atom has a smaller radius than rhodium.

Once the coordination chemistry of SPANamine derivatives was studied, the synthesized complexes were applied in several metal catalyzed reactions.

3.2.2. Rhodium catalyzed hydrogenation of C=C bonds

As a consequence of the small number of publications on rhodium catalyzed hydrogenation of alkenes with amine ligands and in view of the special reactivity of TRAP ligands in hydrogenation;[10–17] the SPANamine was tested as ligand in the Rh catalyzed hydrogenation reaction to check, if like TRAP, a catalyst containing the wide bite angle SPANamine derivatives can hydrogenate selectively C=C double bonds (Scheme 3.10).

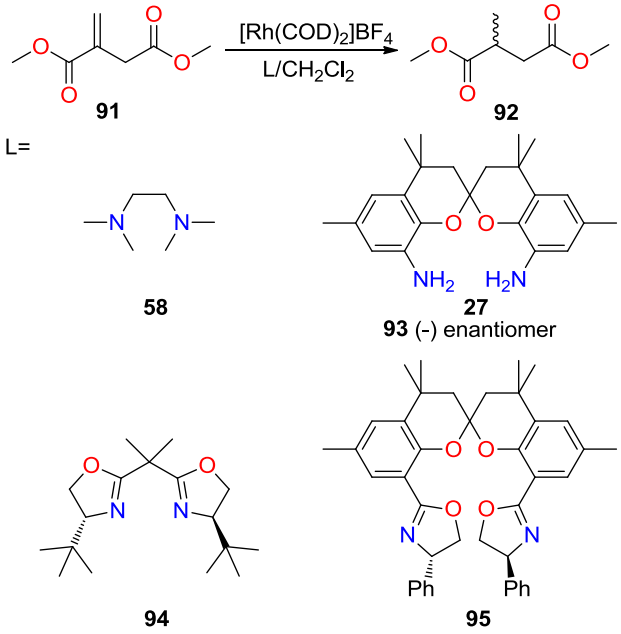

Scheme 3.10 *Rhodium catalysed hydrogenation of dimethyl itaconate.*

The Rh-catalyzed hydrogenation of acrylic derivatives was firstly screened with **58** as ligand for comparatives purposes. Hydrogenation experiments were carried out in dichloromethane at 40 °C for 4h by addition of ligand 58 to $[Rh(COD)_2]BF_4$ (see experimental part). The results of pressure optimization are collected in Table 3.2.

Table 3.2 *Pressure optimization*

Entry	Ligand	P_{H2} (bar)	Conversion %[a] ([b])
1	58	10	0 (0)
2	58	30	0 (0)
3	58	50	36 (32)
4	-	50	78 (74)

Dimethyl itaconate hydrogenation. T=40 ºC, t=4h, S/Rh=100, L/Rh=1.05, $[Rh(COD)_2]BF_4$ as precursor. [a] calculated by ^1H NMR. [b] calculated by GC.

The entries 1-3 (Table 3.2) show the effect pressure in the reaction. 50 bars of hydrogen were required to obtain conversion when ligand **58** was used. Entry 4 was related with a ligand free experiment which was more active. In all the catalytic experiments, the formation of Rh black was observed. Next; a ligand screening was performed and the results are summarized in Graph 3.1.

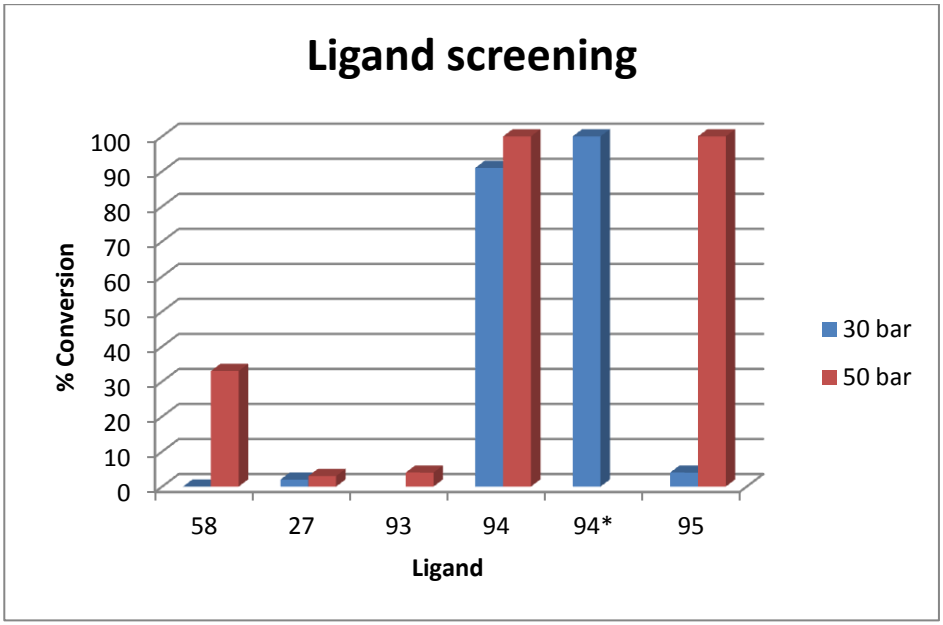

Graph 3.1 *Ligand screening in the Rh-catalyzed asymmetric hydrogenation of dimethyl itaconate. Reaction conditions: T=40 ºC, t=4h, S/Rh=100, L/Rh=1.05, $[Rh(COD)_2]BF_4$ as precursor, conversion calculated by GC. * 2 hours for the formation of complex in situ.*

Graph 3.1 shows the different activities obtained for the N-ligands in the Rh-catalyzed hydrogenation of dimethyl itaconate. Lower conversions were determined for amine ligands, either TMEDA **58** or SPANamine (**27** and **93**). Different catalytic behaviour was observed with 2,2′-isopropylidenebis[(4*S*)-4-*tert*-butyl-2-oxazoline] **94** as a ligand at 50 bar which hydrogenated fully the starting material. Conversion was slightly decreased to 85% when 30 bar of hydrogen were applied. The different behaviour of amines and oxazoline could be explained by their electronic properties. Amines are hard σ-donors and could stabilize COD coordination. Thus the formation of the active species was harder and low conversions were detected. In contrast the oxazoline is a poorer σ-donor than SPANamine and it is a weak π-acceptor, thus π-backdonation to COD was lower and COD is easier displaced. Furthermore, when **94** was used as ligand, the formation of rhodium metal was avoided and the reactivity was attributed to metal complex, which is in agreement with conversions at lower pressure and the better yields obtained when longer incubation times were applied.

In view of the good activities achieved with ligand **94,** we decided to test the SPANoxazoline ligand **95** in the rhodium catalyzed hydrogenation of dimethyl itaconate to investigate the bite angle effect in this reaction. When the reaction was performed under 30 bars of hydrogen less than 5% conversion was obtained. However, under H_2 pressures of 50 bars complete hydrogenation of compound **91** was observed. But under these reaction conditions, rhodium metal was obtained which could be held responsible for most of the substrate hydrogenation. Ligand **95** did not show any enantioselectivity and racemic mixtures were obtained.

To summarize neither SPANamine nor SPANoxazoline are convenient ligands for the rhodium catalyzed hydrogenation of itaconate since full conversions were only obtained when a high pressure (50 bar) was applied and only racemic mixtures were obtained. Furthermore, no bite angle effect was observed in the catalytic transformation using ligands **93** and **95**.

3.2.3. Rhodium catalyzed hydrosilylation of C=O bonds

SPANamine ligand **27** was also applied in the rhodium catalyzed hydrosilylation of acetophenone (Scheme 3.11).

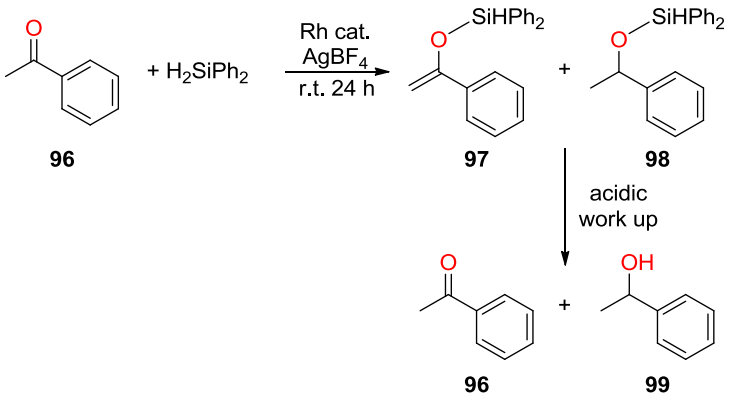

Scheme 3.11 *Schematic representation of rhodium hydrosilylation of acetophenone.*

This reaction was explored with 2,6-bis((S)-4-isopropyl-4,5-dihydrooxazol-2-yl)pyridine (Pybox, **100**) and SPANamine (Figure 3.8).

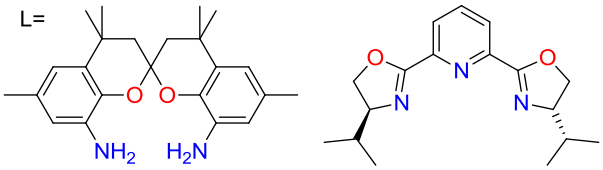

93 (-) enantiomer **100**

Rh= $RhCl_3.6H_2O$, **101** $[Rh(COD)_2]BF_4$, **102** $[RhCl(COD)]_2$ **103**

Figure 3.8 *Ligands and Rh precursors used in the Rh-catalyzed hydrosilylation of acetophenone*

The hydrosilylation experiments were carried out by addition of the corresponding ligands to the rhodium precursors in THF during 30 minutes. The different Rh-complexes were formed *in situ* from Rh(I) and Rh(III) precursor (**101-103**). The results obtained in the hydrosilylation of acetophenone are summarized in Table 3.3.

Table 3.3 *Screening of different Rh precursors in the hydrosilylation of acetophenone*

Entry	Rh	L	% conv.[a]	% sel. 98[a]	%ee[b]
1[c]	**101**	**100**	17	52	0
2[d]	**101**	**100**	96	38	30
3[d]	**101**	**93**	83	61	0
4	**102**	**-**	56	70	0
5	**102**	**100**	47	48	2
6	**102**	**93**	53	50	1
7	**103**	**-**	78	74	0
8	**103**	**100**	24	50	6

*r.t., 24h, L/Rh=1.2, Rh/**96**=100, Rh/Si=150, 2h stirring Rh precursor and ligand in 2 ml THF. [a] calculated by ^1H NMR. [b] calculated by GC. [c] Preparation of the Rh precursor at 70 ºC. [d] Preparation of the Rh precursor at 70 ºC and addition of triethylorthoformate to remove the water.*

When the reaction was performed at room temperature for 24h with **101** as metal precursor with catalyst loadings of 1%, it was observed that the presence of water from **101** had a large influence on the conversion and selectivity (Table 3.3, entry 1 versus 2). In entry 3 when **93** was used as ligand lower conversion was obtained, but the selectivity towards racemic **98** increased up to 61%. A cationic rhodium(I) precursor was tested with several ligands (entries 4-6). Conversion and selectivities for these systems were moderate and did not improve when Rh(III) was used as precursor. When the metal precursor **102** was used without ligand, higher conversion and selectivity were observed. Likewise neutral Rh(I) precursors led to systems with moderate activity and selectivity (entries 7 and 8). With these results in hand and literature precedents,[22] we explored the activities of isolated Rh(III) complexes in the hydrosilylation of acetophenone Figure 3.9.

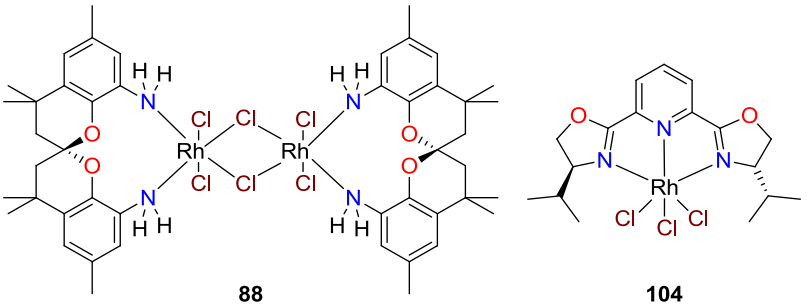

88 **104**

Figure 3.9 *Isolated complexes used in Rh-hydrosilylation.*

To investigate the differences in catalytic activity of *in situ* prepared catalysts and the corresponding isolated complexes, both types were tested in this reaction (Graph 3.2). The isolated pybox complex **104** was much more active and selective than the *in situ* generated system. Thus selectivity to **98** increased from 38% to 93% and enantioselectivity also increased from 30% to 92%. In contrast, both *in situ* and isolated systems of SPANamine showed similar selectivity, although lower conversion was obtained with the isolated complex in this case.

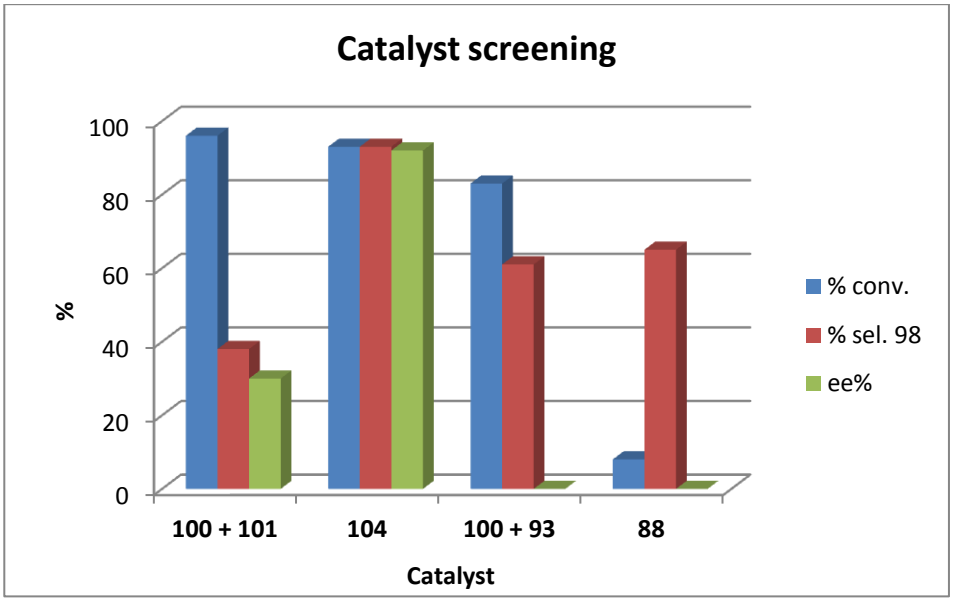

Graph 3.2 *Activity and selectivity comparison in the acetophenone hydrosilylation with isolated and in situ Rh(III) complexes. Reaction conditions: r.t., 24h, Rh/**96**=100, Rh/Si=150, in 2 ml THF. % conv. and % sel. **98** was calculated by ^{1}H NMR and ee% was measured by GC.*

To summarize, the rhodium catalyzed hydrosilylation of acetophenone was performed with SPANamine ligands. *In situ* systems were more active than the isolated one but no enantioselectivity was obtained. Pybox resulted to be the better ligand for this reaction.[22]

3.2.4. Copper catalyzed oxidation of *meso*-hydrobenzoin

Next, the SPANamine ligand was tested in the Cu catalyzed oxidation of *meso*-diols to check if the system containing *trans* bite angle amines can oxidize selectively *meso*-diols likely organometallic catalysts containing bisoxazoline ligands.[55] The benchmark reaction used in this study was the monoxidation of *meso*-hydrobenzoin in the presence of a copper catalyst. The reaction is shown in Scheme 3.12.

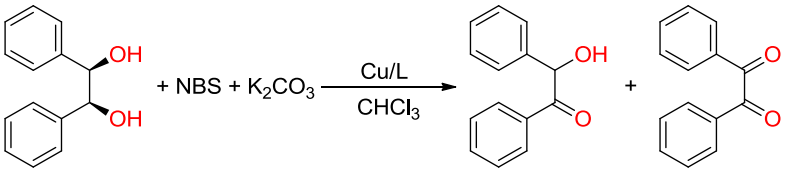

105 **106** **107**

Scheme 3.12 *Oxidation of meso-hydrobenzoin.*

The reaction was optimised with a racemic mixture of SPANamine **27**. Reaction was performed at room temperature in chloroform. The results are summarized in Table 3.4. In entries 1 to 3 it can be observed that conversion and selectivity was affected by the ligand/metal precursor ratio. When the ratio was increased both conversion and selectivity decreased. High conversion and selectivity were obtained for the ligand-free system, in entry 4. This catalytic activity of free metal was known from the literature.[55] The decrease of activity when ligand was present could be attributed to the competitive coordination of the substrate and the ligand to copper. As a consequence, a L/Cu ratio of 1.2 was chosen as the optimal ratio to avoid the presence of free metal in solution.

Table 3.4 *Optimization of reaction time, L/Cu ratio and temperature in the catalytic oxidation of meso-hydrobenzoin.*

Entry	L/Cu	T(h)	T(ºC)	% conv.[a]	% sel. 106[a]
1	1	3	r.t.	88	100
2	1,2	3	r.t.	63	95
3	2	3	r.t.	59	92
4	-	3	r.t.	87	97
5	1,2	3	60	79	30
6	1,2	6	r.t.	100	90
7	1,2	4	r.t.	91	94

105/$Cu(OTf)_2$=10, K_2CO_3/**105**=2, NBS/**105**=2, L=**27**. [a] calculated by ^{1}H NMR.

Once the ligand/metal ratio was optimized other reaction conditions were fine-tuned in order to improve conversion and selectivity. When the temperature was increased (entry 5), an increase in conversion was observed together with a

clear decrease in selectivity, since compound **107** was the major product of the reaction. In entries 6,7 the reaction time was varied. Complete conversion and high selectivity up to 90% was observed for 6 hours of reaction. Although we observed a slight decrease in conversion for 4 hours of reaction time a better selectivity was achieved. Thus the chosen conditions for this catalytic transformation were room temperature and 4 hours of reaction time.

Next, various oxidants were tested in the oxidation of *meso*-hydrobenzoin. The results are summarized in Graph 3.3.

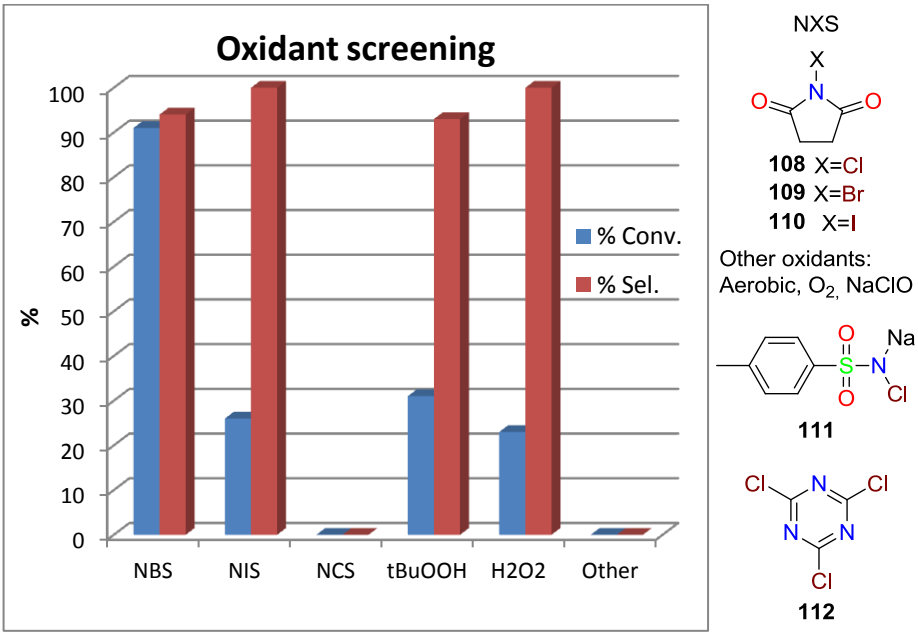

Graph 3.3 *Oxidant screening results in the oxidation of **105**. **105**/Cu(OTf)$_2$=10, K$_2$CO$_3$/**105**=2, oxidant/**105**=2, L/Cu=1.2, L=**27**. [a] calculated by ^{1}H NMR. ^{t}BuOOH, 60ºC and 3 eq. H$_2$O$_2$ 10 eq. Other= NaOCl, 111, 112.*

The most active oxidant in the reaction was NBS, yielding 91% of conversion and 94% of selectivity towards **106**. NIS gave lower conversion but complete selectivity, while in contrast NCS was completely unactive. Some chlorine containing oxidizing agents were tested.[62–64] Like **108**, these different oxidants, sodium hypochloride, chloroamine T, **111**, and cyanuric chloride, **112**, were unactive; only the starting material *meso*-hydrobenzoin was recovered when

they were used. Thus, best results in terms of conversion and selectivity were obtained with NBS.

Hydroperoxide compounds are known to be active in the oxidation of alcohols.[65,66] Thus, they were screened in the copper mediated oxidation of *meso*-hydrobenzoin. *Tert*-butyl hydroperoxide (TBHP) was first tested. The activity was lower than that obtained using NBS. As a consequence, high temperatures, oxidant loadings, or longer reaction times were required. The highest conversion and selectivity were achieved when 3 equivalents were used at 60 ºC. A similar trend was observed when hydrogen peroxide was used as the oxidant, and a large excess of oxidant (up to 10 equivalents) – due to the oxygen evolution – was needed to obtain conversions and high selectivity towards **106**. In view of the results obtained in this oxidant screening, NBS was used for further reactions.

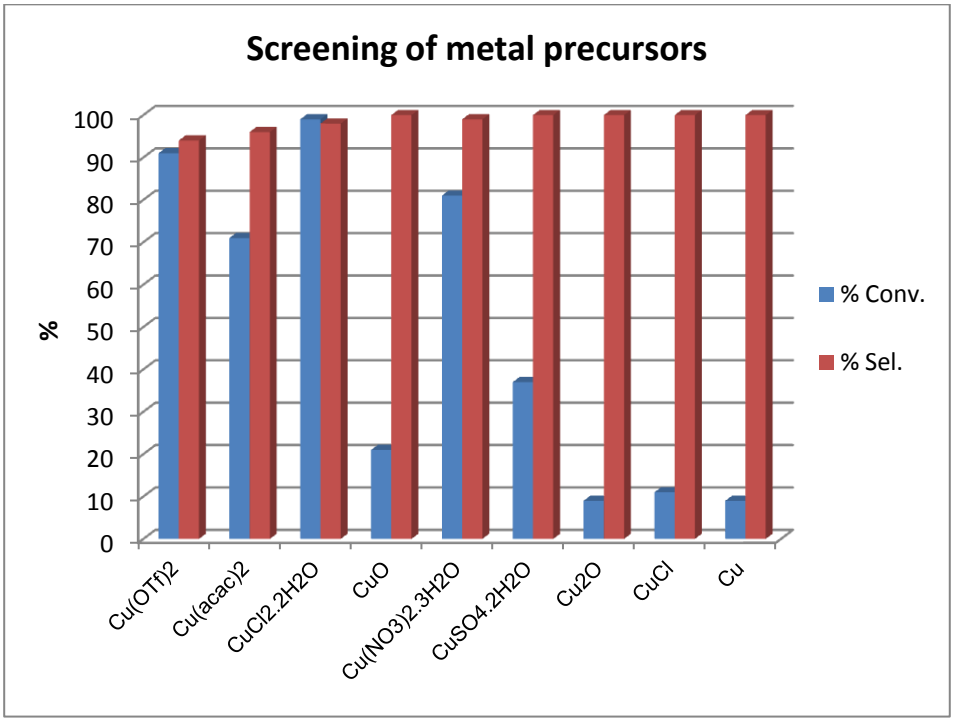

Graph 3.4 *Copper precursors screening in the oxidation of **105**. **105**/Cu=10, K_2CO_3/**105**=2, NBS/**105**=2, L/Cu=1.2, L=**27**. Conversion and selectivity were measured by ^1H NMR.*

Since the nature of the metallic precursor usually plays an important role in catalysis, various precursors were tested. The results in oxidation of different copper precursors are summarized in Graph 3.4. The use of copper (0) and copper(I) species led to low catalytic activities. In contrast, almost all the copper(II) precursors provided high to very high conversion, and very high selectivity to the α-hydroxyketone. Lower conversions were obtained for CuO with only 21% of conversion to **106** and very high selectivity; only α-hydroxyketone was detected. The low activity could be attributed to the solid nature of the catalyst. Regarding the low activity of Cu(0) and Cu(I) species, this may be related to the lower Lewis acidity of these species. Finally the best catalytic precursor was $CuCl_2.H_2O$ with 99% of conversion and 98% of selectivity.

Using this metal precursor a reaction with 1% of metal loading was carried out. Full conversion towards the desired product was obtained together with a high selectivity of up to 97% (Table 3.5, entry 1). Therefore, the next experiments were carried out with this catalyst loading.

Table 3.5 *Solvent screening in the catalytic asymmetric oxidation of meso-hydrobenzoin*

Entry	S	% conv.[a]	% sel. 106[a]	% ee[b]
1	$CHCl_3$	100	97	0
2	CH_2Cl_2	89	98	0
3	THF	95	100	0
4	AcOEt	21	100	0
5	MeOH	2	100	0
6	H_2O	0	0	0

105/Cu=100, L/Cu=1,2, K_2CO_3/S=2, NBS/S=2, r.t., 4h, L=**93**. [a] calculated by ^{1}H NMR. [b] calculated by HPLC.

The influence of the solvent on the activity and selectivity was performed with chiral SPANamine **93**. The nature of the solvent was important for the conversion and selectivity. The results of the solvent screening are summarized in Table 3.5. The use of chloroform, dichloromethane and tetrahydrofuran (entries 1-3) provided high conversion and selectivity. The use of ethyl acetate

as solvent led to low conversion but perfect selectivity (entry 4). Entries 5 and 6 show that low or no conversion was found for methanol and water. The low conversion was attributed to a competitive coordination of the solvent and the substrate to the copper centre. However, the distinct solubilities of the diol and NBS in the solvent could also have contributed to these results. Although conversion was obtained with all solvents, racemic mixtures of the product were obtained in all instances. In the subsequent experiments, chloroform was used.

Table 3.6 *Base screening in the catalytic asymmetric oxidation of meso-hydrobenzoin*

Entry	Base	% conv. [a]	% sel. 106 [a]	% ee[b]
1	K_2CO_3	100	97	0
2	Cs_2CO_3	0	0	0
3	KO^tBu	0	0	0
4	LHMDS	13	100	0

105/Cu=100, L/Cu=1,2, K_2CO_3/S=2, NBS/S=2, r.t., 4h, L=**93**. [a] calculated by ^{1}H NMR. [b] calculated by HPLC.

The last step in the optimization of the reaction conditions was the study of base effects. Results are summarized in Table 3.6. Full conversion and high selectivity was observed when potassium carbonate was used as base (entry 1). No conversion was detected when cesium carbonate or potassium *tert*-butoxide were used as bases (entry 2 and 3) and only 13% of conversion and perfect selectivity was obtained with the use of LHMDS. The low or lack of activity for entries 3 and 4, was attributed to the presence of water in the solvents.

Once the reaction conditions were optimized several amine ligands were tested in the Cu catalyzed asymmetric oxidation of *meso*-hydrobenzoin (Figure 3.10)

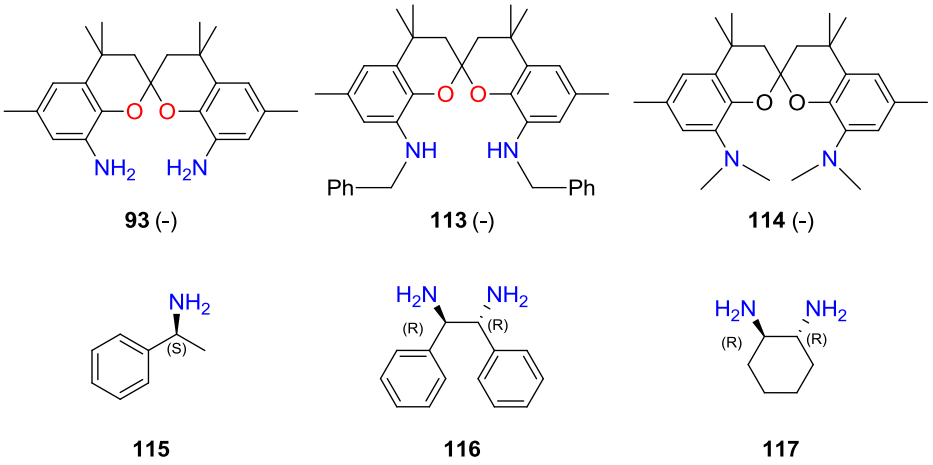

Figure 3.10 *Amines used as ligands in the catalytic asymmetric oxidation of **105**.*

The results of the use of primary amine (**93**, **115**-**117**) as ligands are summarized in Graph 3.5. High conversions and selectivity towards α-hydroxyketone (over 90% for both) were obtained in the oxidation catalysis when mono- and diamines were used as ligands. In all cases the racemic product was obtained. We observed neither an effect of ligand denticitiy nor bite angle.

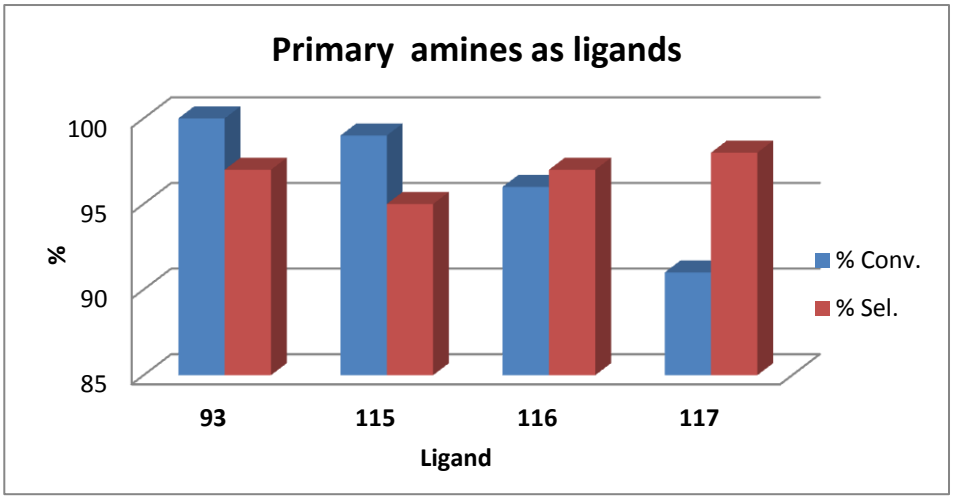

Graph 3.5 *Results of the oxidation of **105** with the usage of primary amines as ligands. **105**/Cu=10, K_2CO_3/**105**=2, NBS/**105**=2, L/Cu=1.2. Conversion and selectivity were calculated by ^{1}H NMR.*

When SPANamine derivatives of secondary and tertiary amines **113** and **114** were used as ligands in the Cu catalyzed oxidation of **105** catalytic activity was also observed. Results are summarized in Graph 3.6. Secondary amine led a catalytic system capable to oxidize **105** with high conversion and selectivity, while in contrast the tertirary amine system only gave 64% of conversion with high selectivity. Unfortunately, the racemic mixture was recovered and apparently the larger steric hindrance does not provide the required chiral pocket to enantiodiscriminate the two diol functions during the oxidation of the substrate. Furthermore, this large steric hindrance is responsible of lower conversions as coordination of the substrate to the metals more difficult. With these results we decided to test oxazoline ligands in the copper catalyzed oxidation of *meso*-hydrobenzoin.

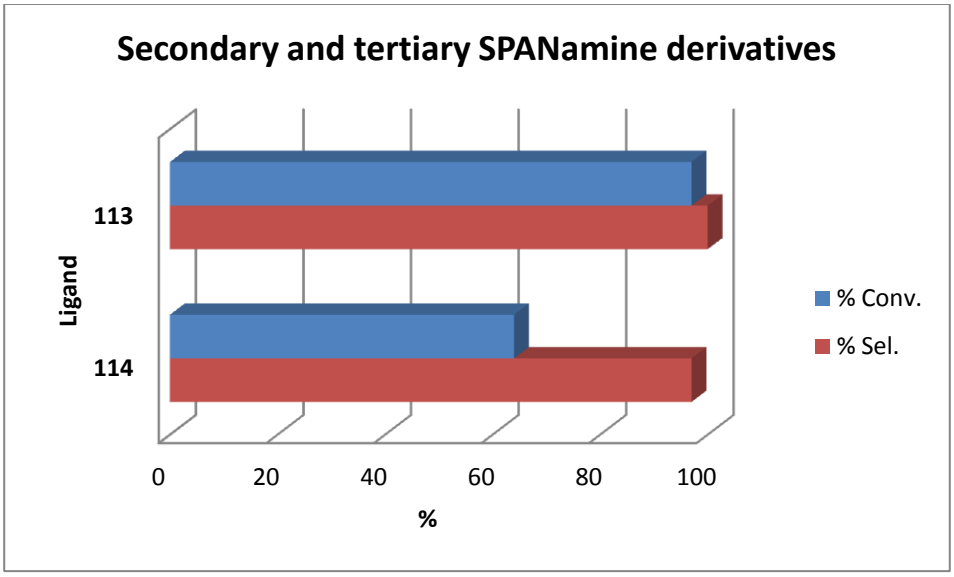

Graph 3.6 *Results in oxidation of **105** with the usage of secondary and tertiary amines as ligands. **105**/Cu=10, K_2CO_3/**105**=2, NBS/**105**=2, L/Cu=1.2. Conversion and selectivity were calculated by ^{1}H NMR.*

In order to investigate the bite angle effects in the asymmetric oxidation of *meso*-hydrobenzoin, several oxazolines, with different bite angle or denticity were explored as ligands in this reaction (Figure 3.11).

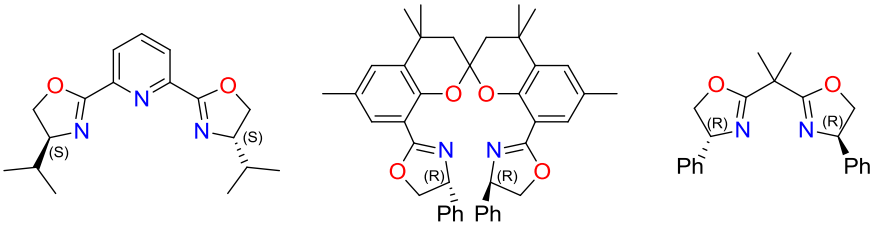

100 **118** (+) **119**

Figure 3.11 *Oxazolines used as ligands in the catalytic asymmetric oxidation of* ***105****.*

The results of the catalyzed copper oxidation of **105** are summarized in Graph 3.7. Ligand **119** was reported in literature as a promising ligand for the oxidation of *meso*-diols.[55,56] Moderate conversions and high selectivities towards **106** were obtained with oxazoline ligands, but low to moderate enantiomeric excesses were obtained. With 10% of catalyst loadings, full conversion, selective formation of the α-hydroxyketone and moderate to good enantioselectivies were observed. **119** was found to be the best ligand for this reaction. An increase of bite angle or denticity of ligand resulted in a reduction of the enantiomeric excess of the product. This may be related with the geometry of copper intermediate. Apparently, larger bite angle ligands or tridentante ligands change the chiral pocket in an unfavourable way.

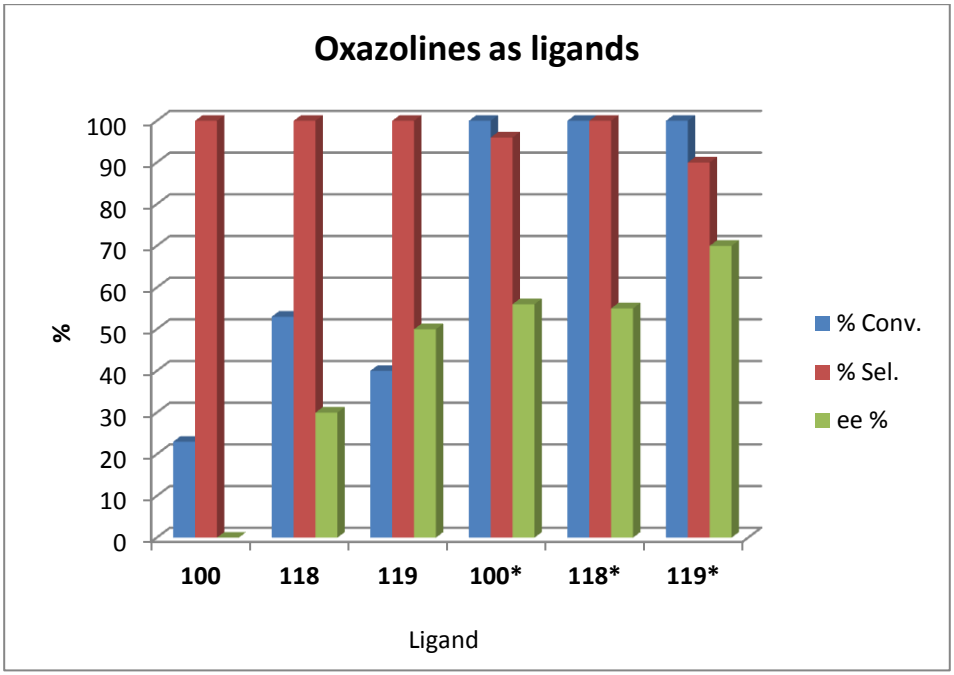

Graph 3.7 *Results in oxidation of **105** with the usage of oxazolines as ligands. **105**/Cu=100, K_2CO_3/**105**=2, NBS/**105**=2, L/Cu=1.2. Conversion and selectivity were measured by ^1H NMR. ee% was* determined by HPLC. * ***105**/Cu=10*

3.2.5. Iron catalyzed oxidation of *meso*-hydrobenzoin

The catalytic oxidation of *meso*-hydrobenzoin using iron complexes was also explored using the same conditions as those for the previously optimised copper mediated catalysis. An iron-catalyzed reaction is of interest due to the high abundance, low toxicity, and price of iron. The reaction is depicted in Scheme 3.13.

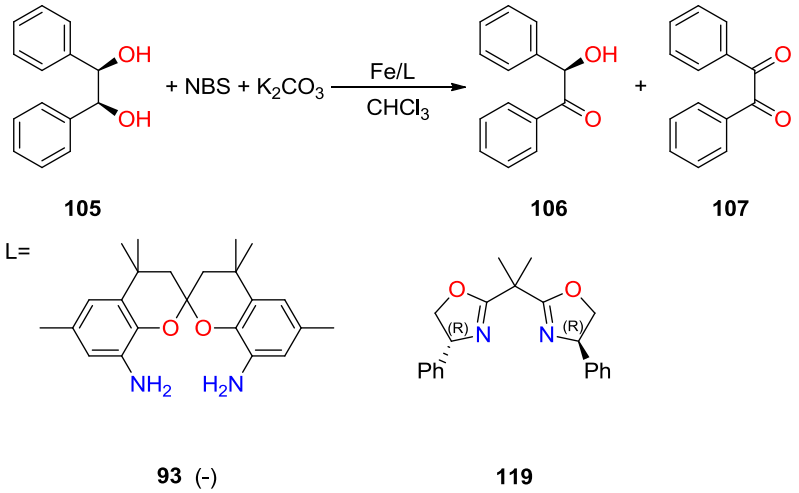

Scheme 3.13 *Iron oxidation of meso-hydrobenzoin.*

SPANamine **93** and BOX **119** were explored in this reaction. The reaction was also carried out in the absence of amine ligand. Conversion to benzoin was detected in all 3 cases. The results are summarized in Graph 3.8 (conversion of starting material) and selectivity towards α-hydroxyketone).

Like copper, iron can act as Lewis acid and iron (0, II or III) precursors promoted the oxidation of **105**. Under the reaction conditions, it is expected that iron (0) is oxidized by the oxidant or air. The nature of the iron counterion was important in the ligand free systems; for instance $Fe(acac)_n$ (n=2 or 3) were good catalyst for the oxidation of **105**. As a general trend, iron-SPANamine catalytic systems presented the higher conversions and selectivities than oxazoline ligand **119**.

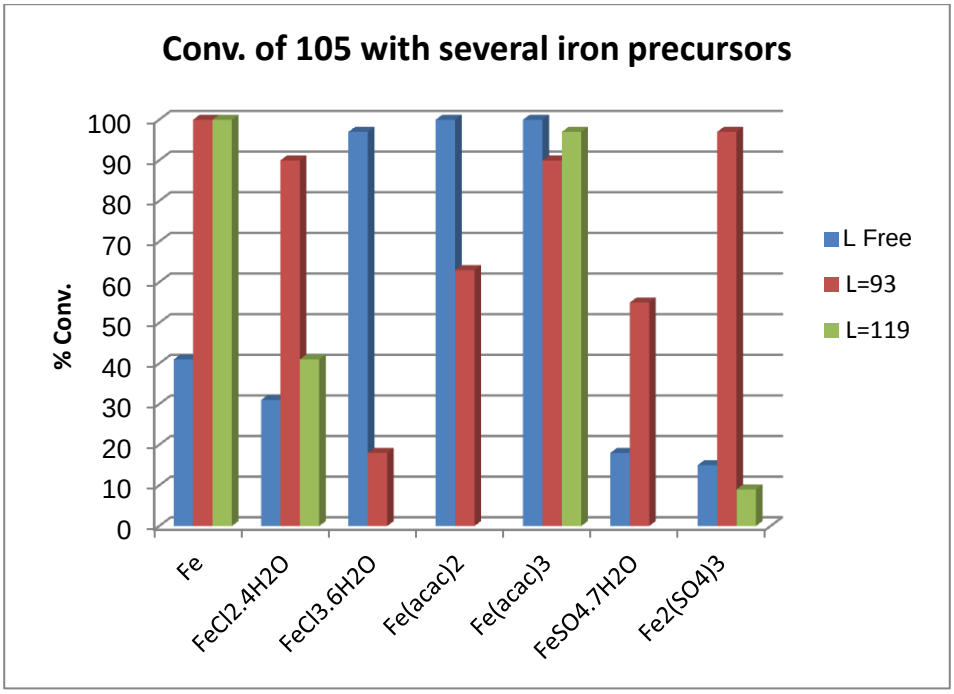

Graph 3.8 *Conversion of **105** in the oxidation promoted by iron precursors.* ***105***/Fe=10, L/Fe=1,2, K_2CO_3/***105***=2, Ox/***105***=2, r.t., t=4h,NBS as oxidant. *Conversion and selectivity were measured by* ^1H *NMR.*

Regarding the selectivity of the reaction (Graph 3.9), values from moderate to very high (70-100%) were obtained. The best results were again achieved with SPANamine with a selectivity ranging from 90 to 100%. However, the use of SPANamine yielded racemic product, and thus no enantiodiscrimination was achieved.

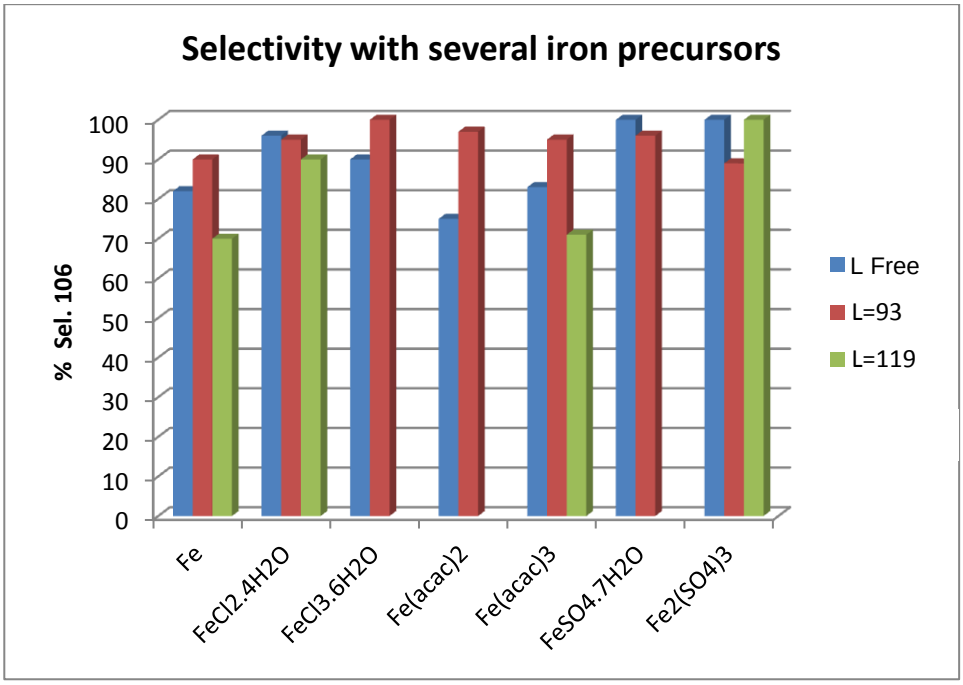

Graph 3.9 *Conversion of **105** in the oxidation promoted by iron precursors.* ***105***/Fe=10, L/Fe=1,2, K_2CO_3/***105***=2, Ox/***105***=2, r.t., t=4h,NBS as oxidant. *Conversion and selectivity were measured by* ^{1}*H NMR.*

To conclude, the combination of SPANamine and iron(III) sulphate was the best system for the oxidation of *meso*-hydrobenzoin with high conversion and selectivity. However, the same as for copper, SPANamine **93** was not able to enantiodiscriminate and hence a racemic mixture was obtained. Compared to copper, conversion and selectivities were similar, but the copper system is better due to its ability to yield enantio-enriched mixtures.

3.3. Conclusions

- Several rhodium, copper and palladium complexes were synthesized containing SPANamine as the ligand. Different structures and geometries were obtained for each metal.

- Rhodium SPANamine complex **88** exhibits a dimeric structure with both Rh centres in an octahedral geometry. For this complex SPANamine shows a bite angle of *ca.* 95º.

- Palladium SPANamine complex **89** is a monomeric species. A *trans*-coordination is expected, as found for the analogous Pd-SPANphos complex.[61]

- Copper SPANamine complex **90** shows a distorted square planar geometry where the ligand bite angle was close to 150º and SPANamine coordinates as a *trans*-ligand.

- The rhodium catalyzed hydrogenation of dimethyl itaconate was explored with SPANamine and SPANoxazoline as ligands. To achieve full conversion, high pressures of hydrogen were necessary. A bite angle effect was not observed in this catalytic transformation and the activity may be due to Rh metal.

- Acetophenone was hydrosilylated by rhodium modified with SPANamine. Different catalytic behaviours were observed for *in situ* and isolated systems, with the former system showing a higher activity. However, similar selectivities were obtained with both systems and no enantioselectivity was achieved.

- Copper-catalyzed oxidation of *meso*-diols was explored with various N-donor ligands. High activities and selectivities were obtained for all the ligands applied in the reaction. Interestingly, only oxazoline ligands were capable of inducing enantioselectivity. When the large bite angle SPANoxazoline ligand **95** was used, no increase in ee was observed when compared to the results measured with oxazoline **119**.

- Iron oxidation of *meso*-diols was explored using the SPANamine and oxazoline ligands **93** and **119**. Iron(0, II, III) precursors modified with SPANamine presented higher conversions and selectivities to α-hydroxyketones than the systems containing the oxazoline ligand. Unfortunately, racemic mixtures of product were obtained in all cases.

3.4. Experimental Part

Unless otherwise stated, all reactions were performed using standard vacuum-line and Schlenk techniques under nitrogen atmosphere. Solvents were purchased from Sigma-Aldrich as HPLC grade and dried with an SPS system of ITC-inc. Reagents were used as commercially available. NMR spectra unless otherwise stated were recorded at the following frequencies: 400.13 MHz (^{1}H) and 100.63 MHz (^{13}C) NMR spectra were recorded using broad band decoupling. Chemical shifts of ^{1}H and ^{13}C NMR spectra are reported in ppm downfield from TMS, used as internal standard. Signals are quoted as s (singlet), d (doublet), t (triplet), m (multiplet), b (broad)). Gas chromatographic analyses were run on a Hewlett-Packard HP 5890A instrument (split/splitless injector, J&W Scientific, IA, 25 m column, internal diameter 0.25 mm, film thickness 0.33 mm, carrier gas: He, F.I.D. detector) equipped with a Hewlett-Packard HP3396 series II integrator. HPLC analyses were run on a HPLC Agilent 1100 apparatus, using a Daicel CHIRALPAK IA column (4.6mm B, 250 mm). The CG-MS are done in HP 6890 Series GC System coupled to HP 5973 Mass Selective Detector, with automatic injector HP 7683 Series Injector. The column is HP 5MS (30 m x 0.25 mm, and 0.25 film thickness µm). High pressure experiments were performed in Berghof Stainless Steel SS316 reactors (25 and 40 ml) equipped with a PTFE liner, magnetic stirring and heating jacket.

Synthesis of $[Rh_2Cl_4(SPANamine)_2(\mu\text{-}Cl)_2]$, 88.

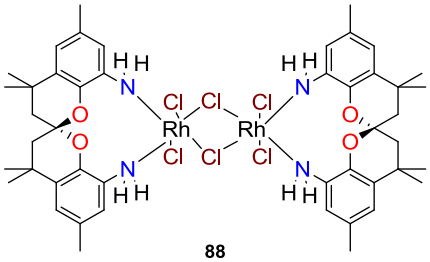

88

A solution of rhodium(III) chloride trihydrate (35.5 mg, 0.14 mmol) and **93** (50 mg, 0.14 mmol) in ethanol (1.5 ml) was heated under reflux under nitrogen atmosphere for 3 h. After the solvent was removed under reduced pressure, the residue was purified by silica gel column chromatography with ethyl acetate and methanol as eluents to give **88** as an orange solid in 65% yield. ^{1}H NMR (401 MHz, Chloroform-*d*) δ = 7.51 – 7.45 (m, 2H), 7.33 – 7.30 (m, 2H), 7.04 (d, *J* = 1.9 Hz, 2H), 7.00 – 6.95 (m, 4H), 5.95 (d, *J* = 11.3 Hz, 2H), 5.75 (d, *J* = 10.7 Hz, 2H), 5.61 (d, *J* = 10.7 Hz, 2H), 2.54 (d, *J* = 14.1 Hz, 2H), 2.42 (d, *J* = 13.9 Hz,

2H), 2.37 (d, *J* = 0.8 Hz, 6H), 2.30 (d, *J* = 14.2 Hz, 2H), 2.24 (d, *J* = 0.8 Hz, 6H), 2.15 (d, *J* = 14.0 Hz, 2H), 1.46 (d, *J* = 11.2 Hz, 12H), 1.32 (d, *J* = 6.6 Hz, 12H). ESI$^+$: calcd. for $C_{46}H_{60}Cl_5N_4O_4Rh_2$ [Rh_2(**27**)$_2Cl_5$] [M+] 1115.11; found 1115.2.

Synthesis of [$PdCl_2$(SPANamine)], 89.

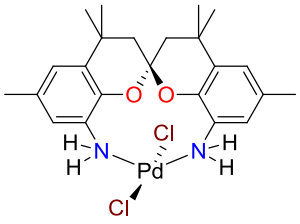

A Schlenk tube was charged with $PdCl_2$ (21.7 mg, 0.12 mmol). The system is sealed with a septum. The flask was evacuated and backfilled with inert gas three times. Deoxygenated acetonitrile was added (1.5 ml). The system was heated up to reflux during 1.5 hours. The system is cooled to r.t. and SPANamine was added (46.2 mg, 0.125 mmol). After two hours the mixture was filtered and washed with Et_2O. A yellow solid was isolated. Yield 73%. ^{1}H NMR (399 MHz, $CDCl_3$) δ = 7.63 (s, 2H), 6.97 (s, 2H), 5.17 (d, J = 9.0 Hz, 2H), 4.20 (d, J = 8.4 Hz, 2H), 2.45 (d, J =14.3 Hz, 2H), 2.41 (s, 6H), 2.18 (d, J = 14.3 Hz, 2H), 1.44 (s, 6H), 1.29 (s, 6H). ESI$^+$: calcd. for $C_{23}H_{30}ClN_2O_2Pd$ [Pd**27**Cl] [M+] 507.10; found 507.

Synthesis of [$CuCl_2$(SPANamine)], 90.

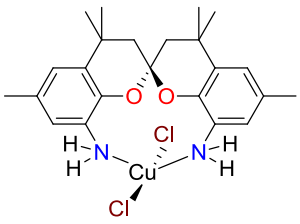

A Schlenk tube was charged with $CuCl_2.H_2O$ (34.4 mg, 0.2 mmol) and SPANamine (73.3 mg, 0.2 mmol). Chloroform was added (1.5 ml). The system was stirred during 2 hours.. After two hours it was filtered and washed with Et_2O. A yellow solid was isolated. Yield 55%. Brown crystals were grown from slow evaporation of a mixture chloroform/acetone (1:1). MALDI$^+$: calcd. for $C_{23}H_{30}N_2O_2Cu$ [Cu**27**] [M+] 429.16; found 429.3.

Synthesis of [$RhCl_3$(Pybox)], 104.[22]

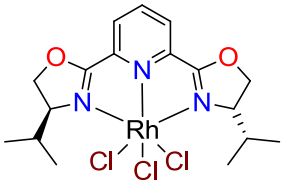

104

A solution of rhodium(III) chloride trihydrate (253 mg, 1 mmol) and **100** (304 mg, 1 mmol) in ethanol (3 ml) was heated at reflux temperature under a nitrogen atmosphere for 3 h. After the solvent was removed under reduced pressure, the residue was purified by

silica gel column chromatography with ethyl acetate and methanol as eluents to give **104** as an orange solid in 83% yield. ^{1}H NMR (399 MHz, $CDCl_3$), δ = 8.43 (t, J = 7.9 Hz, 1 H), 8.09 (d, J = 8.3 Hz, 2 H), 4.98 (dd, J = 10.4, 19.8 Hz, 2 H), 4.94 (dd, J = 7.4, 19.8 Hz, 2 H), 4.62 (ddd, J = 10.4, 7.4, 3.0 Hz, 2 H), 3.04 (m, 2 H), 0.97 (d, J = 6.5 Hz, 6 H), 0.99 (d, J = 6.5 Hz, 6 H

Catalytic hydrogenation reactions. [67]

All reactions were performed in deoxygenated solvents. Conversions were determined by NMR and GC. Enantiomeric excess were determined by GC.

A Schlenk vessel was charged with 1 mmol of dimethyl itaconate, $[Rh(COD)_2]BF_4$ and the ligand. Then three cycles of vacuum/nitrogen were done. Then 6 ml of deoxygenated dichloromethane were added. The solution was moved to an autoclave by syringe in which previously four cycles of vacuum/hydrogen were carried out. After the addition of the solution, the autoclave was charged with the desired hydrogen pressure. The temperature was regulated and the reaction was stopped after four hours. Dichloromethane was removed under reduced presure. ^{1}H NMR spectra were run for determining the conversion ($\delta_{substrate(1H)}$=6.25 (s) ppm, $\delta_{product(1H)}$=2,33 (dd) ppm. The solid remaining was diluted in 15 ml of methanol and filtered through cotton, silica and celite. After that 1 µl of solution was injected to a GC (T oven=80 ºC, $T_{inj}=T_{det}$=250 ºC) for determining the conversions and enantiomeric excesses. T(S)=8.5, T(R)=9.1 and $T_{substrate}$=14.2 min.

Catalytic hydrosilylation reactions.[22,68]

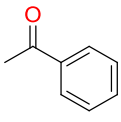

96

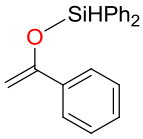

97

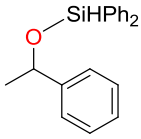

98

A Schlenk tube was charged with acetophenone (0.48 ml, 1 mmol), $AgBF_4$ (15.7 mg, 0.08 mmol), and $RhLCl_3$ (0.01 mmol). The system was sealed with a septum. The flask was evacuated and backfilled with inert gas three times. Deoxygenated THF was added (1 ml). The solution was stirred during 30 minutes. After that the solution was cooled to 0 ºC and H_2SiPh_2 (1.21 ml, 1,2 mmol) was added. The solution was warmed up to r.t. and left stirring during 24h. A sample was taken (0.2 ml), diluted with $CDCl_3$ (0.4ml) and a 1H NMR (400 MHz) was recorded to determine the selectivity towards silylalkyl ether (**98**:(**97**+**98**)) and the degree of

hydrosilylation (conversion of acetophenone, ((**97**+**98**):(**96**+**97**+**98**)). The following integrals were used for the analysis: δ=5.70 ppm (s, Si-H, silylenol ether **97**), δ =5.40 ppm (s, Si-H, silylalkyl ether **98**) and δ =2.50 ppm (s, CH_3, acetophenone **96**)

For the work-up, to the reaction mixture was slowly added methanol (5 mL) at 0 ºC. After gas evolution ceased, the reaction mixture was poured into a solution of hydrochloric acid (1 N, 7 mL) at 0 ºC. The reaction flask was washed with small amounts of methanol and ether, and the washings were also added to the acid solution. The mixture was stirred at 0º C for 1 h and extracted with ether (7.5 mL x 4). The extract was washed with brine (3 ml) and dried over anhydrous $MgSO_4$. The ee was determined by GC analysis.

General procedure for oxidation catalysis.

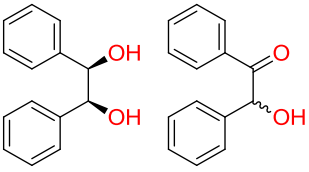

105 **106** **107**

Under an aerobic atmosphere, a solution of $CuCl_2$ (0.9 mg, 0.005 mmol) and ligand (0.006 mmol) in $CHCl_3$ (5 ml) was stirred for 10 min. To the solution were added *meso*-hydrobenzoin (0.5 mmol), potassium carbonate (138 mg, 1.0 mmol), and NBS (178 mg, 1.0 mmol). After stirring for 4 h at r.t., the solution was poured in 10% aqueous $Na_2S_2O_3$ and extracted with CH_2Cl_2 (10 mL x 3). The combined organic layer was dried over $MgSO_4$ and the solvent was removed under reduced pressure. Conversion and selectivity were determined by ^1H NMR. The following integrals were used for the analysis: δ=5.89 ppm (s, C-H (1H), benzoin **A**), δ =4.82 ppm (s, C-H (2H), *meso*-hydrobenzoin **B**) and δ =7.60 ppm (t, CH, benzil **C**). The degree of oxidation was determined using this operation, ((**A**+**B/6**):(**A**+**B/6**+**C/2**)) and selectivity towards benzoin with this one, (**A**:(**A**+**B/6**))

The optical purity of (R)-2a was determined by chiral HPLC: Daicel CHIRALPAK IA column (4.6 mm B, 250 mm), n-hexane/isopropanol = 90:10, wavelength: 210 nm, flow rate: 1.0 ml/min, retention time: 16.5 min ((R)-(+)-2a), 19.9 min ((S)-(-)-2a).

3.5. References

1. S. Bhaduri and D. Mukesh, *Homogeneous Catalysis: Mechanisms and Industrial Applications*, Wiley-Interscience, New York, 2000, vol. 8.
2. P. W. N. M. Leeuwen, *Homogeneous Catalysis: Understanding the Art*, Kluwer, Dordrecht, 2004.
3. B. Cornils and W. A. Herrman, *Applied Homogeneous Catalysis with Organometallic Compounds*, Wiley-VCH, Wienheim, 1996.
4. C. Landis and J. Halpen, *J. Am. Chem. Soc.*, 1987, **5**, 1746-54.
5. H. B. Kagan, *Pure App. Chem.*, 1975, **43**, 401-21.
6. W. S. Knowles, *Angew. Chem. Int. Ed.*, 2002, **41**, 1999-2007.
7. A. Miyashita, A. Yasuda, H. Takaya, K. Toriumi, T. Ito, T. Souchi, and R. Noyori, *J. Am. Chem. Soc.*, 1980, **102**, 7932-4.
8. M. J. Burk, *Acc. Chem. Res.*, 2000, **33**, 363-72.
9. A. Togni, C. Breutel, A. Schnyder, F. Spindler, H. Landert, and A. Tijani, *J. Am. Chem. Soc.*, 1994, **116**, 4062-66.
10. Y. Ito and R. Kuwano, *Phosphorus, Sulfur, and Silicon and the Related Elements*, 1999, **144**, 469-72.
11. R. Kuwano, M. Sawamura, and Y. Ito, *Bull. Chem. Soc. Jap.*, 2000, 2571-8.
12. R. Kuwano, M. Kashiwabara, K. Sato, T. Ito, K. Kaneda, and Y. Ito, *Tetrahedron: Asymmetry*, 2006, **17**, 521-35.
13. R. Kuwano, K. Kaneda, T. Ito, K. Sato, T. Kurokawa, and Y. Ito, *Org. Lett.*, 2004, **6**, 2213-5.
14. M. Tommasino, C. Thomazeau, F. Touchard, and M. Lemaire, *Tetrahedron: Asymmetry*, 1999, **10**, 1813-9.
15. R. T. Halle, A. Breheret, E. Schulz, C. Pinel, and M. Lemaire, *Tetrahedron: Asymmetry*, 1997, **8**, 2101-8.
16. C. Pinel, N. Gendreau-Diaz, A. Bréhéret, and M. Lemaire, *J. Mol. Cat. A, Chem.*, 1996, L157-L161.
17. B. Shainyan, M. Ustinov, V. Bel'skii, and L. Nindakova, *Russ. J. Org. Chem.*, 2002, **38**, 104-10.
18. A. Corma, M. Iglesias, and F. Sa, *J. Organomet. Chem.*, 2002, **655**, 134-45.
19. M. Iglesias, F. Sa, and I. Viani, *J. Organomet. Chem.*, 2000, **601**, 284-92.

20. E. N. Jacobsen, A. Pfaltz, and H. Yamamoto, *Comprehensive Asymmetric Catalysis*, Springer, Heidelberg, 1999.
21. P. C. J. Kamer and P. W. N. M. van Leeuwen, *Phosphorus(III)Ligands in Homogeneous Catalysis: Design and Synthesis*, Wiley, 2012.
22. H. Nishiyama, M. Kindo, T. Nakamura, and K. Itoh, *Organometallics*, 1991, **5**, 500-8.
23. D. Cuervo, J. Díez, M. P. Gamasa, J. Gimeno, and P. Paredes, *Eur. J. Inorg. Chem.*, 2006, **2006**, 599-608.
24. H. Nishiyama, S. Yamaguchi, S. Park, and K. Itoh, *Tetrahedron: Asymmetry*, 1993, **4**, 143-50.
25. P. von Matt and A. Pfaltz, *Angew. Chem. Int. Ed.*, 1993, **32**, 566-8.
26. L. M. Newman, J. M. J. Williams, R. Mccague, G. A. Potter, C. Limited, C. S. Park, and M. Road, *Tetrahedron: Asymmetry*, 1996, **7**, 1597-8.
27. O. Pàmies, C. Claver, and M. Diéguez, *J. Mol. Cat. A, Chem.*, 2006, **249**, 207-10.
28. V. César, S. Bellemin-Laponnaz, H. Wadepohl, and L. H. Gade, *Chem: A Eur. J.*, 2005, **11**, 2862-73.
29. N. Schneider, M. Kruck, S. Bellemin-Laponnaz, H. Wadepohl, and L. H. Gade, *Eur. J. Inorg. Chem.*, 2009, **2009**, 493-500.
30. D. Imao, M. Hayama, K. Ishikawa, T. Ohta, and Y. Ito, *Chem. Lett.*, 2007, **36**, 366-7.
31. R. Kuwano, T. Uemura, M. Saitoh, and Y. Ito, *Tetrahedron: Asymmetry*, 2004, **15**, 2263-71.
32. M. Flückiger and A. Togni, *Eur. J. Org. Chem.*, 2011, **2011**, 4353-60.
33. V. Bette, A. Mortreux, F. Ferioli, G. Martelli, D. Savoia, and J.-F. Carpentier, *Eur. J. Org. Chem.*, 2004, **2004**, 3040-5.
34. J. Gavenonis and T. D. Tilley, *Inorg. Chem.*, 2004, **43**, 4353-62.
35. I. Karamé, M. Lorraine Tommasino, and M. Lemaire, *J. Mol. Cat. A, Chem.*, 2003, **196**, 137-43.
36. T. Inagaki, L. T. Phong, A. Furuta, J.-ichi Ito, and H. Nishiyama, *Chem. Eur. J.*, 2010, **16**, 3090-6.
37. V. M. Mastranzo, L. Quintero, C. Anaya de Parrodi, E. Juaristi, and P. J. Walsh, *Tetrahedron*, 2004, **60**, 1781-9.
38. B. L. Tran, M. Pink, and D. J. Mindiola, *Organometallics*, 2009, **28**, 2234-43.
39. M. B. Smith and J. March, *March's Advanced Organic Chemistry: Reactions, Mechanisms, and Structure, 6th Edition*, Wiley-Interscience, New Jersey, 2007.

40. L. Mandell, *J. Am. Chem. Soc.*, 1956, **78**, 3199-201.
41. A. Shaabani, P. Mirzaei, S. Naderi, and D. G. Lee, *Tetrahedron*, 2004, **60**, 11415-20.
42. D. B. Dess and J. C. Martin, *J. Org. Chem.*, 1983, **48**, 4155-6.
43. S. David and A. Thieffry, *J. Chem. Soc., Perkin Trans. 1*, 1979, 1568-73.
44. P. Gogoi and D. Konwar, *Org.& Bio. Chem.*, 2005, **3**, 3473-5.
45. Y.-Y. Li, X.-Q. Zhang, Z.-R. Dong, W.-Y. Shen, G. Chen, and J.-X. Gao, *Org. Lett.*, 2006, **8**, 5565-7.
46. R. Israel, J. M. M. Smits, C. Smykalla, T. D. System, M. J. Burn, M. G. Fickes, F. J. Hollander, and R. G. Bergman, *Angew. Chem. Int. Ed.*, 1997, **36**, 288-90.
47. S. Arita, T. Koike, Y. Kayaki, and T. Ikariya, *Angew. Chem. Int. Ed.*, 2008, **47**, 2447-9.
48. S. K. Mandal, D. R. Jensen, J. S. Pugsley, and M. S. Sigman, *J. Org. Chem.*, 2003, **68**, 4600-3.
49. S. Hanessian and R. Roy, *J. Am. Chem. Soc.*, 1979, 5839-41.
50. U. Ladziata, J. Carlson, and V. V. Zhdankin, *Tetrahedron Lett.*, 2006, **47**, 6301-4.
51. W. Adam, C. R. Saha-möller, and C.-gui Zhao, *Tetrahedron: Asymmetry*, 1998, **9**, 4117-22.
52. W. Adam, C. R. Saha-Möller, and C.-G. Zhao, *J. Org. Chem.*, 1999, **64**, 7492-97.
53. S. Sayama and T. Onami, *Synlett*, 2004, 2369-73.
54. T. Maki, S. Iikawa, G. Mogami, H. Harasawa, Y. Matsumura, and O. Onomura, *Chem. Eur. J.*, 2009, **15**, 5364-70.
55. O. Onomura, H. Arimoto, Y. Matsumura, and Y. Demizu, *Tetrahedron Lett.*, 2007, **48**, 8668-72.
56. D. Minato, H. Arimoto, Y. Nagasue, Y. Demizu, and O. Onomura, *Tetrahedron*, 2008, **64**, 6675-83.
57. Y. Nakamura, H. Egami, K. Matsumoto, T. Uchida, and T. Katsuki, *Tetrahedron*, 2007, **63**, 6383-7.
58. T. Suzuki, K. Ghozati, T. Katoh, and H. Sasai, *Org. Lett.*, 2009, **11**, 4286-8.
59. X. Sala, E. J. García Suárez, Z. Freixa, J. Benet-Buchholz, and P. W. N. M. van Leeuwen, *Eur. J. Org. Chem.*, 2008, **2008**, 6197-205.
60. C. Jiménez-Rodríguez, F. X. Roca, C. Bo, J. Benet-Buchholz, E. C. Escudero-Adán, Z. Freixa, and P. W. N. M. van Leeuwen, *Dalton Trans.*, 2006, 268-78.

61. O. Jacquet, N. D. Clément, C. Blanco, M. M. Belmonte, J. Benet-Buchholz, and P. W. N. M. van Leeuwen, *Eur. J. Org. Chem.*, 2012, **2012**, 4844-52.
62. L. De Luca, G. Giacomelli, and A. Porcheddu, *J. Org. Chem.*, 2001, **66**, 7907-9.
63. G. A. Mirafzal, A. M. Lozeva, and D. Moines, *Tetrahedron Letters*, 1998, **39**, 7263-66.
64. M. M. Natarajan and V. Thiagarajan, *J. Chem. Soc., Perkin Trans. 2*, 1975, 1590-4.
65. G. Ferguson and A. Nait Ajjou, *Tetrahedron Letters*, 2003, **44**, 9139-2.
66. S. Velusamy and T. Punniyamurthy, *European Journal of Organic Chemistry*, 2003, **2003**, 3913-5.
67. M. Diéguez, A. Ruiz, and C. Claver, *J. Org. Chem.*, 2002, **67**, 3796-801.
68. G. Chelucci, S. Gladiali, M. G. Sanna, and H. Brunner, *Tetrahedron: Asymmetry*, 2000, **11**, 3419-26.

Chapter 4

Amino derivatives of Spirobichroman, Dehydrobenzofurobenzofuran, and Methanodibenzodioxocine; tetradentate ligands in metal catalyzed reactions.

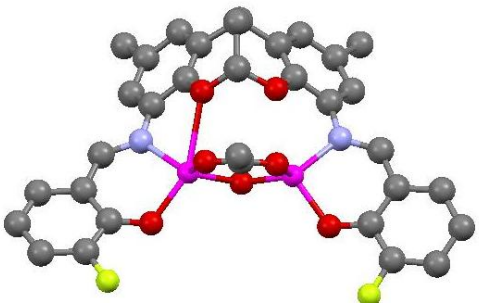

4.1. Catalysis introduction

4.1.1. Metal catalyzed synthesis of cyclic carbonates

Carbon dioxide is widely accepted to be largely responsible for the Greenhouse effect and the increase in the world temperature.[1] Most of the non-natural emissions of carbon dioxide are a result of burning fossil fuels. As more than 80% of the primary energy is derived from the combustion of fossil fuels (Graph 4.1), the concentration of carbon dioxide in atmosphere is growing constantly.[2] In an effort to address this problem, many research activities are nowadays focusing in this area such as for example, green alternative fuel sources, carbon capture and storage, and relevant to this thesis, the use of carbon dioxide as C_1 building block in synthesis.[3,4]

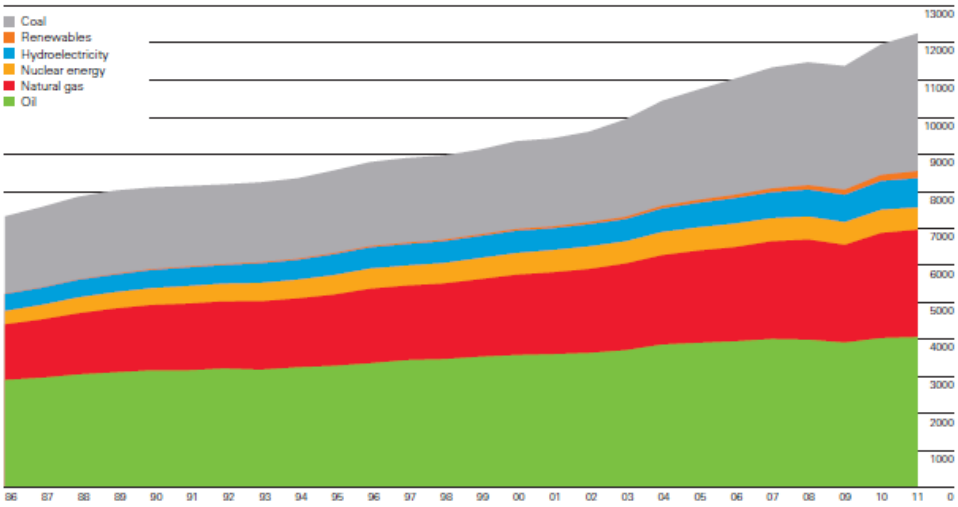

Graph 4.1 *World primary energy consumption in 2011.*

The use of carbon dioxide as starting material to synthesize high-valued compounds is a growing area of interest. [5,6] As an organic, C1 feedstock, CO_2 has several advantages. For instance, it is non-toxic, abundant, economical, and environmentally friendly.[5,6] However, its high thermodynamic stability remains a major hurdle to the effective use of carbon dioxide.[4] As a consequence, high inputs of energy, and thus emissions, are required to transform carbon dioxide.

Several strategies have been employed to realise the chemical utilization of CO_2. Firstly, one can use high-energy, reactive starting materials, for example hydrogen, acetylene, or Grignard reagents.[4] The second approach is to add energy to the system, for example the electrochemical formation of oxalic acid from CO_2 promoted by a copper complex.[7,8] A different strategy relies on shifting the equilibrium of a less favourable reaction by elimination of removable by-products, for example the elimination of water with dehydrating agents .[4] Most relevant to the work presented here was the realisation that it was possible to use carbon dioxide as raw material with moderately high energy compounds such as epoxides, aiming at organic carbonates as the products.[9–11] Examples of these strategies are depicted in Scheme 4.1.

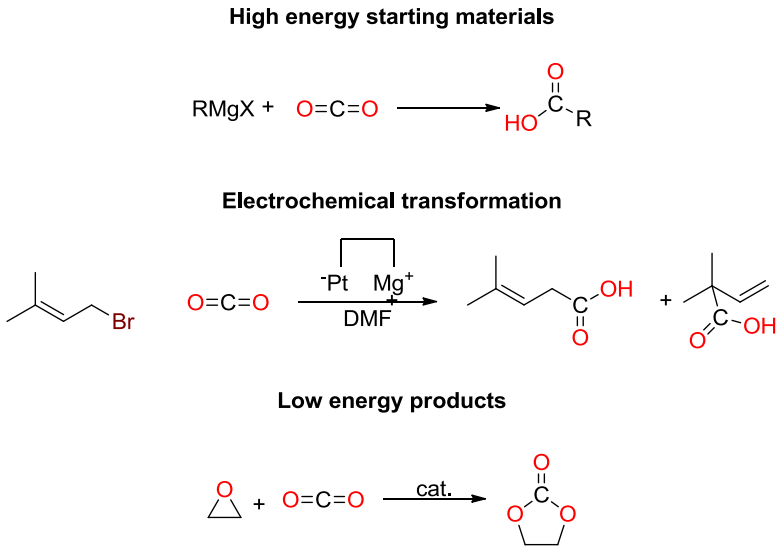

Scheme 4.1 *Different strategies to use CO_2 as raw material.*

Currently, the synthesis of polycarbonates and cyclic carbonates from CO_2 and epoxides is a relevant topic in chemical research because of several advantages. Namely, the synthesis is highly atom economic and it avoids the use of the highly toxic reagent phosgene, required in the classical synthetic routes.[12–14] The polycarbonates are the kinetic products while the cyclic carbonates are formed under thermodynamic conditions.[12,13] The reaction is depicted in Scheme 4.2.

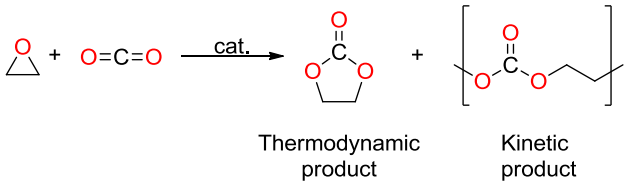

Scheme 4.2 *Formation of carbonates from ethylene oxide and CO_2.*

The great interest in cyclic carbonates arises from their applicability as intermediates in the synthesis of polycarbonates and polyurethanes.[15,16] Other important applications include their usage as environmentally friendly, polar, aprotic solvents, with low odour and toxicity, and as electrolytes for lithium-ion batteries.[17–19]

The organic starting materials for this transformation can be epoxides and oxetanes which can undergo ring expansion with carbon dioxide. The presence of a catalyst is necessary for the reaction to proceed.[20,21] Even in the presence of a suitable catalyst, the reactivity of both substrates is distinct. That is, epoxides are more active than oxetanes. The difference of reactivity is partially a product of the greater ring strain in epoxides.[22] Another important factor that influences the reactivity of epoxides and oxetanes are the steric hindrance and number of substituents on the ring, more hindered substrates requiring harsher conditions.[10,23,24]

The addition of carbon dioxide to epoxides or oxetanes can be catalyzed by nucleophiles, which may be broadly classified as neutral, for instance DMAP (4-dimethylaminopyridine) or charged, such as the halide ions of ammonium or phosphonium derivatives.[25–28] Several examples of these catalyst systems are shown in Figure 4.1.

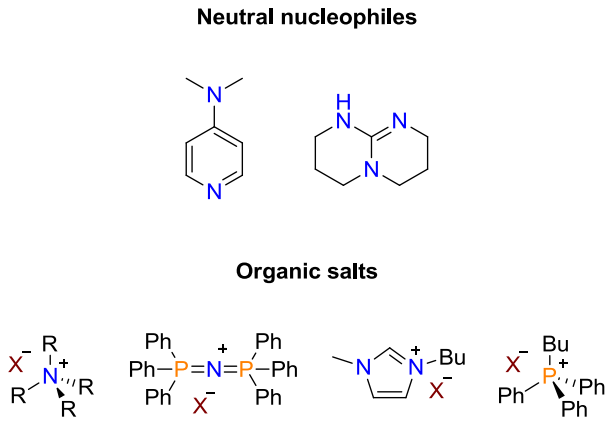

Figure 4.1 *Nucleophiles used in the synthesis of cyclic carbonates.*

The nucleophilicity and leaving group ability (nucleofugacity) are important parameters for the catalyst system. For example, better nucleophiles facilitate the ring opening step thus increasing the reaction rates.[29,30] The leaving group ability is also important for the selectivity to ring closure or polymerization; a low nucleofugacity favours the formation of copolymer as the intermediate anion reacts with a molecule of epoxide.[31,32] Another parameter which can influence the activity is the cation size and usually bulkier cations give higher activity. This can be understood as the result of a weaker interaction between the ion-pair, which increases the nucleophilicity of the anion.[20]

The reaction conditions, temperature and pressure, can be decreased considerably when the nucleophiles described previously are used as co-catalyst to a homogeneous metal catalyst which acts as a Lewis acid.[10,24,33] A wide range of metal complexes are able to promote the addition of carbon dioxide to epoxides, such as Al, Cu, Co, Zn, Fe, Mn, Ni, etc.[11,21,24,34–37]

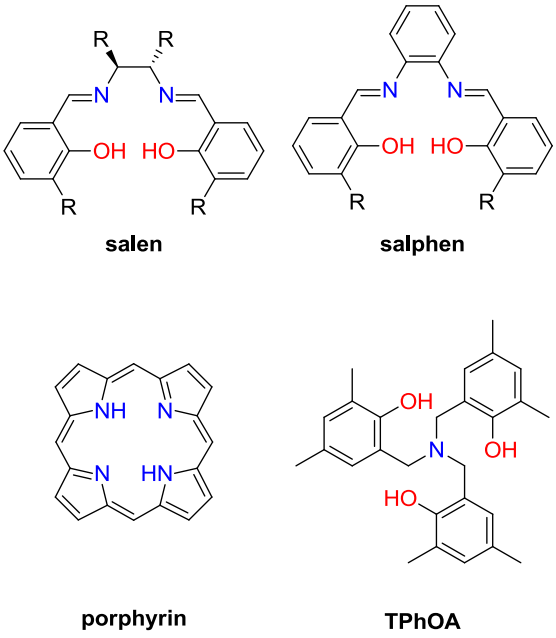

Figure 4.2 *Ligands used in the formation of cyclic carbonates*

Several ligands systems have been utilized to support the metal catalysts, some of which are depicted in Figure 4.2. The most common ligands are based on the salen, salphen and porphyrin families of ligands.[21,38,39] Recently the results obtained using the amine triphenolate ligands (TPhOA) have also been reported. Metal complexes modified by these ligands exhibit high activities and selectivity for sterically demanding epoxides and oxetanes.[11,35] One novel strategy used to improve activity is to modify the ligand by connecting the nucleophile to the structure (Figure 4.3.) A cooperative effect was observed and more active systems were reported based on this modification.[40,41]

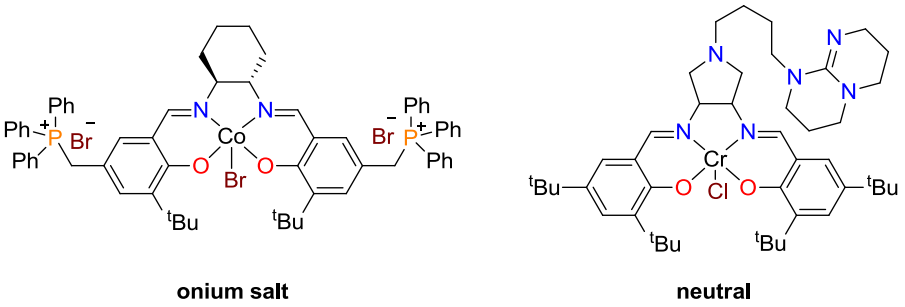

Figure 4.3 *Bifunctional catalyst applied in cyclic carbonate formation.*

The commonly cited catalytic cycle for metal catalyst/nucleophilic co-catalysts systems is depicted in Scheme 4.3.[9,20,36,42] Recently, Bo and coworkers supported this mechanistic proposal for Zn salphen complexes with DFT calculations.[43] The non-metal catalyzed reaction operates *via* a similar mechanism which was also supported by DFT calculations.[44]

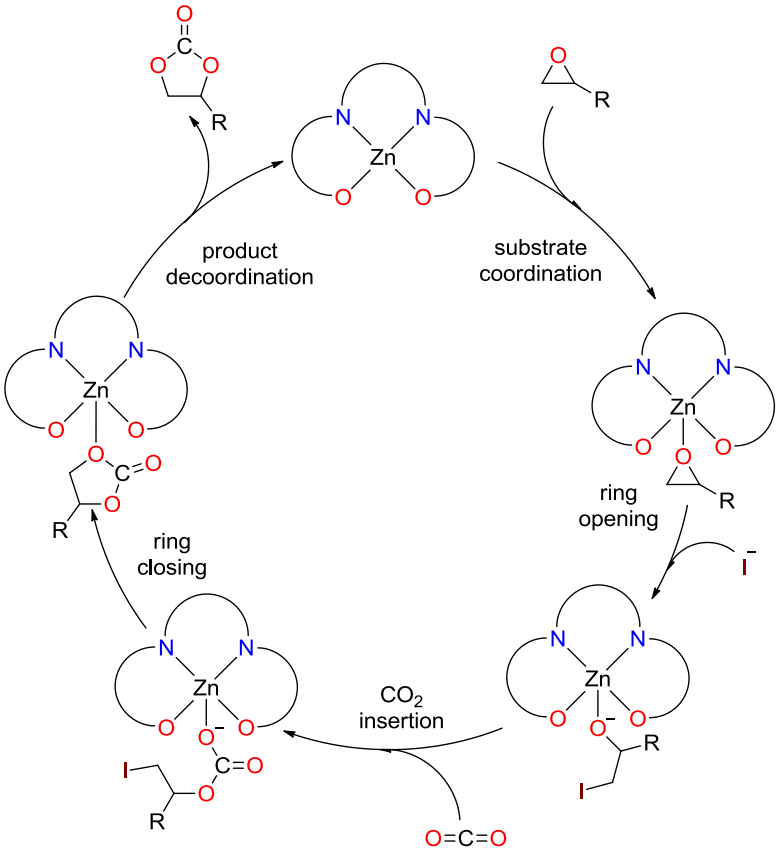

Scheme 4.3 *Proposed catalytic cycle for the Zn promoted formation of cyclic carbonates.*

In the mononuclear systems, the first step is found to be coordination of epoxide to the Lewis acidic zinc. Upon coordination, the epoxide is activated, and can more readily undergo ring opening by the nucleophilic halide. The next step is the CO_2 insertion into the resultant Zn-alkoxide to form the Zn-carbonate intermediate. The key ring closing step occurs via attack of the nucleophilic Zn–O bond to form the coordinated cyclic carbonate with concomitant elimination of halide (back-biting mechanism). The last step is dissociation of the cyclic carbonate to regenerate the catalytically active species.

The cooperative effect of dinuclear organometallic compounds is well known, for instance, with some aluminium complexes. [34,45–47] The reaction mechanism in these instances is closely related to that of the mononuclear compounds. However, a crucial difference is the activation of carbon dioxide by the second,

adjacent metal which is suggested to be the origin of the high activities of these systems. The key mechanistic step in this cooperative mechanism is depicted in Scheme 4.4.

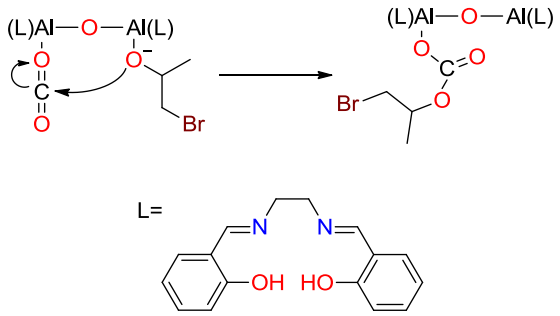

Scheme 4.4 *Cooperative effect in cyclic carbonate formation*

4.1.2. Iron catalyzed oxidations of C–H bonds

The selective oxidation of saturated alkanes is a challenging reaction for an organometallic catalyst due to the high stability required to survive the highly oxidising conditions. As a consequence the selective transformation of C–H bonds is a challenging objective for any homogeneous catalyst.[48] This transformation is of great interest for industry as petroleum and natural gas are mainly composed of saturated hydrocarbons.[49] The general oxidation of alkanes is depicted in Scheme 4.5.

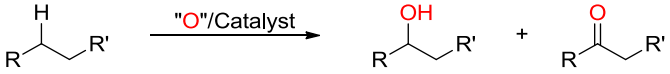

Scheme 4.5 *Representation of alkanes oxidation.*

At the end of nineteenth century, Fenton reported an oxidising system based on Fe(II) complexes and hydrogen peroxide.[50] The application of this system in organic synthesis allows the oxidation of C–H bonds to alcohols or ketones.[51,52] The system is thought to operate via the generation of hydroxyl radicals and hence the reaction proceeds with low selectivity and functional group tolerence.[51] The reaction mechanism is depicted in Scheme 4.6.

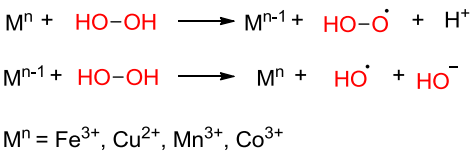

Scheme 4.6 *Formation of radicals by Fenton's reaction*

In contrast, it is well-known that biological systems perform selective oxidation of alkanes under mild conditions. For instance Methane Monoxygenase (MMO) oxidizes methane to methanol (Scheme 4.7).[53] The aliphatic oxidation are catalyzed by two types of enzymes; it can be classified in two families depending in the nature of the active sites named heme and non-heme proteins.[53,54] Cytochrome P450 is an example of heme protein and MMO an example of a non-heme protein (Scheme 4.7). These proteins were used as models to develop new iron catalytic systems that promoted the oxidation of aliphatic compounds.[55]

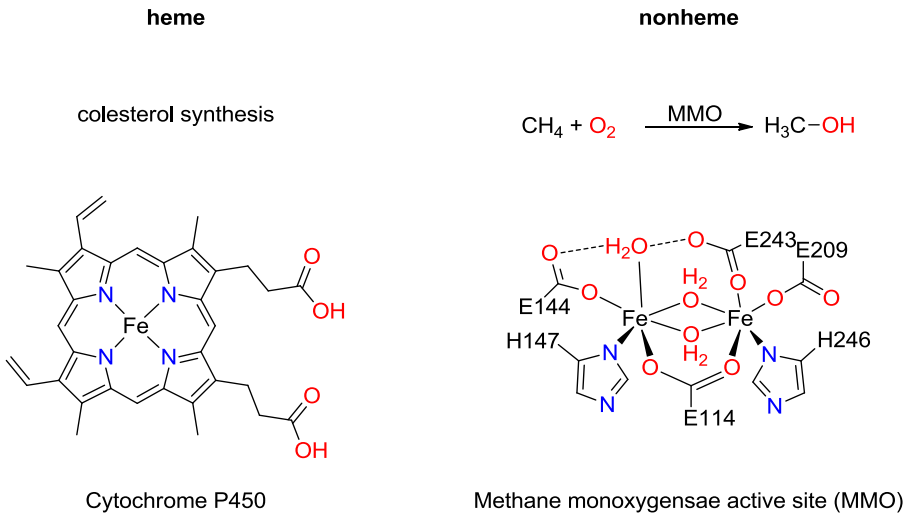

Scheme 4.7 *Examples of heme and non-heme oxidation of aliphatic compounds*

The main drawback in the development of biomimetic ligands is the formation of radicals *via* Fenton chemistry. Thus the developments on ligand design focused on systems that should be capable to oxidize alkanes selectively avoiding the Fenton type oxidations. Non-heme ligands are more attractive ligands due to their tunability compared to heme ligands.

The first example of a stereospecific alkane hydroxylation promoted by an iron catalyst was reported by Que and coworkers.[56] The reaction was catalyzed by a tris(pyridin-2-ylmethyl)amine (TPA) iron complex. Also in 1997, Nishida and coworkers reported N^1,N^2-dimethyl-N^1,N^2-bis(pyridin-2-ylmethyl)ethane-1,2-diamine (BPMEN) as a convenient ligand system for iron promoted oxidations.[57] The two main structures of tetradentate ligands in iron catalyzed oxidation of alkanes are derived from TPA and BPMEN, having tripodal and linear structures, respectively.[58] 1,4-Dimethyl-7-(pyridin-2-ylmethyl)-1,4,7-triazonane (TACN) resulted in an interesting tetradentate N-donor ligand for the oxidation of alkanes.[59,60] A revolution in the iron catalyzed alkane oxidation was reported in 2007 by Chen and White.[61] An iron complex modified with (2S,2'S)-1,1'-bis(pyridin-2-ylmethyl)-2,2'-bipyrrolidine (PDP) resulted in a selective catalyst for the hydroxylation of C–H bonds with good yields. Substrates can be transform with predictable selectivity based on steric and electronic factors.[61–63]

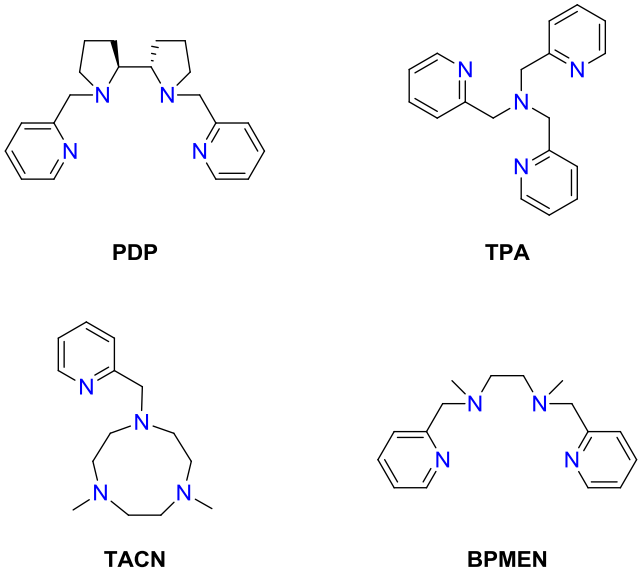

Figure 4.4 *Ligands used in C–H iron oxidations.*

Several parameters are known to affect the activity and selectivity such, as denticity, steric hindrance and the nature of the donors atoms. For example bidentate or tridentate ligands can occupy all iron sites when 3 or 2 ligands coordinate to the iron centre.[64–66]

The systems with tetradentate ligands were more successful in this reaction and other modifications were noted to cause important changes in their catalytic activity. The first important parameter was the rigidity of the backbone. With flexible backbones, different coordination modes are possible and as a consequence the system was shown to be less active.[67] Interestingly, the electronic effects of the backbone in these systems had a negligible effect and the oxidation catalysis was not affected.[68] Finally the steric hindrance has an effect in the hydroxylation reaction; *ortho*-substituents give rise to catalysts with some non-metal based character.[69]

Recently, Bauer and co-workers, reported the use of iminopyridine complexes in the oxidation of C–H bonds (Scheme 4.8.)[70,71] These ligands are highly tuneable and were shown to oxidize alcohols and activated C–H bonds to ketones under mild conditions.

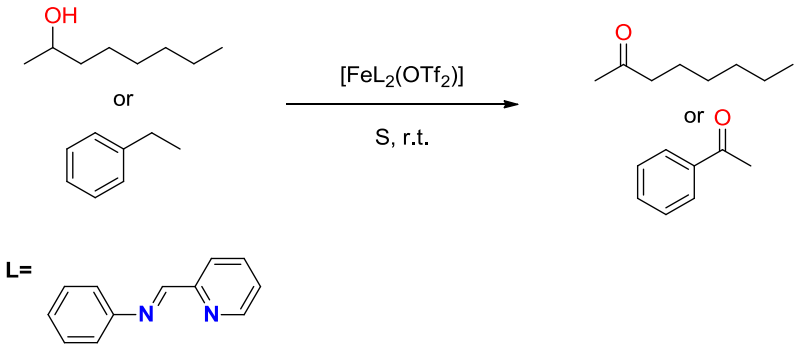

Scheme 4.8 *Oxidation of C–H and alcohols promoted by diiminopyridine iron complex.*

With these precedents in mind, several dinuclear iron and multinuclear zinc complexes will be prepared with the ligands synthesized in Chapter 2. The zinc and iron complexes will be applied as catalyst in the synthesis of cyclic carbonates. The oxidation of C–H bonds will be explored with the iron complexes. It will be studied whether a cooperative effect is present in the multinuclear complexes.

4.2. Results and discussion

4.2.1. Synthesis and characterization of the metal complexes

The synthesis and characterization of molecular complexes of metal DBDOC tetradentate derivatives was considered interesting and preliminary experiments were carried out in order to check if the desired dinuclear complexes were synthetically accessible.

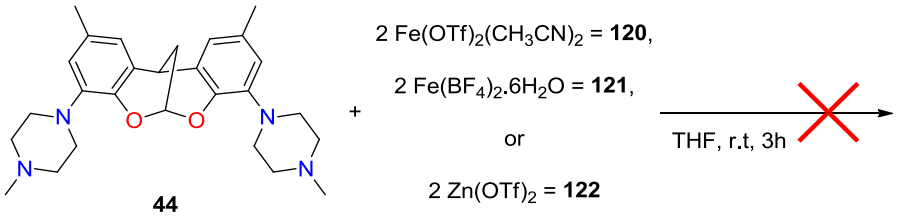

Scheme 4.9 *Unsuccessful synthesis of complexes with compound **44**.*

All attempts to synthesize dinuclear MX_2M with bridging X ligands (X= halide, hydroxide, acetate) failed. Thus we turned to metal precursors with low coordinating counterions.

The coordination chemistry of ligand **44** was studied. Initially iron triflate **120** was utilized as the iron source following a known procedure.[68] No change of colour was observed during the reaction. After work up, proton NMR analysis and mass analysis showed only **44**. The same behaviour was observed when **121** was used as the iron source. It was decided to change the metal for zinc triflate **122** as metal precursor. Unfortunately no coordination of **44** to the metal centre was observed (Scheme 4.9.).

The apparent lack of reactivity of **44** prompted the study of the coordination chemistry of DBDOC iminopyridine derivatives instead. First, the reactivity of **66** with **120** was explored at ligand:metal ratio 1:2 (Scheme 4.10.) which gave a deep purple complex. After work up, an excess of **120** was recovered and the sample analysed by MS and implied the formation of a product with a ligand:metal ratio of (1:1). With this information in hand it was decided to repeat the reaction changing the ligand and metal proportion from 1:2 to 1:1.

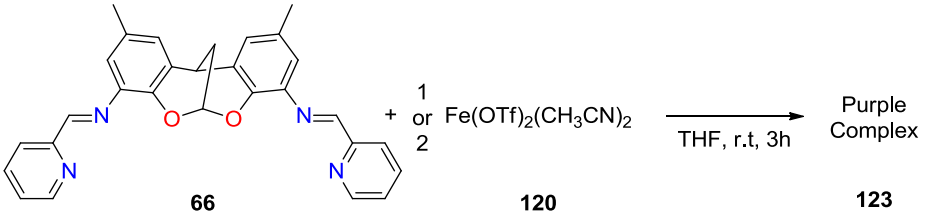

Scheme 4.10 *Synthesis of dinuclear complex with **66** and **120**.*

Crystals of compound **123** were grown from ACN:Et_2O (Figure 4.5.) in which a large intramolecular Fe–Fe distance of 9.273 Å is apparent. This large distance was attributed to the electrostatic repulsion between the iron centres and to the lack of bridging anionic ligands.

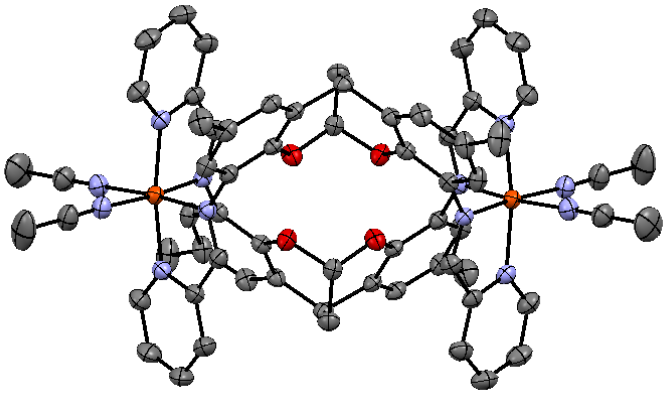

Figure 4.5 *ORTEP-plots (thermal ellipsoids shown at 50% probability levels) of complexes **123**. Non-relevant hydrogen atoms have been omitted for the sake of clarity.*

The iron centres presented an octahedral geometry with angles around 90º and short N–Fe distances, shorter than 2 Å, indicative of low spin complexes.[72] Different isomers could be formed when bidentate imine ligands coordinate to iron centers.[70] The isomers that may form are depicted in Figure 4.6; *cis* and *trans* refers to the position of the acetonitrile ligands. Complex **123** has a C_{2h} symmetry with the pyridine donors *trans* to one another.

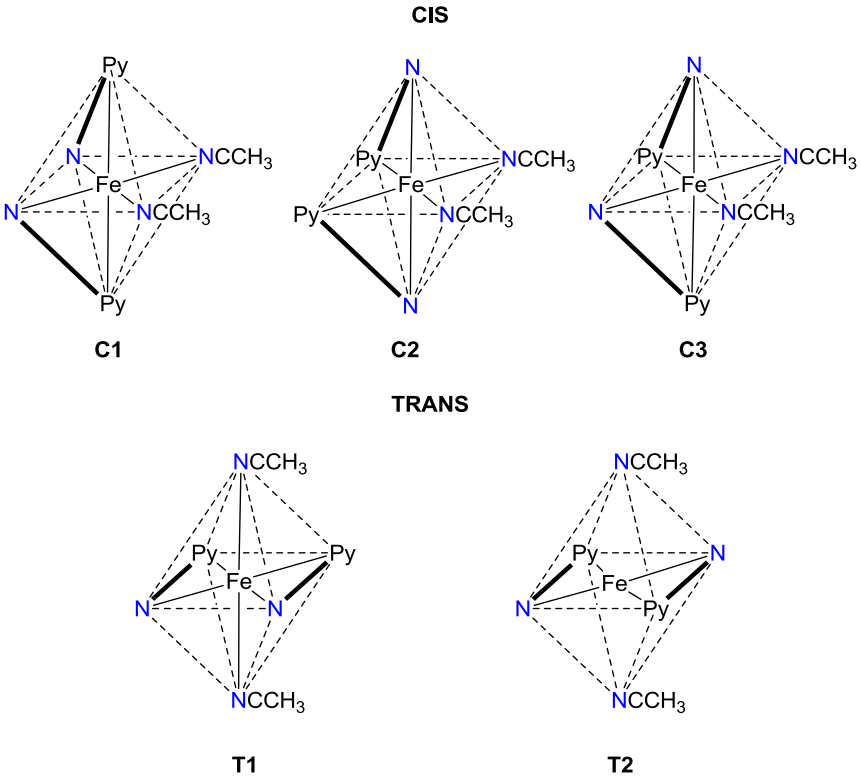

Figure 4.6 *Different coordination modes for the bidentate ligands with iron.*

Different rearrangements of the DBDOC moiety can be expected as outlined before for phosphine complexes of rhodium.[73] The isomers are summarized in Figure 4.7. For compound **123** we observed an *A3* geometry. The formation of this structure could be assisted by the formation of 4 π–π stacking interactions, with a distance between arene and pyridine of adjacent backbones of 3.9 Å (intramolecular) and 4.5 Å (intermolecular).[74,75]

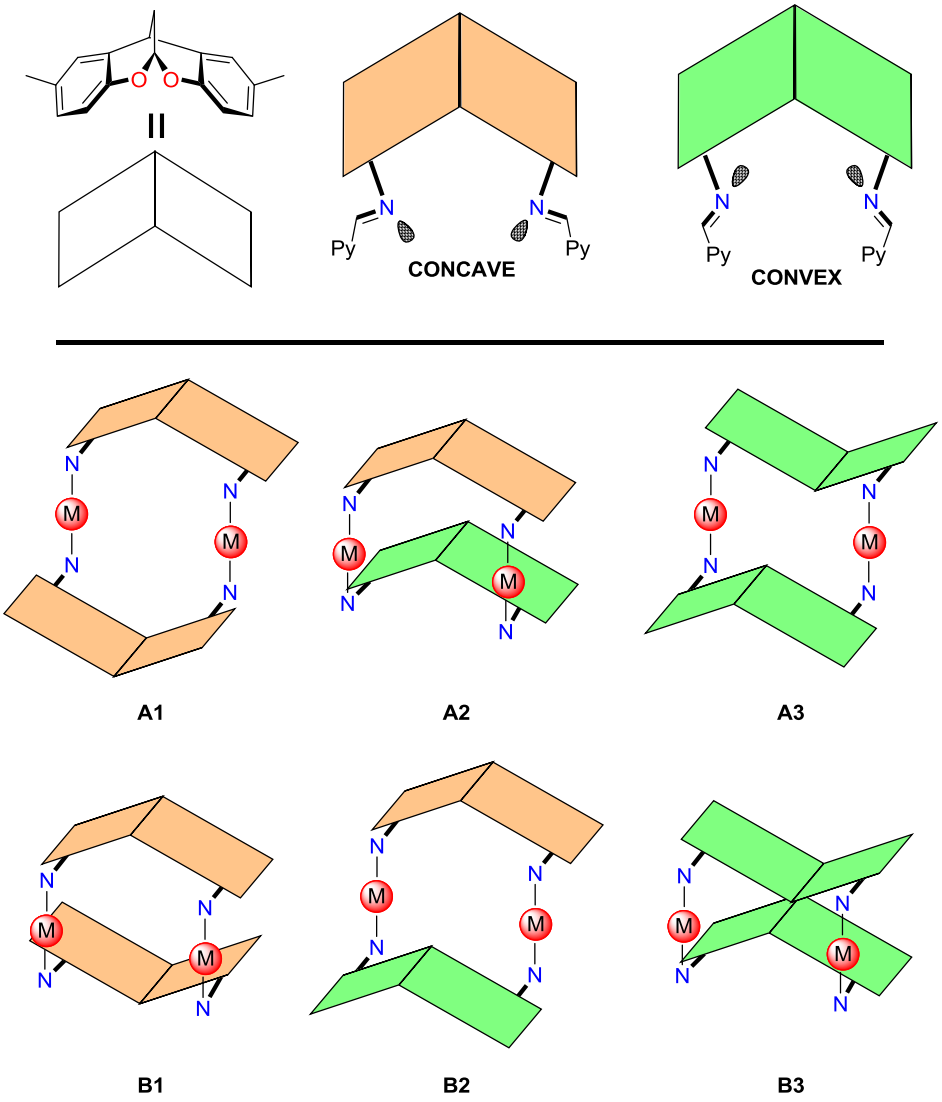

Figure 4.7 *Isomeric face-to-face bimetallic complexes that may form with Cs symmetric ligands derived from DBDOC; three different conformers of each isomer A and B have been depicted, depending on the side (concave or convex) exposed to the metal centres*.

Once the reaction was optimized, the synthesis of new dinuclear complexes with tetradentate ligands was explored. Several iron complexes were prepared with the available DBDOC derivatives, BFBF and SPAN tetradentate

iminopyridine ligands. The reaction conditions and the synthesized complexes are summarized in Scheme 4.11.

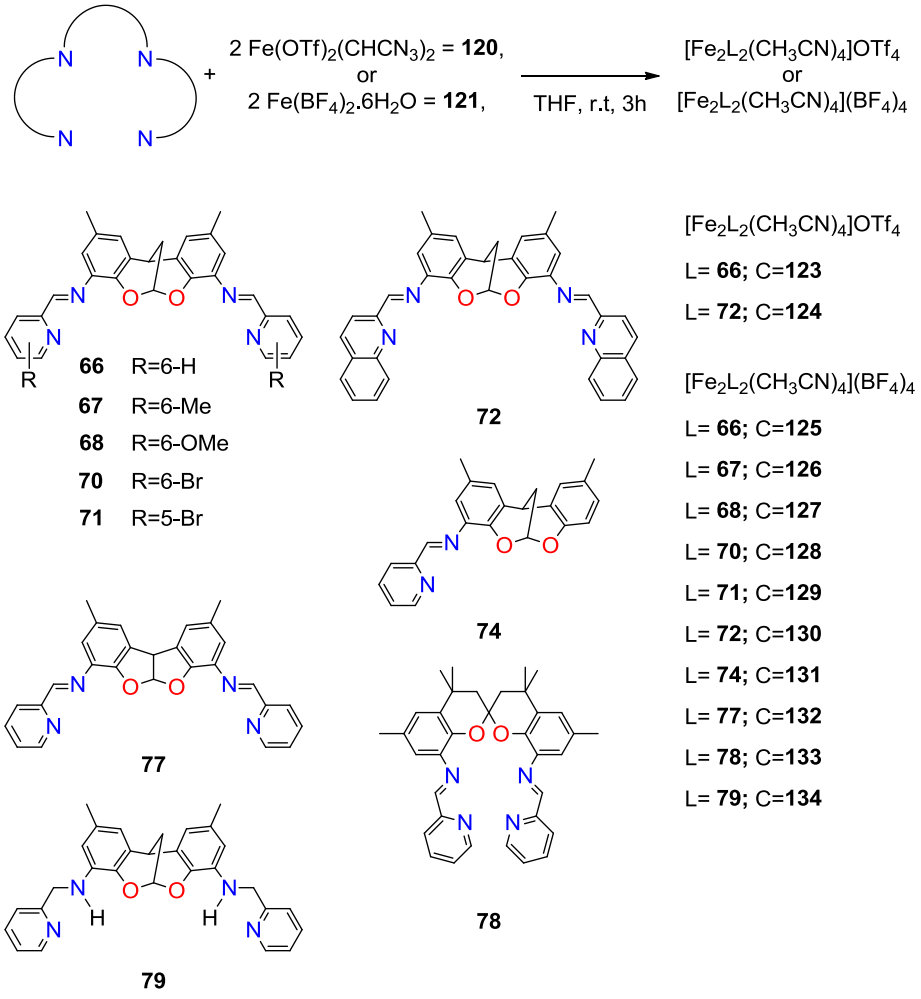

Scheme 4.11 *Synthesis of iron complexes with different tetranuclear ligands*

Crystals of the complexes **124**, **125**, **126**, **127**, **128**, **129.** and **134** suitable for X-ray diffraction were obtained. Analysis of these structures revealed the same arrangement for these complexes; the iron atoms have an octahedral environment and the isomer formed has C_{2h} *symmetry*. As regards the disposition of the DBDOC backbones in all cases we observed the *A3 isomer.*

Moderate steric hindrance and electronic variations in the ligand did not affect the selectivity of the isomers formed.

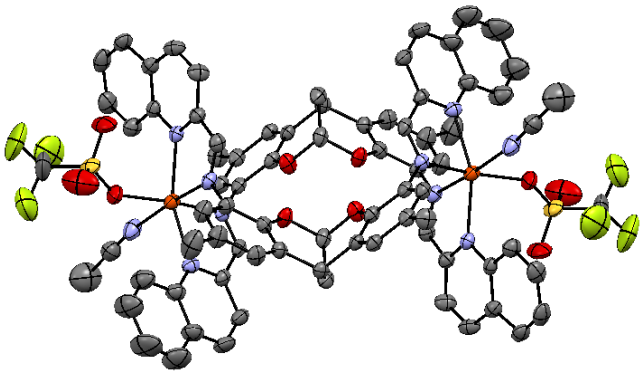

124

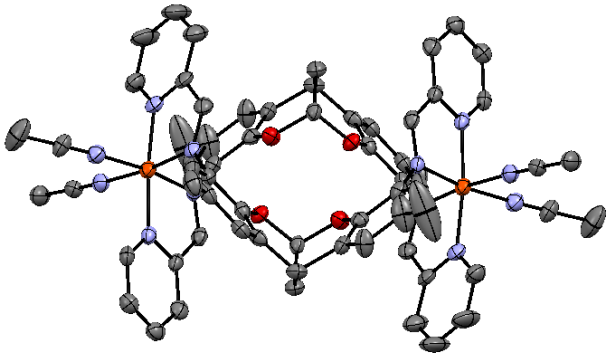

125

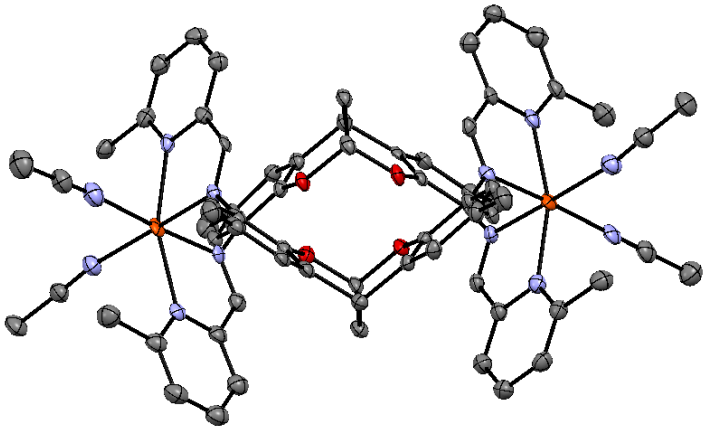

126

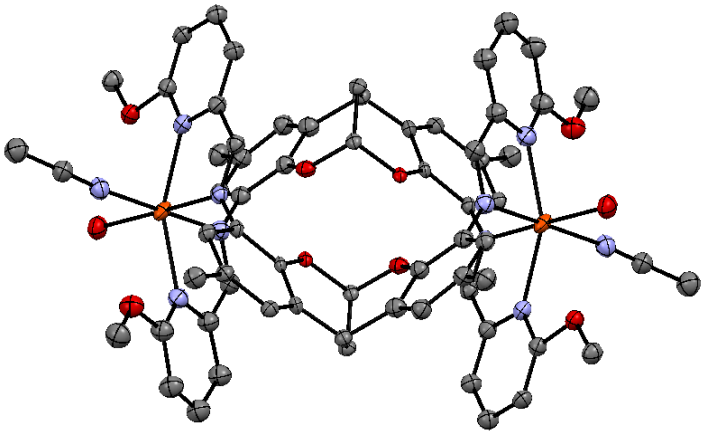

127

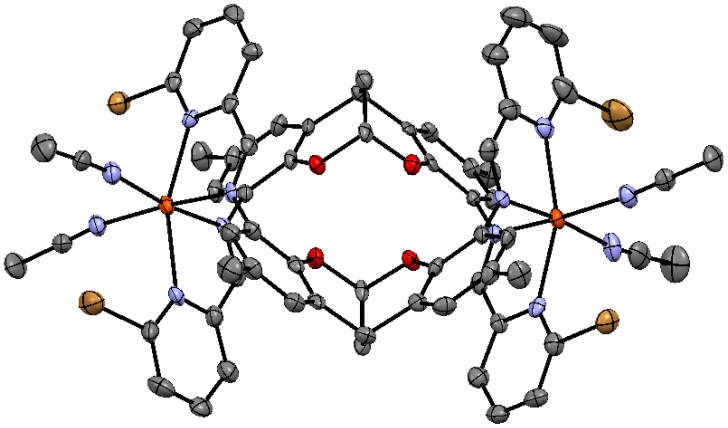

128

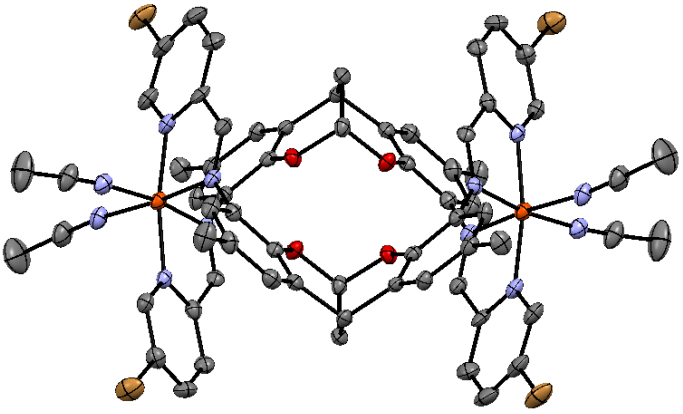

129

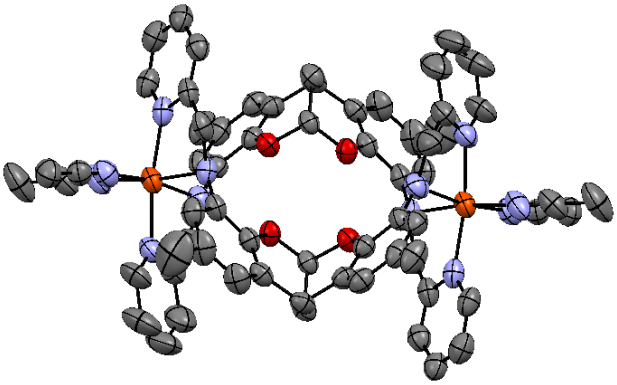

134

Figure 4.8 *ORTEP-plots (thermal ellipsoids shown at 50% probability levels) of complexes* ***124****,* ***125****,* ***126****,* ***127****,* ***128****,* ***129*** *and* ***134****. Non-relevant hydrogen atoms have been omitted for the sake of clarity.*

The geometry of synthesized iron complexes was octahedral in all cases. When the substituents were in *ortho* position of the pyridine nitrogen atom we observed slightly distorted octahedrons, which was attributed to a steric effect. The distortion reduces the ligand field splitting and lowers the symmetry of the orbitals thus promoting the formation of high spin compounds. If the substituent was in *meta* position, low spin complexes were obtained, due to the lack of distortion of the geometry. A low spin complex was formed when aminopyridine derivatives were used. Amines are stronger donors and the quasi octahedral symmetry is achieved in these complexes. In Table 4.1 selected distances of the complexes are summarized.

Table 4.1 *Bond distances in Å for different X-ray structures of synthesized ligands.*

Complex	Bond Distance(*Å*)			
	Fe–Fe	Fe–N[a]	Fe–N[b]	Fe–N[c]
123	9.273	1.973	1.957	1.952
124	9.804	2.210	2.159	2.215
125	9.092	1.961	1.960	1.949
126	9.603	2.170	2.168	2.152
127	9.332	2.190	2.194	2.172

128	9.570	2.235	2.1730	2.167
129	9.918	1.986	1.950	1.940
134	9.222	2.048	2.149	2.029

[a] Nitrogen atom of pyridine. [b] Nitrogen atom of imine. [c] Nitrogen atom of acetonitrile.

The electronic and steric properties of the ligand and the type of anion used affects the Fe–Fe distance. Low spin complexes give shorter Fe–Fe distances and the nature of the anion causes slight differences (Table 4.1, **123** and **125**). The smaller BF_4 anions stay perhaps closer to the Fe cations and the electrostatic repulsion may be lower than in the other complexes, thus decreasing the metal–metal distance . When EWG are present in the molecule (**129** vs. **125**) the distance increases. A plausible explanation is that the ligand in **129** is a weaker σ-donor. As a consequence the iron centres have a lower electron density and the electrostatic repulsion increases. The distortion of the octahedral coordination observed in complexes with *ortho*- substituents in the pyridine moiety affects also the distance between the metals, which increases slightly.

The synthesis of copper complexes with ligand **66** was explored (Scheme 4.12.) Like the aforementioned iron complexes (**124**, **125**, **126**, **127**, **128**, **129** and **134**), complexes with a metal:ligand ratio of 1:1 were formed.

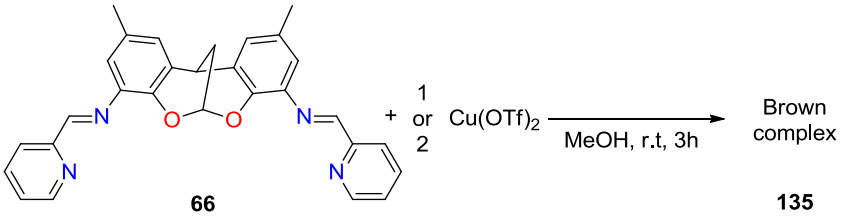

Scheme 4.12 *Synthesis of copper complexes with **66**.*

Crystals of **135** suitable to do X-ray analysis were obtained from MeOH/Et_2O (Figure 4.9). However, two different structures were found in the unit cell, differentiated only by the coordination of OTf (**135a**) or MeOH (**135b**) in the equatorial position. Both species have an *A3* disposition of the DBDOC backbones. The geometry of copper is a distorted trigonal bipyramid.

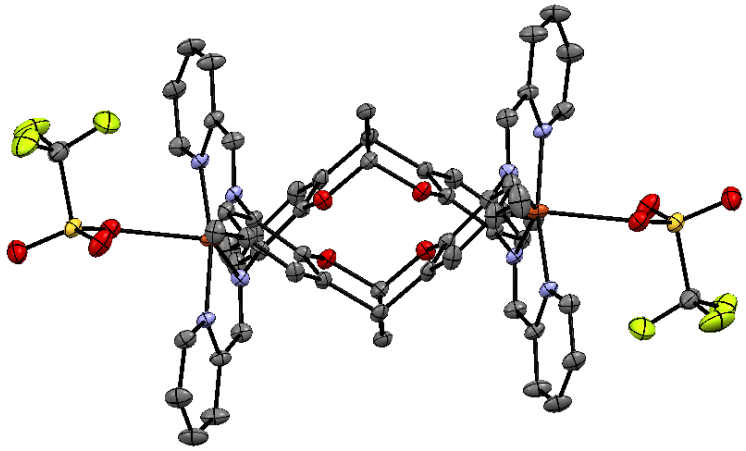

135a

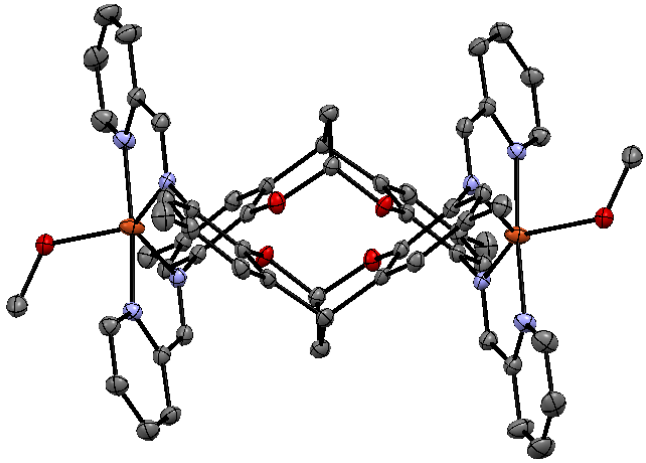

135b

Figure 4.9 *ORTEP-plots (thermal ellipsoids shown at 50% probability levels) of complexes **135**. Non-relevant hydrogen atoms have been omitted for the sake of clarity.*

Some of the relevant bond lengths and angles of complex **135** are summarized in Table 4.2. Of particular interest are the Cu–Cu distances. When the external equatorial position is occupied by anionic triflate, smaller distances are observed. This large difference is attributed to a decrease in electrostatic repulsion between the metals, as the overall positive charge for the Cu unit is 1^+ instead of 2^+ for the methanol complex. Compared with complex **123**, it can be seen that the iron complexes have longer M–M distances (9.2–9.9 Å). A plausible cause could be the different geometries of the metal centres.

Table 4.2 *Selected bond distances and angles for species of complex* ***135****.*

Bond Distance (*Å*)				
Complex	**Cu–N[a]**	**Cu–N[b]**	**Cu–O**	**Cu–Cu**
135a	1.995	1.984	2.433	7.628
135b	2.105	1.984	2.1732	8.278

Angles (º)				
135a	**N_{a1}–Cu–N_{a2}**	**N_{a1}–Cu–N_{b1}**	**N_{a1}–Cu–N_{b2}**	**N_{a2}–Cu–N_{b1}**
	144.96	81.70	104.58	98.86
	N_{a2}–Cu–N_{b2}	**N_{b1}–Cu–N_{b2}**	**O–Cu–N_{a1}**	**O–Cu–N_{a2}**
	81.81	168.9	92.28	122.61
	O–Cu–N_{b1}		**O–Cu–N_{b2}**	
	81.85		87.85	
135b	**N_{a1}–Cu–N_{a2}**	**N_{a1}–Cu–N_{b1}**	**N_{a1}–Cu–N_{b2}**	**N_{a2}–Cu–N_{b1}**
	129.98	79.81	106.29	96.58
	N_{a2}–Cu–N_{b2}	**N_{b1}–Cu–N_{b2}**	**O–Cu–N_{a1}**	**O–Cu–N_{a2}**
	80.96	173.63	88.01	141.92
	O–Cu–N_{b1}		**O–Cu–N_{b2}**	
	92.58		85.90	

[a] Nitrogen of imine group. [b] Nitrogen of pyridine group.

A study of the coordination behaviour of salphen type derivatives of DBDOC and SPAN was performed. Complexes were prepared following recent procedures from the literature.[46] The condensation of **61**, salicylaldehyde, and zinc salt in methanol led to the formation of a yellow Zn complex. The Zn complex was also synthesized via a different protocol, that is isolated ligand **76** was reacted with diethylzinc.[76] Reactions are depicted in Scheme 4.13.

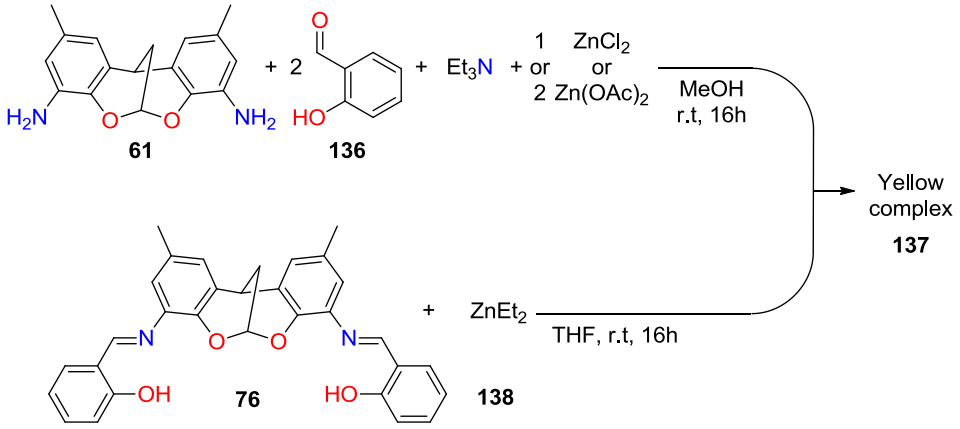

Scheme 4.13 *Synthesis of multinuclear zinc complexes with ligand **76**.*

The metal:ligand ratio and the nature of the zinc precursor did not affect the formation of the yellow complex. MS-MALDI-TOF analysis revealed the presence of an octamer (4435 g/mol) with a metal ligand:ratio of 1:1

Several aldehydes substituted in the 3-position were explored in the synthesis of DBDOCsalphen ligands and SPANsalphen and in all cases $ZnCl_2$ was used as the precursor. The steric hindrance exerted by the R-group was found to play an important role in the nuclearity of the complexes. Less sterically demanding R-groups were found to form complexes with higher nuclearity, for instance octanuclear for R = H, hexanuclear for R = F, tetranuclear for R = Me and dinuclear for R = *tert*-butyl. Furthermore, when the DBDOC backbone was changed for the SPAN backbone, a mononuclear complex was formed.

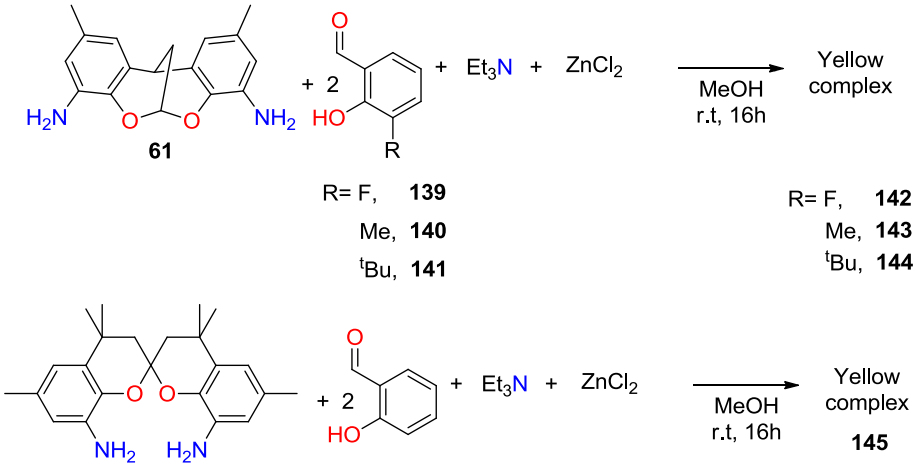

Scheme 4.14 *Zinc-salphen complexes synthesized.*

For aldehyde **139** $Zn(OAc)_2$ was tested as precursor instead of $ZnCl_2$. An unexpected coordination mode was observed and a different complex was formed. X-ray analysis confirmed the formation of a dinuclear species **146** with a metal:ligand ratio of 1:2 (Figure 4.10). Each Zn nucleus exhibits a distorted tetrahedral geometry is bridged by μ-OAc and μ-OH ligands. The oxygen atoms of the backbone are located close to the metal with distances between 2.6-2.8 Å which leads to a favourable interaction with the metal centre; this is best observed in the space-filling representation (Figure 4.10).

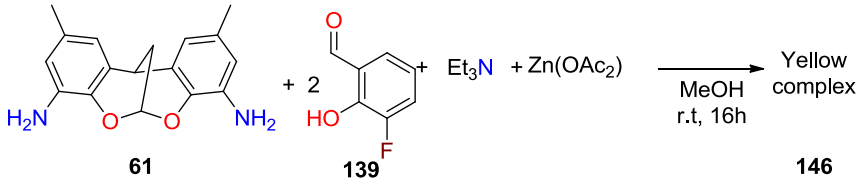

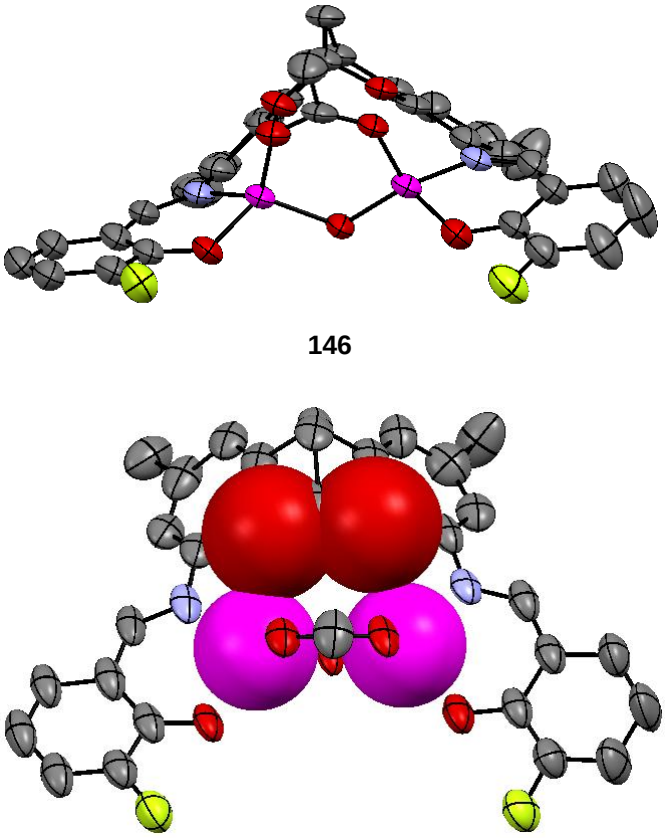

146

O–Zn interaction

Figure 4.10 *ORTEP-plots (thermal ellipsoids shown at 50% probability levels) of complexes **146**. Non-relevant hydrogen atoms have been omitted for the sake of clarity.*

Some relevant bond angles and distances determined from the x-ray structure of complex **146** are summarized in Table 4.3. Of particular interest is the short Zn–Zn distance, which could allow for some kind of cooperative effect in catalysis as proposed for other bimetallic complexes.[40,41] Thus, in the end we did find a complex with the desired bimetallic character containing bridging anions.

Table 4.3 *Selected bond and distances for compound* ***146****.*

Bond Distance(*Å*)					
Zn–Zn	**Zn–N**	**Zn–Oar**	**Zn–OAc**	**Zn–OH**	**Zn–O**
3.280	2.041	1.980	1.967	1.936	2.754

Angles (º)			
N–Zn–Oar	**N–Zn–OAc**	**N–Zn–OH**	**Oar –Zn–OAc**
92.57	125.67	117.40	98.20
Oar –Zn–OH		**OAc–Zn–OH**	**Zn–OH–Zn**
116.79		104.46	117.9

4.2.2. Zinc catalyzed synthesis of cyclic carbonates

It is known from the literature that Zn clusters can catalyse the selective formation of cyclic carbonates from CO_2 and epoxides.[46] In order to test the synthesized ligands and to study the effect of both metal nuclearity and the effect of ligand substituents, we decided to test for activity in a common reaction (Scheme 4.15.)

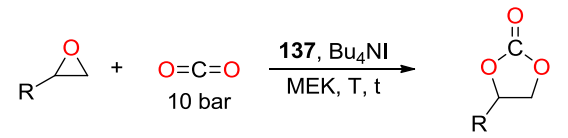

R=Me **147**
R=Bu **148**

R=Me **149**
R=Bu **150**

Scheme 4.15 *Catalytic carbonate formation promoted by* ***138****.*

The results in the optimization of catalyst loadings, complex:ammonium and temperature are summarized in Table 4.4. The first parameter to be optimized was reaction time. In entries 1 and 2 an increase of conversion can be observed when longer reaction time was applied. After 68 h only 82 % yield was obtained. Thus different options were explored to improve these initial results. It was

noted that the alkyl chain length of the epoxide has essentially no impact on yield (entry 3) and further optimizations were carried out using 1,2-epoxyhexane **148**.

Table 4.4 *Optimization of reaction conditions for compound **148**.*

Entry	R	T(ºC)	Zn:Bu_4NI	Yield[a] %
1	Me	45	1:1	37
2[b]	Me	45	1:1	82
3	Bu	45	1:1	38
4[c]	Bu	45	1:1	61
5	Bu	45	1:2	48
6	Bu	45	1:05	23
7	Bu	65	1:1	79
8[d]	Bu	45	1:1	36
9	Bu	85	1:1	100
10[e]	Bu	45	-	2
11[e]	Bu	65	-	11
12[e]	Bu	85	-	55

0.8 mmol substrate, 2.5 mol % catalyst (Zn atoms), pCO_2 = 10 bar, 18 h in 2 mL of MEK. [a] Determined by ^1H NMR (DMSO-d_6) using mesitylene as *internal standard*. [b] 68 h reaction. [c] Double catalyst loading. [d] $Zn(OAc)_2$ as catalyst. [e] Blank 2.5% Bu_4NI.

As might be expected, doubling the catalyst loading gave an increased yield (entry 4). The variation of the metal:ammonium salt ratio had an important effect on the yield. A linear relation between ammonium salt loading and yield was observed. In order to check the specific role of the ligand in the system, $Zn(OAC)_2$ was used as catalyst, and although active (entry 9), the system was less active than that of complex **137**.

The yield was found to increase with temperature and full conversion was obtained at 85 ºC. As the ammonium salt can promote the reaction without the presence of metal catalyst blank reactions were done at different temperatures (entries 10-12), and indeed, at 85 ºC 55% yield was observed in the absence of metal. However, lowering the temperature to 65 ºC resulted in only 11% yield and thus these conditions were chosen to study the reaction so that only a minor participation of the blank, metal-free reaction would be operative.

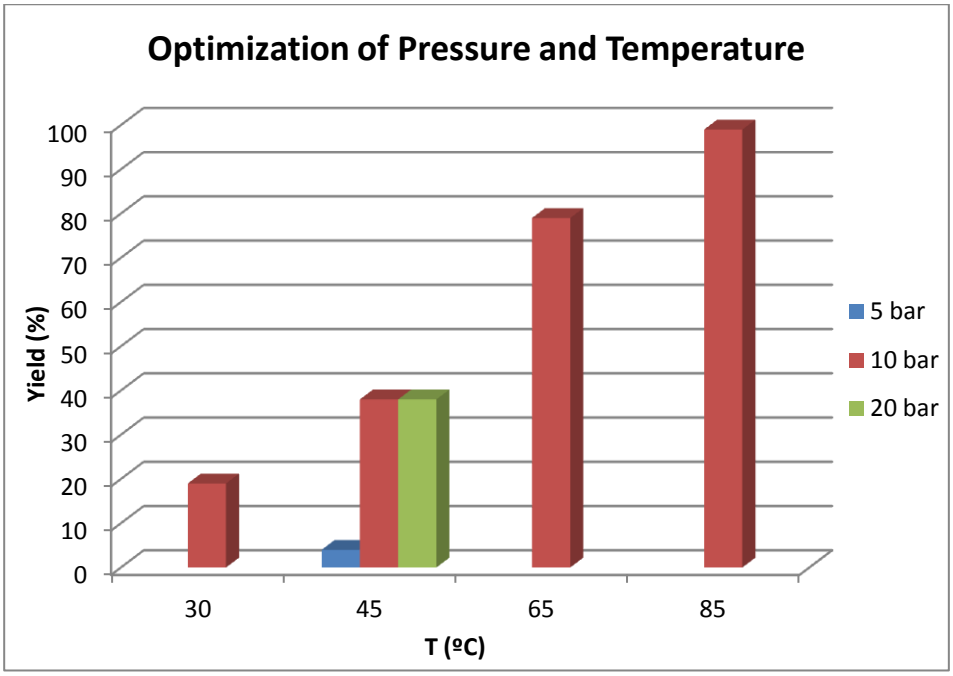

Graph 4.2 *Reaction and temperature optimization for cyclic carbonate synthesis with* ***148****. Reaction conditions: 0.8 mmol substrate, 2.5 mol % catalyst (Zn atoms), 1:1 Zn:I, in 2 mL of MEK, 18h. Chemical yield determined by* ^{1}*H NMR (DMSO-d6) using mesitylene as internal standard.*

The CO_2 pressure is important to increase the amount of CO_2 in solution and the specific effect of pressure and temperature is shown in Graph 4.2. Low yields of less than 10% were observed at low pressures while at 10 bar yields increased up to 38%. It is somewhat surprising that increasing the pressure to 20 bar did not result in a further increase of the yield.

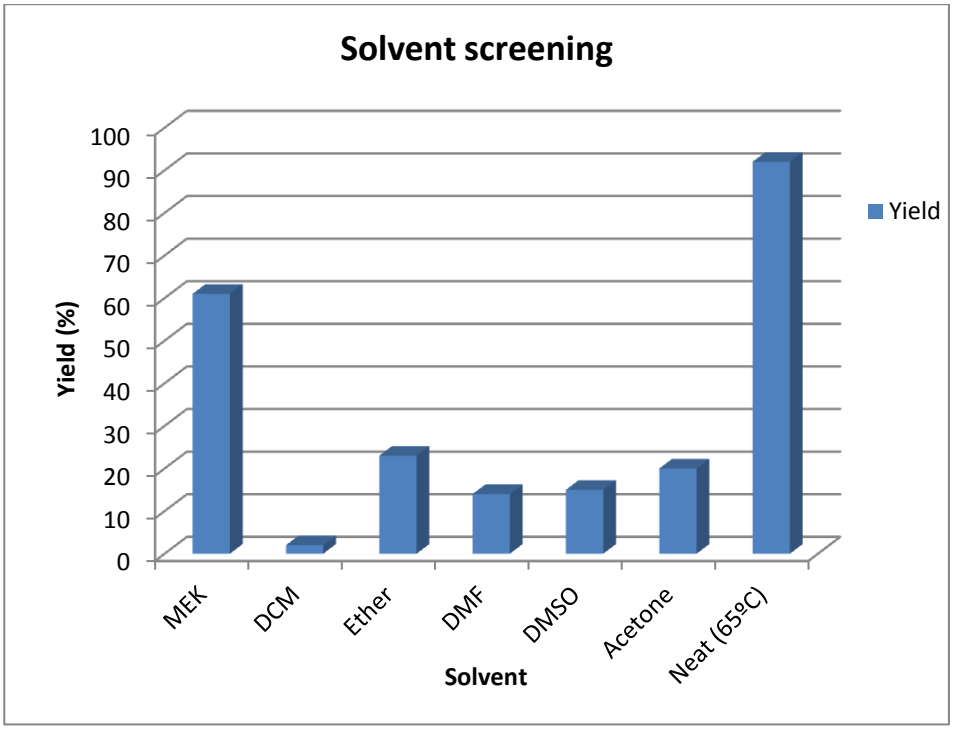

Graph 4.3 *Solvent screening for cyclic carbonate synthesis with **148**. Reaction conditions: 0.8 mmol substrate, 2.5 mol % catalyst (Zn atoms), 1:2 Zn:I, in 2 mL of solvent, pCO_2 = 10 bar, 18h, 45 ºC. Chemical yield determined by 1H NMR (DMSO-d6) using mesitylene as internal standard.*

In the literature it was reported that carbonyl containing solvents are optimal solvents due the high solubility of carbon dioxide in these solvents.[10,29,77] In this case the best solvent was found to be butan-2-one (methylethylketone, MEK). This solvent allowed moderate conversions at 45 ºC. The lower conversion in acetone can be explained by the low solubility of the complex in this medium. The best yields were obtained when the reaction was performed solvent-free, as has been shown to be the case for other systems reported in the literature.[20,21]

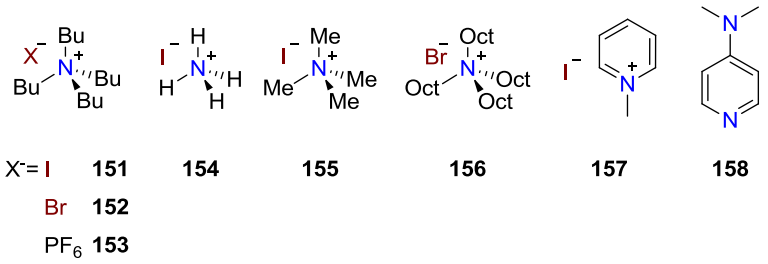

Figure 4.11 *Different screened Co-Catalyst in the ring expansion of **148** with CO_2 to.*

Several co-catalysts with different degrees of anion-nucleophilicity, size, and nature of cation in onium salts were tested (Figure 4.11.).

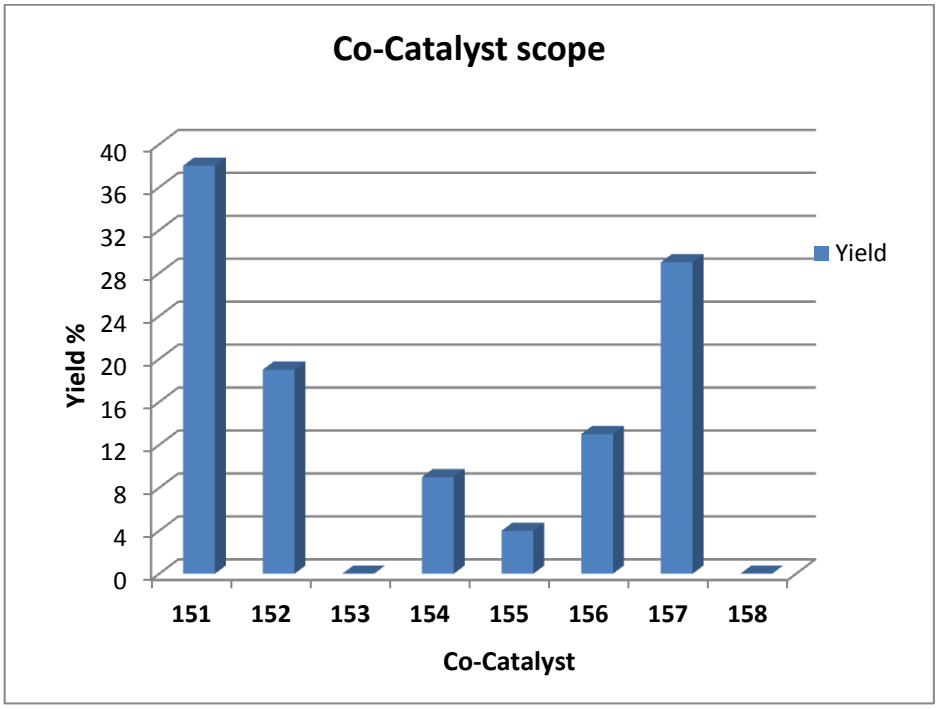

Graph 4.4 *Co-catalyst screening for cyclic carbonate synthesis with **148**. Reaction conditions: 0.8 mmol substrate, 2.5 mol % catalyst (Zn atoms), 1:1 Zn:onium salt, in 2 mL of solvent, pCO_2 = 10 bar, 18h, 45 ºC. Chemical yield determined by ^1H NMR (DMSO-d6) using mesitylene as internal standard.*

The results of co-catalyst screening are summarized in Graph 4.4. Firstly the effect of the anion whilst keeping the size of the cation constant (co-catalyst

151, **152**, and **153**) was investigated. In the literature it was reported that the most active catalytic system was formed by **137** and co-catalyst **151**. This system gave yields of up to 38%, while **137**-**152** gave only 19%. As expected the hexafluorophosphate onium salt **153** was inactive, since it is non-nucleophilic and unable to perform the crucial ring opening step.

The size of the cation was also found to affect the yield (**151**, **154**, and **155** for iodide, **152** and **156** for bromine). On the one hand, decreasing the size of onium salt from NBu_4 to NMe_4 or NH_4 caused a reduction in yield. The ammonium iodide was more active and this was attributed to its ability to form hydrogen bonding with the epoxide substrate, thus activating it towards ring opening. Such stabilization *via* hydrogen bonding is known to facilitate the ring opening.[25,78,79] On the other hand, when the size of the cation was increased, an increase in yield was expected. On the contrary, the opposite behaviour was observed and the yield decreased, which was attributed to the low solubility of **156** in MEK. The effect of the nature of the cation was also scrutinised and it was found that pyridinium salts gave high yields compared to small ammonium salts. Finally, a neutral nucleophile – DMAP – was tested, but no conversion was detected.

After the optimization of the reaction conditions it was found that tetrabutylammonium iodide as co-catalyst in a ratio 2:1 with respect to the Zn catalyst, at 65 ºC, 10 bar of carbon dioxide, and 18 h of reaction time gave the best results. These optimized reaction conditions were applied in the substrate and catalyst screening.

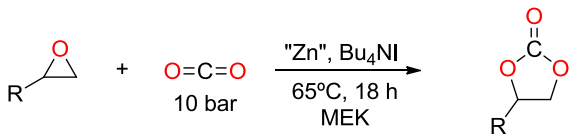

R=Me	**147**	"Zn"=**137,142,**	R=Me	**149**
R=Bu	**148**	**143,144,145**	R=Bu	**150**
R=C_2HOH	**159**		R=C_2HOH	**161**
R=Ph	**160**		R=Ph	**162**

Scheme 4.16 *Catalytic synthesis of cyclic carbonates from monosubstituted epoxides.*

In an effort to expand the substrate scope, this new family of Zn complexes was tested with non-crowded monosubstituted epoxides (Scheme 4.16), the results of which are summarized in Graph 4.5.

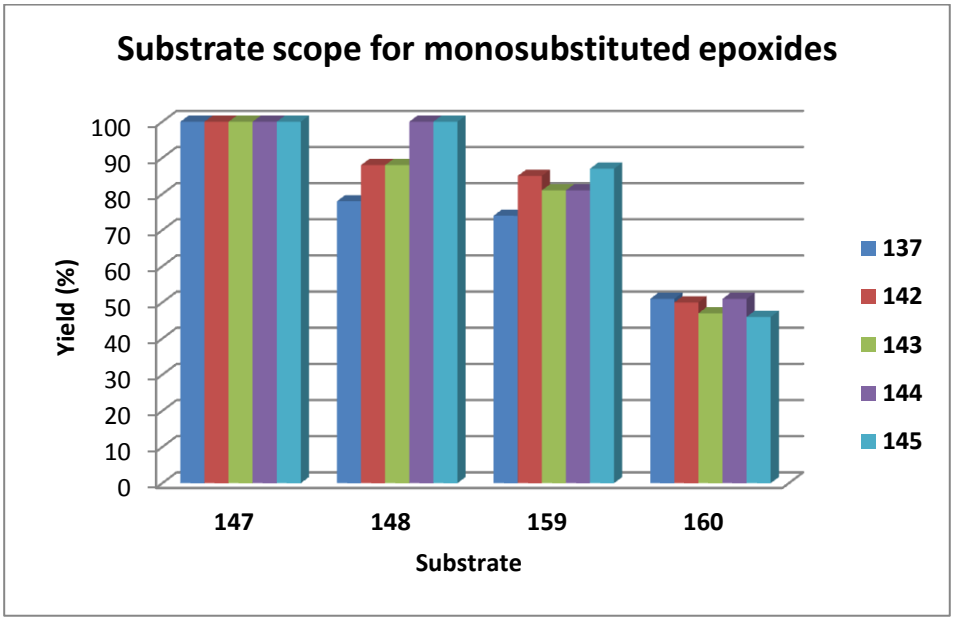

Graph 4.5 *Results in the catalytic synthesis of cyclic carbonates from monosubstitued epoxides. Reaction conditions: 0.8 mmol substrate, 2.5 mol % catalyst (Zn atoms), 1:2 Zn:onium salt, in 2 mL of MEK, pCO_2 = 10 bar, 18h, 65 ºC. Chemical yield determined by ^1H NMR (DMSO-d6) using mesitylene as internal standard.*

Under the previously optimized conditions, the catalyst tested in this transformation gave complete conversion for the least hindered epoxide, epoxypropane **147**. Upon changing the group from methyl to butyl, variations in the activity were noted. The activity of the systems seems to be closely related to the nuclearity of the complexes; dinuclear **144** and mononuclear **145** led the most active systems with yields of 100%. The yield was also affected by the presence of coordinating groups in the epoxide, for example glycidol as the substrate. This substrate was converted in low yield compared to propylene oxide and this may be explained by competitive coordination between alcohol and epoxide for the active site. Compound **159** gave comparable yields for all the catalysts tested. Finally, styrene oxide was converted in moderate chemical

yields. The larger steric hindrance in the epoxide was responsible for the decrease in yields with respect to the other tested epoxides.

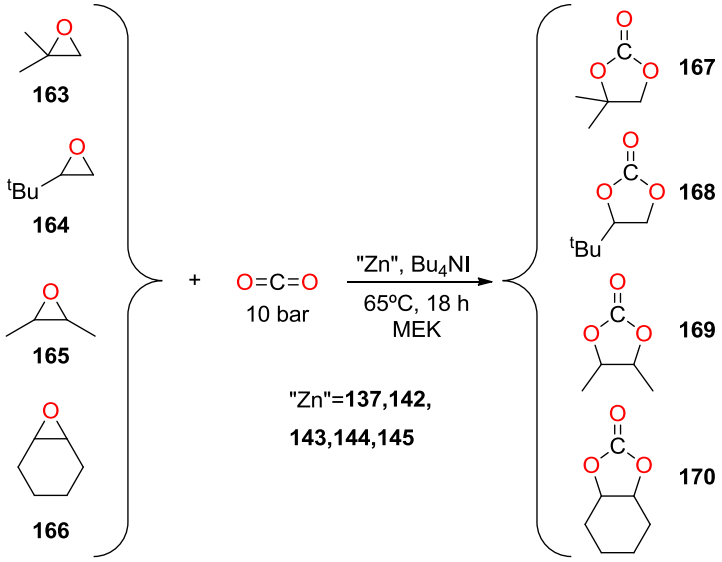

Scheme 4.17 *Catalytic synthesis of cyclic carbonate with hindered epoxides.*

A key challenge in cyclic carbonate synthesis via CO_2/epoxide ring expansion is the transformation of sterically hindered mono- and di-substituted epoxides. [20] Scheme 4.17 and the results of the reaction are summarized in Graph 4.6.

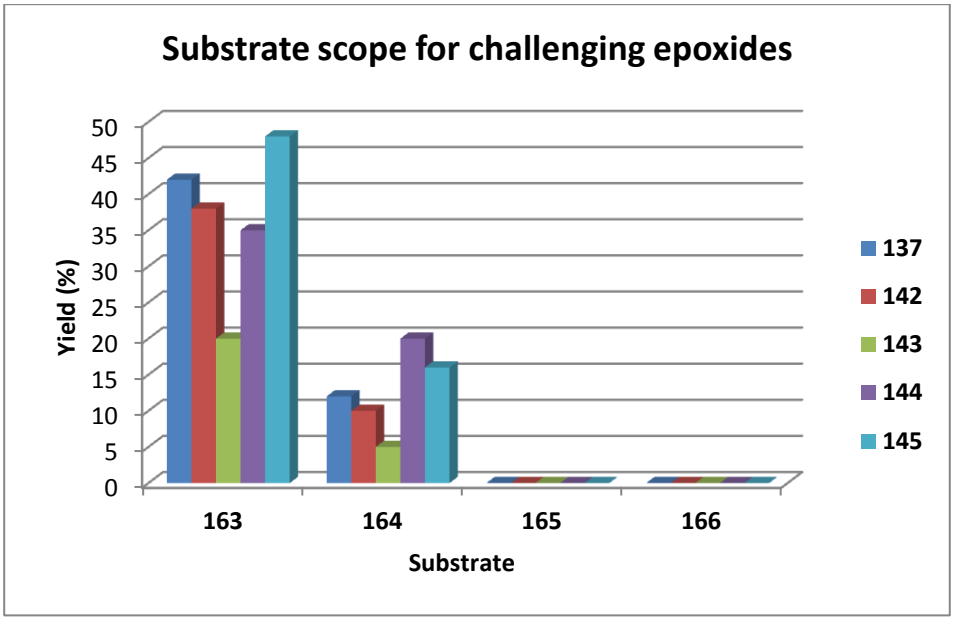

Graph 4.6 *Results in the catalytic synthesis of cyclic carbonates from sterically hindered epoxides. Reaction conditions: 0.8 mmol substrate, 2.5 mol % catalyst (Zn atoms), 1:2 Zn:onium salt, in 2 mL of MEK, pCO_2 = 10 bar, 18h, 45 ºC. Chemical yield determined by ^{1}H NMR (DMSO-d6) using mesitylene as internal standard.*

Different yields were observed with these challenging substrates and it was possible to correlate these activities with the steric bulk of the epoxide substituents. Internal epoxides were recovered from the reaction mixture indicating that no ring opening occurs under these conditions. For mono or disubstituted terminal epoxides some conversion was observed. The less sterically hindered **163** gave moderate yield. The best catalyst for this substrate proved to be **145**. Lower yields were observed with epoxide **164**. The best catalysts for this substrate were **144** and **145**.

To summarize, the most active catalyst for the catalytic ring expansion epoxides with carbon dioxide proved to be the mono and dinuclear complexes **144** and **145**. Better conversions were obtained for less sterically demanding terminal epoxides which is in accordance with the literature.[20,21] Also in line with previous findings was that no conversion of internal epoxides was observed in any case.

4.2.3. Iron catalyzed synthesis of cyclic carbonates

Iron complexes are less well-studied in ring expansion of epoxides with carbon dioxide compared to Zn, Co and Al complexes. Only a few examples are reported in literature.[35,80–82] Most of these reported catalysts are based on Fe(III) complexes.[35,81,82] For this reason we decided to explore the catalytic behaviour of the different Fe(II) dinuclear complexes synthesized previously.

The catalytic conditions were first optimized using complex **125** as the catalyst (Scheme 4.18.)

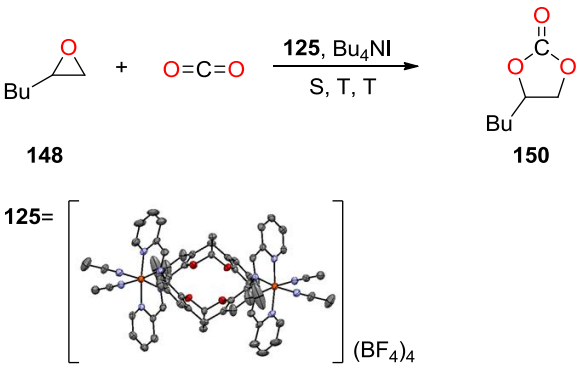

Scheme 4.18 *Ring expansion of **148** with carbon dioxide promoted by iron complex **125**.*

Firstly the temperature and pressure of the reaction were optimized, working below 85 ºC to minimise the metal-free, ammonium-salt catalysed reaction mentioned previously. In line with the previous findings for the Zn catalyst, the yield increased with the temperature. When pressure was kept constant at 10 bar, the highest yield observed was 55%. In contrast to temperature, changes in pressure affected the activity of compound **125** and this sensitivity was not observed for the Zn complexes between 10 and 20 bar. This implies that a different rate determining step exists in this Fe catalysed reaction that is dependent on the pressure of carbon dioxide in the solution. According to literature, the rate determining step, should be the CO_2 insertion or ring closing step.[43] The results of the optimization are summarized in Graph 4.7.

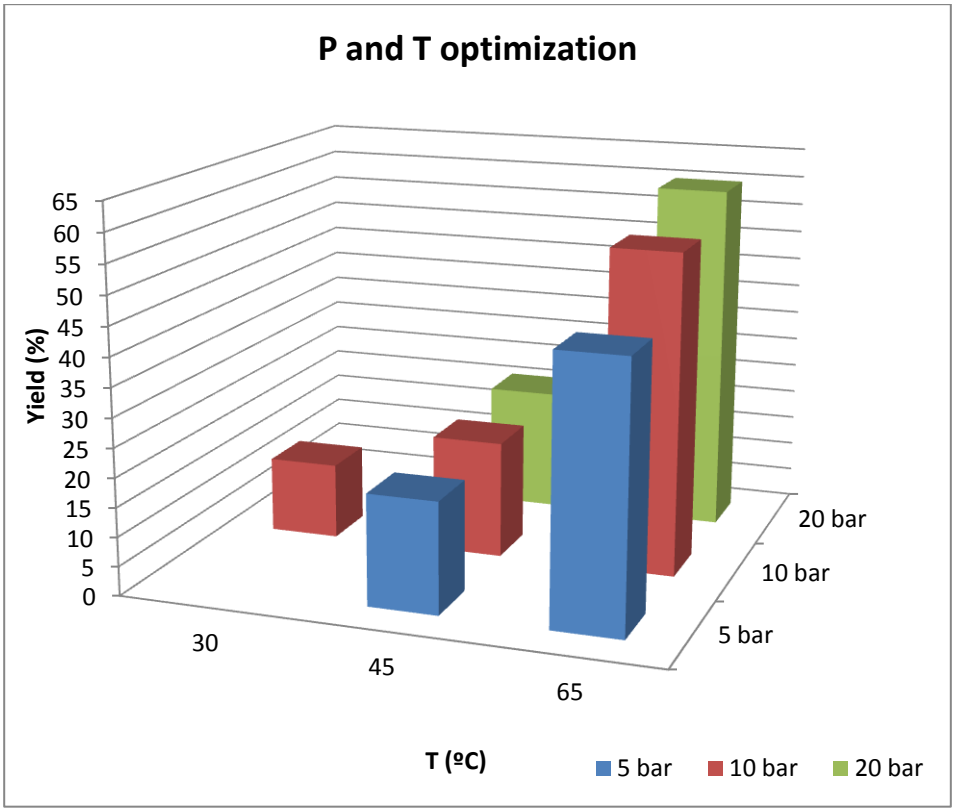

Graph 4.7 *Pressure and temperature optimization in the iron catalytized formation of cyclic carbonates from **148**. Reaction conditions: 0.8 mmol substrate, 1.25 mol % catalyst, 1:2 Fe:onium salt, in 2 mL of MEK. Chemical yield determined by GC using mesitylene as internal standard.*

The results of screening of co-catalysts are summarized in Table 4.5. In the first instance, the importance of complex:co-catalyst ratio was investigated. It was discovered that an iron:co-catalyst ratio of 1:2 was required for an active system, and this was attributed to the coordination of the iodine to iron metal. The nature of the anion (entry 1, 3, and 4) was also found to have an important role. The best yields were obtained with iodide, and this can be attributed to its high nucelofugacity compared with other halides. Furthermore, these findings support the notion of a of ring-closing rate determining step.

Table 4.5 *Co-catalyst screening in ring expansion of **148** with carbon dioxide.*

Entry	Co-catalyst	Chemical Yield[a] (%)
1	Bu_4NI	58
2[b]	Bu_4NI	0
3	Bu_4NBr	44
4	Bu_4NCl	10
5	Me_4NI	10
6	Oct_4NBr	55
7	DMAP	1

0.8 mmol substrate, 2.5 mol %, pCO_2 = 10 bar, 18h, 65 ºC, 1:2 Fe:co-catalyst, in 2 mL of MEK. [a] Chemical yield determined by GC using mesitylene as internal standard. [b] 1:1 Fe:co-catalyst.

Larger cations were also found to improve the yield (entries 1 vs 5 and 3 vs 6). The use of a neutral nucleophile instead of an anionic one dramatically reduced the reactivity and only 1% yield was observed (entry 7). This lack of reactivity was attributed to the poor leaving group ability of DMAP. The results of this screening revealed that the best co-catalyst for iron complexes is tetrabutylammonium iodide.

The poor solubilty of complex **125** limited the solvent scope for solvent optimization to polar ones and the best solvent proved to be methylethylketone giving yields of up to 60%. Acetonitrile and dimethoxyethane were also reasonable solvents, giving yields, above 50% for both. Methanol and acetone were the worst solvents giving yields of only 23% and 4% respectively. In light of this optimization, MEK was chosen as solvent for this transformation.

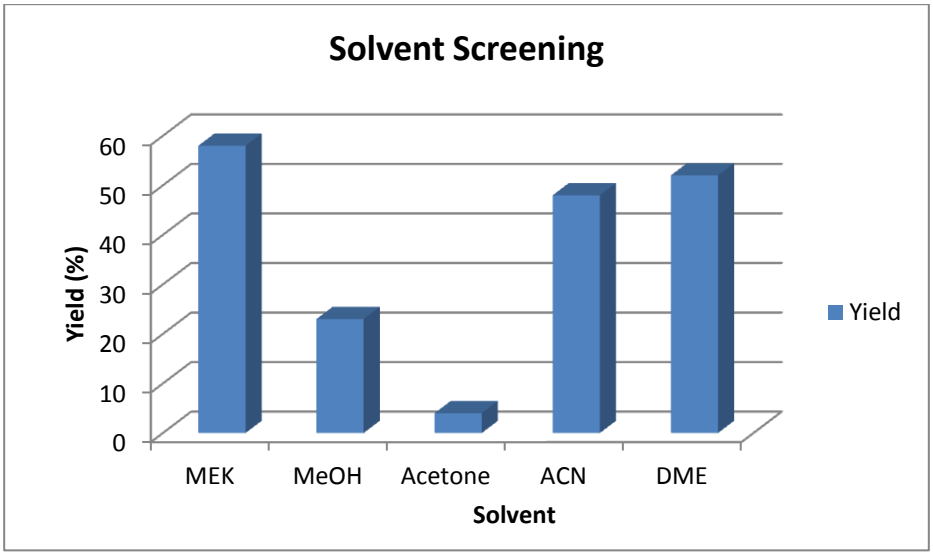

Graph 4.8 *Solvent screening for catalytic formation of cyclic carbonates from **148**. Reaction conditions: 0.8 mmol substrate, 1.25 mol % catalyst, 18h, 65 ºC, 1:2 Fe:Bu_4NI, in 2 mL of solvent. Chemical yield determined by GC using mesitylene as internal standard.*

Once the reaction conditions were optimized, different iron complexes were screened as prospective catalysts (Scheme 4.19.)

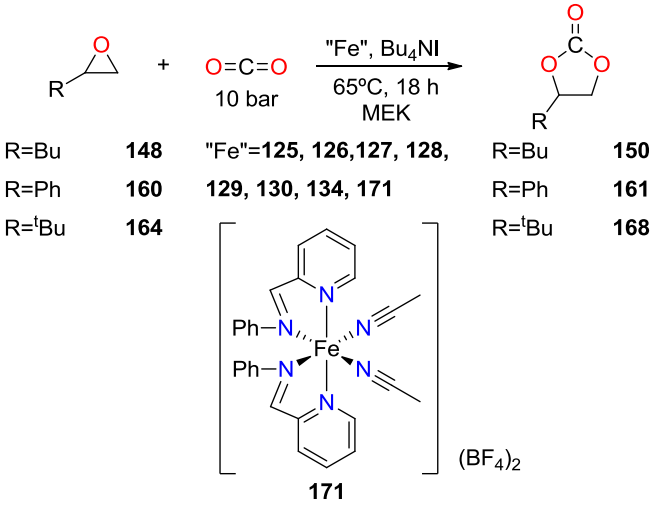

Scheme 4.19 *Cyclic carbonate formation promoted by iron complexes.*

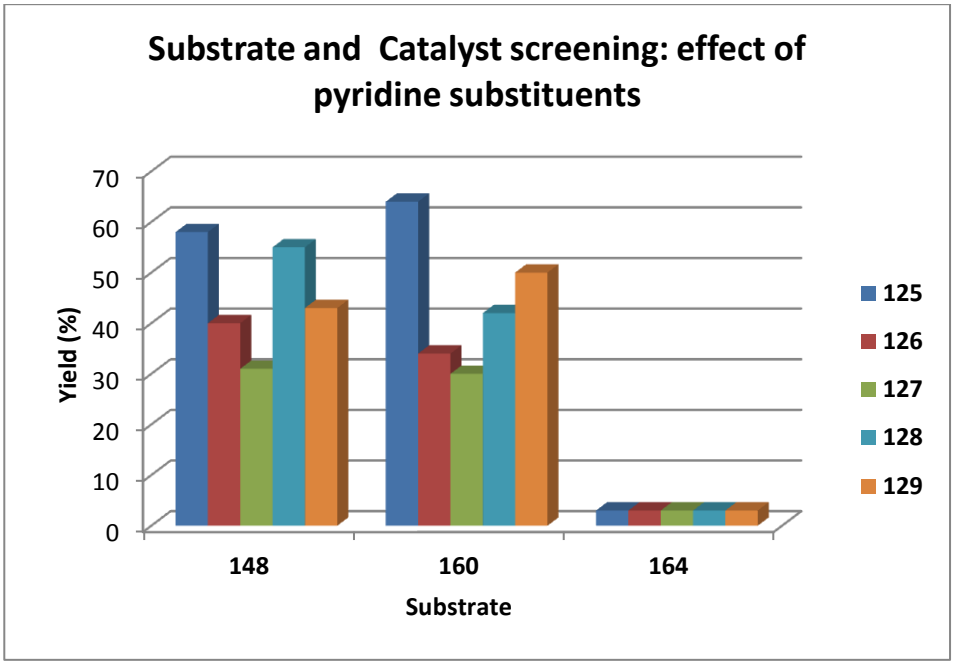

Graph 4.9 *Substrate and catalyst screening for catalytic formation of cyclic carbonates. Reaction conditions: 0.8 mmol substrate, 1.25 mol % catalyst, 18h, 65 ºC, 1:2 Fe:Bu_4NI, in 2 mL of MEK. Chemical yield determined by GC using mesitylene as internal standard.*

The catalytic transformation of several epoxides using iron dinuclear complexes with different steric and electronic properties in the pyridine moiety are summarized in Graph 4.9. The transformation of **148** was initially targeted as a test reaction. The best catalyst for this substrate proved to be complex **125**, giving the expected cyclic carbonate **150** in 58 % yield. It was noted that electron donating substituents in the *ortho*-position from nitrogen of pyridine led to a less active system and this is proposed to be the result of a reduction of the Lewis acidity of these complexes. This notion is supported by the fact that electron withdrawing groups in the *ortho*-position, bromine for example, gave higher yields.

As in the case of **148**, the formation of the corresponding cyclic carbonate from styrene oxide, **160** followed the same trend. The best results were obtained for **125** as catalyst with EWD groups, **128** and **129**. When epoxide **164** was used as substrate, similar very low conversions – above 3% – were observed for all the catalyst systems. This was attributed to the lack of coordination of the

epoxide to the metal. The low conversions observed are attributed to metal-free reaction catalysed by the ammonium salt.

The reactivity of the previously used epoxide were explored with different iron catalysts bearing aminopyiridine coordinating groups, iminoquinoline instead of iminopyridine, or mononuclear iminopyridine iron complexes. The results of these studies are summarized in Graph 4.10.

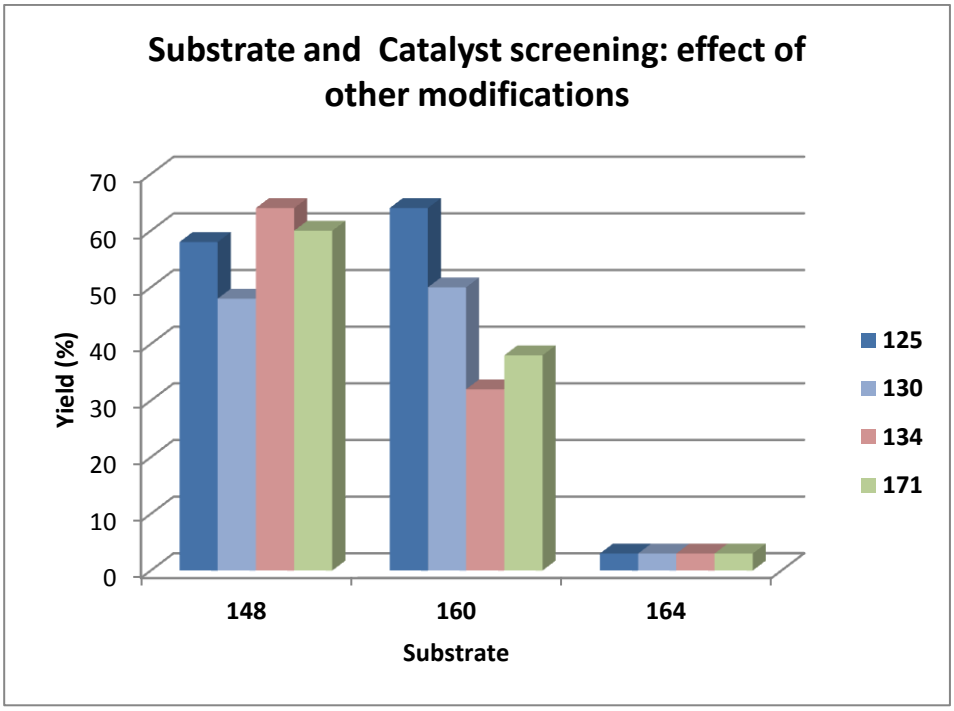

Graph 4.10 *Substrate and catalyst screening with different nitrogen donor applied in the catalytic formation of cyclic carbonates. Reaction conditions: 0.8 mmol substrate, 1.25 mol % catalyst, 18h, 65 ºC, 1:2 Fe:Bu_4NI, in 2 mL of MEK. Chemical yield determined by GC using mesitylene as internal standard*

The yield was comparable between **125**, **134**, and **171** when substrate **148** was used. If we compare **125** and **171** we can disregard any cooperative effect between our iron nuclei and they act as single monomer. Lower yields were obtained when the more crowded complex **130** was used.

When the substrate was changed to **160** lower yields were obtained with **130**, **134** and **171**. The best catalyst was found to be **125**. As we previously described, yields diminished when bulkier R substituents are present in the epoxide substrate.

To summarize, the best catalyst for the ring expansion of epoxides with carbon dioxide was found to be complex **125**. The conversions were affected by the steric properties of the epoxide and the steric and electronic properties of the complex.

4.2.4. Iron catalyzed oxidation of benzylic C–H bonds

The new family of Iron complexes were tested as active catalysts for the oxidation reactions of organic compounds. Recently, iminopyridine complexes were reported as catalyst for the selective oxidation of alcohols and benzylic C–H to ketones.[70,71] Given this precedent we decided to explore this reaction with the dinuclear iron complexes prepared in this work. The oxidation of diphenylmethane **172** was optimized using catalyst **125**. The general reaction is depicted in Scheme 4.20.

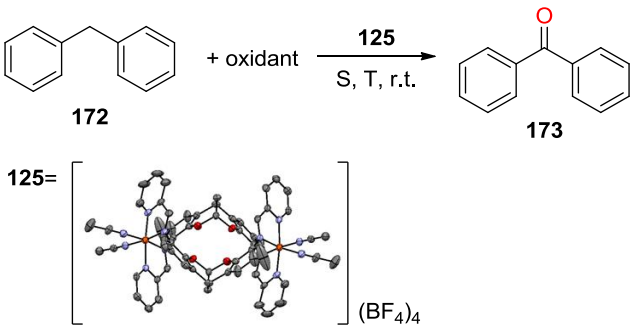

Scheme 4.20 *Benzophenone synthesis via catalytic oxidation of diphenylmethane promoted by **125**.*

Different parameters were shown to influence the reaction and the results of the optimization of some of those parameters are summarized in Table 4.6. Firstly the influence of oxidant loadings was explored. Larger excesses of oxidant can contribute to faster catalyst decomposition, recently it was found that amide was

formed from the iminopyridine which was still active in the catalysis.[71] A positive linear relationship between yield and quantity of oxidant was observed (entries 1-3).

.

Table 4.6 *Diphenylmethane oxidation: optimization of reaction conditions.*

Entry	Solvent	Ox. eq.	Yield[a] (%)
1	ACN	4	30
2	ACN	6	49
3	ACN	8	73
4[b]	ACN	8	57
5[c]	ACN	8	65
6	Py	8	80
7[d]	ACN	8	16

*0.3 mmol of **172**, 0.015 eq. of **125**, oxidant ^{t}BuOOH in 0.5 mL of solvent, 6 h and r.t.. Slow addition of oxidant over 30 min, every five minutes. [a] Chemical yield determined by GC using o-dichlorobenzene as external standard. [b] Internal standard. [c] Fast addition of oxidant. [d] $Fe(BF_4)_2.6H_2O$ as catalyst.*

The usage of an internal standard led to depleted yields and thus an external standard was found to be required. It is suggested that changes in reaction media properties such polarity or solubility upon inclusion of an internal standard were responsible for the decreased yields. The decomposition of the metal centres by peroxides necessitated the slow addition of the peroxide to the system. In our case, when all the peroxide was added at the beginning of the reaction (entry 3 vs 5) the conversion was decreased and gas evolution was observed. Only pyridine and acetonitrile were tested as suitable solvents (entries 3 and 6). Pyridine proved to be a more suitable solvent but since pyridine can readily coordinate to Fe and act as a good ligand, we decided to use acetonitrile as solvent. Finally the nature of the iron precursor was examined, but only low conversions were observed (entry 9), demonstrating that there is a positive stabilization effect of our ligand. From the literature it is

known that benzophenone can be prepared with low yields (8%) via a non-metal catalyzed reaction.[71]

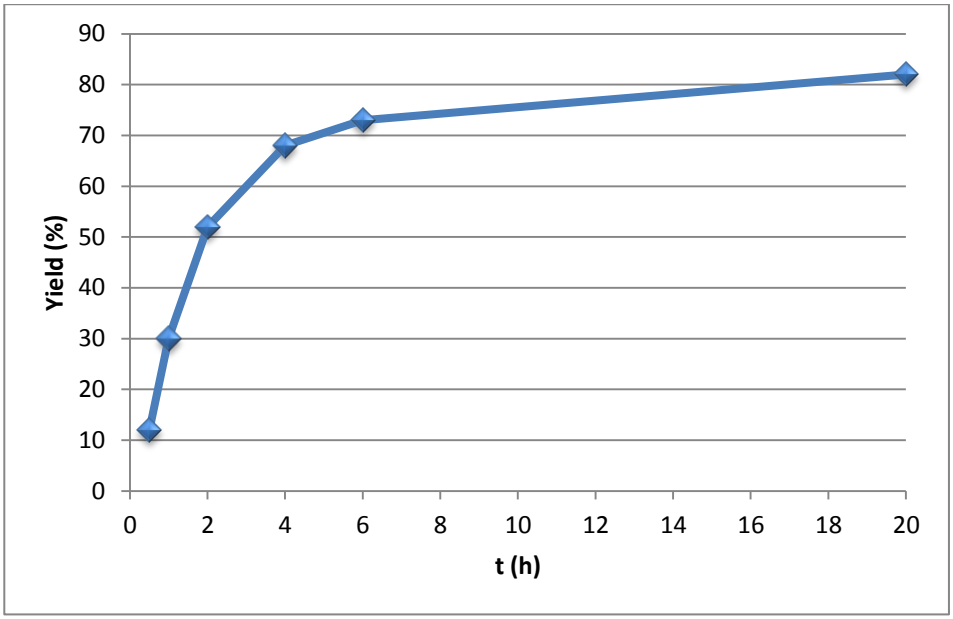

Graph 4.11 *Reaction evolution in time. Reaction conditions: 0.3 mmol of **172**, 0.015 eq. of 125, oxidant ^{t}BuOOH in 0.5 mL of ACN, 6 h and r.t. Slow addition of oxidant, over 30 min, every five minutes. Chemical yield determined by GC using o-dichlorobenzene as external standard.*

The reaction evolved quickly in the first two hours and a chemical yield of 52% was determined. Later the reaction rate decreased and at 4 and 6 hours only 68 and 73% yield were obtained. Despite this decrease in activity, the catalyst was still active, as after 20 h yield the reaction had progressed further to 82%. The concentration of ^{t}BuOOH decreased after 4 hours due to decomposition, this affected the conversion and reaction was almost stopped.

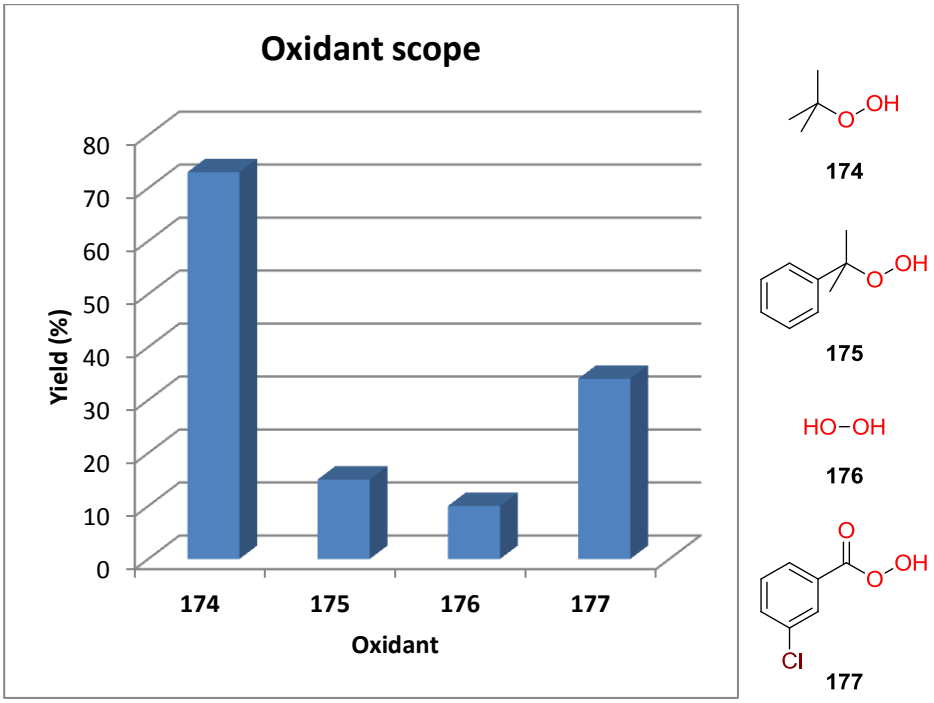

Graph 4.12 *Oxidant scope in the catalytic oxidation of* ***172****. Reaction evolution in time. Reaction conditions: 0.3 mmol of 173, 0.015 eq. of 125, oxidant* ^{t}*BuOOH in 0.5 mL of ACN, 6 h and r.t. Slow addition of oxidant, over 30 min, every five minutes. Chemical yield determined by GC using o-dichlorobenzene as external standard.*

Finally different oxidants were tested in the iron catalytic oxidation of diphenylmethane to benzophenone. The best oxidant for this reaction was found to be *tert*-butyl hydroperoxide which gave 73% yield after 6h hours. Cumene hydroperoxide **175** was determined to be a less suitable oxidant as only 15% of yield was obtained. Surprisingly, hydrogen peroxide gave the lowest yield of all tested oxidants, only 10% which is most likely due to fast decomposition of hydrogen peroxide by the metal catalyst. Lastly *meta*-chloroperbenzoic acid (m-CPBA, **177**) gave yields of up to 34% and this moderate conversion was attributed to the low solubility of the oxidant in the reaction media (410 mg in 0.5 mL of solvent).

Once the reaction was completely optimized different substrates with different electronic and steric properties were tested, along with different Fe complexes. A schematic representation of the reaction is shown in Scheme 4.21.

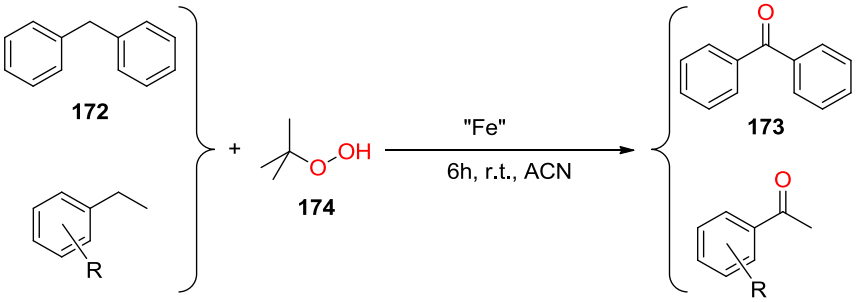

R= H **178** "Fe"= **125, 132, 133, 134, 171** R= H **182**
4-CF_3 **179** 4-CF_3 **183**
4-OMe **180** 4-OMe **184**
2-OMe **181** 2-OMe **185**

Scheme 4.21 *Substrate and catatyst scope in iron catalyzed oxidation of benzylic C–H bonds.*

The results obtained in the oxidation of diphenylmethane with different iron catalyst are summarized in Table 4.7. Low to moderate conversions were obtained for the different catalysts. The best yields were achieved with complex **125** (entry 1). Monomeric species (entries 2 and 5) were found to perform similarly. The nature of the backbone was found to influence the activity of the dimeric compounds, with the catalyst derived from BFBF giving lower conversions.

Table 4.7 *Diphenylmethane oxidation with different iron complexes.*

Entry	Catalyst	Chemical Yield[a] (%)
1	**125**	68
2	**132**	50
3	**133**	41
4	**134**	20
5	**171**	49

*0.3 mmol of **172**, 0.015 eq. of **125**, oxidant ^{t}BuOOH in 0.5 mL of ACN, 6 h and r.t. Slow addition of oxidant over 30 min,*

every five minutes. [a] *Chemical yield determined by GC using o-dichlorobenzene as external standard.*

It can be observed that the conversion is affected by electronic properties of the N-donor. For example, the aminoderivative was the worst catalyst for this transformation with only 20% of isolated yield (entry 5). It is known from literature that secondary amines can be oxidized in the presence of iron and oxidant,[83,84] thus they are less stable than imine complexes and the conversion was decreased for these ligands.

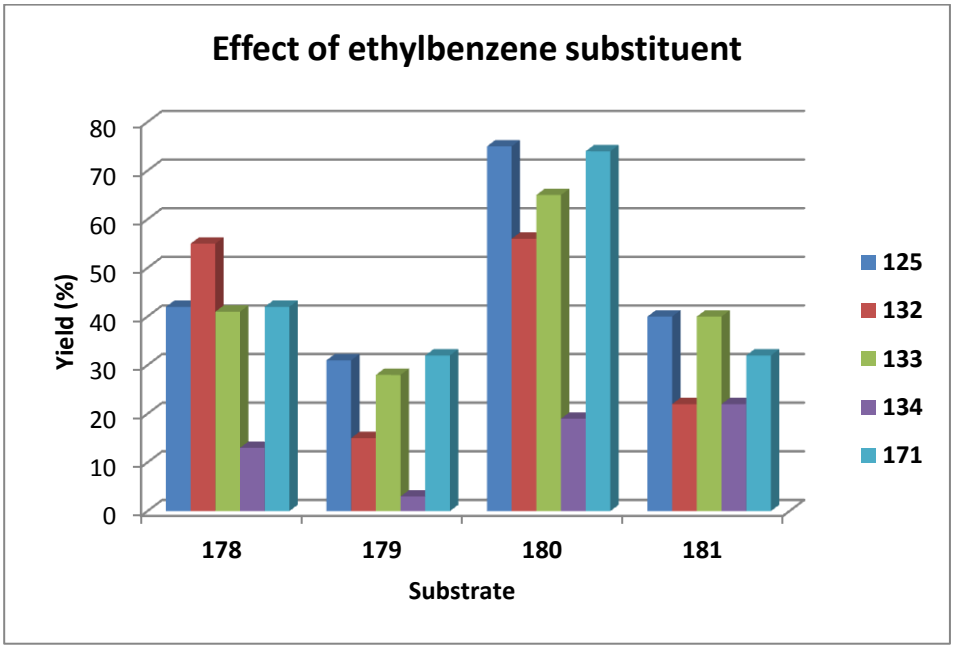

Graph 4.13 *Effect of substituents in ethylbenzene in iron catalyzed oxidation of benzylic C–H bonds. Reaction conditions: 0.3 mmol of 173, 0.015 eq. of 125, oxidant ^{t}BuOOH in 0.5 mL of ACN, 6 h and r.t. Slow addition of oxidant, over 30 min, every five minutes. Chemical yield determined by GC using o-dichlorobenzene as external standard.*

The catalytic oxidation was extended to ethylbenzene derivatives, the results of which are summarized in Graph 4.13. Ethylbenzene is a more challenging substrate than diphenylmethane as it is less activated towards oxidation. A similar trend was observed as before, in that iminopyridine complexes were more active than aminopyridine complexes. Likewise for **172**, no cooperative effect was observed as both mononuclear and dinuclear complexes oxidize

ethylbenzene to acetophenone **182** with comparable yields. Electronic effects were observed for substituents in the *para* position, substrates **179** and **180**. Thus EDG activated the substrate towards oxidation due to an increase of electron density of the ring, **180** was converted up to 75% yield, which is very close to the doubly activated **172**. On the contrary, EWD groups gave only 32% yields. The most hindered substrate, **181** gave lower yields and the best catalytic system gave only 40%. Two different effects could explain this behaviour: a) the steric hindrance could block the approach of the substrate to the iron centre b) the intermediate alcohol could coordinate as chelate to the Fe catalyst, and this chelation could slow down the reaction.

4.3. Conclusions

- A whole range of dinuclear metal complexes were prepared for Fe, Zn and Cu. Unfortunately, the two metal units formed do not interact, although the DBDOC moiety does act as a brigde. Only once the desired type of coordination was observed with a hydroxide and acetate anion acting as the bridging anions.

- Iron complexes assumed an octahedral geometry with a cis coordination of ACN. Non substituted-pyridine promoted the formation of low-spin complexes. *Ortho* substituents deformed the octahedral and favoured the formation of high-spin complexes.

- A distorted bipyramid was observed in the case of Cu complexes with ligand **66**. In the X-ray structure two different compounds were observed which differ in the additional MeOH or TfO ligands in the equatorial face. The nature of the ligands has an influence on the Cu–Cu distance, being longer distance when neutral MeOH is acting as the ligand.

- Different Zn multinuclear cluster were synthesized with DBDOC and SPAN moieties. The nuclearity of the complex depended on the steric hindrance and the structure of the backbone.

- The zinc clusters were applied in the catalytic synthesis of cyclic carbonates. Moderate to high yields were obtained when monosubstituted epoxides were used as substrate under mild conditions. The most challenging epoxides gave low yields or no conversion at all. The best catalysts for this reaction were mono and dinuclear compounds.

- The best catalyst for the catalytic ring expansion of epoxides with carbon dioxide was complex **125**. Conversions were affected by the steric properties of the epoxides and the steric and electronic properties of the complex. In none of the cases we observed a cooperative effect of the iron nuclei.

- Several iminopyridine and aminopyridine iron complexes were applied in the catalytic oxidation of benzylic C–H bonds. This reaction presented moderate to high yields and it was observed that yields were highly affected by electronic and steric properties of the substrate; EWG and steric demanding substrates were the most difficult to oxidize. As general trend the best catalyst was complex **125**. No cooperative effect between the iron nuclei was observed.

4.4. Experimental Part

Unless otherwise stated, all reactions were performed using standard vacuum-line and Schlenk techniques under nitrogen atmosphere. Solvents were purchased from Sigma-Aldrich as HPLC grade and dried with an SPS system of ITC-inc. Reagents were used as commercially available. NMR spectra unless otherwise stated were recorded at the following frequencies: 400.13 MHz (^{1}H) and 100.63 MHz (^{13}C) NMR spectra were recorded using broad band decoupling. Chemical shifts of ^{1}H and ^{13}C NMR spectra are reported in ppm downfield from TMS, used as internal standard. Signals are quoted as s (singlet), d (doublet), t (triplet), m (multiplet), b (broad)). Gas chromatoGraph analyses were run on a Hewlett-Packard HP 5890A instrument (split/splitless injector, J&W Scientific, IA, 25 m column, internal diameter 0.25 mm, film thickness 0.33 mm, carrier gas: He, F.I.D. detector) equipped with a Hewlett-Packard HP3396 series II integrator. HPLC analyses were run on a HPLC Agilent 1100 apparatus, using a Daicel CHIRALPAK IA column (4.6mm B, 250 mm). The CG-MS are done in HP 6890 Series GC System coupled to HP 5973 Mass Selective Detector, with automatic injector HP 7683 Series Injector. The column is HP 5MS (30 m x 0.25 mm, and 0.25 film thickness µm). High pressure experiments were performed in a semiautomatic autoclave (AMTEC, Slurry phase reactor, SPR16) equipped with 16 stainless steel 15 mL reactors. All reactors were connected via a valve system with the gas supply and were equipped with individually adjustable stirring and heating.

Synthesis of Fe complexes with $Fe(OTf)_2(CH_3CN)_2$ as precursor.

A THF (2 mL) solution of ligand (0.1 mmol) was added to a stirring solution of $Fe(OTf)_2(CH_3CN)_2$ (0.1 mmol) in THF (2 mL). The resulting solution was allowed to stir during 3h. Then 10 mL of dry diethyl ether were added and the solution was filtered and dried. The resulting solid was clean 3 times with diethyl ether and dried under vacuum.

Synthesis of $[Fe_2\mathbf{66}_2(CH_3CN)_2](OTf)_4$, 123.

Compound **123** was prepared using the procedure described above for synthesis of Fe complexes with $Fe(OTf)_2(CH_3CN)_2$ as precursor using as **66** as ligand. Yield: 55%. ^{1}H NMR (400 MHz, CD_3CN) δ = 10.50 (s), 9.68 (s), 7.31 (s),

6.35 (s), 6.06 (s), 5.15 (s), 3.67 (s), 3.45 (s), 3.25 (s), 1.30 (s), 1.15 (s), 0.91 (s). LMSIS$^+$: calcd. for $C_{61}H_{48}F_9Fe_2N_8O_{13}S_3^+$ [Fe_2(**66**)$_2$(OTf)$_3$] [M+] 1479.11; found 1479.

Synthesis of [$Fe_2$72$_2$(CH_3CN)$_2$](OTf)$_4$, 124.

Compound **124** was prepared using the procedure described above for synthesis of Fe complexes with $Fe(OTf)_2(CH_3CN)_2$ as precursor using as **72** as ligand. Yield: 40% ^{1}H NMR (500 MHz, Acetonitrile-d_3) δ = 52.08 (d, J = 281.8 Hz), 24.52 (s), 10.12 – 9.39 (m), 8.10 (m), 6.35 (d, J = 73.9 Hz), 5.11 (s), 4.14 – 3.46 (m), -9.07 (s), -14.02 (s), -26.88 (s). LMSIS$^+$: calcd. for $C_{40}H_{28}F_9Fe_2N_4O_{11}S_3^+$ [Fe_2**72**(OTf)$_3$] [M+] 1119.54; found 1120.

Synthesis of Fe complexes with $Fe(BF_4)_2.6H_2O$ as precursor.

A Schlenk tube was charged with $Fe(BF_4)_2.6H_2O$ (34 mg, 0.1 mmol). Then 3 mL of dry THF and 0.1 mL of TEOF (0.6 mmol) were added. The solution was stirred for 30 min and it became light purple. Ligand was added (0.1 mmol) to the stirring solution. The resulting solution was allowed to stir during 3h. Then 10 mL of dry diethyl ether were added and the solution was filtered and dried. The resulting solid was clean 3 times with diethyl ether and dried under vacuum.

Synthesis of [$Fe_2$66$_2$(CH_3CN)$_4$](BF_4)$_4$, 125.

Compound **125** was prepared using the procedure described above for synthesis of Fe complexes with $Fe(BF_4)_2.6H_2O$ as precursor using as **66** as ligand. Yield: 74% ^{1}H NMR (400 MHz, CD_3CN) δ = 10.50 (s), 9.68 (s), 7.31 (s), 6.35 (s), 6.06 (s), 5.15 (s), 3.67 (s), 3.45 (s), 3.25 (s), 1.30 (s), 1.15 (s), 0.91 (s). $C_{66}H_{60}B_4F_{16}Fe_2N_{12}O_4.4H_2O$ (1616.41): calcd. C, 49.05; H, 4.24; found C, 48.81; H, 4.24.

Synthesis of [$Fe_2$67$_2$(CH_3CN)$_4$](BF_4)$_4$, 126.

Compound **126** was prepared using the procedure described above for synthesis of Fe complexes with $Fe(BF_4)_2.6H_2O$ as precursor using as **67** as ligand. Yield: 58%. ^{1}H NMR (500 MHz, Acetonitrile-d_3) δ = 56.41 (b), 24.86 (b), 8.97 (s), 8.52 (s), 8.10 (d, *J* = 34.5 Hz), 7.95 – 7.80 (m), 7.33 (s), 7.03 (s), 2.33

– 2.08 (m), -10.29 (b), -15.27 (b), -29.96 (b). $C_{70}H_{68}B_4F_{16}Fe_2N_{12}O_4.4H_2O$ (1672.34): calcd. C, 50.27; H, 4.58; found C, 50.06; H, 4.59.

Synthesis of $[Fe_2$68$_2(CH_3CN)_4](BF_4)_4$, 127.

Compound **127** was prepared using the procedure described above for synthesis of Fe complexes with $Fe(BF_4)_2.6H_2O$ as precursor using as **68** as ligand. Yield: 63%. ^{1}H NMR (500 MHz, CD_3CN) δ = 75.31 (b), 53.10 (b), 22.31 (b), 9.83 (b), 9.17 (b), 7.89 (b), 7.35 (b), 6.35 (b), -3.02 (b), -7.79 (b), -13.05 (b), -21.85 (b). $C_{70}H_{68}B_4F_{16}Fe_2N_{12}O_8.4H_2O$ (1736.34): calcd. C, 48.42; H, 4.41; found C, 48.58; H, 4.51.

Synthesis of $[Fe_2$70$_2(CH_3CN)_4](BF_4)_4$, 128.

Compound **128** was prepared using the procedure described above for synthesis of Fe complexes with $Fe(BF_4)_2.6H_2O$ as precursor using as **70** as ligand. Yield: 57%. ^{1}H NMR (500 MHz, Acetonitrile-d_3) δ = 10.24 – 9.90 (m), 8.22, (s), 8.11 – 7.72 (m), 7.49 – 7.21 (m), 7.01 (s), 6.35 (s), 4.68 (s), 4.17 (s), 3.16 (s), 2.29 (s), 1.26 (s). $C_{66}H_{56}B_4Br_4F_{16}Fe_2N_{12}O_4.4H_2O$ (1967.07): calcd. C, 40.28; H, 3.48; found C, 40.85; H, 3.43.

.

Synthesis of $[Fe_2$71$_2(CH_3CN)_4](BF_4)_4$, 129.

Compound **129** was prepared using the procedure described above for synthesis of Fe complexes with $Fe(BF_4)_2.6H_2O$ as precursor using as **71** as ligand. Yield: 68%. ^{1}H NMR (500 MHz, Acetonitrile-d_3) δ = 14.85 (bs), 12.21 (bs), 9.76 (s), 7.90 (s), 6.41 (m), 5.13 (s), 4.67 (s), 3.49 (s), 1.96 (s), 1.06 (s). $C_{66}H_{56}B_4Br_4F_{16}Fe_2N_{12}O_4.4H_2O$ (1967.07): calcd. C, 40.28; H, 3.48; found C, 40.78; H, 3.45.

Synthesis of $[Fe_2$72$_2(CH_3CN)_4](BF_4)_4$, 130.

Compound **130** was prepared using the procedure described above for synthesis of Fe complexes with $Fe(BF_4)_2.6H_2O$ as precursor using as **72** as ligand. Yield: 62%. ^{1}H NMR (500 MHz, Acetonitrile-d_3) δ = 52.08 (d, J = 281.8 Hz), 24.52 (s), 10.12 – 9.39 (m), 8.10 (m), 6.35 (d, J = 73.9 Hz), 5.11 (s), 4.14 – 3.46 (m), -9.07 (s), -14.02 (s), -26.88 (s). $C_{82}H_{68}B_4F_{16}Fe_2N_{12}O_4.6H_2O$ (1816.46): calcd. C, 53.16; H, 4.35; found C, 53.18; H, 4.20.

Synthesis of $[Fe_2$74$_2(CH_3CN)_4](BF_4)_4$, 131.

Compound **131** was prepared using the procedure described above for synthesis of Fe complexes with $Fe(BF_4)_2.6H_2O$ as precursor using as **74** as ligand. Yield: 71% ^{1}H NMR (500 MHz, Acetonitrile-d_3) δ = 8.73 (d, *J* = 17.8 Hz), 8.35 (s), 7.78 (s), 7.15 (d, *J* = 30.8 Hz), 6.97 – 6.77 (m), 4.90 (s), 3.78 (d, *J* = 114.6 Hz), 2.70 – 2.07 (m), 1.34 (s). $C_{50}H_{46}B_2F_8FeN_6O_4.3H_2O$ (1616.41): calcd. C, 55.69; H, 4.86; found C, 55.35; H, 4.89.

Synthesis of $[Fe_2$77$_2(CH_3CN)_4](BF_4)_4$, 132.

Compound **132** was prepared using the procedure described above for synthesis of Fe complexes with $Fe(BF_4)_2.6H_2O$ as precursor using as **77** as ligand. Yield: 65%. ^{1}H NMR (500 MHz, Acetonitrile-d_3) δ = 9.35 – 8.66 (m), 8.60 – 7.86 (m), 7.85 – 7.19 (m, 0H), 7.11 – 6.63 (m), 5.12 (m), 3.37 – 2.07 (m), 1.27 (s). $C_{64}H_{56}B_4F_{16}Fe_2N_{12}O_4.4H_2O$ (1516.41): calcd. C, 48.40; H, 4.06; found C, 48.56; H, 4.24

Synthesis of $[Fe_2$78$_2(CH_3CN)_4](BF_4)_4$, 133.

Compound **133** was prepared using the procedure described above for synthesis of Fe complexes with $Fe(BF_4)_2.6H_2O$ as precursor using as **78** as ligand. Yield: 76%. ^{1}H NMR (500 MHz, CD_3CN) δ = 9.02– 8.55 (m), 8.23 –7.38 (m), 7.24 – 6.76 (m),4.94–4.79 (m), 4.51 (s) 3.15 (s), 2.26 (bs), 1.39 – 1.01 (m). $C_{39}H_{42}B_2F_8FeN_6O_2.5H_2O$ (946.32): calcd. C, 48.40; H, 4.06; found C, 49.03; H, 4.

Synthesis of $[Fe_2$79$_2(CH_3CN)_4](BF_4)_4$, 134.

Compound **134** was prepared using the procedure described above for synthesis of Fe complexes with $Fe(BF_4)_2.6H_2O$ as precursor using as **79** as ligand. Yield: 71%. ^{1}H NMR (500 MHz, CD_3CN) δ = 8.54 (s), 8.01 (s), 7.99(s), 7.92 (s), 6.57(s), 6.32 (s), 6.07(s), 4.76 (bs), 3.92 (s), 2.26 (s), 2.22 (s). $C_{66}H_{68}B_4F_{16}Fe_2N_{12}O_4.4H_2O$ (1624.29): calcd. C, 48.80; H, 4.72; found C, 48.52; H, 4.62.

Synthesis of $[Cu_2\mathbf{66}_2(MeOH)_2](OTf)_2$, 135.

A Schlenk tube was charged with $Cu(OTf)_2$ (185 mg, 0.5 mmol). The system was sealed with a septum. The flask was evacuated and backfilled with inert gas three times. Methanol was added (23 mL) and later compound **66** (231 mg, 0.5 mmol). The resulting solution was allowed to stir during 16h. Then 40 mL of dry diethyl ether were added and the solution was filtered and dried. The resulting solid was clean 3 times with diethyl ether and dried under vacuum. The brown solid was solubilized in MeOH and crystallized from slow diffusion of ether. Yield: 70%. $C_{64}H_{56}Cu_2F_{12}N_8O_{18}S_4$ (2327,87): calcd. C, 44.99; H, 3.30; found C, 44.04; H, 3.40. ESI^+: calcd. for $C_{60}H_{54}Cu_2N_8O_6^{2+}$ $[Cu_2\mathbf{66}_2(MeO)_2]$ [M+] 555.13; found 555.1

One pot synthesis of Zn complexes

A solution of amine (0.25 mmol), aldehyde (0.5 mmol), $ZnCl_2$ (0.25 mmol), and triethylamine (0.75 mmol) in MeOH (2 mL) was stirred for 16h at room temperature. The desired salen complex was isolated by filtration, purified by washing with cold MeOH and dried in vacuo to yield the product as a solid.

Synthesis of $Zn_8\mathbf{76}_8$, 137.

From isolated ligand.

To a stirred solution of **78** (140 mg, 0.285 mmol) in THF (3 mL) at room temperature was added Et_2Zn 1M (285 µL, 0.285 mmol) in a under inert atmosphere. The mixture was stirred at room temperature for 18 h, after which the precipitate was filtered and washed with MeOH (20 mL). The solid was dried under reduced pressure. Yield: 82%

From one pot synthesis.

Compound **137** was prepared using the procedure described above for one pot synthesis of Zn complexes, using **61** as amine and **136** as aldehyde. Yield: 74%. ^1H NMR (500 MHz, Methylene Chloride-d_2) δ 8.80 (s, 2H), 8.71 (s, 1H), 8.54 (d, J = 19.9 Hz, 2H), 8.32 (s, 2H), 8.28 – 8.13 (m, 2H), 7.63 (s, 2H), 7.25 – 7.11 (m, 16H), 7.02 (td, J = 3.9, 1.8 Hz, 8H), 6.80 – 6.60 (m, 16H), 6.51 (ddd, J = 7.8, 6.8, 1.2 Hz, 4H), 6.38 (dd, J = 8.4, 1.2 Hz, 2H), 6.22 (dd, J = 8.7, 1.2 Hz,

2H), 6.03 (t, J = 7.2 Hz, 2H), 5.85 – 5.78 (m, 2H), 5.71 – 5.50 (m, 6H), 5.29 (ddd, J = 8.0. 7.0. 1.2 Hz, 2H), 5.04 – 4.97 (m, 2H), 4.86 – 4.81 (m, 2H), 4.64 (q, J = 1.9 Hz, 2H), 3.62 (d, J = 2.2 Hz, 2H), 3.33 (s, 1H), 2.55 (d, J = 8.4 Hz, 12H), 2.40 – 2.33 (m, 8H), 2.32 – 2.18 (m, 10H), 2.06 (s, 6H), 1.90 (s, 6H). $C_{248}H_{192}N_{16}O_{32}Zn_8$ (4431,31): calcd. C, 67.22; H, 4.37; found C, 66.89; H, 4.53. MALDI$^+$: calcd. for $C_{248}H_{192}N_{16}O_{32}Zn_8$ [M+] 4431,31; found 4435.

Synthesis of complex 142.

Compound **142** was prepared using the procedure described above for one pot synthesis of Zn complexes, using **61** as amine and **139** as aldehyde. Yield: 54%. ^{1}H NMR (400 MHz, Chloroform-*d*) δ = 14.10 (s, 2H), 8.73 (d, *J* = 1.2 Hz, 2H), 7.20 – 7.18 (m, 2H), 7.18 – 7.16 (m, 2H), 7.00 (d, *J* = 2.1 Hz, 2H), 6.90 (dd, *J* = 2.1, 0.8 Hz, 2H), 6.35 (d, *J* = 1.9 Hz, 1H), 4.01 (s, 1H), 2.34 (m, 8H). $C_{186}H_{132}F_{12}N_{12}O_{24}Zn_6$ (3539,37): calcd. C, 63.12; H, 3.76; found C, 62.81; H, 3.92. MALDI$^+$: calcd. for $C_{186}H_{132}F_{12}N_{12}O_{24}Zn_6$ [M+] 3539,37; found 3547.

Synthesis of complex 143.

Compound **143** was prepared using the procedure described above for one pot synthesis of Zn complexes, using **61** as amine and **140** as aldehyde. Yield: 52%. ^{1}H NMR (400 MHz, DMSO-d_6) δ 8.92 (s, 2H), 7.42 (d, *J* = 7.6 Hz, 2H), 7.29 (d, *J* = 6.5 Hz, 2H), 7.17 (d, *J* = 11.4 Hz, 2H), 7.11 (d, *J* = 17.7 Hz, 2H), 6.90 – 6.82 (m, 2H), 6.46 (s, 1H), 4.71 (s, 1H), 2.27 (m, 8H), 2.23 (s, 6H). $C_{132}H_{112}N_8O_{16}Zn_4$ (2327,87): calcd. C, 68.11; H, 4.85; found C, 67.16; H, 5.13. ESI$^+$: calcd. for $C_{132}H_{112}N_8O_{16}Zn_4Na^+$ [M+] 2349,52; found 2349.5.

Synthesis of complex 144.

Compound **144** was prepared using the procedure described above for one pot synthesis of Zn complexes, using **61** as amine and **141** as aldehyde. Yield: 50%. ^{1}H NMR (300 MHz, Chloroform-*d*) δ 14.09 (s, 2H), 8.66 (s, 2H), 7.38 (dd, *J* = 7.8, 1.6 Hz, 2H), 7.24 (dd, *J* = 7.7, 1.7 Hz, 2H), 6.96 (d, *J* = 2.1 Hz, 2H), 6.91 – 6.79 (m, 4H), 6.37 (q, *J* = 2.0 Hz, 1H), 2.34 – 2.28 (m, 8H), 1.48 (s, 18H). $C_{78}H_{80}N_4O_8Zn_2$ (1332,25): calcd. C, 70.32; H, 6.05; found C, 69.81; H, 6.30. MALDI$^+$: calcd. for $C_{78}H_{80}N_4O_8Zn_2$ [M+] 1332.45; found 1332.5.

Synthesis of complex 145.

Compound **145** was prepared using the procedure described above for one pot synthesis of Zn complexes, using **27** as amine and **136** as aldehyde. Yield: 76%. ^{1}H NMR (500 MHz, DMSO-d_6) δ 8.44 (s, 1H), 8.13 (s, 1H), 7.38 – 7.32 (m, 2H), 7.28 (ddd, *J* = 8.8, 6.9, 1.9 Hz, 1H), 7.22 (dd, *J* = 7.7, 1.7 Hz, 1H), 7.07 (d, *J* = 2.1 Hz, 1H), 6.92 (ddd, *J* = 13.0. 8.0. 1.6 Hz, 3H), 6.88 – 6.84 (m, 1H), 6.68 (d, *J* = 2.0 Hz, 1H), 6.63 – 6.59 (m, 1H), 6.56 – 6.51 (m, 1H), 2.30 (s, 3H), 2.17 (s, 3H), 2.16 – 1.96 (m, 4H), 1.38 (d, *J* = 8.9 Hz, 6H), 1.27 (d, *J* = 4.7 Hz, 6H). $C_{37}H_{36}N_2O_4Zn.4H_2O$ (1384.24): calcd. C, 64.2; H, 6.84; found C, 63.23; H, 5.99. MALDI$^+$: calcd. for $C_{37}H_{37}N_2O_4Zn$ [M+] 637.2; found 637.2.

General procedure for Zn catalyzed synthesis of cyclic carbonates

A stainless steel 15 mL reactor was charged with Zn complex (0.05 mmol in Zn atoms) and NBu_4I (0.1 mmL). Then the reactor was screwed to AMTEC, Slurry phase reactor. Three cycles of pressurisation and depressurisation of the reactor (with CO_2 at 5 bar) were carried out. Then 2 mL of a 10 mM solution of epoxide and mesitylene (as internal standard) in MEK were added. The system was pressurized to 10 bars of CO_2 and the solution was stirred at 65 ºC for 18 h. 0.2 mL of the solution were dissolved in 0.4 mL of ^{d6} DMSO and the yield was determined by ^{1}H NMR

General procedure for Fe catalyzed synthesis of cyclic carbonate

A stainless steel 15 mL reactors was charged with Fe complex (0.025 mmol and NBu_4I (0.1 mmL). Then the reactor was screwed to AMTEC, Slurry phase reactor. Three cycles of pressurisation and depressurisation of the reactor (with CO_2 at 5 bar) were carried out. Then 2 mL of a 10 mM solution of epoxide and mesitylene (as internal standard) in MEK were added. The system was pressurized to 10 bars of CO_2 and the solution was stirred at 65 ºC for 18 h. 0.2 mL of the solution were dissolved in 1 mL of DCM and the yield was determined by GC.

General procedure for Fe catalyzed synthesis of cyclic carbonate.

A stainless steel 15 mL reactors was charged with Fe complex (0.025 mmol and NBu_4I (0.1 mmL). Then the reactor was screwed to AMTEC, Slurry phase

reactor. Three cycles of pressurization and depressurization of the reactor (with CO_2 at 5 bar) were carried out. Then 2 mL of a 10 mM solution of epoxide and mesitylene (as internal standard) in MEK were added. The system was pressurized to 10 bars of CO_2 and the solution was stirred at 65 ºC for 18 h. 0.2 mL of the solution were dissolved in 1 mL of DCM and the yield was determined by GC. After that 1 µl of solution was injected to a GC (Pressure=52 KPa of He, $T_{oven\text{-}initial}$=50 ºC during 0 min, ramp temperature 20 ºC/min, $T_{oven\text{-}final}$=325 ºC during 10 min., T_{inj}=T_{det}=250 ºC)

General procedure for Fe catalyzed oxidation of benzylic C–H bonds.

A Schlenk tube was charged with the substrate (0.3 mmol) and the catalyst (4,5 µmol) were dissolved in ACN (0.5 mL). The oxidant ^{t}BuOOH (0.32 mL, 70 wt% in H_2O, 2.4 mmol) was slowly added within 30 min, and then solution was shaken for 6 h at room temperature. 0.2 mL of the solution were dissolved in 1 mL of DCM and the yield was determined by GC. After that 1 µL of solution was injected to a GC (Pressure=111.7 KPa of He, $T_{oven\text{-}initial}$=50 ºC during 0 min, ramp temperature 15 ºC/min, $T_{oven\text{-}final}$=200 ºC during 10 min., T_{inj}=T_{det}=250 ºC). Conditions were different for diphenylmethane (Pressure=111.7 KPa of He, $T_{oven\text{-}initial}$=100 ºC during 0 min, ramp temperature 25 ºC/min, $T_{oven\text{-}final}$=320 ºC during 10 min., T_{inj}=T_{det}=250 ºC).

4.5. References

1. T. M. Lenton, *Climatic Change*, 2006, **76**, 7–29.
2. *British Petroleum BP Statistical Review of World Energy*, 2012, http://www.bp.com/statisticalreview.
3. *The Global Status of CCS: 2012*, http://www.globalccsinstitute.com/publications/glo.
4. T. Sakakura, J.-C. Choi, and H. Yasuda, *Chem. Rev.*, 2007, **107**, 2365–87.
5. X. Xiaoding and J. Moulijn, *Energy & fuels*, 1996, 305–25.
6. H. Arakawa, M. Aresta, J. N. Armor, M. a Barteau, E. J. Beckman, a T. Bell, J. E. Bercaw, C. Creutz, E. Dinjus, D. a Dixon, K. Domen, D. L. DuBois, J. Eckert, E. Fujita, D. H. Gibson, W. a Goddard, D. W. Goodman, J. Keller, G. J. Kubas, H. H. Kung, J. E. Lyons, L. E. Manzer, T. J. Marks, K. Morokuma, K. M. Nicholas, R. Periana, L. Que, J. Rostrup-Nielson, W. M. Sachtler, L. D. Schmidt, A. Sen, G. a Somorjai, P. C. Stair, B. R. Stults, and W. Tumas, *Chem. Rev.*, 2001, **101**, 953–96.
7. M. Tokuda, T. Kabuki, Y. Katoh, and H. Suginome, *Tetrahedron letters*, 1995, **36**, 3345–8.
8. R. Angamuthu, P. Byers, M. Lutz, a. L. Spek, and E. Bouwman, *Science*, 2010, **327**, 313–5.
9. A. Sibaouih, P. Ryan, M. Leskelä, B. Rieger, and T. Repo, *App. Cat. A: General*, 2009, **365**, 194–8.
10. A. Decortes, M. Martínez Belmonte, J. Benet-Buchholz, and A. W. Kleij, *Chem. Comm.*, 2010, **46**, 4580–2.
11. C. J. Whiteoak, N. Kielland, V. Laserna, E. C. Escudero-Adán, E. Martin, and A. W. Kleij, *J. Am. Chem. Soc.*, 2013, **135**, 1228–31.
12. D. Darensbourg, *Chem. Rev.*, 2007, **107**, 2388–410.
13. G. W. Coates and D. R. Moore, *Angew. Chem. Int. Ed.*, 2004, **43**, 6618–39.
14. T. Sakakura and K. Kohno, *Chem. Comm.*, 2009, 1312–30.
15. S. Fukuoka, M. Kawamura, K. Komiya, M. Tojo, H. Hachiya, K. Hasegawa, M. Aminaka, H. Okamoto, I. Fukawa, and S. Konno, *Green Chem.*, 2003, **5**, 497–507.
16. B. Ochiai, K. Koda, and T. Endo, *J. Pol. Sci. P. A: Pol. Chem.*, 2012, **50**, 47–51.

17. P. Lenden, P. M. Ylioja, C. González-Rodríguez, D. a. Entwistle, and M. C. Willis, *Green Chem.*, 2011, **13**, 1980–2.
18. T. Ogasawara, A. Débart, M. Holazapfel, P. NováK, and P. G. Bruce, *J. Am. Chem. Soc.*, 2006, **128**, 1390–3.
19. B. Schäffner, F. Schäffner, S. P. Verevkin, and A. Börner, *Chem. Rev.*, 2010, **110**, 4554–81.
20. P. P. Pescarmona and M. Taherimehr, *Catal. Sci. & Tech.*, 2012, **2**, 2169–87.
21. A. Decortes, A. M. Castilla, and A. W. Kleij, *Angew. Chem. Int. Ed.*, 2010, **49**, 9822–37.
22. K. B. Wiberg, *Angew. Chem. Int. Ed.*, 1986, **25**, 312–22.
23. C. Beattie, M. North, P. Villuendas, and C. Young, *J. Org. Chem.*, 2013, **78**, 419–26.
24. M. a Fuchs, T. a Zevaco, E. Ember, O. Walter, I. Held, E. Dinjus, and M. Döring, *Dalton Trans.*, 2013, **42**, 5298–305.
25. J. Sun, J. Ren, S. Zhang, and W. Cheng, *Tetrahedron Lett.*, 2009, **50**, 423–6.
26. V. Calo, A. Nacci, A. Monopoli, and A. Fanizzi, *Org. Lett.*, 2002, **4**, 1552–4.
27. R. a. Shiels and C. W. Jones, *J. Mol. Cat. A, Chem.*, 2007, **261**, 160–6.
28. K. M. K. Yu, I. Curcic, J. Gabriel, H. Morganstewart, and S. C. Tsang, *J. Phys. Chem. A*, 2010, **114**, 3863–72.
29. W. Clegg, R. W. Harrington, M. North, and R. Pasquale, *Chem. Eur. J.*, 2010, **16**, 6828–43.
30. Y. Zhao, J.-S. Tian, X.-H. Qi, Z.-N. Han, Y.-Y. Zhuang, and L.-N. He, *J. Mol. Cat. A, Chem.*, 2007, **271**, 284–9.
31. X.-B. Lu and Y. Wang, *Angew. Chem. Int. Ed.*, 2004, **43**, 3574–7.
32. X. Lu, L. Shi, Y. Wang, R. Zhang, Y. Zhang, X. Peng, Z. Zhang, and B. Li, *J. Am. Chem. Soc.*, 2006, **128**, 1664–74.
33. D. Anselmo, V. Bocokić, A. Decortes, E. C. Escudero-Adán, J. Benet-Buchholz, J. N. H. Reek, and A. W. Kleij, *Polyhedron*, 2012, **32**, 49–53.
34. J. Meléndez, M. North, and R. Pasquale, *Eur. J. Inorg. Chem.*, 2007, **2007**, 3323–6.
35. C. J. Whiteoak, E. Martin, M. M. Belmonte, J. Benet-Buchholz, and A. W. Kleij, *Adv. Syn. & Cat.*, 2012, **354**, 469–76.
36. Y.-M. Shen, W.-L. Duan, and M. Shi, *J. Org. Chem.*, 2003, **68**, 1559–62.
37. S. Kumar, S. L. Jain, and B. Sain, *Catal. Lett.*, 2012, **142**, 615–8.
38. D. Bai, S. Duan, L. Hai, and H. Jing, *ChemCatChem*, 2012, **4**, 1752–8.

39. R. L. Paddock, Y. Hiyama, J. M. McKay, and S. T. Nguyen, *Tetrahedron Lett.*, 2004, **45**, 2023–6.
40. T. Chang, L. Jin, and H. Jing, *ChemCatChem*, 2009, **1**, 379–3.
41. X. Zhang, Y.-B. Jia, X.-B. Lu, B. Li, H. Wang, and L.-C. Sun, *Tetrahedron Lett.*, 2008, **49**, 6589–2.
42. M. North, R. Pasquale, and C. Young, *Green Chemistry*, 2010, **12**, 1514.
43. F. Castro-Gómez, G. Salassa, A. W. Kleij, and C. Bo, *Chem. Eur. J.*, 2013, **19**, 6289–98.
44. J.-Q. Wang, K. Dong, W.-G. Cheng, J. Sun, and S.-J. Zhang, *Catal. Sci. & Tech.*, 2012, **2**, 1480–4.
45. M. North and R. Pasquale, *Angew. Chem. Int. Ed.*, 2009, **48**, 2946–8.
46. R. M. Haak, A. Decortes, E. C. Escudero-Adán, M. Martínez Belmonte, E. Martin, J. Benet-Buchholz, and A. W. Kleij, *Inorg. Chem.*, 2011, **50**, 7934–6.
47. Y. Yang, Y. Hayashi, Y. Fujii, T. Nagano, Y. Kita, T. Ohshima, J. Okuda, and K. Mashima, *Catal. Sci. & Tech.*, 2012, **2**, 509–13.
48. A. E. Shilov and G. B. Shul'pin, *Chem. Rev.*, 1997, **97**, 2879–932.
49. J. F. Brazdil, *Top. Catal.*, 2006, **38**, 289–94.
50. H. J. H. Fenton, *J. Chem. Soc., Trans.*, 1894, **65**, 899–910.
51. J. Prousek, *Pure App. Chem.*, 2007, **79**, 2325–38.
52. C. Pavan, J. Legros, and C. Bolm, *Adv. Syn. & Cat.*, 2005, **347**, 703–5.
53. S. Friedle, E. Reisner, and S. J. Lippard, *Chem. Soc. Rev.*, 2010, **39**, 2768–79.
54. F. P. Guengerich, *Chem. Res. Toxicol.*, 2001, **14**, 611–50.
55. L. Que and W. B. Tolman, *Nature*, 2008, **455**, 333–40.
56. C. Kim, K. Chen, J. Kim, and L. Que, *J. Am. Chem. Soc.*, 1997, **7863**, 5964–5.
57. T. Okuno, S. Ito, S. Ohba, and Y. Nishida, *Dalton Trans.*, 1997, 3547–51.
58. K. Chen and L. Que, *Chem. Comm.*, 1999, 1375–6.
59. A. Company, L. Go, M. Gu, X. Ribas, and J. M. Luis, *J. Am. Chem. Soc.*, 2007, **129**, 15766–7.
60. G. Roelfes, M. Lubben, R. Hage, L. Que, and B. L. Feringa, *Chem. Eur. J.*, 2000, **6**, 2152–9.
61. M. S. Chen and M. C. White, *Science*, 2007, **318**, 783–7.
62. M. C. White, *Science*, 2012, **335**, 807–9.
63. M. S. Chen and M. C. White, *Science*, 2010, **327**, 566–71.
64. M. D. Godbole, M. P. Puig, S. Tanase, H. Kooijman, A. L. Spek, and E. Bouwman, *Inorg. Chim. Acta*, 2007, **360**, 1954–60.

65. N. Carvalho, A. Horn, and O. Antunes, *App. Cat. A: General*, 2006, **305**, 140–5.
66. G. J. P. Britovsek, J. England, S. K. Spitzmesser, A. J. P. White, and D. J. Williams, *Dalton Trans.*, 2005, 945–55.
67. M. Costas and L. Que, *Angew. Chem. Int. Ed.*, 2002, **41**, 2179–81.
68. J. England, R. Gondhia, L. Bigorra-Lopez, A. R. Petersen, A. J. P. White, and G. J. P. Britovsek, *Dalton Trans.*, 2009, 5319–34.
69. K. Chen and L. Que, *J. Am. Chem. Soc.*, 2001, **123**, 6327–37.
70. P. Shejwalkar, N. P. Rath, and E. B. Bauer, *Dalton Trans.*, 2011, **40**, 7617–31.
71. M. Lenze, E. T. Martin, N. P. Rath, and E. B. Bauer, *ChemPlusChem*, 2013, **78**, 101–16.
72. S. C. Bart, E. Lobkovsky, E. Bill, K. Wieghardt, and P. J. Chirik, *Inorg. Chem.*, 2007, **46**, 7055–63.
73. J. M. López-Valbuena, E. C. Escudero-Adán, J. Benet-Buchholz, Z. Freixa, P. W. N. M. van Leeuwen, and P. W. N. M. Leeuwen, *Dalton Trans.*, 2010, **39**, 8560–74.
74. G. B. McGaughey, M. Gagne, and A. K. Rappe, *J. Biol. Chem.*, 1998, **273**, 15458–63.
75. M. O. Sinnokrot, E. F. Valeev, and C. D. Sherrill, *J. Am. Chem. Soc.*, 2002, **124**, 10887–93.
76. G. A. Morris, H. Zhou, C. L. Stern, and S. T. Nguyen, *Inorg. Chem.*, 2001, **40**, 3222–7.
77. A. Decortes and A. W. Kleij, *ChemCatChem.*, 2011, **3**, 831–4.
78. L. Han, H.-J. Choi, S.-J. Choi, B. Liu, and D.-W. Park, *Green Chem.*, 2011, **13**, 1023–8.
79. J. Sun, W. Cheng, W. Fan, Y. Wang, Z. Meng, and S. Zhang, *Catal. Today*, 2009, **148**, 361–7.
80. J. E. Dengler, M. W. Lehenmeier, S. Klaus, C. E. Anderson, E. Herdtweck, and B. Rieger, *Eur. J. Inorg. Chem.*, 2011, **2011**, 336–43.
81. M. a Fuchs, T. a Zevaco, E. Ember, O. Walter, I. Held, E. Dinjus, and M. Döring, *Dalton Trans.*, 2013, **42**, 5298–305.
82. J. Gao, Q.-W. Song, L.-N. He, C. Liu, Z.-Z. Yang, X. Han, X.-D. Li, and Q.-C. Song, *Tetrahedron*, 2012, **68**, 3835–42.
83. A. Machkour, D. Mandon, M. Lachkar, and R. Welter, *Eur. J. Inorg. Chem.*, 2005, **2005**, 158–61.
84. J. Larsen and K. A. Jsrgensen, *J. Chem. Soc., Perkin Trans. 2*, 1992, 1213–7.

Chapter 5
Concluding remarks.

The work presented in this doctoral Thesis focuses on the synthesis of new tetranitrogen ligands with a large N–N distance between two dinitrogen bidentate ligands designed for the formation of bimetallic complexes to be applied in bimetallic catalysis. The results, organized as ligand synthesis, metal complex synthesis and catalytic applications, lead to the following general conclusions.

Ligand synthesis

The synthesis of the various N-donor ligands prepared in this work followed the same synthetic procedure involving the ensuing sequence of steps: formation of the backbones by a condensation reaction, halogenation of the backbones, and formation of the C–N bonds *via* a cross-coupling reaction. Subsequently the aminoderivatives were condensed with pyridinecarboxaldehyde or salicylaldehyde derivatives to give to the the final ligands.

The main characteristics of the steps are indicated below:

a) The three backbones were synthesized from *p*-cresol by an acid catalysed condensation with different carbonyl derivatives. SPAN, BFBF and DBDOC backbones were obtained with moderate yields. The success of the condensation was affected by the position of the substituents in the phenol derivatives. The condensation was inhibited when substituents were present in the position *ortho* to the hydroxy group. Electron donating groups did not affect the condensation when they were present in the *meta* position, but the reaction did not proceed when the *para* substituents were electron withdrawing groups.

b) For the second step – the halogenation – NBS is still the brominating agent of choice. Other bromine source gave promising yields and selectivities, for instance the Selectfluor and sodium bromide systems. As regards the monobromination of the DBDOC backbone, good selectivities were achieved with benzyl tribromide.

c) Surprisingly, the three backbones showed very dissimilar reactivity in the C–N bond formation and for each one a distinct method had to be developed. For instance SPANamine was synthesized efficiently *via* a Buchwald–Hartwig coupling reaction with benzylamine. The synthesized SPANbenzylamine was

reduced to SPANamine in high yield and selectivity. In the case of DBDOC the amination was performed *via* an Ullmann coupling with ammonia in high yields. Finally, BFBFamine was prepared *via* an Ullmann coupling with sodium azide.

d) Finally the tetradentate derivatives were firstly prepared *via* Schiff condensation with different pyridinecarboxaldehyde derivatives for DBDOC, BFBF, and SPAN amine derivatives. These ligands were obtained in moderate to high yield. Phenolcarboxaldehyde reacted with DBDOC in high yield. All imines were highly sensitive to hydrolysis.

Two different synthetic routes were successfully applied in the synthesis of aminopyridine derivative of DBDOC **79**. The first one concerned the reduction of iminopyridines with a range of reducing agents; the best results were obtained with DIBALH. The second route involved the reductive amination of the imine yielding compound **79** in high yields and selectivies when PEMB was used as the reducing agent.

The formation of the tertiary amine or the amide required the use of strong bases due to the low nucleophilicity of DBDOCamine. The thus formed NH^- anion was sufficiently nucleophilic to attack dimethyl sulphate or methyl 2-pyridinecarboxylate. Eventually compounds **80** and **87** were isolated with moderate yields.

Bidentate complexes and their application in catalysis

SPANamine was used as ligand in the synthesis of several metal complexes showing different structures, geometries and nuclearity. Firstly, rhodium trichloride SPANamine complex **88** was synthesized; it exhibited a dimeric structure with both Rh centres in an octahedral geometry. For this complex SPANamine presented a bite angle of *ca.* 95º. In contrast copper SPANamine complex was isolated as a monomer with a distorted square planar geometry in which the ligand bite angle was close to 150º and is best described as a *trans*-ligand coordination. Finally, palladium SPANamine complex **89** was obtained as a monomeric species; a *trans*-coordination was expected as for the analogous Pd-SPANphos complex.[1]

The rhodium catalyzed hydrogenation of dimethyl itaconate was explored with SPANamine or SPANoxazoline ligands. To achieve full conversion high pressures of hydrogen were necessary. No bite angle effect was observed in this catalytic transformation.

Acetophenone was hydrosilylated by rhodium complexes modified with SPANamine. A distinct catalytic behaviour was observed for *in situ* prepared catalysts and pre-isolated complexes, the former showing a higher activity. However, similar selectivities were obtained with both systems and no enantioselectivity was achieved.

Copper-catalyzed oxidation of *meso*-diols was explored with various N-donor ligands. High activities and selectivities were obtained for all ligands applied in the reaction. Interestingly, only oxazolines ligands were capable of inducing enantioselectivity. When the large bite angle SPANoxazoline ligand **118** was used, no increase in ee was observed with respect tooxazoline **119**.

Iron oxidation of *meso*-diols was explored using the SPANamine and oxazoline ligands **93** and **119**. Iron (0, II, III) precursors modified with SPANamine gave higher conversions and selectivities to α-hydroketones than the systems containing the oxazoline ligand. However, racemic mixtures of product were obtained in all cases.

Tetradentate complexes and their application in catalysis

Several dinuclear metal complexes based on Fe, Zn and Cu were prepared, but unfortunately two independent metal units were formed; only DBDOC moiety acted as a bridge and we did not succeed in incorporating bridging, small anions. Only once the desired type of coordination was observed.

Iron complexes of the pyridine-imine ligands showed octahedral geometry with a *cis* coordination of the acetonitrile ligands. Nonsubstituted-pyridine derivatives promoted the formation of low-spin complexes. *Ortho* substituents deformed the octahedral geometry and favoured the formation of high-spin complexes.

The formation of a distorted bipyramid was observed for the Cu complex with ligand **66**. In the X-ray structure two different compounds were found differing in

the ligand coordinated in the external equatorial face, MeOH or TfO. The nature of the ligands influences the Cu–Cu distance showing a longer distance when neutral MeOH is acting as the ligand.

Different Zn multinuclear clusters were synthesized with DBDOC and SPANbased ligands. The nuclearity of the complex depended on the steric hindrance and the structure of the backbone.

The zinc clusters were applied in the catalytic synthesis of cyclic carbonate through reaction of CO_2 and epoxide. Moderate to high yields were obtained when monosubstituted epoxides were used as the substrate . The most hindered epoxides gave low yield or no conversion at all. The best catalysts for this reaction were Zn dinuclear compounds.

The best catalyst for the catalytic ring expansion of epoxides with carbon dioxide was complex **125**. Conversions were affected by the steric properties of the oxirane and the steric and electronic properties of the complex. In none of the cases we observed a cooperative effect between the iron nuclei.

Several iminopyridine and aminopyridine iron complexes were applied in the catalytic oxidation of benzylic C–H bonds. This reaction showed moderate to high yields, highly affected by electronic and steric properties of the substrate; substrates containing electron withdrawing groups or sterically demanding groups were the most difficult to oxidize. As a general trend the best catalyst was complex **125**. No cooperative effect between the iron nuclei was observed.

Chapter 6
Appendix.

Congress contributions

Oral Communications

- *Title:* Dioxocin nitrogen derivates: novel ligands for dinuclear complexes
  Authors: Oriol Martínez-Ferraté; Josep Maria López-Valbuena ; George J. P. Britovsek, Carmen Claver; Piet W. N. M. van Leeuwen
  Kind of participation: Flash-poster presentation
  Conference: 5th CaRLa Winter School 2012
  City: Heidelberg, Germany *Year:* 2012

Posters

- *Title:* Dioxocin nitrogen derivates: novel ligands for dinuclear complexes
  Authors: Oriol Martínez-Ferraté; Josep Maria López-Valbuena ; George J. P. Britovsek, Carmen Claver; Piet W. N. M. van Leeuwen
  Conference: 18th International Symposium on Homogeneous Catalysis
  City: Toulouse, France *Year:* 2012
- *Title:* Dioxocin nitrogen derivates: novel ligands for dinuclear complexes
  Authors: Oriol Martínez-Ferraté; Josep Maria López-Valbuena ; George J. P. Britovsek, Carmen Claver; Piet W. N. M. van Leeuwen
  Conference: XXX Reunión del Grupo Especializado de Química Organometálica
  City: Toulouse, France *Year:* 2012
- *Title:* Spanaminas: Nueva ruta sintética y su aplicación en catálisis
  Authors: Oriol Martínez; Olivier Jacquet; Nicolas Clément; Carmen Claver; Piet W. N. M. van Leeuwen
  Conference: XXVIII Reunión del Grupo Especializado de Química Organometálica
  City: Punta Umbría, Spain *Year:* 2010
- *Title:* Spanamines: New efficient synthetic route and their application in catalysis

Authors: Oriol Martínez; Olivier Jacquet; Nicolas Clément; Carmen Claver; Piet W. N. M. van Leeuwen
Conference: 17th International Symposium on Homogeneous Catalysis
City: Poznan, Poland *Year:* 2010

Research abroad

- *Center:* Imperial College London
  Place: Londres, United Kingdom *Year:* 2011
  Duration: 3 Months
  Issue: Synthesis of dinuclear complexes

Other scientific activities

- *Activity:* Consolider Intecat Meeting
  Dates: 27/10/2009 - 28/10/2009
  City: Huesca, Spain
- *Activity:* ICIQ Summer-school.
  Dates: 20/07/2009 - 24/07/2009
  City: Tarragona, Spain